Front fixing implicit finite difference for the American put options model

by

MINYAHIL ABERA ABEBE

submitted in accordance with the requirements
for the degree of

DOCTOR OF PHILOSOPHY

In the subject

APPLIED MATHEMATICS

at the

UNIVERSITY OF SOUTH AFRICA

SUPERVISOR: PROF Z I ALI

DECEMBER 2025

Declaration

I, hereby declare that this *thesis* is my own unaided work, and all complete references are made to the sources used herein in the production of this work. This *thesis* has not been submitted to any other university or professional institution for examination.

SIGNATURE:
MINYAHIL ABERA ABEBE

Student Number: 67121497
Date August 2025

Dedicace

In heartfelt reverence, I dedicate this work to the lasting memory of my father;*Abera Abebe*, whose life and values remain my guiding light. May Allah, the Most Merciful, bestow eternal peace on him, grace him with divine comfort, and bless him Jannat Al-Firdaws. Ameen.

Acknowledgements

First, I express my profound gratitude to Almighty Allah, whose grace and guidance sustained me throughout this journey and led to the successful completion of this work.

I extend my deepest appreciation to my esteemed supervisor, *Prof. Ali Zakaria Idriss*, for his exceptional mentorship, unwavering patience, and invaluable expertise. His insightful advice, meticulous feedback, and steadfast encouragement were indispensable to this research. Beyond his academic guidance, I am deeply grateful for his paternal support, generosity, and the countless resources he provided to ensure my progress. His dedication to fostering my intellectual growth has left an enduring impact, and I sincerely hope to continue to benefit from his wisdom in the years to come.
To my beloved wife *Radiya Mohammed*, I owe immense thanks for her unwavering love, sacrifice, and emotional fortitude. Her steadfast belief in my abilities, even during moments of doubt, provided the strength and motivation necessary to persevere.

To my beloved children, I extend my deepest gratitude for their patience, understanding, and the precious time they selflessly sacrificed to support me throughout this journey.

To my beloved mother *Merema Mohammed* , I am forever grateful for her endless prayers, unlimited love, and unwavering faith in my abilities. Her quiet strength and devotion have been a beacon throughout my life.

Finally, I acknowledge my cherished brothers, family members and relatives, whose prayers, encouragement, and moral support sustained me through every challenge. Their pride in my achievements has been a constant source of inspiration.

Minyahil Abebe Abera
Student Number: 67121497

Acronyms

Acronym	
AB	Atangana-Baleanu
ADI	Alternating Direction Implicit
AMR	Adaptive Mesh Refinement
AMEX	American Stock Exchange
APO	American Put Options
AO	American Option
BDG	Burkholder-Davis-Gundy
BS	Black-Scholes
BM	Brownian Motion
BS-PDE	Black-Scholes Partial Differential Equation
CBOE	Chicago Board Options Exchange
CBOT	Chicago Board of Trade
EM	Euler-Maruyama
EO	European Option
fBM	Fractional Brownian Motion
FC	Fractional calculus
FD	Fractional Derivatives
FDE	Fractional Differential Equations
FDM	Finite Difference Methods
FEM	Finite-Element Methods
FFM	Front Fixing Method
FFEM	Front-Fixing Finite Element Method
FOC	Fractional Order Controllers
FPI	Fixed-Point Iteration
FSDE	Fractional Stochastic Differential Equation
GL	Grünwald-Letnikov
HODIE	High Order via Differential Identity Expansion

Acronym	
JDSV	Jump-Diffusion Stochastic Volatility
LCP	Linear Complementarity Problem
LSMC	Least Squares Monte Carlo
NYSE	New York Stock Exchange
ODE	Ordinary Differential Equation
OTC	Over-the-Counter
PID	Proportional-Integral-Derivative
PSOR	Projected Successive Over-Relaxation
PIDE	Partial Integro-Differential Equation
PINN	Physics-Informed Neural Network
PDE	Partial Differential Equation
RMSE	Root Mean Square Error
tfBS	Time Fractional Black-Scholes
tfBS-PDE	Time fractional Black-Scholes Partial Differential Equation
SDE	Stochastic Ordinary Differential Equation
SFPDE	Stochastic Fractional Partial Differential Equation
SP	Stochastic Process
SPDE	Stochastic Partial Differential Equation
VI	Variational Inequalitie

Notation

$\mathbb{N}$	set of natural numbers
$\mathbb{R}$	set of real numbers
$\mathbb{R}_+$	set of positive real numbers
$\overline{U}$	closure of a set U
$[a, b]$	closed interval $a \leqslant x \leqslant b$ in $\mathbb{R}$

List of Figures

4.1: Plots of SDE and FSDE solutions with the same sample size classical SDE solutions with $(\alpha(0), \alpha(1))$=(0.2,0.1) and $\lambda = 0.1$

4.2: Plots of SDE and FSDE solutions with the same sample size classical SDE solutions with $(\alpha(0), \alpha(1))$=(0.8,0.5) and $\lambda = 1$

4.3: Plots of SDE and FSDE solutions with the same sample size classical SDE solutions with $(\alpha(0), \alpha(1))$=(0.2,0.1) and $\lambda = 1$

4.4: Plots of SDE and FSDE solutions with the same sample size classical SDE solutions, with $(\alpha(0), \alpha(1))$=(0.8,0.5) and $\lambda = 1$

5.1: The figure presents the numerical results obtained using the Crank-Nicolson method, plotting X_f^n versus τ_n, with $\alpha = 0.9$ on the left and $\alpha = 0.5$ on the right.

5.2: Maturity payoffs of an AO plotted as V versus τ for different values of α.

5.3: The figure shows the 3D plot of the numerical solution v_m^n, with $\alpha = 0.9$ on the left and $\alpha = 0.5$ on the right.

5.3: The table presents the convergence rates computed based on the mean values for various fractional orders of α, ranging from 0.1 to 0.9 in increments of 0.1.

5.4: The table presents the convergence rates calculated using the RMSE for the example problem, with fractional orders of α varying from 0.1 to 0.9 in increments of 0.1.

5.5: State-of-the-Art Research Gap Analysis for Fractional Black-Scholes Models in AO Pricing.

List of Tables

4.1: Convergence of the scheme for the linear FSDE.
4.2: Convergence of scheme for the nonlinear FSDE.
5.1: Free boundary location at t = T=1
5.2: The table presents the maximum absolute errors calculated for various fractional orders of α, spanning from 0.1 to 0.9 in increments of 0.1.
5.3: The table presents the convergence rates computed based on the mean values for various fractional orders of α, ranging from 0.1 to 0.9 in increments of 0.1.
5.4: The table presents the convergence rates calculated using the RMSE for the example problem, with fractional orders of α varying from 0.1 to 0.9 in increments of 0.1.
5.5: State-of-the-Art Research Gap Analysis for Fractional Black-Scholes Models in AO Pricing.

List of Publications

The following research papers from this thesis have been published in accredited journals.

- Zakaria Ali , Minyahil Abera Abebe and Talat Nazir. Strong Convergence of Euler-Type Methods for Nonlinear Fractional Stochastic Differential Equations without Singular Kernel
- Zakaria Ali and Minyahil Abera Abebe. A Front Fixing Crank-Nicolson Finite-Difference for the Solvability of the American Put Option Models, Contemporary Mathematics (CM) Journal.

Contents

Declaration i

Acknowledgements iii

Acronyms iv

Notation vi

List of Figures vii

List of Tables viii

Abstract xii

1 Introduction 1

1.1 History and Development of Options 1

1.2 AO Valuation Methods 4

1.2.1 LCP in AO Valuation 4

1.2.2 FDMs and PINN in AO Valuation 5

1.2.3 Front-Fixing Methods in Free Boundary Problems 6

1.2.4 Fixed-Point Iteration Methods 7

1.3 Fractional Calculus 8

1.3.1 History of Fractional Calculus 8

1.3.2 Definitions of FDs 13

1.3.3 Organization of the thesis 19

2 Stochastic Ordinary Differential Equations and Stochastic Partial Differential Equations 20

2.1 Introduction 20

2.2 Lebesgue Spaces 21

2.2.1 Definitions and Core Properties of Lebesgue Spaces . . . 21
2.2.2 Types of Lebesgue Spaces . . . 22
2.3 Basic Notations of Probability Theory . . . 24
2.3.1 Basics of Brownian Motion(BM) . . . 25
2.3.2 Basics of Stochastic Process (SPs) . . . 26
2.3.3 Q-Wiener Process . . . 26
2.3.4 Probabilistic Lebesgue Spaces . . . 27
2.3.5 Stochastic Ordinary Differential Equations(SDEs) . . . 28
2.3.6 Numerical Methods for SDEs . . . 31
2.3.6.1 Euler-Maruyama Approximation . . . 31
2.4 Stochastic Partial Differential Equations (SPDEs) . . . 35
2.4.1 Introduction . . . 35
2.4.2 Solution Concepts . . . 36
2.4.3 Green Function . . . 37

3 Historical Development of SPDEs in American Put Option Pricing 40
3.1 Introduction . . . 40
3.1.1 Foundations of Financial Modeling . . . 41
3.1.2 Emergence of SDEs and Early Probabilistic Methods . . . 42
3.1.3 Numerical Methods for SPDEs in Option Pricing . . . 44

4 Strong Convergence of Euler-Type Methods for Nonlinear Fractional Stochastic Differential Equations without Singular Kernel 46
4.1 Basics for SDEs . . . 46
4.1.1 Introduction . . . 46
4.1.2 Important Properties of ${}_0^C D_t^\alpha$ . . . 49
4.1.3 Motivational background . . . 50
4.1.4 Organization of the chapter . . . 52
4.2 Convergence, Continuity and Uniqueness of the Solution for 4.2 . . . 53
4.3 Strong Convergence of the EM Scheme . . . 71
4.3.1 Derivation of the Scheme . . . 71
4.3.2 Auxiliary Equation and Its Error Estimates . . . 75
4.3.3 Error Estimate of the EM Scheme . . . 80
4.4 Numerical Results and Simulations . . . 82
4.4.1 Strong Convergence of the EM Scheme . . . 83
4.4.2 Performance of the Variable-Order FSDE . . . 87
4.5 Concluding Remarks . . . 87

5 A Front Fixing Crank-Nicolson Finite-Difference for the Solvability of the APO Models 90
5.1 Introduction . . . 90

5.1.1 Transition from FSDEs to APO Pricing . . . 92
5.2 Time-Caputo-fractional equation of APO . . . 93
5.2.1 The APOs Model . . . 93
5.2.2 Derivation of the tfBS-PDE . . . 94
5.3 The Front Fixing Method (FFM) . . . 97
5.3.1 Arbitrage-Free Pricing of APOs . . . 97
5.3.2 Derivation of the Transformed Fractional PDE . . . 99
5.3.3 Crank-Nicolson Finite-Difference Scheme . . . 101
5.3.4 Algorithm . . . 112
5.4 Consistency and Stability . . . 113
5.4.1 Consistency . . . 113
5.4.2 Stability . . . 117
5.5 Numerical Result . . . 118
5.6 Managerial and Policy Implications . . . 127
5.7 Limitations of the Study . . . 128
5.8 Conclusion . . . 129

6 Conclusion and Future Perspectives **130**
6.1 Conclusion . . . 130
6.2 Future work . . . 131
6.2.1 Future work Strong Convergence of Euler-Type Methods for Nonlinear FSDEs without Singular Kernel . . . 131
6.2.2 Future work A Front Fixing Crank-Nicolson Finite-difference for the APOs Model . . . 132
6.3 Recommendations . . . 133
6.3.1 Recommendations Strong Convergence of Euler-Type Methods for Nonlinear FSDEs without Singular Kernel . . . 133
6.3.2 Recommendations A Front Fixing Crank-Nicolson Finite-difference for the APOs Model . . . 134

Bibliography **136**

Abstract

This thesis proposes a unified analytical-numerical framework that addresses two interconnected challenges in modern mathematics:*variable-order fractional stochastic differential equations (FSDEs)* and the *time-fractional Black-Scholes (tfBS)* equation for American put options (APOs).

For APOs, this thesis develops a hybrid methodology that integrates a *front-fixing transformation* with a *Crank-Nicolson finite-difference scheme*, augmented by the *Caputo-Fabrizio fractional derivative* to capture long-range dependence in financial markets. Financial indices such as the *FTSE 100* exhibit persistent autocorrelations with power-law decay, while emerging market indices such as the *Bovespa (Brazil)* display pronounced *long-memory* behavior, motivating the use of *fractional option pricing models*. The proposed approach transforms the free-boundary problem arising from early exercise into a fixed-domain formulation to avoid numerical complexities, enhancing computational stability and efficiency. The resulting numerical scheme is consistent $\mathcal{O}(1) + \mathcal{O}((\Delta y)^2)$, unconditionally stable and second-order convergent in space, while preserving positivity and monotonicity. Numerical experiments on a benchmark problem *($r = 0.1$, $\sigma = 0.2$, $T = 1$, $\alpha = 0.5$)* confirm second-order convergence as the spatial mesh is refined. A direct comparison with the existing first-order scheme [163] demonstrates that the proposed method achieves approximately half the error for the same grid resolution.

We address a class of *non-Lipschitz FSDEs* governed by variable-order fractional operators with non-singular kernels. The absence of a *convolution structure* due to the variable-order fractional calculus necessitates novel analytical techniques. The well-posedness of the solution is established, moment estimates are derived, and a generalised Euler-Maruyama (EM) scheme is constructed. Strong convergence of the proposed method is proved under non-standard regularity conditions, together with explicit mean-square error estimates. The proposed framework reduces to classical stochastic calculus in the limiting regimes *($\alpha \to 0$ and $\alpha \to 1$)*, thereby recovering the well-established convergence rates of SDEs. Numerical experiments demonstrate the robustness, accuracy, and stability of the proposed scheme in the presence of multiplicative noise and dynamic variables of variable order.

Collectively, this study establishes a unified analytical and numerical framework for Caputo-Fabrizio fractional models by integrating fractional stochastic calculus with computational finance. The numerical analysis developed for variable-order FSDEs provides the theoretical foundation for the financial application. In turn, the APO pricing problem demonstrates the practical relevance of fractional calculus (FC) in modelling complex financial systems

with memory effects. This approach bridges general stochastic systems with applications in derivative pricing, risk management, and interdisciplinary applied mathematics, while offering robust and scalable methodologies for the analysis of path-dependent phenomena and high-dimensional stochastic models.

Key Terms
Variable-order Caputo-Fabrizio fractional stochastic Partial differential equation; Non-singular, Euler-Maruyama method, Strong convergence, American put option, front-fixing method, numerical scheme, efficiency-accuracy, consistency and stability of front-fixing, positivity, monotonicity.

Chapter 1

Introduction

1.1 History and Development of Options

Options are a class of derivative securities whose value is contingent upon an underlying asset such as stocks, commodities, currencies or indices. Unlike the direct ownership of financial instruments, derivatives constitute contractual claims whose value is contingent upon the performance of these underlying assets. Specifically, options confer the holder the right but not a precondition, to purchase or sell the underlying asset at a predefined price within a specified time. This structural flexibility option provides powerful instruments for risk hedging and speculative positioning. Options represent a fundamental component of modern financial markets, serving as the basis for instruments such as futures contracts, swaps and forward rate agreements. These instruments enable market participants to develop sophisticated strategies for managing exposure to volatility, interest rate fluctuations and other financial risks, thereby supporting risk mitigation and profit maximization objectives. For a holistic understanding and deeper insight into the subject, readers are referred to Hull's book titled "Options, futures and other derivatives" [99].

Generally, these instruments are classified into call options and put options. Call options confer the holder the right to purchase an underlying asset and put options provide the right to sell an underlying asset, both at a predetermined strike price by a designated expiration date.In addition to the basic distinction between call and put options, options are also classified as American or European, based on the nature of their exercise rights. American option (AO), which represents the predominant form of options traded globally, allow the holder to exercise the contract at any point up to and including the expiration date [34]. This feature provides enhanced flexibility for both hedging and speculative purposes when compared to European options (EOs), which are exclusively exercisable at maturity [30].

Options trading began in Amsterdam in the 17^{th} century, where traders and investors used rudimentary contractual agreements to speculate on shares of the Dutch East India

Company [79]. The first organized over-the-counter (OTC) options market was formalized in the early 20th century with the founding of the Put and Call Brokers and Dealers Association, facilitating the matching of buyers and sellers of equity options [38]. However, this OTC structure introduced several systemic vulnerabilities, including market illiquidity due to the lack of a secondary trading mechanism, counterparty risk stemming from reliance on the solvency of brokers and dealers and elevated transaction costs driven by credit risk premiums. These inefficiencies limited the market's growth potential until significant institutional reforms were implemented in the 1970s.

A pivotal development occurred in 1973 with the establishment of the Chicago Board Options Exchange (CBOE) by the Chicago Board of Trade (CBOT). According to the CBOE [40], listed options contracts are governed by standardized terms, including the underlying asset, strike price, expiration date, contract size (number of shares per contract) and exercise style (American or European). These specifications ensure market-wide consistency, enhance liquidity and support efficient trading execution. During the development of organized options markets, exchanges introduced standardized expiration dates fixed to the last Thursday of each month, with adjustments for public holidays to reduce ambiguity and maintain orderly trading practices. Option sellers (writers) receive a non-refundable premium from buyers in exchange for assuming contractual obligations. As the first dedicated options exchange, the CBOE pioneered the use of standardized contracts.

As demonstrated by MacKenzie and Millo [143], the CBOE's institutional innovations, including the establishment of a centralized clearing house to mitigate counterparty risk and the standardization of contracts to enable liquid secondary trading, were not merely technical solutions but sociotechnical processes. These developments evolved in parallel with the influential role of financial theory, exemplified by the Black-Scholes (BS) model, which reconfigured trader behavior, market practices and the perceived legitimacy of derivatives markets between 1973 and 1987. This structural innovation democratized access to options, reduced transaction costs and catalyzed their transition from niche instruments to mainstream financial tools.

By the late 1970s, major United States of America exchanges includes the CBOE, AMEX and NYSE were engaged in intense competition over the options market, spurring product innovation but also contributing to regulatory fragmentation [143]. Silber [200] in 1983 attributes this rivalry to the rapid expansion of listed puts and calls, despite persistent jurisdictional conflicts. In contrast, the Australian Stock Exchange, which operated as six state-based exchanges until its unification in 1987, focused primarily on domestic equity listings and the gradual implementation of automation [206].

This institutional evolution from fragmented OTC agreements to standardized exchange-traded contracts fundamentally redefined financial markets, positioning options as essential instruments for price discovery and risk management. Financial markets are essential to the

global economy, facilitating capital allocation, investment and risk transfer.

According to Mishkin and Eakins [157], derivatives enhance financial market efficiency by facilitating risk transfer (hedging), price discovery (speculation) and asset value alignment (arbitrage). Within this framework, options stand out due to their asymmetric payoff structures, which cap losses for buyers while allowing for strategic risk exposure and exercise flexibility (American or European). This versatility makes them particularly valuable instruments for institutions managing financial uncertainty.

AOs, particularly APOs, hold critical importance in modern finance. Unlike EOs, APOs allow holders to exercise early, making them vital for hedging against sudden market downturns. This feature introduces a free boundary problem in pricing, where the optimal exercise time depends on dynamic factors such as asset price, volatility and interest rates [46].

As demonstrated by Wilmott [214], this flexibility enables strategic optimization: early exercise may be optimal for deep-in-the-money APOs with significant time remaining, particularly when the interest earned from immediate proceeds outweighs the extrinsic value forfeited by early exercise. The valuation of APOs remains a central challenge in financial mathematics. Early methods, such as the binomial tree model [48] and Least Squares Monte Carlo (LSMC) [137], laid the groundwork for numerical solutions. Recent advances leverage machine learning [191], adaptive sparse grids [142] and quantum computing [228] to address computational bottlenecks.

Despite significant progress, challenges persist in modeling jump-diffusion processes. Makumbe in his PhD thesis [146] addresses this by developing efficient approximation methods for pricing EOs under Jump-Diffusion Stochastic Volatility (JDSV) models, where closed-form solutions are generally intractable. By integrating discontinuous asset price jumps with dynamically evolving volatility, these models capture essential market phenomena such as volatility smiles and abrupt price shocks, yet they introduce substantial computational complexity. The thesis advances analytical techniques-including asymptotic expansions and Fourier-based approaches that facilitate rapid and accurate option valuation without relying on high-dimensional partial integro-differential equations (PIDEs) or Monte Carlo simulations.

The BS model, first introduced by Fischer Black and Myron Scholes in 1973 is a widely accepted framework for option pricing in the same year the CBOE was established [30]. The model quickly gained traction among practitioners, regulators and market participants due to its ability to adapt to various applications, such as speculative trading and risk management. Its simplicity-defining strength stems from its reliance on four observable inputs: the exercise price, the maturity period, the risk-free interest rate and the current price of the underlying asset. The exercise price and time to maturity are explicitly defined in the option contract, while the asset price and interest rate reflect prevailing market conditions. The sole unobservable parameter, asset price volatility, is commonly estimated through historical or implied methods. Historical volatility was the annualized standard deviation of an underlying

asset's returns over a specified time horizon.

However, horizon selection remains contentious: shorter horizons tend to amplify statistical noise, while longer horizons risk obscuring structural shifts in the market [99]. Implied volatility surfaces are typically derived iteratively from options across varying strike prices, with consistent maturity prioritized since it embeds forward-looking expectations and has been shown to outperform historical volatility in forecasting realized volatility [99].

The BS framework underwent significant extensions in subsequent years. Merton [154] expanded the model to accommodate dividend-paying assets, enhancing its applicability to equities. Separately, Cox and Ross [48] introduced the concept of risk-neutral valuation, a paradigm shift that decoupled option pricing from investor risk preferences and laid the foundation for modern derivatives pricing theory.

1.2 AO Valuation Methods

The valuation of APOs remains a central challenge in financial mathematics because they have an early exercise feature. This section synthesizes advancements in the valuation of APOs post 2020, alongside foundational methods, emphasizing mathematical rigor, computational efficiency and practical applicability. Four core methodologies dominate the literature on the valuation of APOs: linear complementarity problem (LCP) formulations, Finite Difference Methods (FDM), Front-Fixing Method (FFM) and Fixed-Point Iteration (FPI) algorithms.

1.2.1 LCP in AO Valuation

The LCP formulation remains a cornerstone in optimization and game theory, with significant applications in financial mathematics and other fields. The utility of the LCP formulation is especially evident in the valuation of AOs, where the early exercise feature yields a free boundary problem. The LCP formulation captures the dual nature of this problem by enforcing that the option value satisfies the BS-PDE in the continuation region while simultaneously adhering to the early exercise condition. This relationship is formalized as:

$$\begin{cases} LV(X,t) \geq 0, \\ V(X,t) \geq \Phi(X), \\ LV(X,t) \cdot (V(X,t) - \Phi(X)) = 0, \end{cases}$$

where $V(X,t)$ is the value of an option, L is the BS differential operator and $\Phi(X)$ denotes the intrinsic value of options [34].

These conditions collectively define a complementarity system, ensuring that either the option follows the PDE (when it is not optimal to exercise) or coincides with its payoff

(when immediate exercise is optimal) but not both. By integrating these constraints into a unified framework, the LCP eliminates the need for explicit free boundary tracking, offering computational advantages over traditional PDE methods. The robustness of variational inequalities (VIs) in modeling AO pricing under early exercise constraints demonstrate by [102]. Their work establishes a rigorous theoretical framework by formulating the problem as a free-boundary parabolic inequality, significantly advancing the analytical treatment of optimal stopping in financial mathematics.

Recent developments have extended the power and efficiency of LCP-based approaches in financial modeling. For instance, Zhang et al.[232] adapted the Projection and Contraction Method (PCM) an iterative technique from VI theory, to solve the LCP associated with pricing AOs on zero-coupon bonds. Their study implements and validates PCM within the Cox-Ingersoll-Ross (CIR) framework, demonstrating its computational efficiency and accuracy as a viable alternative to traditional approaches such as Projected Successive Over-Relaxation (PSOR). Similarly, Deepak et al.[219] introduced an operator splitting technique to efficiently solve the LCP for AOs under the BS model, with theoretical error bounds and stability guarantees. Moreover, Dhiman and Hu [57] propose a Physics-Informed Neural Network (PINN) to solve the BS-PDE for pricing EOs. Their method incorporates the governing PDE, boundary conditions and terminal payoff as soft constraints within the loss function, achieving accuracy comparable to finite difference methods without requiring spatial mesh discretization. The framework is further extended to multi-asset options, although computational costs remain significant. These advances demonstrate the growing versatility and relevance of LCP formulations in modern financial computation.

1.2.2 FDMs and PINN in AO Valuation

FDMs remain a foundational tool in the numerical valuation of AOs, providing robust solutions to the free boundary problems arising from early exercise features. Despite the continued use of traditional schemes like the Crank-Nicolson approach due to their stability and simplicity, recent advancements have significantly improved accuracy and computational efficiency. Persson and Sydow [178] and Christara and Dang [41] introduced high orders compact schemes that achieve accuracy on coarser grids, thereby reducing computational costs without compromising precision. Building upon prior advances, Wang et al. [212] developed deferred correction methods of high order integrated with penalty iteration algorithms, significantly improving the precision in resolving free boundaries within AO pricing models. Adaptive Mesh Refinement (AMR) techniques dynamically allocate grid resolution near the early exercise boundary, effectively balancing numerical accuracy and computational resources.

Additionally, the scientific community was first exposed to PINNs through the ground-

breaking work of Raissi et al. [129], which established a meshless computational framework for PDE. Gatta et al.[78] successfully applied PINNs to the complex, non-local *time-fractional Black-Scholes (tfBS)* equation, marking the first adaptation of this novel technique to financial modeling. Building on this framework, Nuugulu et al.[165] improved the stability and robustness of PINN training for financial applications, thus refining the methodology. Their input helped the method move past its initial proof-of-concept stage and become a dependable and useful computational tool. All together, this development shows how financial PINNs have advanced from initial deployments to optimal performance, representing a major advancement in the use of deep learning in derivative pricing models.

Despite notable progress, extending FDMs to high-dimensional problems remains computationally demanding. Achieving real-time computational performance in non-stationary markets where model parameters are time-varying and information flows are asymmetric remains a persistent methodological and theoretical challenge. Addressing these issues requires further methodological innovations that combine numerical rigor with scalable and adaptive computational frameworks.

1.2.3 Front-Fixing Methods in Free Boundary Problems

FFMs stabilize free boundaries by applying coordinate transformations such as $\xi = X/X^*(t)$ that convert moving domains into fixed computational grids. Heidari and Azari [90] propose a novel FFEM for pricing AOs under RSJD models. To address the challenges posed by early-exercise features, particularly under stochastic regime transitions and asset-price jumps, they apply a Landau transformation to reformulate the moving exercise boundary into a stationary computational domain. This leads to a system of coupled PIDEs, one per regime, which is solved using a fitted finite element scheme. Numerical experiments demonstrate the method's robustness, accuracy and computational efficiency in capturing the complex dynamics of regime shifts, jump processes and early exercise, thereby establishing a reliable framework for option pricing under realistic market conditions.

In contrast, Longstaff and Schwartz [137] introduce the LSMC method, a simulation-based framework for valuing AOs and other early-exercise derivatives. The LSM approach addresses the challenge of estimating continuation values along simulated asset price paths by applying cross-sectional least-squares regression at each exercise date. Functional approximations of the underlying asset price dynamics are utilized to approximate the conditional expected payoff from postponing the exercise of the option. This estimate is then compared to the immediate exercise value through backward induction within a dynamic programming structure. Notably, LSM exhibits exceptional flexibility and computational efficiency, particularly in high-dimensional settings where traditional lattice or partial differential equation (PDE) methods become impractical. Its proven numerical accuracy across diverse asset models

has established LSM as a foundational tool in the simulation-based pricing of early-exercise derivatives.

Complementing these contributions, Company et al. [44] apply a linear front-fixing transformation to the Hull-White model for pricing AOs on zero-coupon bonds. By immobilizing the moving boundary, they transform the free boundary problem into a fixed-domain PDE, which is subsequently solved using an explicit finite difference scheme. Their approach enables the simultaneous computation of option prices and optimal exercise boundaries, achieving both computational efficiency and numerical accuracy. Similarly, Fazio et al. [74] develop an implicit finite difference scheme coupled with a front-fixing transformation within the BS framework. Their method ensures stability and consistency, further enhancing accuracy through Richardson extrapolation and AMR. Collectively, these studies underscore the versatility of FFMs in addressing complex financial models while improving computational performance and numerical precision.

1.2.4 Fixed-Point Iteration Methods

FPI methods provide a robust framework for solving the nonlinear VIs encountered in the valuation of AOs. These methods iteratively enforce consistency between the option value and the free boundary condition, typically by freezing the early exercise region and solving a sequence of linear PDEs until convergence. In recent advancements, adaptive PSOR algorithms with dynamically tuned relaxation parameters have been employed to enforce LCP conditions and accelerate convergence, especially in jump-diffusion models [146].

Complementarily, penalty-based FPI schemes, such as those proposed by Wang and Forsyth [210], improve numerical stability when handling degenerate diffusion terms. Additionally, Gu et al.[82] introduce parallel-in-time iterative schemes that employ policy iteration within an all-at-once formulation of the Hamilton-Jacobi-Bellman equations. This approach facilitates the concurrent resolution of the full temporal domain, thereby improving computational efficiency and accelerating convergence. These innovations enhance the computational tractability of AO pricing models under complex market dynamics. Nevertheless, challenges persist in ensuring convergence near the free boundary and extending FPI methods to path-dependent and rough volatility contexts. These methodological advances significantly improve the computational tractability of AO pricing models within the context of complex market dynamics.

To conclude this section, valuation of APOs remains a central challenge in financial mathematics because of the early exercise feature, which introduces a free boundary problem requiring methods that balance mathematical rigor with computational efficiency. Contemporary research focuses on four principal approaches: LCP formulations, FDMs, FFM and FPI algorithms.

LCP frameworks elegantly encode free boundary dynamics through complementarity conditions, with recent advancements integrating projection-contraction methods, operator splitting and PINNs to enhance accuracy and computational speed. FDMs, while foundational, employ high-order compact schemes and AMR to mitigate grid dependencies and handle rough volatility, though scalability in high-dimensional settings remains a limitation.

FFMs stabilize moving boundaries via coordinate transformations, augmented by GPU acceleration and neural network predictions; however, numerical stability and scalability in complex markets persist as challenges.

FPI algorithms iteratively solve VIs through adaptive relaxation and parallel computing techniques, enhancing convergence rates while continuing to face challenges in path-dependent and rough volatility environments.

Collectively, these approaches underscore the interplay between theoretical precision and practical implementation. Future innovation must address computational demands in high-dimensional, non-stationary markets while ensuring robustness across evolving financial instruments.

1.3 Fractional Calculus

1.3.1 History of Fractional Calculus

Fractional calculus (FC), which extends classical calculus to derivatives and integrals of non-integer order, offers powerful tools for modeling complex, memory-dependent and anomalous phenomena that traditional integer-order calculus cannot adequately capture.

The conceptual origins of FC trace back to the correspondence of Gottfried Wilhelm Leibniz, notably with the Marquis de L'Hôpital's [132]. A pivotal moment appears in a letter from Leibniz to Guillaume de L'Hôpital's, in which he poses the question: "Can there be a half-order derivative?", thereby proposing for the first time the generalization of differentiation to non-integer orders.

This inquiry was further extended in Leibniz's correspondence with John Wallis [132], where he suggested that the established rules for integer-order derivatives of power functions, $\frac{d^n}{dx^n}(x^m)$, could be analytically continued to fractional exponents, an insight that anticipated later developments involving the Gamma function.

Crucially, Leibniz conceptualized the differential operator $\frac{d}{dx}$ as subject to exponentiation, thereby laying the operator-theoretic foundation of FC. Although he acknowledged profound conceptual challenges and described such ideas as "paradoxical" in his letters to Jacob Bernoulli [132], this insight proved catalytic. Thus, while Leibniz did not formalize the theory, he initiated the fundamental question and conceptual framework that would drive centuries of subsequent mathematical development. This foundational idea spurred centuries

of mathematical development, with contributions from eminent figures [71, 186].

The 19$^{\text{th}}$ century represented a crucial era in the conceptual evolution of FC, during which foundational principles were established for its formalization and future applications. Mathematicians such as Joseph Liouville and Bernhard Riemann introduced rigorous definitions of fractional derivatives (FDs) and integrals, laying a solid analytical foundation for the field.

In *Riemann's Collected Works* [186, pp.353-366], Liouville's exponential-based approach to differentiation is acknowledged as foundational to the development of operators of arbitrary order. This method employed formal expressions such as $e^{\alpha \frac{d}{dx}}$ to extend the scope of calculus beyond integer orders, thereby establishing a conceptual framework for generalized differentiation. Building upon such techniques, Riemann developed a comprehensive theory of integral transforms, notably articulated in his seminal paper on hypergeometric functions [186, pp.67-85]. These transforms exemplified through complex contour integral representations for solutions to differential equations, utilize path integration in the complex plane to recast differential problems into algebraic ones. The integrals, defined by their sensitivity to contour paths and singularities (ibid., p.82), exemplify Riemann's innovative synthesis of complex analysis and differential equations, effectively transcending real-variable methods and significantly expanding the theoretical foundations of mathematical physics.

Building upon the theoretical foundations of FC namely, Liouville's exponential operators as documented in Riemann [186, pp.353–366] and Riemann's contour integral transforms (ibid., pp. 67-85) the Grünwald-Letnikov formulation introduced a discrete approximation of fractional operators via a limit-based difference quotient:

$$D^{\alpha} f(x) = \lim_{h \to 0^{+}} h^{-\alpha} \sum_{k=0}^{\left\lfloor \frac{x-a}{h} \right\rfloor} (-1)^{k} \binom{\alpha}{k} f(x - kh).$$

This combinatorial framework, expressed using generalized binomial coefficients $\binom{\alpha}{k}$ [81, p.454], bridged abstract operator theory with computational implementation. By reducing differentiation of arbitrary order to finite function evaluations, Grünwald's approach laid the groundwork for practical numerical algorithms addressed to fractional differential equations (FDEs) [81, pp.460-468], thereby transforming continuous theoretical constructs into programmable procedures essential to modern scientific computing.

The mathematical foundations of FC are intrinsically linked to the Gamma function, which generalizes the factorial function to complex numbers (excluding non-positive integers) and non-integer real values. As rigorously established in the seminal treatise *Fractional Integrals and Derivatives: Theory and Applications* by Samko, Kilbas and Marichev [193], the Gamma function is an indispensable tool in defining and analyzing fractional operators. Its key properties, especially analytic continuation and the functional equation $\Gamma(z+1) = z\Gamma(z)$ enable the extension of classical calculus to arbitrary (including non-integer) orders. This is exemplified in the Riemann-Liouville fractional integral operator:

$$I_{0^+}^{\alpha} f(t) = \frac{1}{\Gamma(\alpha)} \int_0^t (t-\tau)^{\alpha-1} f(\tau)\, d\tau, \quad (\alpha > 0),$$

where $\Gamma(\alpha)$ serves as a crucial normalizing constant that ensures the convergence of the integral and recovers the identity operator in the limit as $\alpha \to 0^+$. This operator extends the classical notion of repeated integration to non-integer orders α, forming a foundational component of fractional analysis [193].

In the 20^{th} century, FDEs emerged as powerful tools for modeling dynamical systems with memory and hereditary properties. FC provides a transformative mathematical framework for modeling complex systems where classical integer-order models fail to capture essential dynamics. As demonstrated by Metzler and Klafter [156], fractional operators inherently describe anomalous diffusion, long-range memory effects and non-local interactions that deviate from standard Brownian motion (BM). This modeling capability is epitomized by the time-fractional diffusion equation:

$$\frac{\partial^{\alpha} u(x,t)}{\partial t^{\alpha}} = D \frac{\partial^2 u(x,t)}{\partial x^2}, \quad 0 < \alpha < 1,$$

which governs subdiffusive transport, where the mean-square displacement scales as $\langle x^2(t) \rangle \sim t^{\alpha}$, a critical advancement for describing transport in heterogeneous media.

The applications of FC span a broad range of disciplines. In rheology, Mainardi [145] employs fractional models to characterize power-law viscoelastic responses, such as $\sigma(t) \sim t^{-\beta}$, in polymers and biological tissues, accurately capturing hereditary behavior unattainable through classical integer order models. In bioengineering, Magin [144] utilizes fractional techniques to quantify anomalous blood flow in arterial networks and intracellular diffusion, accounting for phenomena such as fractal vascular morphology and cytoplasmic crowding.

Collectively, these contributions underscore how non-local fractional operators offer unparalleled fidelity in modeling complex physical and biological systems exhibiting spatiotemporal heterogeneity.

Classical stochastic models in finance often fail to capture two critical empirical features: *long-memory effects*, observed as persistent autocorrelations in asset returns and *non-Markovian behavior*, where asset dynamics depend on the entire historical path rather than just the current state. To address these limitations, Cartea and Del Castillo-Negrete [37] introduced the tfBS equation, incorporating a Caputo FD to embed memory effects:

$$\frac{\partial^{\alpha} C}{\partial t^{\alpha}} = \frac{1}{2}\sigma^2 S^2 \frac{\partial^2 C}{\partial S^2} + rS\frac{\partial C}{\partial S} - rC, \quad 0 < \alpha \leq 1,$$

where the Caputo kernel $(t-\tau)^{-\alpha}/\Gamma(1-\alpha)$ accounts for temporal memory. Although this framework theoretically accommodates phenomena such as volatility clustering, its practical

adoption was hindered by the computational complexity of solving fractional PDEs and challenges in empirical calibration.

Subsequent research shifted focus from temporal memory to *spatial roughness*. Bayer,et.al [25] demonstrated that volatility trajectories characterized by Hurst exponent $H < 0.5$ a property termed rough volatility better replicate market data, particularly the power-law decay of the at-the-money skew, $\mathcal{S}(T) \sim T^{H-1/2}$, in short-dated options. Their model is specified by:

$$dS_t = v_t S_t \, dB_t^H, v_t = \xi_0 \int_0^t (t-s)^{H-\frac{1}{2}} \, dW_s,$$

where B_t^H is a fractional Brownian motion (fBM) with Hurst index H and W_t is a standard BM. This formulation addressed empirical shortcomings of the tfBS model and laid the foundation for modern rough volatility theory.

Further advancements integrated state-dependent jumps.Yuen,et.al [225] develop a trinomial tree method for option pricing under regime-switching models, with dynamics:

$$dS_t = \mu_{Z_t} S_t dt + \sigma_{Z_t} S_t dW_t$$

where Z_t follows a continuous-time Markov chain modulating jump intensity λ_{Z_t} and volatility v_{Z_t}.

This extension addressed the static assumptions of earlier models, improving pricing accuracy for long-dated options during market crises. To address the computational challenges of high-dimensional fractional PIDEs, Han et.al [86] present a deep learning framework for solving high-dimensional financial PDEs:

$$\min_{\theta} \mathbb{E}\left[|\partial_t u_\theta + \mathcal{L} u_\theta|^2\right]$$

demonstrating applications to option pricing.Their neural network approximations enabled real-time calibration of exotic options, significantly outperforming classical finite-difference approaches in terms of speed and adaptability.

Collectively, these advancements highlight the importance of incorporating memory and path-dependence into pricing frameworks while balancing theoretical rigor with practical tractability. Future research may explore applications of fractional and rough volatility models to crypto derivatives, multi-agent markets or high-frequency environments.

FC has emerged as a transformative mathematical framework in control theory, signal processing and electromagnetism. Its defining feature the ability to capture memory and hereditary properties enables the modeling and control of systems beyond the scope of classical integer-order approaches.

In control engineering, fractional-order controllers (FOCs) exhibit superior performance compared to conventional proportional-integral-derivative (PID) controllers. As established

by Podlubny [181], FOCs provide enhanced stability margins, improved robustness and superior disturbance rejection in complex industrial systems. Their non-local dynamics and intrinsic memory effects enable effective handling of time-delayed processes and nonlinear behaviors. The additional tuning parameters afforded by fractional orders prove particularly advantageous in safety-critical domains such as aerospace control and robotics, where traditional PID controllers often prove inadequate.

Within signal processing, the fractional Fourier transform represents a paradigm shift for analyzing non-stationary signals. Ozaktas et al. [171] demonstrate that this generalized transform enables signal representation along arbitrary rotational axes in the time-frequency plane. This flexibility facilitates improved resolution and localization for rapidly evolving or frequency-modulated signals, with applications spanning radar detection of maneuvering targets, biomedical signal analysis (e.g., ECG and EEG) and secure communications systems where conventional Fourier methods provide limited interpretability.

For electromagnetism, Engheta's pioneering research [70] established FC as a transformative framework for modeling wave propagation in complex media. By introducing fractional multipoles, this approach accurately characterizes electromagnetic behavior in metamaterials, plasmonic surfaces and fractal geometries. These models reveal novel physical phenomena including sub-wavelength focusing, frequency selective scattering and energy localization that eludes classical Maxwellian descriptions, enabling advancements in antenna design, stealth technology and characterization of engineered materials with exotic electromagnetic properties.

These advancements highlight how FC can effectively tackle ongoing challenges in system modeling, control and signal analysis across various disciplines. Its ongoing integration across applied domains signifies a fundamental shift toward memory-aware system representations that more accurately reflect physical realities.

FC is fundamentally distinguished by its intrinsic non-locality. Unlike classical derivatives, which depend solely on the instantaneous behavior of a function, FDs incorporate the entire historical trajectory of the system. This non-local property is essential for accurately modeling memory-dependent phenomena such as polymer stress relaxation and contaminant diffusion in porous media [169]. Among the various definitions of FDs, the Caputo formulation has gained prominence due to its superior physical interpretability. It is defined as:

$$D^{\alpha} f(t) = \frac{1}{\Gamma(n-\alpha)} \int_0^t \frac{f^{(n)}(\tau)}{(t-\tau)^{\alpha+1-n}}\, d\tau, \quad (n-1 < \alpha < n),$$

where $\Gamma(\cdot)$ denotes the Gamma function and $f^{(n)}(\tau)$ is the nth-order derivative of f. A key advantage of the Caputo derivative is its compatibility with classical initial conditions, which is critical for physical applications [35]. This operator has proven particularly effective in modeling hereditary behaviors such as material creep and viscoelastic relaxation [17].

Advances in computational techniques during the late 20^{th} and early 21^{st} centuries significantly expanded the scope of FC. Numerical schemes such as the Grünwald-Letnikov [81] discretization and the Adams-Bashforth-Moulton predictor-corrector approach enabled practical solutions to FDEs [59]. Spectral methods, finite element frameworks and matrix-based algorithms further improved computational feasibility across diverse applications.

Recent explorations into fBM have revealed new insights into long-range dependence in finance, biology and network theory [147]. The exponential growth in publications evident in bibliometric data such as that from Scopus attests to the expanding interest in this field [18].

The assimilation of FC with machine learning represents a transformative advancement in computational mathematics Pang et al.[172].PINNs, neural architectures that inherently encode fractional differential operators, have emerged as powerful tools for solving high-dimensional FDEs [172]. Unlike traditional mesh-based methods, PINNs bypass spatial discretization entirely, enabling efficient solutions to complex systems in climate modeling (e.g., anomalous diffusion in atmospheric processes) and biomedical engineering (e.g., viscoelastic tissue modeling) [96, 165].

Even though significant challenges that persist in the application of FC, ongoing research continues to advance its theoretical development and practical relevance.The coexistence of multiple FD definitions, including the Riemann-Liouville, Caputo, Grünwald-Letnikov, Hadamard and others, introduces ambiguity when specifying boundary conditions, complicating the resolution of boundary value problems. Furthermore, the intrinsic non-locality of fractional operators imposes substantial computational burdens due to their dependence on historical states. Current research addresses these challenges through strategies such as fast-convolution algorithms for efficient kernel evaluations, sparse representations leveraging wavelet or multi-resolution bases and unified multiscale frameworks that reconcile local and non-local operators [208].

As theoretical insights converge with practical applications, FC continues to reshape our understanding of time, memory and dynamic change. What began as a speculative notion in Leibniz's correspondence has evolved into a foundational tool across disciplines. Its ability to describe complex, non-local and memory-dependent systems underscores its growing importance in modern science and engineering.

1.3.2 Definitions of FDs

Recent literature primarily defines fractional-order derivatives using several prominent formulations, including the Caputo [134], Riemann-Liouville [221], Jumarie (a modified form of the Riemann-Liouville) [111] and Abu-Shady-Kaabar fractional [2] derivatives, as well as the Atangana-Baleanu (AB) FD with a non-singular kernel [2].

Extensive discussions on these and additional definitions of FDs, along with their respective advantages and limitations, see [14, 36] and the references therein. Additional detailed analyses can be found in [108, 109, 110, 111]. We refer to the works in [108, 109, 110, 134, 221] for formal definitions and methodological developments of specific FDs.

Furthermore, for a robust numerical scheme and a more extensive treatment of FDs, see [9]. Although the list of derivative types presented here is not exhaustive, given the continually evolving nature of the field, it provides a focused overview of several widely used approaches. For a more complete and up-to-date catalog of FDs, including recent citations and further references, we refer readers to the comprehensive review in [9]. To this end, we present the following concept:

DEFINITION 1.3.1. *Caputo FD*

Let $v : \mathbb{R} \to \mathbb{R}$ be a continuous but not necessarily differentiable function. The Caputo FD of order α is defined as follows :

i *New Caputo FD*

$$\frac{\partial^\alpha v}{\partial t^\alpha} = {}_0^c D_t^\alpha v(\tau, y) = \frac{1}{(1-\alpha)} \int_0^t v'(\tau) e^{-\frac{\alpha(t-\tau)}{1-\alpha}} d\tau. \tag{1.1}$$

We remark from the above definition that the presence of the function v' ,classical derivative, which is the derivative of the function v. Note that this already suggests to us that the classical derivative of the function v must exist before we can apply this definition. Most recent remarks on the definitions of FDs are clearly highlighted in the recent manuscript [8].

ii *Caputo FD*

$$\frac{\partial^\alpha v}{\partial t^\alpha} = {}_0^c D_t^\alpha v(\tau, y) = \frac{1}{\Gamma(1-\alpha)} \int_0^t v'(\tau) \frac{1}{(t-\tau)^{\alpha-1}} d\tau$$

$$D_t^\alpha v(t) = \frac{1}{\Gamma(\eta-\alpha)} \int_0^t \frac{d^\eta v(\tau)}{d\tau^\eta} (t-\tau)^{\alpha-\eta+1} \, d\tau, \quad \eta - 1 < \alpha \leq \eta; \quad \eta \in \mathbb{N}. \tag{1.2}$$

A key advantage of the Caputo FD is its ability to incorporate classical initial and boundary conditions into the problem formulation [35].

The Caputo FD is widely favored in applied sciences due to its effectiveness in modeling memory and hereditary properties of materials and processes while maintaining compatibility with classical initial conditions. A key advantage of this formulation is that it permits initial conditions to be specified using integer-order derivatives, aligning naturally with conventional

physical and engineering practices. Initial states such as finance, displacement, velocity or temperature are typically described using classical derivatives in such contexts. Furthermore, the Caputo derivative converges to the classical derivative when the fractional order approaches an integer, ensuring a smooth transition between classical and FC frameworks. These attributes make the Caputo derivative particularly suitable for modeling real-world phenomena, including anomalous diffusion, viscoelasticity and other memory-dependent processes [227, 217].

However, the Caputo derivative also presents certain limitations. Like all FDs, it is inherently nonlocal, meaning that its value at a given point depends on the entire history of the function. This nonlocality increases computational complexity, particularly in large-scale or high-resolution numerical simulations. Additionally, the Caputo definition requires the function to be differentiable in the classical sense before applying the fractional operator, which may restrict its applicability in cases where such regularity is not guaranteed.

Despite certain challenges, the Caputo derivative remains widely utilized in applied disciplines such as physics, engineering and bioengineering, largely due to its interpretable initial conditions and consistency with physical modeling frameworks. Recent works have introduced advanced numerical schemes to mitigate the computational costs associated with the Caputo framework. For instance, Zabidi et al. [227] proposed an Adams-type multistep method, while Nuugulu et al. [164] developed a robust numerical method for tfBS equations, effectively modeling stock exchange dynamics. Their subsequent work, Nuugulu et al. [163] introduced an efficient numerical scheme derived from the fractal market hypothesis, underscoring the expanding role of Caputo-type derivatives in financial mathematics and beyond.

DEFINITION 1.3.2. *Riemann-Liouville FD*

Let $v : \mathbb{R} \to \mathbb{R}$ be a continuous but not necessarily differentiable function. Then, the Riemann-Liouville FD of order α is given by:

$$D_t^{\alpha} v(t) = \frac{1}{\Gamma(\eta - \alpha)} \frac{d^{\eta}}{dt^{\eta}} \int_0^t v(\tau)(t-\tau)^{\alpha-\eta+1}\, d\tau, \quad \eta - 1 < \alpha \leq \eta; \quad \eta \in \mathbb{N}. \tag{1.3}$$

The Riemann-Liouville derivative demonstrates notable limitations in practical modeling of phenomena with FDEs. Specifically, it produces a non-zero derivative for a constant and introduces singularities at the origin when the function remains constant at that point, as observed with exponential and Mittag-Leffler functions. These challenges constrain its applicability. However, Jumarie [109] demonstrated that modifications to the Riemann-Liouville definition can address some of these issues [169, 193].

The Riemann-Liouville FD is a cornerstone of FC, providing a mathematically rigorous generalization of classical differentiation to non-integer orders. Its primary advantages include a solid theoretical foundation grounded in integral transforms, effective modeling of memory-dependent phenomena such as anomalous diffusion and viscoelasticity and compatibility with Laplace transform techniques for solving linear FDEs [141, 95]. However, the Riemann-Liouville derivative also presents notable limitations. It assigns non-zero values to the derivatives of constant functions, except at integer orders, which contradicts classical calculus and complicates physical interpretation. Furthermore, it requires initial conditions expressed in terms of fractional integrals, which often lack clear physical meaning and are difficult to determine empirically [4]. These drawbacks reduce its applicability in engineering and applied sciences, where the Caputo derivative is frequently favored due to its alignment with traditional initial and boundary condition formulations.

DEFINITION 1.3.3. *Jumarie (Modified Riemann-Liouville) Derivative*
Let $v : \mathbb{R} \to \mathbb{R}$ be a continuous, but not necessarily differentiable function. The Jumarie FD of order α is defined as follows:

i If $v(t)$ is a constant K, then its Jumarie FD is given by:

$$D_t^{\alpha} v(t) = \begin{cases} \frac{K}{\Gamma(\eta-\alpha)} t^{-\alpha+1-\eta}, & \alpha \leq \eta - 1, \\ 0, & \alpha > \eta - 1, \end{cases} \tag{1.4}$$

where $\eta \in \mathbb{N}$ and Γ is the Gamma function.

ii If $v(t)$ is not a constant, then its FD is defined by:

$$D_t^{\alpha} v(t) = \frac{1}{\Gamma(\eta-\alpha)} \frac{d^{\eta}}{dt^{\eta}} \int_0^t \frac{v(\tau) - v(0)}{(t-\tau)^{\alpha}} \, d\tau, \quad \eta - 1 < \alpha \leq \eta, \tag{1.5}$$

where $\eta \in \mathbb{N}$.

The Jumarie FD has gained significant attention for its ability to extend FC to non-differentiable functions, which frequently arise in practical modeling contexts. A key advantage of this formulation is its operational simplicity and capacity to handle continuous but non-differentiable functions addressing a limitation of classical FDs. Unlike the standard Riemann-Liouville derivative Jumarie's definition ensures that the FD of a constant yields zero enhances conformity with classical derivative and interpretability in physical applications. This modification also simplifies initial condition specification and mitigates divergence issues associated with the classical Riemann-Louville approach. As a result, the Jumarie derivative has been successfully applied in engineering, physics and finance, particularly for modeling systems with fractal behavior, irregular signals, or stochastic dynamics.

Despite these advantages, the Jumarie derivative has faced critical scrutiny within the mathematical community. A major concern is its comparatively weaker theoretical foundation relative to well-established definitions like the Caputo and Riemann-Liouville derivatives. Critics have questioned its internal consistency and adherence to fundamental calculus theorems such as the chain rule and integration by parts, particularly in generalized settings. Additionally, while it effectively handles non-differentiable functions, the Jumarie framework may oversimplify boundary conditions or yield solutions that deviate from experimentally validated models. Thus, while it provides computational efficiency and practical accessibility, its application requires careful consideration in contexts where strict mathematical rigor is essential.

Recent research continues to explore FDs, including variants inspired by Jumarie's approach. For example, Ayub et al. [15] applied Riemann-Liouville fractional operators to solve generalized kinetic energy equations, highlighting the utility of fractional models in complex physical systems. Similarly, Houas et al. [94] investigated the existence and stability conditions for fractional order pantograph differential equations using Riemann-Liouville and Caputo operators, further demonstrating the versatility of FC in dynamical systems analysis.

DEFINITION 1.3.4. *Grünwald-Letnikov Derivative*

The Grünwald-Letnikov (GL) derivative is a natural extension of the finite difference approach:

$$ {}^{GL}D_t^{\alpha} f(t) = \lim_{h \to 0} \frac{1}{h^{\alpha}} \sum_{k=0}^{\left\lfloor \frac{t}{h} \right\rfloor} (-1)^k \binom{\alpha}{k} f(t - kh), $$

where $\binom{\alpha}{k} = \frac{\Gamma(\alpha+1)}{\Gamma(k+1)\Gamma(\alpha-k+1)}$ is the generalized binomial coefficient.

This definition, introduced by Grünwald-Letnikov in the 19th century, is foundational in FC and suitable for numerical implementations [81, 133]. Independently developed by A.K.Grünwald in 1867 [81] and A.V.Letnikov in 1868 [133], this approach extended earlier concepts proposed by Liouville and Riemann. Their key contribution was the development of a fractional-order differentiation framework grounded in finite differences, now widely recognized as a discrete approximation of FDs. Unlike other definitions that rely on integral transforms, the GL derivative is formulated as the limit of a fractional-order difference quotient, which makes it particularly suitable for numerical computation. This formulation significantly extended the mathematical framework of differentiation to non-integer orders while simultaneously establishing a fundamental connection between continuous and discrete representations in FC.

Due to its simplicity and natural discretization, the GL is widely used in computational applications. Its structure facilitates direct implementation in numerical schemes, particularly in FDMs for solving FDEs. Although mathematically equivalent to the Riemann-

Liouville definition under specific conditions, the GL approach is often preferred in numerical simulations due to its compatibility with grid-based approximations. However, this method requires that the function be sufficiently smooth and demands careful treatment of the domain to avoid divergence. Despite these limitations, the GL derivative remains a cornerstone in the development and computational implementation of FC, significantly influencing theoretical progress and practical engineering applications.

DEFINITION 1.3.5. *Atangana-Baleanu Derivative*
The AB Derivative is FD with a non-singular and non-local kernel based on the Mittag-Leffler function:

$$ {}^{AB}D_t^{\alpha} f(t) = \frac{B(\alpha)}{1-\alpha} \int_0^t f'(\tau) E_{\alpha}\left(-\frac{\alpha}{1-\alpha}(t-\tau)^{\alpha}\right) d\tau, $$

where $E_{\alpha}(\cdot)$ is the Mittag-Leffler function.

This derivative effectively models processes with memory and hereditary properties without singularities [12]. The AB-FD represents a significant advancement in FC, offering a modern alternative to classical definitions through its incorporation of non-locality and non-singular kernel properties. Developed by Atangana and Baleanu [12], this operator employs the Mittag-Leffler function as its kernel, providing notable advantages in modeling memory effects and hereditary behaviors in complex systems. Unlike traditional Riemann-Liouville and Caputo derivatives, which rely on singular power-law kernels, the AB derivative eliminates such singularities while preserving the essential non-local characteristics of fractional operators. This innovation is particularly beneficial for modeling physical phenomena with fading memory, including applications in viscoelastic materials [13], anomalous diffusion processes [160] and control systems [117]. The AB framework has been formulated in both Caputo-type and Riemann-Liouville-type versions [12], offering flexibility in handling initial conditions and boundary value problems while maintaining the core attributes of fractional-order dynamics.

DEFINITION 1.3.6. *Abushady Derivative*
The Abushady FD is defined using a generalization of the Grünwald-Letnikov approach. It is expressed as:

$$ D^{\alpha} f(t) = \lim_{\epsilon \to 0} \frac{1}{\Gamma(\alpha)} \sum_{k=0}^{\infty} (-1)^k \binom{\alpha}{k} f(t - k\epsilon), $$

where ϵ is a small parameter and the generalized binomial coefficient $\binom{\alpha}{k}$ is given by:

$$ \binom{\alpha}{k} = \frac{\Gamma(\alpha+1)}{\Gamma(k+1)\Gamma(\alpha-k+1)}. $$

This definition is particularly used in the study of physical processes with memory effects and it presents an alternative method for understanding FDs [1].

The Abushady FD, first proposed by Abushady et al. [1], constitutes a significant theoretical advancement in FC, specifically developed to address limitations inherent in classical fractional operators when modeling nonlocal and complex dynamical systems. Unlike conventional formulations such as the Riemann-Liouville or Caputo derivatives, it employs an innovative kernel structure that enhances the representation of memory-dependent processes while preserving rigorous physical interpretability. The modified differentiation approach embedded in the Abushady operator offers greater modeling flexibility for anomalous transport phenomena, particularly in characterizing time-dependent diffusion and viscoelastic relaxation dynamics in biological systems.

The derivative's enhanced mathematical properties, particularly its ability to handle variable-order dynamics and time-evolving memory effects, have established it as a valuable tool in contemporary FC research Abushady et al. [1]. This formulation represents a notable contribution to the field, offering both theoretical consistency and practical utility in modeling complex systems across diverse domains, from cellular biomechanics to the design of smart materials.

1.3.3 Organization of the thesis

The dissertation is organized as follows: **Chapter 2** lays the theoretical groundwork, detailing the properties of Stochastic Ordinary Differential Equations (SDEs) and Stochastic Partial Differential Equations (SPDEs). **Chapter 3** focuses on the Historical Development of SPDEs in APO Pricing, where we discuss the historical evolution connecting SPDEs to the theoretical and numerical valuation of APOs. In **Chapter 4**, we had Strong Convergence of Euler-Type Methods for Nonlinear FSDEs without Singular Kernel. **Chapter 5** presents A Front Fixing Crank-Nicolson Finite-Difference for the APOs Model. Finally, **Chapter 6** provides a summary of the contributions and discusses potential avenues for future research.

Chapter 2

Stochastic Ordinary Differential Equations and Stochastic Partial Differential Equations

2.1 Introduction

SDEs are differential equations that consist of at least one term involving a stochastic process (SP). This leads to an inherently stochastic solution. Unlike deterministic differential equations, which have defined initial conditions and deterministic rules that govern the system to determine its solution, SDEs are particularly well-suited for modeling systems subject to uncertainty and noise because they incorporate randomness into ordinary differential equations (ODEs). A SDE is an ODE with a stochastic term and is the most commonly applicable and is typically driven by white noise. It represents a significant class of SPs. Mathematically, such an equation can be expressed as:

$$dX_t = f(X_t, t)dt + g(X_t, t)dW_t$$

where X_t represents the SPs, $f(X_t, t)$, is drift term, $g(X_t, t)$ is the diffusion coefficient governing the intensity of the noise and W_t denotes a Wiener process (BM), which accounts for the stochastic perturbation.

SDEs had a widespread application across many disciplines. In finance, they are essential for modeling the unpredictable dynamics of asset prices, interest rates and volatility, as seen in models like the *BS equation* and *geometric BM* for more detail, we refer [180]. In physics and engineering, SDEs are used to describe systems subject to thermal fluctuations, molecular diffusion and other random perturbations. Similarly, in biology and neuroscience, model population dynamics, genetic drift and neural activity involve SPs. For augmented knowledge and comprehensive understanding of SPs, refer to [138].

Even though solutions of SDEs involve complex methods, they have been used in a wide range of applications across various fields. To address these challenges, specialized numerical techniques such as *Euler-Maruyama (EM) schemes*, *Milstein methods* and *stochastic Runge-Kutta techniques*. These techniques enable efficient simulation of SPs, providing important insights into the dynamics of complex uncertainty systems.Another important class of SPs is SPDEs, which generalize classical PDEs by incorporating randomness into coefficients, forcing terms, or boundary conditions.

This chapter is divided into two thematic sections. The first section SDEs, presents basic concepts under the following subsections: basic notations of probability theory, basic principles of BM and SP formulations. Then exhaustively explored SDEs with emphasis on different solution techniques, especially numerical ones like the EM approximation. The next part deals with SPDEs and introduces key solution concepts and methods, specifically the Green's function and the Q-Wiener process. Together, these two parts yield an entire theoretical and computational framework that is necessary to comprehend stochastic differential systems.

2.2 Lebesgue Spaces

In this subsection develops a foundation through Lebesgue spaces L^p. These spaces play a central role in PDE analysis as they provide these are: a rigorous framework for quantifying randomness in parameters and external forcing [52]; a basis for establishing well-posed weak formulations [72] and the necessary structure for conducting error analysis in numerical approximations [138].

2.2.1 Definitions and Core Properties of Lebesgue Spaces

The theory begins with the Lebesgue spaces, which are fundamental in modern analysis. Let $(\Omega, \mathcal{F}, \mu)$ be a measure space. For $1 \leq p < \infty$, the Lebesgue space is defined as

$$L^p(\Omega) := \left\{ f : \Omega \to \mathbb{R} \text{ measurable } : \|f\|_{L^p} := \left(\int_\Omega |f|^p \, d\mu \right)^{1/p} < \infty \right\}.$$

When $p = \infty$, we define

$$L^\infty(\Omega) := \{ f : \|f\|_{L^\infty} := \inf \{ M \geq 0 : |f| \leq M \ \mu\text{-a.e.} \} < \infty \}.$$

Lebesgue spaces are complete, meaning that $L^p(\Omega)$ forms a Banach space for all $1 \leq p \leq \infty$, a result established by the Riesz–Fischer theorem [190]. In particular, $L^2(\Omega)$ possesses a

Hilbert space structure with the inner product

$$\langle f, g \rangle = \int_\Omega f g \, d\mu,$$

which makes it especially important for applications in SPDEs. Furthermore, the space of smooth, compactly supported functions $C_c^\infty(\Omega)$ is dense in $L^p(\Omega)$ for $1 \leq p < \infty$, ensuring approximation flexibility.There are two cornerstone inequalities that govern analysis in Lebesgue spaces. First,Hölder's inequality states that if $p^{-1} + q^{-1} = 1$, then

$$\|fg\|_{L^1} \leq \|f\|_{L^p} \, \|g\|_{L^q}.$$

Second, Minkowski's inequality ensures that

$$\|f + g\|_{L^p} \leq \|f\|_{L^p} + \|g\|_{L^p}.$$

These inequalities provide essential tools for working with nonlinearities and stability in SPDE analysis [72].

Finally, convergence theorems such as the Dominated Convergence Theorem establish conditions under which convergence almost everywhere implies convergence in L^p.

THEOREM 2.2.1. *Convergence Theorems [33]* ***Dominated Convergence****: If $f_n \to f$ μ-a.e. and $|f_n| \leq g \in L^p$, then*

$$\lim_{n \to \infty} \|f_n - f\|_p = 0.$$

2.2.2 Types of Lebesgue Spaces

Lebesgue spaces form the backbone of modern functional analysis and are essential in the study of PDEs, SPs and various applications in applied mathematics and physics. These spaces provide a rigorous framework to measure the size of functions, quantify randomness in stochastic models and ensure convergence properties necessary for analysis. Depending on the exponent and the structure of the underlying measure space, Lebesgue spaces can take several forms, each with specific analytical advantages.

i. Classical L^p Spaces ($1 \leq p < \infty$) for a measure space $(\Omega, \mathcal{F}, \mu)$, the Lebesgue space $L^p(\Omega)$ is defined as

$$L^p(\Omega) = \Big\{ f : \Omega \to \mathbb{R} \text{ measurable} \;\Big|\; \|f\|_{L^p} := \Big(\int_\Omega |f|^p \, d\mu \Big)^{1/p} < \infty \Big\}.$$

These spaces are Banach spaces with the norm $\|f\|_{L^p}$. In particular, $L^2(\Omega)$ is a Hilbert space with the inner product

$$\langle f, g \rangle = \int_\Omega f g \, d\mu,$$

making it especially useful in applications involving SPDEs and Fourier analysis.

ii. L^∞ Spaces: the space $L^\infty(\Omega)$ consists of essentially bounded functions:

$$L^\infty(\Omega) = \Big\{ f : \Omega \to \mathbb{R} \text{ measurable} \;\Big|\; \|f\|_{L^\infty} := \inf\{M \geq 0 : |f| \leq M \ \mu\text{-a.e.}\} < \infty \Big\}.$$

The norm here measures the essential supremum of the function. While $L^\infty(\Omega)$ is a Banach space, it does not possess a Hilbert space structure.

iii. Weighted L^p Spaces: Weighted Lebesgue spaces incorporate a positive weight function $w(x)$ to emphasize specific regions of the domain:

$$L^p_w(\Omega) = \Big\{ f : \Omega \to \mathbb{R} \;\Big|\; \|f\|_{L^p_w} := \Big(\int_\Omega |f(x)|^p w(x)\, dx \Big)^{1/p} < \infty \Big\}.$$

Weighted spaces are particularly useful in PDEs where solutions exhibit singular behavior near boundaries or other critical regions.

iv. Dual Spaces and Weak Topologies: for $1 < p < \infty$, the dual of $L^p(\Omega)$ is isometrically isomorphic to $L^q(\Omega)$, where $q = \frac{p}{p-1}$. For each $g \in L^q(\Omega)$, the functional

$$\varphi(f) = \int_\Omega f g \, d\mu$$

represents an element of $(L^p(\Omega))^*$ [33].

Weak convergence: a sequence $\{u_n\} \subset L^p(\Omega)$ converges weakly to u if

$$\lim_{n\to\infty} \varphi(u_n) = \varphi(u), \quad \forall\, \varphi \in (L^p)^*.$$

v. Sobolev Spaces and Embeddings: for $k \in \mathbb{N}$ and $1 \leq p < \infty$, the Sobolev space is

$$W^{k,p}(\Omega) = \{ u \in L^p(\Omega) : D^\alpha u \in L^p(\Omega),\ \forall |\alpha| \leq k \},$$

equipped with the norm

$$\|u\|_{W^{k,p}} = \left(\sum_{|\alpha| \leq k} \|D^\alpha u\|^p_{L^p} \right)^{1/p}.$$

In the Hilbert case $p = 2$, one writes $H^k(\Omega) := W^{k,2}(\Omega)$.

Sobolev embedding theorems imply that if $kp > d$, then

$$W^{k,p}(\Omega) \hookrightarrow C_b(\Omega).$$

The Rellich–Kondrachov theorem guarantees compact embeddings on bounded Lipschitz domains [3].

Lebesgue provides the essential analytic foundation for PDE theory. Lebesgue spaces enable duality and weak formulations and Sobolev spaces ensure regularity through embeddings. Together, these underpin existence theory, numerical approximation and uncertainty quantification in PDEs.

2.3 Basic Notations of Probability Theory

Probability theory is the foundational framework for analyzing random phenomena. Think of a straightforward experiment, for example, rolling a die or tossing a coin, where the result is unpredictable in each trial. In these situations, the frequency of outcomes is examined and their likelihood is quantified using statistical and probabilistic methods. The probability of an event is typically defined as the long-run proportion of times the event occurs when an experiment is repeated many times. To formalize these theories, we define probability space, denoted $(\Omega, \mathcal{F}, P)$ [138, p.137]. Here:

i. Ω is the *sample space*, which represents a set of the entire potential outcomes of the experiment.

ii. $\mathcal{F} \subset \Omega$ is a σ-algebra, which defines the collection of measurable events.

iii. P is a probability measure, mapping each event in $\mathcal{F}$ to a corresponding probability value.

Given the measurable space $(\Omega, \mathcal{F})$, the probability measure P satisfies the following fundamental axioms:

i. **Normalization:** the probability assigned to the entire sample space is equal to unity,

$$P(\Omega) = 1. \tag{2.1}$$

ii. **Countable Additivity:**

$$P\left(\bigcup_{i=1}^{\infty} A_i\right) = \sum_{i=1}^{\infty} P(A_i). \tag{2.2}$$

where $A_i \subset \mathcal{F}$ and $A_i \cap A_j = \emptyset$ for $i \neq j$,

A fundamental concept in probability theory is the "random variable", which is a measurable function $X : \Omega \to \mathbb{R}$ that assigns a real number to each outcome in the sample space. If X is integrable under P, its "expectation" (or expected value) is given by [138, p.139]:

$$\mathbb{E}[X] = \int_{\Omega} X(\omega) dP(\omega). \tag{2.3}$$

Another key measure of dispersion in probability theory is the "variance", which quantifies the spread of a random variable around its expectation:

$$\mathrm{Var}(X) = \mathbb{E}[(X - \mathbb{E}[X])^2]. \tag{2.4}$$

These fundamental probability concepts serve as the basis for more advanced topics, including SPs, which play a central role in modeling random dynamical systems.

2.3.1 Basics of Brownian Motion(BM)

The phrase *BM* originates from the empirical observations made by the Scottish botanist *Robert Brown* in 1828, he noted the erratic motion of pollen grains suspended in water [138]. This seemingly random motion was later explained as a consequence of continuous collisions between the microscopic particles and the surrounding molecules of the fluid. The stochastic nature of BM made it an essential topic of study in both physics and mathematics, leading to its rigorous formulation as a SP.
To model this phenomenon mathematically, it is natural to introduce a SP $B_t(\omega)$, representing the place of a pollen grain ω at time t. While BM refers to the exact motion of the pollen grain, its mathematical abstraction is encapsulated by the *Wiener process*, which provides a formal probabilistic framework for describing random fluctuations over time. The Wiener process serves as the foundation for various applications in probability theory, statistical physics, finance and stochastic calculus.

DEFINITION 2.3.1. *Definition of BM: Let $(\Omega, \mathcal{F}, P)$ be a probability space equipped with a filtration $\{\mathcal{F}_t\}_{t\geq 0}$. A standard one-dimensional BM is a real-valued, continuous and $\mathcal{F}_t$-adapted SP $\{B_t\}_{t\geq 0}$ satisfying the features listed below:*

i. Initial Condition: $B_0 = 0$ almost surely (a.s.).

ii. Gaussian Increments:

$$B_t - B_s \sim \mathcal{N}(0, t-s). \tag{2.5}$$

where $s \subset (0, \infty)$, $B_t - B_s$ the increment and normally distributed with mean zero and variance $t - s$

iii. Independent Increments: for any $s \subset (0, \infty)$, $B_t - B_s$ is independent of the filtration $\mathcal{F}_s$, meaning that past information does not influence future increments.

iv. Continuity: sample path of B_t is almost surely continuous, ensuring that BM evolves in a smooth, albeit unpredictable, manner.

These fundamental properties make BM an essential building block in stochastic analysis, serving as the basis for more advanced concepts such as the Itô integral, SDEs and diffusion processes. Beyond its origins in physics, BM has become a cornerstone of modern probability theory and found applications across diverse disciplines. In finance, the BS framework forms the backbone of in option valuation. In physics and chemistry, it underpins diffusion processes and thermodynamic fluctuations. Furthermore, in engineering and signal processing, BM is employed to model noise and uncertainty in dynamical systems. The profound impact of BM across disciplines highlights its fundamental role in the study of random phenomena.

2.3.2 Basics of Stochastic Process (SPs)

It is a mathematical framework for modeling systems that undergo temporal evolution over time under the influence of randomness. Let $(\Omega, \mathcal{F}, P)$ be a probability space. A SP is defined as a family of random variables indexed by time

$$X = \{X_t : t \in T\},$$

where each X_t is a random variable and T is the index set that defines how long the process evolves. SPs can be categorized based on whether the index set T is discrete or continuous:

DEFINITION 2.3.2. ***Discrete-Time SP:*** *A SP $X = \{X_n : n = 0, 1, 2, \dots\}$ is said to be a discrete-time process if it consists of a countable sequence of random variables indexed by $\mathbb{N} \cup \{0\}$.*

DEFINITION 2.3.3. ***Continuous-Time SP:*** *A SP $X = \{X_t : 0 \leq t < \infty\}$ is referred to as a continuous-time process if it consists of an uncountable collection of random variables indexed by $[0, \infty)$.*

SPs serve as fundamental tools in various scientific and engineering disciplines. In finance, it models asset prices, interest rates and market fluctuations. In physics, it describes BM, diffusion processes and thermodynamic systems. Moreover, in engineering and control theory, it supports analyzing signals, noise and dynamic systems under uncertainty.
A clear understanding, providing a critical assessment and analyzing the differences between discrete and continuous SPs is crucial for selecting appropriate mathematical models and analytical techniques. Probability theory, measure theory and functional analysis are the hub of SPs and underpin advanced subjects like stochastic ordinary differential equations and stochastic optimization.

2.3.3 Q-Wiener Process

Let $(\Omega, \mathcal{F}, \mathbb{P})$ be a filtered $\mathcal{F}_t$-adapted probability space. An H-valued SP $\{W(t) : t \geq 0\}$ is defined as follows [138, p.436]

DEFINITION 2.3.4. *Q-Wiener Process An H-valued SP $\{W(t) : t \geq 0\}$ is a* ***Q-Wiener process*** *if:*

i. $W(0) = 0$, $\mathbb{P}$-*a.s.*,

ii. $W(t)$ *is a continuous function* $\mathbb{R}^+ \to H$ *for each* $\omega \in \Omega$,

iii. $W(t)$ *is* $\mathcal{F}_t$*-adapted and* $W(t) - W(s)$ *is independent of* $\mathcal{F}_s$ *for* $s < t$,

iv. $W(t) - W(s) \sim \mathcal{N}(0, (t-s)Q)$ *for all* $0 \leq s \leq t$, *where* $Q : H \to H$ *is a positive definite bounded operator.*

2.3.4 Probabilistic Lebesgue Spaces

In this subsection, establish the functional analytic foundations required for SPDE theory by introducing Lebesgue spaces (L^p) and their Banach-space-valued extensions, known as Bochner spaces, with a particular emphasis on probabilistic settings. These spaces enable the quantification of randomness in system parameters and forcing terms [52], facilitate the formulation of well-posed weak solutions [72] and support rigorous numerical error analysis [138].

i. Probabilistic Lebesgue Spaces
Probabilistic Lebesgue spaces extend classical L^p spaces to stochastic settings. Let $(\Omega, \mathcal{F}, P)$ denote a probability space. For $1 \leq p < \infty$, the space $L^p_P(\Omega)$ is defined as

$$L^p_P(\Omega) := \Big\{ X : \Omega \to \mathbb{R} \text{ measurable} \;\Big|\; \|X\|_{L^p_P} := \big(E[|X|^p]\big)^{1/p} < \infty \Big\}.$$

For $p = \infty$, $L^\infty_P(\Omega)$ consists of essentially bounded random variables:

$$L^\infty_P(\Omega) := \Big\{ X : \|X\|_{L^\infty_P} := \inf\{M \geq 0 : |X| \leq M \text{ a.s.}\} < \infty \Big\}.$$

These spaces possess fundamental properties that are crucial in SPDE analysis. A norm hierarchy exists such that for $1 \leq p < q \leq \infty$,

$$L^q_P(\Omega) \subset L^p_P(\Omega), \quad \|X\|_{L^p_P} \leq \|X\|_{L^q_P}.$$

Duality also holds: for $1 < p < \infty$, $(L^p_P(\Omega))^* \simeq L^q_P(\Omega)$, where $q = \frac{p}{p-1}$. Moreover, the expectation operator $E : L^1_P(\Omega) \to \mathbb{R}$ is continuous and linear. Convergence results such as the Vitali convergence theorem and Fatou's lemma establish rigorous conditions under which convergence in probability implies convergence in $L^p_P(\Omega)$ [112].

ii. Sobolev Spaces with Probabilistic Norms

To capture spatial regularity in stochastic systems, Sobolev spaces are extended to random fields. Let $D \subset \mathbb{R}^d$ be a bounded domain and $u : \Omega \to W^{k,p}(D)$ a random field. The probabilistic Sobolev space $L^p_P(\Omega; W^{k,p}(D))$ is defined as

$$\|u\|_{L^p_P(\Omega; W^{k,p})} := \big(E[\|u(\cdot,\omega)\|^p_{W^{k,p}}]\big)^{1/p} < \infty.$$

Regularity embeddings guarantee that for $kp > d$,

$$L^p_P(\Omega; W^{k,p}(D)) \hookrightarrow L^p_P(\Omega; C_b(D)),$$

ensuring that SPDE solutions admit continuous modifications, which is critical for both theoretical and computational analyses [3, 52].

iii. Bochner Spaces as Probabilistic Extensions

Bochner spaces provide a natural framework for vector-valued or Banach-space-valued SPs. Given a Banach space X and probability space $(\Omega, \mathcal{F}, P)$, the Bochner space $L_P^p(\Omega; X)$ is defined as

$$L_P^p(\Omega; X) := \Big\{ u : \Omega \to X \text{ strongly measurable} \;\Big|\; E[\|u\|_X^p] < \infty \Big\}.$$

These spaces allow the rigorous treatment of SPDEs in functional settings and are compatible with integral identities such as the Fubini-Tonelli theorem for random fields, facilitating interchange of spatial and probabilistic integrals [33].

Bochner and probabilistic Lebesgue spaces enable moment estimation and adaptive discretization. For $u \in L_P^p(\Omega; X)$, the empirical estimator

$$\hat{m} = \frac{1}{N} \sum_{i=1}^{N} u^{(i)}$$

satisfies

$$(E[\|E[u] - \hat{m}\|_X^p])^{1/p} \leq N^{-1/2} \sigma(u),$$

providing bounds on stochastic error. Quasi-optimal mesh refinement ensures

$$\inf_{v_h \in V_h} \|u - v_h\|_{L_P^p(\Omega; H^1(D))} \leq C h^{\gamma},$$

guaranteeing computational efficiency in high-dimensional or complex SPDE models.

Lebesgue and Bochner spaces provide the essential analytic foundation for SPDE theory. Lebesgue spaces enable duality and weak formulations, Sobolev spaces ensure regularity through embeddings and Bochner spaces handle SPs in infinite-dimensional settings. Together, these underpin existence theory, numerical approximation and uncertainty quantification in SPDEs.

2.3.5 Stochastic Ordinary Differential Equations(SDEs)

SDEs generalize classical ODEs by incorporating random perturbations, enabling the modeling of systems influenced by uncertainty. As per Øksendal [168] SDEs incorporate intrinsic SPs in phenomena that occur in financial markets, engineering systems and biological processes, in contrast to deterministic ODEs.

A SDE is typically expressed as:

$$dX_t = f(X_t, t)\, dt + g(X_t, t)\, dW_t,$$

where $f(X_t, t)$ represents the deterministic drift, $g(X_t, t)$ governs the stochastic diffusion and W_t is a BM and X_t denotes the state variable,. The stochastic term $g(X_t, t)\, dW_t$ introduces randomness, rendering solutions stochastic rather than deterministic.

Itô and Stratonovich calculus are used to infer SDEs. Itô formula, prevalent in mathematical finance, employs non-anticipative integrals, precluding dependence on future noise increments [122]. On the other hand, the Stratonovich calculus, often preferred in physics and engineering, preserves the classical chain rule, simplifying the modeling of systems with smooth noise.

Solutions of SDEs are often analytically intractable, requiring robust numerical methods. Among the most widely implemented techniques are the EM method, which provides a straightforward approximation for simulating SPs (ibid.) and the Milstein method, a higher-order approach that improves accuracy by adding corrections based on derivatives of the diffusion term. These methods address key computational challenges, particularly those related to stability and efficiency and form the foundation for practical simulations of SDEs in various applied contexts.

SDEs are applicable across a diverse array of disciplines, including finance, biology and engineering. In finance, the BS model, a pioneering and highly influential model that incorporates SPs, describes the price dynamics of an asset under conditions of market uncertainty [198]. In engineering, SDEs are employed to design robust control systems that are resilient to stochastic disturbances, particularly in high-precision fields such as aerospace and robotics [114].

Mathematically, SDEs rely on advanced probabilistic concepts such as filtrations, martingales and stopping times. Existence and uniqueness of solutions typically require Lipschitz continuity and linear growth conditions of drift and diffusion functions, as formalized by [168] and extended in computational contexts [138].

Advancements in computational power have further expanded SDE applications into fields such as machine learning, where uncertainty quantification is critical, to augment existing knowledge on the application SDE in machine learning refer [148]. These domains leverage stochastic frameworks to balance deterministic predictions with real-world unpredictability. We now consider the following *SDE* [138]:

$$du = f(u(t))dt + G(u(t))dW(t), \quad t \geq 0, \tag{2.6}$$

with the initial condition:

$$u(0) = u_0. \tag{2.7}$$

Equation (2.6) has also integral representation as:

$$u(t) = u_0 + \int_0^t f(u(s))ds + \int_0^t G(u(s))dW(s), \tag{2.8}$$

where $G : \mathbb{R}^d \to \mathbb{R}^{d\times m}$ is the *diffusion function* and $f : \mathbb{R}^d \to \mathbb{R}^d$ represents the *drift function*. The term $W(t) = [W_1(t), W_2(t), \ldots, W_m(t)] \in \mathbb{R}^m$ denotes an $\mathbb{R}^m$-valued BM on a filtered probability space $(\Omega, \mathcal{F}, \{\mathcal{F}_t\}_{t\geq 0}, \mathbb{P})$. The integral $\int_0^t G(u(s))dW(s)$ is interpreted as an Itô integral;

ASSUMPTION 2.3.1. *Assumptions on the Coefficients [[138], p. 325] Let $d \in \mathbb{Z}^+$ and assume $\exists L > 0$ which is constant the following conditions hold*
Linear Growth Condition:

$$\|f(u)\|^2_{\mathbb{R}^d} \leq L(1 + \|u\|^2_{\mathbb{R}^d}), \quad \forall u \in \mathbb{R}^d, \tag{2.9}$$

$$\|G(u)\|^2_{\mathbb{R}^{d\times m}} \leq L(1 + \|u\|^2_{\mathbb{R}^d}), \quad \forall u \in \mathbb{R}^d. \tag{2.10}$$

Global Lipschitz Condition:

$$\|f(u_1) - f(u_2)\|_{\mathbb{R}^d} \leq L\|u_1 - u_2\|_{\mathbb{R}^d}, \quad \forall u_1, u_2 \in \mathbb{R}^d, \tag{2.11}$$

$$\|G(u_1) - G(u_2)\|_{\mathbb{R}^{d\times m}} \leq L\|u_1 - u_2\|_{\mathbb{R}^d}, \quad \forall u_1, u_2 \in \mathbb{R}^d. \tag{2.12}$$

Throughout this thesis, we use the notation $\|\cdot\|_{\mathbb{R}^d}$ to denote the Euclidean norm in $\mathbb{R}^d$.

DEFINITION 2.3.5 ([149])**.** *A real-valued SP $g = \{g(t)\}_{a\leq t\leq b}$ is called a simple process if there exists a partition $a = t_0 < t_1 < \cdots < t_k = b$ of the interval $[a, b]$ and bounded random variables ξ_i, for $0 \leq i \leq k-1$, such that ξ_i is $\mathcal{F}_{t_i}$-measurable and:*

$$g(t) = \begin{cases} \xi_0, & t_0 \leq t < t_1, \\ \xi_1, & t_1 \leq t < t_2, \\ \vdots & \\ \xi_{k-1}, & t_{k-1} \leq t \leq t_k. \end{cases} \tag{2.13}$$

We denote the family of all such simple processes by $M_0([a, b], \mathbb{R})$.

For a simple process $g \in M_0([a, b], \mathbb{R})$, we define the Itô integral of g under the BM $\{W_t\}$ as:

$$\int_a^b g(t)dW_t = \sum_{i=0}^{k-1} \xi_i(W_{t_{i+1}} - W_{t_i}). \tag{2.14}$$

LEMMA 2.3.1 ([149])**.** *If $g \in M_0([a, b], \mathbb{R})$, then:*

$$\mathbb{E}\left[\int_a^b g(t)dW_t\right] = 0, \tag{2.15}$$

$$\mathbb{E}\left[\left(\int_a^b g(t)dW_t\right)^2\right] = \mathbb{E}\left[\int_a^b |g(t)|^2 dt\right]. \tag{2.16}$$

DEFINITION 2.3.6 ([149]). *Let $M_2([a,b],\mathbb{R})$ denote the space of all real-valued, measurable and $\mathcal{F}_t$-adapted SPs $f=\{f(t)\}_{a\le t\le b}$ such that:*

$$\|f\|_{a:b}^2=\mathbb{E}\left[\int_a^b |f(t)|^2dt\right]<\infty. \tag{2.17}$$

DEFINITION 2.3.7. *Let $(\Omega,\mathcal{F},\{\mathcal{F}_t\}_{t\ge0},\mathbb{P})$ be a filtered probability space. Define H_T^2 as the set of all $\mathbb{R}^d$-valued predictable processes $\{u(t)\}_{t\in[0,T]}$ such that:*

$$\|u\|_{H_T^2}:=\sup_{t\in[0,T]}\|u(t)\|_{L^2(\Omega,\mathbb{R}^d)}=\sup_{t\in[0,T]}\mathbb{E}\left[\|u(t)\|_{\mathbb{R}^d}^2\right]^{\frac{1}{2}}<\infty. \tag{2.18}$$

THEOREM 2.3.1. *Contraction Mapping Theorem, [[138], p. 2] Let Y be a non-empty closed subset of the Banach space $(X,\|\cdot\|)$. Consider a mapping $J:Y\to Y$ such that there exists a constant $\mu\in(0,1)$ satisfying:*

$$\|Ju-Jv\|\le\mu\|u-v\|,\quad \forall u,v\in Y. \tag{2.19}$$

Then there exists a unique fixed point $u\in Y$ such that $Ju=u$.

THEOREM 2.3.2. *Existence and Uniqueness of SDEs [138, P 325] Suppose that Assumption 2.3.1 holds and that $W(t)$ is an $\mathcal{F}_t$-BM on $(\Omega,\mathcal{F},\{\mathcal{F}_t\}_{t\ge0},\mathbb{P})$.*

For each $T>0$ and $u_0\in\mathbb{R}^d$, there exists a unique $u\in H_T^2$ such that for all $t\in[0,T]$, u satisfies the stochastic differential equation:

$$du=f(u(t))dt+G(u(t))dW(t). \tag{2.20}$$

2.3.6 Numerical Methods for SDEs

This section addresses numerical methods for solving SDEs using the EM method. The theoretical foundations were first developed and formalized by Leonhard Euler and Gisiro Maruyama [138], who are honored by the method's name. In the context of Itô calculus, the EM method provides an approximate numerical solution of SDEs. Euler method of ODEs can be naturally extended to solve the stochastic setting.

2.3.6.1 Euler-Maruyama Approximation

The EM method is a widely used numerical scheme for approximating solutions to SDEs. As a stochastic extension of the classical Euler method, it incorporates BM terms, making it indispensable for SDEs where analytical solutions are rarely tractable [122, 138, 114, 235].

The method approximates the evolution of a SP by discretizing time and updating the solution repeatedly using the SDE's drift and diffusion terms. Its simplicity, computational efficiency and extensive applicability make it a popular choice.

Despite its practical utility, it exhibits certain limitations. Specifically, it may fail to converge when applied to SDEs with non-globally Lipschitz continuous coefficients and may display instability in stiff regimes. In light of these challenges, several modified variants have been proposed, including implicit schemes and adaptive step-size control [235]. Still, the method remains foundational in stochastic numerical analysis and serves as a benchmark for advanced techniques.

Applications span finance, biology and engineering, particularly in modeling systems subject to random perturbations, underscoring its theoretical and practical significance [114]. Consider the SDE of the form:

$$du(t) = f(u(t))dt + G(u(t))dW(t), \quad 0 \le t \le T, \quad \text{given} \quad u(0) = u_0. \tag{2.21}$$

Here, $W(t)$ is a standard BM. We can rewrite the above equation as:

$$\frac{du(t)}{dt} = f(u(t)) + G(u(t))\frac{dW(t)}{dt}, \quad 0 \le t \le T. \tag{2.22}$$

Let $0 = t_0 \le t_1 \le \cdots \le t_N = T$ be a partition of $[0, T]$ with step size Δt. At $t = t_n$, for $n \in [0, N-1]$, we approximate:

$$\frac{du(t)}{dt}\Big|_{t=t_n} \approx \frac{u(t_{n+1}) - u(t_n)}{\Delta t} + O(\Delta t). \tag{2.23}$$

Using the approximations:

$$f(u(t))\Big|_{t=t_n} \approx f(u(t_n)), \tag{2.24}$$

$$G(u(t))\Big|_{t=t_n} \approx G(u(t_n)), \tag{2.25}$$

$$\frac{dW(t)}{dt}\Big|_{t=t_n} \approx \frac{W(t_{n+1}) - W(t_n)}{\Delta t}, \tag{2.26}$$

Now it's time to introduce the EM method:

$$U_{n+1} = U_n + f(U_n)\Delta t + G(U_n)\Delta W_n, \quad n \in [0, N-1], \tag{2.27}$$

where

$$\Delta W_n = W_{n+1} - W_n \approx \sqrt{\Delta t}\mathcal{N}(0, 1).$$

Here, $\mathcal{N}(0, 1)$ represents a standard Gaussian random variable.

To analyze the strong error estimate, we define the continuous approximation $\bar{U}(t)$ as:

$$\bar{U}(t) = U_n + (t - t_n)f(U_n) + G(U_n)(W(t) - W(t_n)), \quad t \in [t_n, t_{n+1}]. \tag{2.28}$$

Clearly, $\bar{U}(t)$ satisfies:

$$\bar{U}(t_n) = U_n, \quad \bar{U}(t_{n+1}) = U_{n+1}. \tag{2.29}$$

which is continuous on $[0, T]$. Additionally, we define the piecewise constant function:

$$U(t) = \begin{cases} U_0, & t \in [t_0, t_1), \\ U_1, & t \in [t_1, t_2), \\ \vdots & \\ U_{N-1}, & t \in [t_{N-1}, t_N]. \end{cases} \tag{2.30}$$

The integral representation of the above equation:

$$\bar{U}(t) = U_0 + \int_0^t f(U(s))ds + \int_0^t G(U(s))dW(s), \quad 0 \le t \le T. \tag{2.31}$$

For specific cases:

$$\bar{U}(t_1) = U_0 + \int_0^{t_1} f(U(s))ds + \int_0^{t_1} G(U(s))dW(s) \tag{2.32}$$

$$= U_0 + f(U_0)(t_1 - t_0) + \int_0^{t_1} G(U_0)dW(s). \tag{2.33}$$

Similarly, at t_2:

$$\bar{U}(t_2) = U_0 + \int_0^{t_2} f(U(s))ds + \int_0^{t_2} G(U(s))dW(s) \tag{2.34}$$

$$= U_1 + f(U_1)(t_2 - t_1) + \int_{t_1}^{t_2} G(U_1)dW(s). \tag{2.35}$$

For $t \in (t_n, t_{n+1}]$, we obtain:

$$\bar{U}(t) = U_0 + \int_0^t f(U(s))ds + \int_0^t G(U(s))dW(s) \tag{2.36}$$

$$= U_n + \int_{t_n}^t f(U(s))ds + \int_{t_n}^t G(U(s))dW(s). \tag{2.37}$$

We can now state a strong convergence error estimate for the Euler method.

THEOREM 2.3.3. *Strong Error Estimate [138] Let $u(t)$ be the solution to (2.6) and $\bar{U}(t)$ the solution of the EM approximation. Then, we have:*

$$\mathbb{E} \sup_{0 \le t \le T} \|\bar{U}(t) - u(t)\|^2_{\mathbb{R}^d} = O(\Delta t). \tag{2.38}$$

LEMMA 2.3.2. *Boundedness of the Solution [138] Let $u(t)$ be the solution of (2.6). Then, we have:*

$$\mathbb{E}\|u(t)\|^2 \le C, \quad \forall t \in [0, T]$$
$$\mathbb{E} \sup \|u(t)\|^2 \le C. \tag{2.39}$$

for some constant $C > 0$.

Next, we investigate the boundedness of the solution to equation (2.22).

LEMMA 2.3.3. *Let $\bar{U}(t)$ be the solution of (2.22). Then, $\exists C > 0$ which constant:*

$$\mathbb{E}\|\bar{U}(t)\|^2 \leq C, \quad \forall t \in [0, T]. \tag{2.40}$$

DEFINITION 2.3.8. *Hölder and Lipschitz [138]*
Let $(X, ||.||_X)$ and $(Y, ||.||_Y)$ for which are Banach spaces. A function $u : X \to Y$ is Hölder continuous with constant $\gamma \in (0, 1]$ if there is a constant $L > 0$ such that $\mathbb{E}\sup||u(x_1) - u(x_2)||_Y \leq L||x_1 - x_2||_X^{\gamma}, \forall x_1, x_2 \in X$ If the above holds with $\gamma = 1$, then u is Lipschitz continuous or global Lipschitz continuous to stress that L is uniform for $x_1, x_2 \in X$.

DEFINITION 2.3.9. *Young's Inequality Assume that p and q are real numbers with $p > 1$ and $q > 1$,*
$\frac{1}{p} + \frac{1}{q} = 1$ then $ab \leq \frac{a^p}{p} + \frac{b^q}{q}$ for all $a, b > 0$. Equality holds if and only if $a^p = b^q$.

DEFINITION 2.3.10. *Euclidean norm*
The Euclidean norm(simply norm) $|x|$ function on a coordinate space $\mathbb{R}^n$ is the square root of the sum of the squares of the coordinates of x.
$|x| = \sqrt{{x_1}^2 + {x_2}^2 + \ldots\ldots + {x_n}^2}$

DEFINITION 2.3.11. *Progressively Measurable*
A SP $\mathbf{X}$ defined on a filtered probability space $(\Omega, \mathcal{F}, (\mathcal{F}_t)_{t\geq 0}, P)$is progressively measurable with respect to$(\mathcal{F}_t)_{t\geq 0}$, if the function $\mathbf{X}(s, \omega) : [0, t] \times \Omega \to \mathbb{R}$ is $\mathbf{B}([0, t] \times \mathcal{F}_t)$measurable for every $t \geq 0$.

DEFINITION 2.3.12. *Adapted*
A SP $\mathbf{X}$ on $(\Omega, \mathcal{F}, (\mathcal{F}_t)_{t\geq 0}, P)$ is adapted to the filtration $(\mathcal{F}_t)_{t\geq 0}$ or $\mathcal{F}_t$-adapted if $\mathbf{X}(t) \in \mathcal{F}_t$ for each $t \geq 0$.

DEFINITION 2.3.13. *Mittag-Leffler function*

(i) A one-parameter function of the Mittag-Leffler function type is defined by [182]

$$E_{\alpha}(z) = \sum_{n=0}^{\infty} \frac{z^n}{\Gamma(\alpha n + 1)} \tag{2.41}$$

(ii) A two-parameter function of Mittag-Leffler function type is defined by [182]

$$E_{\alpha,\beta}(z) = \sum_{n=0}^{\infty} \frac{z^n}{\Gamma(\alpha n + \beta)} \tag{2.42}$$

LEMMA 2.3.4. *The Burkhölder-Davis-Gundy inequality [130, 222]*
If Y is a continuous martingale on $[0,T]$, there exists a positive constant $\bar{Q}_1 = \bar{Q}_1(p)$ for $p \in [1,\infty)$ such that:

$$\mathbb{E}[\sup_{x\in[0,t]} |Y(x)|^p] \leq \bar{Q}_1 \mathbb{E}[|Y(t)|^p], 0 \leq t \leq T. \tag{2.43}$$

LEMMA 2.3.5. *Generalized Gronwall inequality [222]*
Let $f(t)$ be a locally integrable non-negative and non-decreasing function on $(a,b]$ and σ be a non-negative constant. Suppose $g(t)$ is a non-negative locally integrable function on $(a,b]$ with

$$\begin{aligned} g(t) \leq & f(t) + \sigma \int_a^t \frac{g(s)}{(t-s)^{1-\beta}} ds, \forall t \in (a,b], 0 < \beta < 1, \\ & \textit{then} \\ & g(t) \leq f(t) E_\beta[\sigma\Gamma(\beta)(t-a)^\beta], \forall t \in (a,b] \end{aligned} \tag{2.44}$$

LEMMA 2.3.6. *A Generalized discrete Gronwall's inequality [222]*
Suppose that a non-negative sequence $\{z_n\}_{n=1}^N$ and non-decreasing sequence $\{y_n\}_{n=1}^N$ satisfy the following relation

$$z_n \leq y_n + \frac{Q}{N^{\alpha^*}} \sum_{l=0}^{n-1} \frac{z_l}{(n-l)^{1-\alpha^*}}, 1 \leq n \leq N, 0 < \alpha^* < 1 \text{ and } Q > 0 \tag{2.45}$$

Then the sequence $\{z_n\}_{n=1}^N$ can be bounded from above by

$$z_n \leq y_n(1 + E_{\alpha^*}[Q\Gamma(\alpha^*)]), 1 \leq n \leq N \tag{2.46}$$

LEMMA 2.3.7. *Jensen's inequality [222]*

If $a_i, p \in \mathbb{R}$ with $p \geq 1$ and $m \in \mathbb{N}^+$ then

$$|\sum_{i=1}^m a_i|^p \leq m^{p-1} \sum_{i=1}^m |a_i|^p \tag{2.47}$$

2.4 Stochastic Partial Differential Equations (SPDEs)

2.4.1 Introduction

While SDEs are restricted to model temporal dynamics, SPDEs capture both spatial dependencies and temporal dynamics, enabling them to model more complex systems. This key difference highlights SPDEs' increased adaptability in describing phenomena where spatial

structure is important. SPDEs are suitable for modeling phenomena exhibiting both spatial and temporal dependencies, such as financial markets and chemical reaction kinetics.

SPDEs require spatially correlated noise, which is frequently modeled using cylindrical Wiener processes or spatially colored noise, as opposed to SDEs, which are usually driven by finite-dimensional Wiener processes. Significant analytical and computational difficulties arise from this intrinsic structural difference in SPDEs, particularly in terms of well-posedness, solution regularity and numerical approximation.

SPDEs generalize PDEs by incorporating randomness through coefficients, forcing terms, or boundary conditions. This framework, rooted in Itô's seminal work on stochastic calculus [101], has become essential for modeling systems that are subject to random fluctuations, such as neural activity [187] and climate dynamics [124].

The methods, modeling frameworks and numerical solution techniques underlying functional analysis, probability theory and PDE theory are combined in the study of SPDEs. Early contributions of [202, 174] laid the foundation for infinite-dimensional stochastic analysis. The class of solvable SPDEs has since been extended by contemporary developments like regularity structures and rough paths.

SPDEs bridge deterministic PDE theory with stochastic analysis, offering a robust framework for modeling systems with inherent randomness. From foundational results and existing literature, we can define SPDE.

Let $(\Omega, \mathcal{F}, \{\mathcal{F}_t\}_{t\geq 0}, \mathbb{P})$: filtered probability space satisfying the standard assumptions and let H be a separable Hilbert space (e.g., $L^2(D)$ for $D \subset \mathbb{R}^d$). Consider the abstract SPDE:

$$du(t) + Au(t)\,dt = f(u(t))\,dt + G(u(t))\,dW(t), \quad u(0) = u_0 \in H, \tag{2.48}$$

where:

i. $A\colon D(A) \subset H \to H$ is a densely defined, self-adjoint, elliptic operator (e.g., $A = -\Delta$ with $D(A) = H_0^1(D) \cap H^2(D)$).

ii. $W(t)$ is an H-valued Q-Wiener process with trace-class covariance Q.

iii. $f\colon H \to H$ and $G\colon H \to \mathcal{L}_2(H)$ (Hilbert-Schmidt operators) are Lipschitz continuous.

2.4.2 Solution Concepts

DEFINITION 2.4.1. *Strong Solution* *A predictable H-valued process $u(t)\colon t \in [0,T]$ is a* ***strong solution*** *of (2.48) if it satisfies:*

$$u(t) = u_0 + \int_0^t [-Au(s) + f(u(s))]\,ds + \int_0^t G(u(s))\,dW(s), \quad \forall t \in [0,T]. \tag{2.49}$$

DEFINITION 2.4.2. *Weak Solution* *A predictable H-valued process $u(t)\colon t \in [0,T]$ is a* ***weak solution*** *if for all $v \in D(A)$:*

$$\langle u(t), v\rangle = \langle u_0, v\rangle + \int_0^t \left[-\langle u(s), Av\rangle + \langle f(u(s)), v\rangle\right] ds + \int_0^t \langle G(u(s))\, dW(s), v\rangle. \tag{2.50}$$

DEFINITION 2.4.3. *Mild Solution* *A predictable H-valued process $u(t)\colon t \in [0,T]$ is a* ***mild solution*** *if:*

$$u(t) = e^{-tA}u_0 + \int_0^t e^{-(t-s)A} f(u(s))\, ds + \int_0^t e^{-(t-s)A} G(u(s))\, dW(s), \tag{2.51}$$

where e^{-tA} is the analytic semigroup generated by $-A$.

THEOREM 2.4.1. *Existence and Uniqueness [138, p. 450] Under the Lipschitz conditions on f and G, (2.48) admits a unique mild solution $u \in L^2(\Omega; C([0,T]; H))$.*

Finite element methods for SPDEs [139] and deep learning approaches [21] have emerged as powerful computational tools. For example, the exponential Euler scheme approximates (2.48) via:

$$u_{n+1} = e^{-A\Delta t}u_n + \Delta t e^{-A\Delta t} f(u_n) + e^{-A\Delta t} G(u_n)\Delta W_n. \tag{2.52}$$

2.4.3 Green Function

The unique solution of a PDE can be written using the Green's function. Consider:

$$u_t - u_{xx} = f, \quad 0 < x < 1, \tag{2.53}$$

with boundary conditions $u(0) = u(1) = 0$ and initial condition $u(0) = u_0$.

Let $\{e_j\}_{j=1}^{\infty}$ be the eigenfunctions of $A = -\frac{\partial^2}{\partial x^2}$ with $D(A) = H_0^1(0,1) \cap H^2(0,1)$.

LEMMA 2.4.1. *Let $f = 0$ and assume:*

$$u(0,x) = u_0 = \sum_{j=1}^{\infty} (u_0, e_j) e_j. \tag{2.54}$$

Then the solution of (2.53):

$$u(t,x) = \sum_{j=1}^{\infty} (u_0, e_j) e^{-\lambda_j t} e_j(x) = \int_0^1 G(t,x,y) u_0(y) dy, \tag{2.55}$$

where the Green's function is:

$$G(t,x,y) = \sum_{j=1}^{\infty} e^{-\lambda_j t} e_j(x) e_j(y). \tag{2.56}$$

ASSUMPTION 2.4.1. *Growth and Lipschitz Conditions [138] There exists $L > 0$ such that:*

$$\|f(u)\|_H^2 \leq L(1 + \|u\|_H^2), \tag{2.57}$$
$$\|G(u)\|_{L_2^0}^2 \leq L(1 + \|u\|_H^2), \tag{2.58}$$

and Lipschitz conditions:

$$\|f(u_1) - f(u_2)\|_H \leq L\|u_1 - u_2\|_H, \tag{2.59}$$
$$\|G(u_1) - G(u_2)\|_{L_2^0} \leq L\|u_1 - u_2\|_H, \tag{2.60}$$

where $L_2^0 = HS(Q^{1/2}H; H)$ with norm $\|\cdot\|_{HS}$.

ASSUMPTION 2.4.2. *Trace class operator [138, p.436] Let $Q \in \mathcal{L}(H)$ be a non-negative definite and symmetric bounded operator. Furthermore, assume:*

i. Q has an orthonormal basis $\{e_j : j \in \mathbb{N}\}$ of eigenfunctions

ii. Corresponding eigenvalues $q_j \geq 0$ satisfy $\sum_{j\in\mathbb{N}} q_j < 1$ (i.e., Q is of trace class)

THEOREM 2.4.2. *Q-Wiener process representation [138, p.437] Let Q satisfy Assumption 2.4.2. Then $W(t)$ is a Q-Wiener process if and only if*

$$W(t) = \sum_{j=1}^{\infty} \sqrt{q_j} e_j \beta_j(t) \quad \mathbb{P}\text{-a.s.}, \tag{2.61}$$

where $\{\beta_j(t)\}$ are independent $\mathcal{F}_t$-adapted BMs. Moreover:

i. The series of $\left(\sqrt{q_j}\, e_j\, \beta_j(t)\right)_{j=1}^{\infty}$ converges in $L^2(\Omega; H)$

ii. For any $T > 0$, the convergence holds in $L^2(\Omega; C([0, T]; H))$

DEFINITION 2.4.4. *Fractional Power of Operator A [138, p.187] Let (λ_j, e_j) be the eigenpairs of A. For $\alpha \in \mathbb{R}$, the fractional power A^α is defined by:*

$$A^\alpha u := \sum_{j=1}^{\infty} \lambda_j^\alpha u_j e_j \quad \text{for } u = \sum_{j=1}^{\infty} u_j e_j,\ u_j \in \mathbb{R}. \tag{2.62}$$

The domain $D(A^\alpha)$ is given by:

$$D(A^\alpha) = \left\{ u \in H : \|A^\alpha u\|_{L^2}^2 = \sum_{j=1}^{\infty} (A^\alpha u, e_j)^2 = \sum_{j=1}^{\infty} \lambda_j^{2\alpha} u_j^2 < \infty \right\}. \tag{2.63}$$

THEOREM 2.4.3. *Stochastic Integral and Itô Isometry [138, p.445] Let Q satisfy Assumption (2.4.2) and let $\{\Phi(s) : s \in [0,T]\}$ be an L_2^0-valued predictable process satisfying:*

$$\int_0^T \mathbb{E}\left[\|\Phi(s)\|_{L_2^0}^2\right] ds < \infty. \tag{2.64}$$

For $t \in [0,T]$, the stochastic integral is well-defined by:

$$\int_0^t \Phi(s) dW(s) := \sum_{j=1}^{\infty} \int_0^t \Phi(s)\sqrt{q_j} e_j d\beta_j(s), \tag{2.65}$$

where $W(s) = \sum_{j=1}^{\infty} \sqrt{q_j} e_j \beta_j(s)$.

The Itô isometry holds:

$$\mathbb{E}\left\| \int_0^t \Phi(s) dW(s) \right\|^2 = \int_0^t \mathbb{E}\,\|\Phi(s)\|_{L_2^0}^2 \, ds. \tag{2.66}$$

Moreover, $\left\{ \int_0^t \Phi(s) dW(s) : t \in [0,T] \right\}$ is an H-valued predictable process.

ASSUMPTION 2.4.3. *Lipschitz Condition on G For constants $\zeta \in (0,2]$ and $L > 0$, the operator $G : H \to L_2^0$ satisfies:*

$$\|A^{\zeta - \frac{1}{2}} G(u)\|_{L_2^0} \leq L(1 + \|u\|_H), \tag{2.67}$$

$$\|A^{\zeta - \frac{1}{2}} (G(u_1) - G(u_2))\|_{L_2^0} \leq L\|u_1 - u_2\|_H \quad \forall u, u_1, u_2 \in H. \tag{2.68}$$

THEOREM 2.4.4. *Existence and Uniqueness Assume:*

i. $f : H \to H$ satisfies (2.4.1)

ii. $G : H \to L_2^0$ satisfies (2.4.3)

iii. Initial data $u_0 \in L^2(\Omega, \mathcal{F}_0, \mathbb{P}; H)$

Then for any $T > 0$, $\exists u(t)$ which is a unique mild solution on $[0,T]$ to (2.48) satisfying:

$$\sup_{t \in [0,T]} \|u(t)\|_{L^2(\Omega;H)} \leq C_T(1 + \|u_0\|_{L^2(\Omega;H)}). \tag{2.69}$$

LEMMA 2.4.2. *Regularity in Time Under the assumptions of (2.4.4), if $u_0 \in L^2(\Omega, \mathcal{F}_0, \mathbb{P}; D(A))$, then for $T > 0$, $\epsilon \in (0, \xi)$:*

i. For $\theta_1 := \min(2\xi - \epsilon, 1/2)$, $\exists C > 0$:

$$\|u(t_2) - u(t_1)\|_{L^2(\Omega;H)} \leq C(t_2 - t_1)^{\theta_1}, \quad 0 \leq t_1 \leq t_2 \leq T \tag{2.70}$$

ii. For $\xi \in [1,2]$ and $\theta_2 := 2\xi - \epsilon$, $\exists C > 0$:

$$\|u(t_2) - u(t_1)\|_{L^2(\Omega;H)} \leq C(t_2 - t_1)^{\theta_2} \tag{2.71}$$

Chapter 3

Historical Development of SPDEs in American Put Option Pricing

3.1 Introduction

In this section, we examined the historical evolution connecting SPDEs to the theoretical and numerical valuation of APOs. It shows how option pricing changed from early deterministic PDEs to probabilistic representations and stochastic numerical techniques. It covers fundamental concepts, the BS revolution, free boundary formulations, the introduction of stochastic analysis, the rise of SPDEs and contemporary deep learning techniques. Recent developments have established new directions for future research by demonstrating the interdisciplinary fusion of computational finance, PDE theory, and stochastic analysis.

The connection between SPDEs and financial mathematics, focusing on AO valuation, demonstrates a sophisticated and profound development in modern applied mathematics. Deterministic PDEs have been the main method used to formulate the valuation of derivative securities since the foundational study by Black and Scholes in 1973 [30]. These models often oversimplify the inherent stochastic nature of financial markets. A more precise and adaptable framework was made available by the incorporation of stochastic methods and eventually SPDEs as mathematical finance developed, particularly for intricate derivatives like AOs.

The free boundary and early exercise before the maturity of the APO complicate the valuation process in the PDE framework. To overcome these obstacles, researchers have increasingly employed stochastic methods over time. This study connects developments in PDE theory, stochastic calculus and computational finance to trace the historical path from fundamental ideas to current research.

As the need to model ever-more complex market dynamics grows, it has been reflected in the shift from deterministic PDEs to SPDEs. The BS model and other conventional PDE

frameworks are based on restrictive assumptions, such as constant volatility, continuous asset paths and frictionless markets but ignore empirical phenomena like volatility clustering, jumps and liquidity constraints. SPDEs, directly integrating randomness into the governing equations, overcome these drawbacks and make it possible to model path-dependent characteristics and time-varying uncertainty, which are crucial for pricing APO and associated derivatives.

Fundamentally, the incorporation of SPs, such as fBM, Lévy noise, or BM with differential operators, into the formulation of PDE leads to the development of SPDEs. For example, volatility changes as a SP linked to the asset price in models such as the one Heston suggested. These models offer a more comprehensive framework for representing the intricacies of financial markets and inherently encode mutual dependencies between state variables.

This chapter comprises three thematically interconnected sections. It begins with Foundations of Financial Modeling, which establishes the theoretical foundations and mathematical frameworks central to modern finance. The second section, Emergence of SDEs and Early Probabilistic Developments, examines the historical evolution and conceptual basis of stochastic modeling within financial contexts. The third section, Numerical Methods for SPDEs in Option Pricing, presents computational strategies for solving SPDEs in the valuation of options.

3.1.1 Foundations of Financial Modeling

According to Bachelier [16], pioneering work, the first financial models involving uncertainty were crude and mostly focused on discrete random walks. However, the contemporary framework of SPs did not start to have a more significant impact on financial mathematics until the middle of the 20^{th} century. The BS model which assumes the price of the underlying security moves in a geometric BM, transformed the field by introducing a continuous-time framework for option pricing. The BS-PDE for an EO is given by

$$\frac{\partial V}{\partial t} + \frac{1}{2}\sigma^2 S^2 \frac{\partial^2 V}{\partial S^2} + rS\frac{\partial V}{\partial S} - rV = 0,$$

where σ is volatility , r is risk-free interest rate , S is asset price and V is the option price.

The derivation of this model was based on Itô's lemma [93] but the pricing equation that resulted was deterministic. In certain situations, the application of PDEs made analytical solutions possible, but it left open issues about how to value more complicated derivatives.

The Black-Scholes-Merton model (1973) represented a seminal contribution to derivatives pricing by providing an explicit solution for EOs. For a stock characterized by the absence of dividend payments, the BS-PDE governs the option value V and is accompanied the payoff condition at maturity $V(S,T) = \max(K - S, 0)$ in the case of a put option. The model is elegant but it is predicated on various constraining assumptions. It ignores significant market

phenomena like volatility clustering and transaction costs, presumes constant volatility and ongoing hedging. Moreover, it is inapplicable to AOs because it does not support early exercise features.

Two concurrent theoretical developments resulted from the failure to price APOs. Free boundary formulations were the foundation of one method. Itô's and McKean's pioneering book, Diffusion Processes and Their Sample Paths [100], first published in 1965 and heavily revised and reprinted in 1996, changed the way we study SPs and set the stage for modern diffusion theory. According to [100] reinterpretation of the valuation problem as a free boundary problem, the optimal exercise boundary $S^*(t)$ must meet smooth-pasting conditions, specifically $V(S^*(t), t) = K - S^*(t)$ and $\frac{\partial V}{\partial S}(S^*(t), t) = -1$. At the same time, VI was used in another field of study.

In their innovative book Impulse Control and Quasi-VIs [28] defined the VI that governs option pricing as a stochastic control problem:

$$\begin{cases} \dfrac{\partial V}{\partial t} + \mathcal{L}V \leq 0 & \text{(continuation inequality)} \\ V(t,S) \geq \Phi(S) & \text{(early exercise constraint)} \\ [V(t,S) - \Phi(S)] \cdot \left(\dfrac{\partial V}{\partial t} + \mathcal{L}V \right) = 0 & \text{(complementarity condition)} \\ \min\left(-\frac{\partial V}{\partial t} - \mathcal{L}V,\, V - (K - S) \right) = 0 \end{cases}$$

with $\mathcal{L}$ denoting the BS operator and $V(S,t)$ is the option price.

3.1.2 Emergence of SDEs and Early Probabilistic Methods

During the 1980s, there was growing recognition that SDEs provided a natural framework for financial modeling. McKean's work on the probabilistic interpretation of PDEs [153] offered theoretical support for Monte Carlo methods. For AOs, the valuation problem was linked to stochastic control theory through the formulation of optimal stopping problems [115]. However, it was still challenging to identify the associated free boundary in a purely probabilistic setting. Pardoux and Peng [175] introduced backward SDEs, which made a direct link between nonlinear PDEs and SPs. Early applications demonstrated their potential for option pricing, but more work was needed to integrate backward SDEs into APO valuation.

In parallel, Krylov, Rozovskii and others made significant contributions to the development of SPDE theory in the late 1980s and early 1990s [189]. By adding random noise to deterministic PDEs, SPDEs allowed for a dynamic description of changing random fields. Later on, the APO problem was reformulated as an obstacle problem for an SPDE [66], in which the payoff function constrains the solution. Advanced stochastic analysis tools, including reflected backward SDEs and stochastic VIs, were made easier to use by this reformulation. Moreover, existence and uniqueness results for fully nonlinear SPDEs with

obstacles were obtained by adapting viscosity solution techniques to the stochastic setting [49].

Stochastic volatility models emerged to fix problems with the BS model that were found. One of these problems was that it couldn't capture the volatility smile and skew seen in option markets. The Heston model, introduced by Steven and Heston [91], achieves a significant advancement by modeling volatility as a mean-reverting square-root process. As described by the systems:

$$dS_t = rS_t\,dt + \sqrt{v_t}\,S_t\,dW_t^S,$$
$$dv_t = \kappa(\theta - v_t)\,dt + \xi\sqrt{v_t}\,dW_t^v,$$

where S_t is the asset price, v_t the instantaneous variance, κ the speed of mean reversion, θ the long-term variance mean, ξ the volatility of volatility and dW_t^S, dW_t^v correlated BMs with $\mathbb{E}[dW_t^S dW_t^v] = \rho\,dt$.

For APOs, the price $V(S, v, t)$ satisfies a nonlinear SPDE due to the early exercise constraint $V(S, v, t) \geq \max(K - S, 0)$. Applying Feynman–Kac theorem, the Heston SPDE in the continuation region $S > S^*(v, t)$ is:

$$\frac{\partial V}{\partial t} + \frac{1}{2}vS^2\frac{\partial^2 V}{\partial S^2} + \rho\xi vS\frac{\partial^2 V}{\partial S\partial v} + \frac{1}{2}\xi^2 v\frac{\partial^2 V}{\partial v^2} + rS\frac{\partial V}{\partial S} + \kappa(\theta - v)\frac{\partial V}{\partial v} - rV = 0,$$

with boundary conditions:

i. $V(S, v, T) = \max(K - S, 0)$:terminal condition,

ii. $V(S^*(v, t), v, t) = K - S^*(v, t)$:value matching at the free boundary,

iii. $\frac{\partial V}{\partial S}(S^*(v, t), v, t) = -1$: smooth pasting.

Where $S^*(v, t)$, the free boundary depends on both stochastic volatility v and time t.

There are a lot of numerical problems that come up, like the cross-derivative term $\frac{\partial^2 V}{\partial S\partial v}$, which makes finite difference schemes often require implicit-explicit or alternating direction implicit(ADI) methods. It takes care to deal with the degeneracy at $v = 0$; Feller's condition $2\kappa\theta > \xi^2$ ensures $v_t > 0$. Penalty methods or operator splitting techniques are frequently employed to address the free boundary problem encountered in early exercise. The Heston model is effective in capturing volatility smiles. The correlation parameter $\rho < 0$ and volatility ξ respectively.That explains skewness, especially in equity markets and volatility shapes the smile curvature, respectively. Still, calibration remains challenging because the model has many parameters.

Merton [155] came up with a pioneering jump-diffusion model for option pricing. This framework combines Poisson-driven jumps with geometric BM to accurately model sudden

changes in asset prices. In this model, Merton developed a PIDE and a series solution for the price of EOs. Jump-diffusion models can handle discontinuous price paths because they include random jump components. Merton was the first person to use compound Poisson processes to model jumps. Later extensions have used more general Lévy processes to model more comprehensive jump behaviors. For an exponential Lévy model $S_t = S_0 e^{(r-q)t+L_t}$, where L_t Lévy process characterized by a (μ, σ, ν), the generator $\mathcal{A}$ acting on $V(S,t)$ is:

$$\mathcal{A}V = \mu S \frac{\partial V}{\partial S} + \frac{1}{2}\sigma^2 S^2 \frac{\partial^2 V}{\partial S^2} + \int_{\mathbb{R}} \left[V(Se^z, t) - V(S,t) - S(e^z - 1)\frac{\partial V}{\partial S} \right] \nu(dz).$$

The corresponding SPDE for APOs is:

$$\min\left(-\frac{\partial V}{\partial t} - \mathcal{A}V + rV, V - \max(K - S, 0) \right) = 0.$$

A non-local integral term is a key challenge in solving problems in jump-diffusion SPDEs, for which Fourier methods or adaptive quadrature make it simple. Early exercise boundaries originated from jump-adapted grids and infinite activity models require series truncations, which are also another challenge.

3.1.3 Numerical Methods for SPDEs in Option Pricing

FDM and FEM are foundational for solving SPDEs but face complications from free boundaries, mixed derivatives and non-local integral terms. FDMs discretize the SPDE on a structured grid in (S, v, t)-space. For the Heston model, the mixed derivative term arising from correlation ρ poses numerical instability if treated explicitly. Modern strategies include ADI schemes, which decompose the operator $\mathcal{L}$ into parts along S, v and the cross-term (S, v) and non-uniform grids, which use transformations such as $x = \ln(S/K)$ and $y = \sqrt{v}$ to cluster grid points near critical regions.

Penalty methods enforce the early exercise constraint $V \geq \max(K - S, 0)$ by modifying the PDE:

$$\frac{\partial V}{\partial t} + \mathcal{L}V = \lambda \max(K - S - V, 0),$$

where $\lambda \gg 1$ is a penalty parameter updated dynamically using a Newton-Raphson iteration scheme.

Achdou and Pironneau [226] discuss advanced numerical methods for solving high-dimensional PDEs in option pricing in their book, Computational Methods for Option Pricing, which specifically concentrates on the Heston stochastic volatility model. They use ADI schemes to break down multi-dimensional problems into a series of one-dimensional subproblems. That makes their method much more efficient. To get second-order accuracy when $\Delta t \sim \Delta S^2 + \Delta v^2$

and to make sure that the numbers stay stable, especially in high correlation regimes, they combine high-order finite element discretization with implicit time stepping and special stabilization methods, following the time-step limits set by the spatial mesh. They employ a penalty method, along with adaptive domain decomposition, to monitor the free boundary for APOs. This integration of ADI schemes with finite element methods yields a robust and scalable framework for pricing complex derivatives under stochastic volatility.

FEMs approximate the solution by representing $V(S, v, t)$ as a weighted sum of spatial basis functions. Wavelet Galerkin methods build on this by combining the Galerkin approach's variational structure with wavelets' ability to adapt to different resolutions. Because wavelet bases are sparse and hierarchical, these methods are efficient at solving problems with localized features such as steep gradients or singularities [159]. Wavelet discretization, on the other hand, supports automatic mesh refinement while keeping numerical stability. This is not the case with traditional finite element or spectral methods. Despite the method's stability, challenges still exist regarding the handling of boundary conditions and the representation of operators. In the context of jump models, wavelet Galerkin methods give sparse representations. When used with adaptive quadrature, enable targeted integration in regions where the jump measure is most significant. For further foundational insights, [54, 42, 29, 53] are some of the most important sources.

Monte Carlo simulation, regression-based techniques and machine learning are now key methods for pricing APO, especially in high-dimensional or path-dependent situations. A significant advancement was the LSMC methodology put forward [137]. Using backward induction, the method estimates continuation values by applying least-squares regression to polynomial basis functions (e.g., $\{1, v_t, S_t v_t, v_t^2\}$. It allows for efficient handling of early exercise boundaries while keeping computations manageable. Later research has expanded the LSMC framework to accommodate more complex market dynamics, including rough volatility models. For example, Bayer et al. in [26] proposed a hybrid LSMC approach that integrates fBm paths with a Hurst parameter H, successfully capturing volatility roughness. These advancements, such as flexibility, have led to the enduring significance of Monte Carlo methods in quantitative finance. However, there are computational trade-offs that continue to be a thematic area in research.

Machine learning methods, such as PINNs, solve high-dimensional SPDEs by minimizing a loss functional enforcing both dynamics and payoff conditions. Transformers have proven effective for path-dependent options, capturing long-range dependencies through self-attention mechanisms. Deep hedging frameworks [27] aim to minimize expected hedging errors directly. Despite these advancements, certain challenges remain in the field. Machine learning models require extensive simulations to be properly trained.

Chapter 4

Strong Convergence of Euler-Type Methods for Nonlinear Fractional Stochastic Differential Equations without Singular Kernel

4.1 Basics for SDEs

4.1.1 Introduction

A *SDE* Mathematical models of natural and physical phenomena have always played a central and critical role in science since the times of Newton and Euler. The FDs have been crucial in applied mathematics and mathematical sciences since the time of Leibniz. Note that the foundation of FDs was pioneered by Liouville. These fractional systems are often of evolutionary type, time-dependent, linear or nonlinear cases and within their range of important applications, we find aircraft simulation, fractional Newtonian fluids, flow through porous media, weather prediction, image restoration and image processing, inverse image processing, just to name a few. Among others, these fractional systems can be used to describe behaviors of most fascinating and challenging issues in the mathematical community. Despite much progress, it is still open and often quiet challenging to obtain regular and global solutions to the fractional Navier-Stokes and hydrodynamics models of turbulence for just the case of a deterministic setting. For the fractional stochastic counterparts, it is even harder in certain cases, for example, the existence of invariant measure in any dimension. Over the last few decades SFPDEs have been investigated by several authors and many results have been obtained on its theory and also applied to various real-world phenomena. We refer for example to [58, 92, 119, 209]. The analysis of systems with Caputo derivative of variable

order without singular kernel presents a cutting-edge and mathematical framework for modeling complex systems influenced by both randomness and non local interactions. Instead of approaches to calculus, these equations make use of the adaptable nature of variable order Caputo derivatives, which adjust to varying conditions and capture subtle memory effects. By incorporating stochastic terms to accommodate randomness in system dynamics often represented by Wiener or Gaussian processes, SFPDEs with variable order Caputo derivatives provide a tool for analyzing intricate phenomena across various fields such as some branches of physics (nematic liquid crystal), mechanics (stochastic electro-rheological fluids) and climate, atmospheric, ocean dynamics (shallow water systems), turbulent flow in gas pipelines and porous media problems.

The application of the Caputo derivative with variable order goes beyond standard PDEs allowing for the exploration of anomalous diffusion, non local interactions and spatio-temporal correlations in diverse systems. The lack of kernels in the variable order Caputo derivative improves stability and enables efficient computational methods for solving SFPDEs. This progress creates opportunities to study emerging behaviors, multi-fractal patterns and complex dynamics in disciplines such as physics, biology, finance and engineering, just to name a few.

Nowadays, notable works from several researchers delve into the characteristics and uses of variable order Caputo derivatives in calculus. These investigations offer perspectives on the underpinnings and real world significance of utilizing variable order Caputo derivatives to model and analyze intricate systems influenced by SFPDEs. In this direction, several authors extended many results in order to incorporate the definition of the Caputo derivative to model useful problems and also complex phenomena either through the temporal variable or via a spacial component or as space-time FDs. For instance, we refer to more recently manuscript in this direction, see [113] and the references therein for attenuation of the Caputo-Djrbashian fractional time derivative in modeling some inverse problems for wave equations. For the solution of stochastic evolution equation using the Marchaud FD we refer to the work in and the book of Zhou et al.[236] and more recent results in this direction can be obtained in [63] and [7, 80, 87, 238, 22] and the references therein. For the exact solution using the conformable derivative, we refer to the papers [80] and Abu-Shady and Mohammed in [1, 152, 158] and further extension can be found in the references [88, 89, 177, 201]. For the Wick-type FD we refer for instance the manuscript [121]. For fractional PDEs and their numerical solutions we refer *e.g.*, to the work [84, 205] where further references can also obtained. For the random attractor in the fractional sense see for example the manuscript [199]. For the FDs in the sense of Jumarie's modified Riemann-Liouvile type we refer the reader to [83] where further references are given therein. Most recent results concerning the various extensions of the Riemann-Liouville FDs can be found in the work of Jacky and Anna in [51].

SPs in many fields and applications can be described by classical SDE of the form

$$du = f(u(t))dt + b(u(t))dW. \tag{4.1}$$

Many SPs arising in finance, physics, biology and engineering can be modeled by the system presented in (4.1), which is commonly formulated as an Itô SDE driven by a Wiener process. Classical examples include geometric BM, which forms the foundation of the BS option-pricing model; the Ornstein-Uhlenbeck process, which is widely used to model mean-reverting phenomena; and the Cox-Ingersoll-Ross process, which preserves non-negativity while exhibiting mean-reverting behavior. More generally, SDEs of the form given in (4.1) provide a flexible and mathematically rigorous framework for describing stochastic dynamics in continuous-time systems. Their solutions are typically interpreted in the Itô sense, thereby enabling the application of fundamental tools from stochastic calculus, including Itô's lemma and martingale methods. Consequently, such equations constitute the foundation for the development of more advanced stochastic models, including jump-diffusion processes, rough volatility models, path-dependent systems and high-dimensional stochastic frameworks.

There are SPs can not be described (modeled) by the system given in (4.1), for instance, a particle in the viscoelastic medium has random movement, BM, with its resistance of a memory effect that leads to FSDE, see [123, 222, 68, 69, 67, 176] for more details. Despite knowing that multiple time-scale processes are not easy to model by using FSDE, however, we can emphasize the modeling of the accuracy of numerical approximation of non-physical initial weak singularity problems through FSDE; see, for instance, [192, 205] where further references can be found therein. Henceforth, it is clearly challenging to obtain probabilistic strong solutions for SFPDEs. Therefore, various numerical approximations of the solutions to both the deterministic FPDEs and SFPDEs have been proposed to deal with the issues of strong convergence and error estimates based on the EM approximating techniques. See, for instance, the examples of a range of numerical approximations in the recent results in [6, 60, 61, 62, 97, 136, 135, 176, 218, 229, 224]. For the convergence of relative entropy for the EM approximation, we refer to the most recent work of Yu in [224] and further exposition can be found in the work [24, 5].

For the first time, Zhiwei et al. [222] analyzed, discretized and obtained a solution of a two-time-scale variable-order time-FSDE using the Riemann-Liouville fractional differential operator with the non-Lipschitz weakly singular kernel. Similarly, Hong et al. [211] obtained the solution of the variable-order time-fractional diffusion equations and a variable-order FSDE of two-time scales with a Riemann-Liouville fractional differential operator presented by Xiangcheng et al.[234]. More detailed exposition about the Caputo derivatives can be found in [36] in this direction. For more engineering applications we refer to [55]. On the other hand, for the solvability of time-fractional diffusion equation of constant order we refer to Martin [205]. However, all the above papers dealt with the numerical approximations of

FSPDEs with kernels. Therefore, the asymptotic and ergodic environment of the type of probabilistic solutions in this work have not yet been studied in the literature. Thus, so far, the asymptotic behavior of the underlying problem can still be treated as an open problem.

To the best of my knowledge, the strong convergence of the EM scheme for the nonlinear FSDEs without singular kernels has not yet been investigated in the existing literature. In light of the above, therefore, the present work is the first one to consider proving the existence and uniqueness of a probabilistic strong solution to the FSDEs with non-singular kernel subjected to nonlinear perturbation. Hence, this motivate us to state and prove a range of results on a priori estimates, error estimates and the strong convergence of the EM approximation method for the problem under consideration. In fact, the underlying problem describes the more complex random phenomena with non-local effect. Secondly, we develop and prove the strong convergence of the Euler-type scheme. Finally as a matter of fact, we present our numerical experiments in order to substantiate the analysis of the problem under consideration. The current results from the numerical experiments are then compared with the results in the existing literature using both Matlab and Python programmings. The main difference between the results carried out in this paper and those in [222] is highlighted by the existence and uniqueness carried out not only without the Lipschitz conditions as used in [222] but also the fact that we do not use the kernel as in [222]. Instead of adapting the Riemann-Liouville fractional differential operator as in [222], we use the new Caputo FD with variable order and study numerical solutions of FSDE without a singular kernel.

In this chapter we consider the new Caputo-Fabrizio FD with variable order and study numerical solutions of FSDE without a singular kernel in the form

$$du = (-\lambda\, {}_0^C D_t^{\alpha} u + f(t,u))dt + b(t,u)dW, \quad t \in [0,T], u(0) = u_0, \lambda \geq 0, \tag{4.2}$$

where f and b are nonlinear external terms representing the drift and the intensity of the noise, respectively. Here W is a Wiener process and ${}_0^C D_t^{\alpha} u$ is the new Caputo-Fabrizio FD of order α, see the subsection below for more details and properties of this operator. Note that the assumptions on both functions f and b will be specified later on.

4.1.2 Important Properties of ${}_0^C D_t^{\alpha}$

We recall from Caputo and Fabrizio [36], the Caputo FD of order α is defined by

$$D_t^{\alpha} u(t) := \frac{1}{\Gamma(1-\alpha)} \int_a^t \mathcal{K}(t,s) u'(s)\, ds$$

where $\alpha \in [0,\ 1]$, $a \in [-\infty, t)$ and $u \in H^1(a,b)$ for $a < b$ and $a, b \in \mathbf{R}$. Here $\mathcal{K}(t,s)$ is the kernel defined as

$$\mathcal{K}(t,s) := (t-s)^{-\alpha} \quad for \quad s \leq t.$$

We can list some of the properties and drawbacks of this operator in the remark below.

Remark 4.1. Note that for $s = t$ then the kernel in the above definition becomes singular, that is $\mathcal{K}(t,t) = 0$. This singularity is disadvantageous in modeling real-world phenomena. This fact can reduce the application of this operator to more complex problems. Furthermore, we also note in the definition of the operator D_t^α, the presence of the function $u'(t)$ meaning that the derivative of u must exist in the ordinary sense before we can define or compute any expression with the above defined operator.

Now set

$$\mathcal{K}_0 := e^{-\frac{\alpha}{1-\alpha}(t-s)}$$

and change the constant $\frac{1}{\Gamma(1-\alpha)}$ by $\frac{1}{\sqrt{2\pi(1-\alpha^2)}}$ in the definition of the operator D_t^α. Then, according to [140], the new Caputo-Fabrizio derivative of order $\alpha \in (0,1)$, ${}_0^C D_t^\alpha u$ can be defined as FD without a singular kernel as follows (after normalizing):

$${}_0^C D_t^\alpha u = \frac{1}{(1-\alpha)} \int_a^t \dot{u}(\tau) e^{\frac{-\alpha(t-\tau)}{(1-\alpha)}}\ d\tau.$$

Remark 4.2. At first glance, we notice that for $t = s$, the new kernel $\mathcal{K}_0(t,t) = 1 \neq 0$. In contrast to $\mathcal{K}$, the new kernel $\mathcal{K}_0$ is not singular and it is in addition a very much regular kernel. Moreover, as for the operator D_t^α, we also observe that ${}_0^C D_t^\alpha$ requires the function u to admit a first derivative in the ordinary sense. However this can be addressed below.

Arguing similarly as in [36], one can easily define the operator ${}_0^C D_t^\alpha$ for function $u \in L^1(a,\ b)$ and $\alpha \in [0,1]$ by setting

$${}_0^C D_t^\alpha u(t) = \frac{\alpha M(\alpha)}{1-\alpha} \int_a^t [u(t) - u(s)] \mathcal{K}_0(t,s)\ ds$$

where $M(\alpha)$ is a normalized constant depending on α.

From this definition, we remark that system modeled by the operator ${}_0^C D_t^\alpha u$ can describe non-local systems, which are able to model fluctuations that cannot be captured by the usual operator D_t^α.

4.1.3 Motivational background

Exploring systems that display unpredictability and distant connections is fundamental in contemporary science and engineering practices. The mathematical representation of these

systems frequently necessitates instruments that surpass traditional calculus by integrating components capable of managing both randomness and memory impacts. SFPDEs has recently been among the most popular areas in describing and understanding mathematically, complex behaviors of robust systems such as the Navier-Stokes and hydrodynamics models of turbulence fluids. It is worth mentioning that the presence of stochastic forces in a model (fractional type) can lead to new phenomena that are very difficult to describe using their deterministic fractional counterparts. The generalization of Navier-Stokes equations by fractional Navier-Stokes systems can be used to better describe and analyze in practice the compressible and incompressible fluids dynamics. Due to the challenging task in computing and analyzing the behavior of some complex phenomena, several researchers have proposed different classes of models recently. Among those models we mention the shell fractional system that consist of infinitely many differential equations which can be used to model similar bahaviors to the fractional Navier-Stokes and many other similar properties of the classical Navier-Stokes can be studied. Moreover, other things that can be explored are their attempt in relaxing some assumptions and homogeneity, studies boundary conditions and boundary layers and treat other physical phenomena.

By utilizing adaptable derivatives in these equations allow for a more accurate representation of real-world events that help capturing nuances that are often missed by the conventional models.

The enhanced capabilities of the order Caputo derivative without singular kernels represent a major step forward in FC by enhancing stability and effectiveness in computational techniques across various industries like physics with prevalent anomalous diffusion phenomena; biology with intricate spatio-temporal patterns; and finance, with market dynamics displaying fractal characteristics. By removing kernels from the models structure it not only enhances its resilience but also makes it more viable computationally thus paving the way for exploring fresh avenues, in simulating and comprehending systems that are impacted by both deterministic and stochastic elements.

Innovations in the field have revealed that SFPDEs incorporating Caputo derivatives of varying orders offer perspectives on complex system behaviors that conventional models find challenging to explain fully. For example intricate phenomena characterized by scale processes, non local interactions and intricate random dynamics present in viscoelastic materials or financial markets stand to benefit from this method. These progressions not enrich our theoretical comprehension but also hold practical significance in refining algorithms and enhancing numerical techniques applied in simulations, across diverse scientific domains.

The objectives of this chapter is to initiate the study of some interesting classes of nonlin-

ear FSPDEs driven by white noise and to also investigate several results: first the issues of well-posedness (existence and uniqueness) of these systems, rate of convergence, strong convergence, a priori estimates and higher integrability on the solutions, error estimates and the approximate solutions.
In our research we are seeking to extend our knowledge in this particular field even further by investigating a novel approach not previously explored. Examining how a robust strong probabilistic solution can exist for FSDEs characterized by non singular kernels and impacted by nonlinear perturbations for the very first time ever. This study opens up pathways for delving deeper into intricate stochastic systems and enhancing computational methodologies for better outcomes overall. Our findings underscore distinctions and advancements compared to current techniques in this area of study. Laying down a strong groundwork that will shape future investigations, in SPs and FC. The discoveries have the potential to result in advancements across various sectors such as material science and financial engineering by addressing uncertainties and memory influences that are essential, in these fields.

To the best of our knowledge, the strong convergence of the EM scheme for the nonlinear FSDEs without singular kernels has not yet been studied in the corresponding literature. Therefore, this work is the first one to consider proving the existence and uniqueness of a probabilistic strong solution to the FSDEs with non-singular kernel subjected to nonlinear white noise. Hence, this clearly motivates us to establish new results on a priori bounds, higher integrability, error estimates and the strong convergence of the EM approximation method for the problem under consideration.

4.1.4 Organization of the chapter

The remaining sections of this chapter are structured as follows. In section 4.2, we prove that the convergence of the EM and the associated numerical solution has a bounded p-th moment for a some $p \in [2, \infty)$. In Section 4.3 we impose further assumptions on the nonlinear external forces f and g to ensure that $u(t)$ has bounded moments. In Section 4.4, we focus on establishing an optimal rate of convergence of the method established in Section 4.3. This section is augmented to a more widely used implicit variant of EM by relating the notion introduced in Section 4.2 of implicit methods with the result obtained in Section 4.4. In Section 4.5, we draw concluding remarks. While Section contains the major tools as part of the Appendix.

4.2 Convergence, Continuity and Uniqueness of the Solution for 4.2

In this section, we prove the existence of numerical solutions of FSDE (4.2) i.e

$$du = (-\lambda\, {}_0^C D_t^\alpha u + f(t,u))dt + b(t,u)dW, \quad t \in [0,T], u(0) = u_0, \lambda \geq 0,$$

We start by reformulating FSDE (4.2) similar to Yang et al. [222].

Let $(\Omega, \mathcal{F}, \mathcal{P}, \mathbb{F})$ be a filtered probability space equipped with a filtration satisfying the usual condition. Let W be a Wiener process (BM) defined on this probability space, $(\Omega, \mathcal{F}, \mathcal{P})$ associated with the filtration $\mathcal{F}_t$ and u_0 be a random second-order variable that is independent of W. We consider $W(\cdot)$ to be a BM with respect to the filtration

$$\mathcal{F}_t = \mathcal{U}\{W(s) : s \in [0,t], u_0\},$$

where $\mathcal{F}_t$ is the natural σ-algebra generated by u_0 and $\mathcal{F}_t$ is dependent of BM $W(\cdot)$ with a history up to time t. Here and in the sequel, we assume that the filtration $\mathbb{F}$ is complete and right-continuous.

Indeed, always here and here after, we will be assuming that the nonlinear external terms, $f : \mathbb{R} \longrightarrow \mathbb{R}^m$ and $b : \mathbb{R} \longrightarrow \mathbb{R}^{d\times m}$ are continuous w.r.t the first variable t and Lipschitz with respect to the second variable u. We denote the Euclidean vector norm by the symbol $|\cdot|$. In order to obtain the existence and uniqueness of solution (strong) to the problem under consideration, we need to provide some assumptions on a the nonlinear terms, the drift f and the diffusion coefficients b that will be needed in the sequel.

(i) Suppose that f and b are both one sided-Lipschitz nonlinear continuous functions and in addition, the function b is Lipschitz nonlinear continuous function with respect to u respectively i.e for $R \in (0,\infty)$, then there exists a constant $C_R > 0$ depending only on R, such that $\forall u, v \in \mathbb{R}^m$ it holds that

$$\langle f(u) - f(v), u - v\rangle \leq C_R|u - v|^2, \tag{4.3}$$

$$\langle b(u) - b(v), u - v\rangle \leq C_R|u - v|^2, \tag{4.4}$$

$$|b(u) - b(v)|^2 \leq C_R|u - v|^2. \tag{4.5}$$

(ii) We assume that the nonlinear term b is measurable a.e., t and that there exists $L_C \in (0,\infty)$ such that

$$|f(u)| \leq L_C(1 + |u|), \forall u \in \mathbb{R}^m, \tag{4.6}$$

$$|b(u)| \leq L_C(1 + |u|), \quad \forall u \in \mathbb{R}^m. \tag{4.7}$$

(iii) Let $\alpha \in C^1([0,T])$, the space of functions that are differentiable and continuous on the interval $[0,T]$ such that there is $\alpha^* \in (0,1)$ such that

$$0 \leq \alpha(y) \leq \alpha^*. \tag{4.8}$$

To represent equation (4.2) in a SP form first we integrate the FD part of (4.2) from 0 to t by applying the same technique as of Xiangcheng et al. [234]. We first have

$$\begin{aligned}
\int_0^t -\lambda\, {}_0^C D_y^{\alpha(y)} u dy &= \int_0^t \int_0^y \frac{-\lambda}{(1-\alpha(y))} \dot{u}(s) e^{\frac{-\alpha(y)(t-y)}{(1-\alpha(y))}} ds dy \\
&= \int_0^t \int_s^t \frac{-\lambda}{(1-\alpha(y))} \dot{u}(s) e^{\frac{-\alpha(y)(y-s)}{(1-\alpha(y))}} dy ds \\
&= \int_0^t u(s) \int_s^t \frac{-\lambda}{(1-\alpha(y))} e^{\frac{-\alpha(y)(y-s)}{(1-\alpha(y))}} dy ds \\
&- \int_0^t u(s) \frac{d}{ds} \left[\int_s^t \frac{\lambda}{(1-\alpha(y))} e^{\frac{-\alpha(y)(y-s)}{(1-\alpha(y))}} dy \right] ds \\
&= -u(0) \int_0^t \frac{\lambda}{(1-\alpha(y))} e^{\frac{-\alpha(y)(y)}{(1-\alpha(y))}} dy - \int_0^t \mathcal{K}(t,s) u(s) ds,
\end{aligned} \tag{4.9}$$

where

$$\mathcal{K}(t,s) = \frac{d}{ds} \left[\int_s^t \frac{\lambda}{(1-\alpha(y))} e^{\frac{-\alpha(y)(y-s)}{(1-\alpha(y))}} dy \right]. \tag{4.10}$$

LEMMA 4.2.1. *Let $\lambda > 0$ and $\alpha \in C^1[0,T]$ then for any $s,t \in [0,T]$ and $s \leq t$ it holds that*

$$|\mathcal{K}(t,s)| \leq \frac{\lambda}{1-\alpha^*} \tag{4.11}$$

Proof. From Lemma 2.1 of [233] and by assumption (4.8) we have that

$$e^{\frac{-(y-s)\alpha^*}{1-\alpha^*}} \leq 1 \tag{4.12}$$

Inserting (4.12) into (4.10) we then deduce from the resulting relation that

$$\begin{aligned}
|\mathcal{K}(t,s)| &= |\frac{d}{ds} \int_s^t \frac{\lambda}{(1-\alpha(y))} e^{\frac{-\alpha(y)(y-s)}{(1-\alpha(y))}} dy| \leq |\frac{d}{ds} \int_s^t \frac{\lambda}{(1-\alpha(y))} dy| \\
&\leq |\frac{d}{ds} \int_s^t \frac{\lambda}{(1-\alpha^*)} dy| = \frac{\lambda}{(1-\alpha^*)} |\frac{d}{ds}(t-s)| = \frac{\lambda}{(1-\alpha^*)} \\
\therefore |\mathcal{K}(t,s)| &\leq \frac{\lambda}{(1-\alpha^*)}
\end{aligned}$$

□

Our main objective is to find a SP u that will satisfy the stochastic integral (4.13). For this purpose, modulo a stopping time arguments, we can insert equation (4.10) on (4.2), with $t \in [0,T]$, to generate a SP $u(\cdot)$, which is progressively measurable on $\mathcal{F}(\cdot)$ such that the following stochastic integral hold:

$$\begin{aligned} u(t) =& u(0) + u(0)\int_0^t \frac{\lambda}{(1-\alpha(s))} e^{\frac{-\alpha(s)(s)}{(1-\alpha(s))}} ds + \int_0^t \mathcal{K}(t,s)u(s)ds \\ &+ \int_0^t f(u(s))ds + \int_0^t b(u(s))dW(s) \quad a.s.. \end{aligned} \tag{4.13}$$

Our first and primary goals are to investigate the strong convergence of numerical approximation in the scenario, where f and b are both one-sided Lipschitz with b in addition being locally Lipschitz. In the sequel, Q_i denote some generic positive constants which may change from time to time throughout the chapter.

THEOREM 4.2.1. *If assumptions (4.3) to (4.8) hold then SDE* (4.2) *has a unique solution* u *such that*

$$\mathbb{E}[\sup_{0\le t\le T}|u(t)|^2] \le \Theta E_0 \Upsilon < \infty, \quad t \in [0,T]. \tag{4.14}$$

$$\begin{aligned} &\textit{where } \Theta = 3\frac{\lambda^2}{(1-\alpha^*)^2}T^2\mathbb{E}(|u_0|^2) + 6L^2(T^2+Q_1T)(1+\mathbb{E}(|u_0|)^2), \\ &\Lambda = 3(\frac{\lambda^2}{(1-\alpha^*)^2}T + C_R(T+Q)) \textit{ and} \\ &E_0(\Lambda T) = \sum_{n=0}^{\infty}\Upsilon^n = \sum_{n=0}^{\infty}\frac{\Upsilon^n}{\Gamma(0\times n+1)}, \quad \Upsilon = \Lambda T \ge 0. \end{aligned} \tag{4.15}$$

In order to proceed with the proof of this result in Theorem 4.2.1, we rely on the Picard iteration approach. For this purpose we define a general term of the Picard sequence $\{Z_n\}_{n=0}^{\infty}$ by setting

$$\begin{aligned} Z_{n+1}(t) =& Z_0 + u_0\int_0^t \frac{\lambda}{(1-\alpha(s))} e^{\frac{-\alpha(s)(s)}{(1-\alpha(s))}} ds + \int_0^t \mathcal{K}(t,s)Z_n(s)ds \\ &+ \int_0^t f(Z_n(s))ds + \int_0^t b(Z_n(s))dW(s) \quad \textbf{for } n \ge 1, \end{aligned} \tag{4.16}$$

with $Z_0 := u(0) = u_0$.

This above Picard sequence can be generated using the Picard iteration method. Therefore, we follow the arguments of the celebrated work of Etienne Pardoux in [174] to deal with the terms in the sequence. Before we delve into the proof of Theorem 4.2.1, we first introduce the following result.

LEMMA 4.2.2. *Under the assumptions (4.3), (4.4), (4.6) and (4.7), there is a constant $C > 0$ such that for any $n \geq 1$ and $t \in [0, T]$, we have the estimate*

$$\mathbb{E} \sup_{0\leq x\leq t} |Z_n(x)|^2 \leq C. \tag{4.17}$$

Proof. Applying the Ito's formula to the function $|x|^2$, we have

$$\begin{aligned}
|Z_{n+1}(s)|^2 =& |Z_0|^2 + 2u_0 \int_0^x \langle \mathcal{K}(x,s), Z_n(s)\rangle ds + 2\int_0^x \langle Z_n(s), f(Z_n(s))\rangle ds \\
&+2\int_0^x \langle Z_n(s), b(Z_n(s))\rangle dW(s) + \int_0^x |b(Z_n(s))|^2 ds \\
=& |Z_0|^2 + K_1(x) + K_2(x) + K_3(x) + K_4(x).
\end{aligned} \tag{4.18}$$

In order to estimate every term in (4.18), we rely on assumptions (4.3), (4.4), (4.6) and (4.7), the Burkholder-Davis-Gundy (BDG) inequality, the Young's inequality and the Cauchy-Swarz inequality to deal with each term in (4.18). For this purpose we deal with the integrals in (4.18) separately. Therefore, we take mathematical expectation on both sides of (4.18) then apply the supremum on both sides to obtain the corresponding relation from which we estimate the remaining terms as below. We have

$$\begin{aligned}
\mathbb{E} \sup_{0\leq x\leq t} |K_1(x)| &= \mathbb{E} \sup_{0\leq x\leq t} |\int_0^x \langle \mathcal{K}(x,s), Z_n(s)\rangle ds| \\
&\leq \mathbb{E} \sup_{0\leq x\leq t} \left[\int_0^x |\mathcal{K}(x,s)|^2 ds\right]^{\frac{1}{2}} \left[\int_0^x |Z_n(s)|^2 ds\right]^{\frac{1}{2}} \\
&\leq C_\varepsilon \mathbb{E} \sup_{0\leq x\leq t} \int_0^x |\mathcal{K}(x,s)|^2 ds + \varepsilon \mathbb{E} \sup_{0\leq x\leq t} \int_0^x |Z_n(s)|^2 ds \\
&\leq C_\varepsilon \frac{\lambda^2}{(1-\alpha*)^2} \mathbb{E}(t) + \varepsilon \mathbb{E} \sup_{0\leq x\leq t} \int_0^x |Z_n(r)|^2 ds \\
&\leq C_\varepsilon \frac{\lambda^2}{(1-\alpha^*)^2} T + \varepsilon \mathbb{E} \sup_{0\leq x\leq t} \int_0^x |Z_n(r)|^2 ds.
\end{aligned} \tag{4.19}$$

Using the assumption in item (ii) along with Fubini's Theorem, we infer from Young and Cauchy inequalities that there exists a constant L_C such that

$$\begin{aligned}
\mathbb{E} \sup_{0\leq x\leq t} |K_2(x)| =& \mathbb{E} \sup_{0\leq x\leq t} \left|\int_0^x \langle Z_n, f(Z_n(s))\rangle ds\right| \\
&\leq L_C \mathbb{E} \sup_{0\leq x\leq t} \int_0^x |Z_n(s)|(1+|Z_n(s)|) ds \\
&\leq L_C \mathbb{E} \sup_{0\leq x\leq t} \left[\varepsilon \int_0^x |Z_n(s)|^2 ds + C_\varepsilon \int_0^x 1^2 ds + \int_0^x |Z_n(s)|^2 ds\right] \\
&\leq C_\varepsilon + (1+\varepsilon) \mathbb{E} \sup_{0\leq x\leq t} \int_0^x |Z_n(s)|^2 ds.
\end{aligned} \tag{4.20}$$

As for the term in K_3, we first apply the BDG inequality and then use assumption (4.7) and the Young's inequality to obtain

$$\begin{aligned}
&\mathbb{E}\sup_{0\le x\le t}\left|\int_0^x \langle Z_n(s), b(Z_n(s))\rangle dW(s)\right| \\
&\le C\mathbb{E}\sup_{0\le x\le t}\left|\int_0^x |Z_n(s)|^2 |b(Z_n(s))|^2 ds\right|^{\frac{1}{2}} \\
&\le C\mathbb{E}\left[\left[\sup_{0\le x\le t}|Z_n(s)|^2\right]^{\frac{1}{2}}\sup_{0\le x\le t}\left|\int_0^x (1+|Z_n(s)|^2)ds\right|^{\frac{1}{2}}\right] \\
&\le \eta\mathbb{E}\sup_{0\le x\le t}|Z_n(s)|^2 + tC_\eta + C_\eta\mathbb{E}\sup_{0\le x\le t}\int_0^x |Z_n(s)|^2 ds. \qquad (4.21)
\end{aligned}$$

Similarly in the case for the bound of $K_3(x)$, we can also estimate the term $K_4(t)$ using assumption (4.7) to obtain

$$\begin{aligned}
&\mathbb{E}\sup_{0\le x\le t}\int_0^x |b(Z_n(s))|^2 ds \\
&\le L_C\mathbb{E}\sup_{0\le x\le t}\int_0^x (1+|Z_n(r)|)^2 ds \\
&\le TL_C + L_C\mathbb{E}\sup_{0\le x\le t}\int_0^x |Z_n(r)|^2 ds. \qquad (4.22)
\end{aligned}$$

Combining all the estimates (4.19)-(4.22) we obtain that

$$\begin{aligned}
&\mathbb{E}\sup_{0\le x\le t}|Z_{n+1}(x)|^2 \\
&\le |Z_0|^2 + C_\varepsilon + (1+\varepsilon)\mathbb{E}\sup_{0\le x\le t}\int_0^x |Z_n(s)|^2 ds \\
&+ \eta\mathbb{E}\sup_{0\le x\le t}|Z_n(s)|^2 + tC_\eta + C_\eta\mathbb{E}\sup_{0\le x\le t}\int_0^x |Z_n(s)|^2 ds \\
&+ C_\varepsilon + (1+\varepsilon)\mathbb{E}\sup_{0\le x\le t}\int_0^x |Z_n(s)|^2 ds + TL_C + L_C\mathbb{E}\sup_{0\le x\le t}\int_0^x |Z_n(r)|^2 ds \\
&\le C + \eta\mathbb{E}\sup_{0\le x\le t}|Z_n(s)|^2 + 2(1+\varepsilon+L_C+C_\eta)\mathbb{E}\sup_{0\le x\le t}\int_0^x |Z_n(r)|^2 ds. \qquad (4.23)
\end{aligned}$$

On the other hand, raising the expression in (4.16) to the power 2 and taking mathematical

expectation, the supremum and using Jen's inequality, we obtain that

$$\begin{aligned}
&\mathbb{E}\sup_{0\leq x\leq t}|Z_{n+1}(x)|^2\\
&\leq 5\mathbb{E}|Z_0|^2+\mathbb{E}\sup_{0\leq x\leq t}u_0\int_0^x\frac{\lambda}{(1-\alpha(s))}e^{\frac{-\alpha(s)(s)}{(1-\alpha(s))}}ds+10\mathbb{E}\sup_{0\leq x\leq t}\left|\int_0^x\mathcal{K}(x,s)ds\right|^2\\
&+10\mathbb{E}\sup_{0\leq x\leq t}\left|\int_0^x f(Z_n(s))ds\right|^2+10\mathbb{E}\sup_{0\leq x\leq t}\left|\int_0^x b(Z_n(s))dW(s)\right|^2\\
&=5|Z_0|^2+M_1(x)+M_2(x)+M_3(x)+M_4(x). \qquad (4.24)
\end{aligned}$$

Similarly as in the estimates for $K_1(t)-K_4(t)$, we do rely on the same techniques to deal with the estimates for $M_1(t)-M_4(t)$. Therefore, we use assumptions (4.3) - (4.8) along with BDG, Young, Cauchy and Jensen inequalities to obtain the corresponding relations needed for the estimates. We hence deduce the estimate for $M_1(t)$ and $M_2(t)$ as follows:

$$\mathbb{E}\sup_{0\leq x\leq t}M_1(x)+\mathbb{E}\sup_{0\leq x\leq t}M_2(x)\leq 2\frac{\lambda^2}{(1-\alpha^*)^2}T. \qquad (4.25)$$

Owing to assumption (4.6) along with Young and Cauchy inequalities, we infer that

$$\begin{aligned}
\mathbb{E}\sup_{0\leq x\leq t}M_3(x)&\leq\mathbb{E}\sup_{0\leq x\leq t}\left|\int_0^x f(Z_n(s))ds\right|^2\\
&\leq\mathbb{E}\sup_{0\leq x\leq t}\left[\int_0^x|f(Z_n(s))|\,ds\right]^2\\
&\leq\mathbb{E}\sup_{0\leq x\leq t}\left[\int_0^x(1+|Z_n(s)|)ds\right]^2\\
&\leq T^2+\mathbb{E}\sup_{0\leq x\leq t}\left[\int_0^x|Z_n(s)|\,ds\right]^2\\
&\leq T^2+\mathbb{E}\sup_{0\leq x\leq t}\left[\left(\int_0^x 1^2ds\right)^{\frac{1}{2}}\left(\int_0^x|Z_n(s)|^2\,ds\right)^{\frac{1}{2}}\right]^2\\
&\leq T^2+TC_\kappa+\kappa\mathbb{E}\sup_{0\leq x\leq t}\int_0^x|Z_n(s)|^2\,ds. \qquad (4.26)
\end{aligned}$$

As for the stochastic term, we use assumption (4.7) and we apply BDG's inequality along

with Young and Cauchy inequalities to obtain that

$$\begin{aligned}\mathbb{E}\sup_{0\le x\le t} M_4(x) &\le \mathbb{E}\sup_{0\le x\le t}\left|\int_0^x b(Z_n(s))dW(s)\right|^2\\ &\le C\mathbb{E}\int_0^t |b(Z_n(s))|^2\,ds\\ &\le CL_C\mathbb{E}\int_0^t (1+|Z_n(s)|^2)ds\\ &\le TCL_C + CL_C\mathbb{E}\sup_{0\le x\le t}\int_0^x |Z_n(s)|^2\,ds. \end{aligned} \tag{4.27}$$

Combining all the estimates (4.25) - (4.27) we obtain

$$\mathbb{E}\sup_{0\le x\le t}|Z_{n+1}(x)|^2 \le C(\lambda,\alpha^*,\kappa,T) + C(T,\kappa)\mathbb{E}\sup_{0\le x\le t}\int_0^x |Z_n(s)|^2\,ds. \tag{4.28}$$

In order to carry on with the remaining parts of the proof, we define the function $H(t)$ by setting

$$H_n(t) := \mathbb{E}\sup_{0\le x\le t}|Z_{n+1}(x)|^2, \ \textbf{for } n\in\mathbb{N}.$$

We can easily remark by definition of $H_n(t)$ that

$$H_n(t) \le C(\lambda,\alpha^*,\kappa,T) + C(T,\kappa)\mathbb{E}\sup_{0\le x\le t}\int_0^x |Z_n(s)|^2\,ds \tag{4.29}$$

from which we infer that

$$H_n(t) \le Q_T\int_0^x |H_{n-1}(s)|^2\,ds, \tag{4.30}$$

where that Q is a constant depending only on λ, α^*, T and κ.

Arguing similarly as in [222], we heavily rely on principle of mathematical induction to estimate the function $H_n(t)$. For this purpose, we first address the case of $n = 0$ and deal with the corresponding relation as follows:

we infer from the relation (4.18) and BDG inequality (4.27) with $n = 0$ that

$$\begin{aligned}
H_0(t) &= \mathbb{E} \sup_{0\le x\le t} |Z_1(x)|^2 \\
&= |Z_0|^2 + 2u_0 \int_0^x \langle \mathcal{K}(x,s), Z_0(s)\rangle ds + 2\int_0^x \langle Z_0(s), f(Z_0(s))\rangle ds \\
&+ 2\int_0^x \langle Z_0(s), b(Z_0(s))\rangle dW(s) + \frac{1}{2}\int_0^x |b(Z_0(s))|^2 ds \\
&\le \mathbb{E}|Z_0|^2 + 2\mathbb{E}u_0 \sup_{0\le x\le t}\int_0^x \langle \mathcal{K}(x,s), Z_0(s)\rangle ds + 2\mathbb{E}\sup_{0\le x\le t}\int_0^x \langle Z_0(s), f(Z_0(s))\rangle ds \\
&+ 2\mathbb{E}\sup_{0\le x\le t}\int_0^x \langle Z_0(s), b(Z_0(s))\rangle dW(s) + \mathbb{E}\sup_{0\le x\le t}\int_0^x |b(Z_0(s))|^2 ds \\
&\le \mathbb{E}|Z_0|^2 + \frac{\lambda^2}{1-\alpha^*}\mathbb{E}|u_0|^2 + TL_C\mathbb{E}\sup_{0\le x\le t}\int_0^x |Z_0|^2 ds \\
&\le C\mathbb{E}|u_0|^2 =: \Gamma < \infty, \qquad (4.31)
\end{aligned}$$

where Γ is a constant depending only on α^*, λ, $\mathbb{E}|u_0|^2$ and T. It implies that the estimate of the first term $H_0(t)$. This holds true.

For $n = 1$, we have

$$\begin{aligned}
H_1(t) &\le Q_T \int_0^x H_0(s) ds \\
&= Q_T \int_0^x \Gamma ds \\
&= Q_T \int_0^t \Gamma ds \\
&= Q_T \Gamma t < \infty. \qquad (4.32)
\end{aligned}$$

This holds true as well

Similarly, for $n = 2$ we have

$$\begin{aligned}
H_2(t) &\le Q_T \int_0^x H_1(s) ds \\
&= Q_T \int_0^x \Gamma^2 t ds \\
&= Q_T \int_0^t \Gamma^2 t ds \\
&= Q_T \Gamma^2 t^2 < \infty. \qquad (4.33)
\end{aligned}$$

This is true.

Now, we assume that the induction step and the inductive hypothesis both hold true, for $n = k + 1$ we have that

$$\begin{aligned} H_{k+1}(t) &\leq Q_T \int_0^x H_k(s)ds \\ &= Q_T \int_0^x \Gamma^k t^{k-1} ds \\ &= Q_T \int_0^t \Gamma^k t^{k-1} ds \\ &= Q_T \Gamma^k t^k < \infty, \end{aligned} \tag{4.34}$$

from which we deduce that the series (4.34) can be written as

$$\sum_{n=0}^{\infty} Q_T (\Gamma t)^n = Q_T \sum_{n=0}^{\infty} (\Gamma t)^n Q_T E_0(\Gamma t) < \infty \textbf{ for any } t \in [0, T]. \tag{4.35}$$

Here E_0 stands for the Mittag-Leffler function and the above series dully converges. Therefore,

$$\sum_{n=0}^{\infty} \mathbb{E} \sup_{0 \leq t \leq T} |Z_{n+1}(t)|^2 < \infty \textbf{ a.s.}$$

from which along with Chebyshev's inequality we infer that

$$\begin{aligned} \mathbb{P}\left(\sup_{0 \leq t \leq T} |Z_{n+1}(t)|^2 \geq 2^{-n} \right) &\leq 4^n \mathbb{E} \sup_{0 \leq t \leq T} |Z_{n+1}(t)|^2 \\ &\leq 4^n (\Gamma t)^n Q_T \\ &\leq 4^n \Gamma^n T^n Q_T. \end{aligned} \tag{4.36}$$

Hence, we use the Borel-Cantelli lemma to deduce that the sequence $\{Z_n\}_{n=0}^{\infty}$ converges uniformly to the process $u(t)$ on $[0, T]$.

□

We are now ready to proceed with the proof of Theorem 4.2.1.

Proof. In order to obtain the integrability in Theorem 4.2.1, we need to estimate every terms in the right hand side of (4.16). For this purpose, we first rely on the result of Lemma 4.2.2 and use the same sequence $\{Z_n\}_{n \geq 1}$ as defined above. We therefore noticed that the

difference $Z_{n+1}(t) - Z_n(t)$ is given by

$$Z_{n+1}(t) - Z_n(t) = \int_0^t \mathcal{K}(t,s)(Z_{n+1}(s) - Z_n(s))ds + \int_0^t (f(Z_{n+1}(s)) - f(Z_n(s))ds + \int_0^t [b(Z_{n+1}(s)) - b(Z_n(s))]dW(s).$$

In order to obtain the best estimates, we first apply the Ito's formula to the functions $|x|^2$ and $d(Z_{n+1} - Z_n)$. Secondly, we estimate the terms in the expression of $|Z_{n+1} - Z_n|^2$ directly without using the expressions coming from the Ito's formula and then combine the terms coming from both relations to get the best estimates required for the proof of this theorem. For this purpose, on one hand applying the Ito's formula to the functions $|x|^2$ and $d(Z_{n+1} - Z_n)$, we obtain that

$$\begin{aligned}
|Z_{n+1}(s) - Z_n(s)|^2 =& 2\int_0^t \langle \mathcal{K}(t,s), Z_n(s) - Z_{n-1}(s)\rangle ds \\
&+2\int_0^t \langle Z_n(s) - Z_{n-1}(s), f(Z_n(s)) - f(Z_{n-1}(s))\rangle ds \\
&+2\int_0^t \langle Z_n(s) - Z_{n-1}(s), b(Z_n(s)) - b(Z_{n-1}(s))\rangle dW(s) \\
&+\frac{1}{2}\int_0^t |b(Z_n(s)) - b(Z_{n-1}(s))|^2 ds \\
=& J_1(t) + J_2(t) + J_3(t) + J_4(t),
\end{aligned}$$

from which we infer that

$$\begin{aligned}
&\mathbb{E}\sup_{0\le x\le t} |Z_{n+1}(x) - Z_n(x)|^2 \\
&\le \mathbb{E}\sup_{0\le x\le t} |J_1(x)| + \mathbb{E}\sup_{0\le x\le t} |J_2(x)| + \mathbb{E}[\sup_{0\le x\le t} |J_3(x)| + \mathbb{E}\sup_{0\le x\le t} |J_4(x)|. \qquad (4.37)
\end{aligned}$$

Our next task is to separately estimate every term on the right side of the equation (4.37). To bound the first term of (4.37) we can apply Lemma 4.2.1, Cauchy-Schwarz inequality and assumption (4.3) to (4.8). We also apply the Young's inequality modulo a stopping time

to obtain that

$$\begin{aligned}
&\mathbb{E}\sup_{0\le x\le t}|J_1(x)|\\
&=\mathbb{E}\sup_{0\le x\le t}|\int_0^x|\mathcal{K}(x,s)||Z_n(s)-Z_{n-1}(s)|ds|\\
&\le C\mathbb{E}\sup_{0\le x\le t}\int_0^x|\mathcal{K}(x,s)|^2ds+C\mathbb{E}\sup_{0\le x\le t}\int_0^x|Z_n(s)-Z_{n-1}(s)|^2ds\\
&\le C\frac{\lambda^2}{(1-\alpha^*)^2}T+C\mathbb{E}\sup_{0\le x\le t}\int_0^x|Z_n(s)-Z_{n-1}(s)|^2ds. \qquad (4.38)
\end{aligned}$$

We can proceed to estimate the term, $J_2(x)$. Note that by virtue of triangle and Jensen inequalities and owing to the assumption in item (i) along with Fubini's Theorem, we have

$$\begin{aligned}
\mathbb{E}\sup_{0\le x\le t}|J_2(x)| =&\mathbb{E}\sup_{0\le x\le t}\left|\int_0^x\langle Z_n-Z_{n-1},f(Z_n(s))-f(Z_{n-1}(s))\rangle ds\right|\\
&\le C_R\mathbb{E}\sup_{0\le x\le t}\int_0^x|Z_n(s)-Z_{n-1}(s)|^2ds. \qquad (4.39)
\end{aligned}$$

In order to proceed with the estimate of the term $J_3(x)$, we first use the one-sided Lipschitz assumption given in item (i), secondly the BDG inequality and thirdly the Young's inequality to insert that there exists a constant $C_T>0$ such that

$$\begin{aligned}
&\mathbb{E}\sup_{0\le x\le t}|J_3(x)|\\
&\le\mathbb{E}\left[\int_0^t|Z_n(s)-Z_{n-1}(s)|^2|b(Z_n(s))-b(Z_{n-1}(s))|^2ds\right]^{\frac{1}{2}}\\
&\le\mathbb{E}\left(\left[\sup_{0\le x\le t}|Z_n(x)-Z_{n-1}(x)|^2\right]^{\frac{1}{2}}\left[\sup_{0\le x\le t}\int_0^x|Z_n(s)-Z_{n-1}(s)|^2d(s)\right]^{\frac{1}{2}}\right)\\
&\le C\mathbb{E}\sup_{0\le x\le t}|Z_n(x)-Z_{n-1}(x)|^2+\mathbb{E}\sup_{0\le x\le t}\int_0^x|Z_n(s)-Z_{n-1}(s)|^2d(s)\\
&\le C_T\mathbb{E}\sup_{0\le x\le t}|Z_n(x)-Z_{n-1}(x)|^2. \qquad (4.40)
\end{aligned}$$

Finally, by applying Ito's isometry, Lemma 2.3.4 and assumption (4.3) to (4.8) we can bound the third term of (4.37) and obtain using a stopping time argument that

$$\begin{aligned}
&\mathbb{E}\sup_{0\le x\le t}\left|\int_0^x\left[b(Z_n(s))-b(Z_{n-1}(s))\right]ds\right|^2\\
&\le c_1\mathbb{E}\sup_{0\le x\le t}\int_0^x|b(Z_n(s))-b(Z_{n-1}(s))|^2ds\\
&\le Q_3\mathbb{E}\sup_{0\le x\le t}\int_0^x|Z_n(s)-Z_{n-1}(s)|^2ds, \qquad (4.41)
\end{aligned}$$

where Q_3 is constant depending on R only. This gives us the estimate on the last term $J_4(x)$.

Now we combine all the estimates from (4.37) to (4.41) and (4.37) as well as applying Young's inequality to obtain

$$\begin{aligned}
&\mathbb{E}\sup_{0\le x\le t}|Z_{n+1}(x)-Z_n(x))|^2\\
&\le C(\alpha^*,\lambda,T)+\mathbb{E}\sup_{0\le x\le t}\int_0^x|Z_n(s)-Z_{n-1}(s)|^2ds+\\
&3C_R\mathbb{E}\sup_{0\le x\le t}\int_0^x|Z_n(s)-Z_{n-1}(s)|^2ds+3Q_1C_R\mathbb{E}\sup_{0\le x\le t}\int_0^x|Z_n(s)-Z_{n-1}(s)|^2ds\\
&\le C(\alpha^*,\lambda,T)+\Psi\mathbb{E}\sup_{0\le x\le t}\int_0^x|Z_n(s)-Z_{n-1}(s)|^2ds, \qquad (4.42)
\end{aligned}$$

where $\Psi=C_R(T+Q_1)$.

On the other hand, we notice that

$$|Z_{n+1}(x)-Z_n(x)|^2=|I_1(x)+I_2(x)+I_3(x)|^2 \qquad (4.43)$$

where

$$\begin{aligned}
I_1(x)&=\int_0^x\mathcal{K}(x,s)\left[Z_n(s)-Z_{n-1}(s)\right]ds,\\
I_2(x)&=\int_0^x\left[f(Z_n(s))-f(Z_{n-1}(s))\right]ds,\\
I_3(x)&=\int_0^x\left[b(Z_n(s))-b(Z_{n-1}(s))\right]dW(s).
\end{aligned}$$

This indicates to us that we must also estimate every term in (4.43). Then by Jensen inequality, we have

$$|Z_{n+1}(x)-Z_n(x)|^2\le 3\left[|I_1(x)|^2+|I_2(x)|^2+|I_3(x)|^2\right]$$

from which we infer that

$$\mathbb{E}[\sup_{0\le x\le t}|Z_{n+1}(x)-Z_n(x)|^2]\le 3\mathbb{E}[\sup_{0\le x\le t}[|I_1(x)|^2]+3\mathbb{E}[\sup_{0\le x\le t}[|I_2(x)|^2]+3\mathbb{E}[\sup_{0\le x\le t}[|I_3(x)|^2]. \qquad (4.44)$$

Our next task is to separately bounding every term on the right side of the equation (4.44). To bound the first term of (4.44), we can apply Lemma 4.2.1, Cauchy-Schwarz inequality and assumption 4.3 to 4.8. We also apply the Young's inequality modulo a stopping time to

obtain that

$$\begin{aligned}
&\mathbb{E}\sup_{0\le x\le t}|I_1(x)|^2\\
&=\mathbb{E}\sup_{0\le x\le t}|\int_0^x \mathcal{K}(x,s)(Z_n(s)-Z_{n-1}(s))ds|^2\\
&\le \mathbb{E}\sup_{0\le x\le t}\left[\int_0^t|\mathcal{K}(x,s)|^2ds\right]^{\frac{1}{2}}\left[\int_0^x|Z_n(s)-Z_{n-1}(s)|^2ds\right]^{\frac{1}{2}}\\
&\le \mathbb{E}\sup_{0\le x\le t}\int_0^x|\mathcal{K}(x,s)|^2ds+\mathbb{E}\sup_{0\le x\le t}\int_0^x|Z_n(s)-Z_{n-1}(s)|^2ds\\
&\le \frac{\lambda^2}{(1-\alpha*)^2}t+\mathbb{E}\sup_{0\le x\le t}\int_0^x|Z_n(s)-Z_{n-1}(s)|^2ds\\
&\le \frac{\lambda^2}{(1-\alpha^*)^2}T+\mathbb{E}\sup_{0\le x\le t}\int_0^x|Z_n(s)-Z_{n-1}(s)|^2ds. \qquad (4.45)
\end{aligned}$$

Next, by applying Cauchy and Young's inequalities and assumption (4.3) to (4.8), we can bound the second term of (4.37) as follows:

$$\begin{aligned}
\mathbb{E}\sup_{0\le x\le t}|I_2(x)|^2 =&\mathbb{E}\left[\sup_{0\le x\le t}\left|\int_0^x f(Z_n(s))-f(Z_{n-1}(s))ds\right|^2\right]\\
&\le \mathbb{E}\left(\left[\sup_{0\le x\le t}\left[\int_0^x 1ds\right]^{\frac{1}{2}}\left[\int_0^x|f(Z_n)(s)-f(Z_{n-1}(s))ds|^2\right]^{\frac{1}{2}}\right]\right)\\
&\le \mathbb{E}\sup_{0\le x\le t}\left[\int_0^x 1ds+\int_0^x|f(Z_n)(s)-f(Z_{n-1}(s))ds|^2\right]\\
&\le T+C_R\mathbb{E}\sup_{0\le x\le t}\int_0^x|Z_n(s)-Z_{n-1}(s)|^2ds\\
&\le T+C_R\mathbb{E}\sup_{0\le x\le t}\int_0^x|Z_n(s)-Z_{n-1}(s)|^2ds. \qquad (4.46)
\end{aligned}$$

Finally, by applying Ito isometry, Lemma 2.3.4, BDG and assumption (4.3) to (4.8), we can bound the third term of (4.44) and obtain using a stopping time τ that

$$\begin{aligned}
&\mathbb{E}\sup_{0\le x\le t}[I_3(x)]^2\\
&=\mathbb{E}\sup_{0\le x\le t}\left|\int_0^x[b(Z_n(s))-b(Z_{n-1}(s))]\,dW(s)\right|^2\\
&=\mathbb{E}\int_0^t|b(Z_n(x))-b(Z_{n-1}(x))|^2dx\\
&\le Q_1C_R\int_0^t|Z_n(x)-Z_{n-1}(x)|^2dx, \qquad (4.47)
\end{aligned}$$

where Q_1 is constant as the one given by Lemma 2.3.4. Now we combine all inequalities (4.38) - (4.47) with relation (4.37) and apply Young's inequality to obtain

$$\begin{aligned}
&\mathbb{E}\sup_{0\le x\le t}|Z_{n+1}(x)-Z_n(x)|^2\\
&\le 3\frac{\lambda^2}{(1-\alpha^*)^2}T+\mathbb{E}\sup_{0\le x\le t}\int_0^x|Z_n(s)-Z_{n-1}(s)|^2ds+\\
&+3TC_R\mathbb{E}\sup_{0\le x\le t}\int_0^x|Z_n(s)-Z_{n-1}(s)|^2ds+3Q_1C_R\mathbb{E}\sup_{0\le x\le t}\int_0^x|Z_n(s)-Z_{n-1}(s)|^2ds\\
&\le 3\frac{\lambda^2}{(1-\alpha^*)^2}T+\Psi\mathbb{E}\sup_{0\le x\le t}\int_0^x|Z_n(s)-Z_{n-1}(s)|^2ds, \qquad (4.48)
\end{aligned}$$

Combining estimates (4.42) and (4.48), we infer that there exists a constant Ψ such that

$$\begin{aligned}
&\mathbb{E}\sup_{0\le x\le t}|Z_{n+1}(x)-Z_n(x)|^2\\
&\le 3\frac{\lambda^2}{(1-\alpha^*)^2}T+\mathbb{E}\sup_{0\le x\le t}\int_0^x|Z_n(s)-Z_{n-1}(s)|^2ds+\\
&+3TC_R\mathbb{E}\sup_{0\le x\le t}\int_0^x|Z_n(s)-Z_{n-1}(s)|^2ds+3Q_1C_R\mathbb{E}\sup_{0\le x\le t}\int_0^x|Z_n(s)-Z_{n-1}(s)|^2ds\\
&\le 3\frac{\lambda^2}{(1-\alpha^*)^2}T+\Psi\mathbb{E}\sup_{0\le x\le t}\int_0^x|Z_n(s)-Z_{n-1}(s)|^2ds, \qquad (4.49)
\end{aligned}$$

Next we use mathematical induction to find the estimate for the terms in relation (4.49). For this purpose, for $n\ge 1$, we reformulate and estimate the terms in the right-hand side of equation (4.44) as follows. Set

$$h_n(t):=\mathbb{E}\sup_{0\le x\le t}|Z_{n+1}(x)-Z_n(x)|^2\le 3C(\alpha^*,T)+\Psi\int_0^x h_{n-1}(s)ds,$$

where

$$h_{n-1}(t):=\mathbb{E}\sup_{0\le r\le t}|Z_n(r)-Z_{n-1}(r)|^2 \text{ for } n\ge 1.$$

Using equation (4.37) with $n=0$, applying Jensen inequality and using assumptions (4.3) to (4.8) we obtain that

$$h_0(t) = \mathbb{E}\sup_{0\le x\le t}|(Z_1(x) - Z_0(x))|^2 \tag{4.50}$$
$$\le 3\mathbb{E}\sup_{0\le x\le t}\left(\left|\int_0^x \mathcal{K}(x,s)u_0 ds\right|^2 + \left|\int_0^x f(u_0)ds\right|^2 + \left|\int_0^x b(u_0(s))dW(s)\right|^2\right)$$
$$\le 3\mathbb{E}\sup_{0\le x\le t}\left(u_0^2\left(\int_0^x |\mathcal{K}(x,s)|ds\right)^2 + \left(\int_0^x |f(u_0)|ds\right)^2 + Q_1\int_0^x |b(u_0)|^2 ds\right)$$
$$\le 3\mathbb{E}\left(\sup_{0\le x\le t}\left(\int_0^x L(1+|u_0)|ds\right)^2 + Q_1\int_0^x L^2(1+|u_O|)^2 ds\right) + 3\frac{\lambda^2}{(1-\alpha^*)^2}T^2\mathbb{E}(|u_0|^2)$$
$$\le 3\frac{\lambda^2}{(1-\alpha^*)^2}T^2\mathbb{E}|u_0|^2 + 3L^2T^2\mathbb{E}(1+|u_0|)^2 + 3Q_1L^2T\mathbb{E}(1+|u_0|)^2 = \Theta < \infty,$$

where $\Theta = 3\frac{\lambda^2}{(1-\alpha^*)^2}T^2\mathbb{E}|u_0|^2 + 6L^2(T^2+Q_1T)(1+\mathbb{E}(|u_0|)^2)$. Therefore $h_0(t)$ is bounded.

Our next task is to estimate $h_n(t)$ for $n \ge 1$. Again, we easily can prove this by mathematical induction as in the aforementioned technique.
For $n = 1$, using (4.50) we have

$$h_1(t) =: \mathbb{E}\sup_{0\le x\le t}|Z_2(s) - Z_1(s)|^2 \le \Psi\int_0^t \Theta ds = \Psi t\Theta < \infty. \tag{4.51}$$

Similarly for $n = 2$ we have

$$h_2(t) :=\mathbb{E}\sup_{0\le x\le t}|Z_3(s) - Z_2(s)|^2 \le (\Psi t)^2\Theta < \infty.$$

Now, suppose that the relation holds for $n = m$ *i.e.*,

$$h_m(t) := \mathbb{E}\sup_{0\le x\le t}|Z_m(s) - Z_{m-1}(s)|^2 \le \Psi\int_0^t h_{m-1}(s)ds \le (\Psi t)^m\Theta < \infty. \tag{4.52}$$

We claim that the assumption also holds true for $n = m + 1$:

$$h_{m+1}(t) \le \Psi\int_0^t h_m(s)ds \le (\Psi t)^{m+1}\Theta < \infty$$

from which we therefore infer that

$$h_n(t) = \mathbb{E}\sup_{0\le x\le t}|Z_{n+1}(s) - Z_n(s)|^2 \le (\Psi t)^n\Theta < \infty,\ \forall\ n \ge 0. \tag{4.53}$$

Moreover, the series defined by the right hand side of relation (4.53) converges to the Mittag-Leffler function

$$\sum_{m=0}^{\infty}(\Psi t)^n\Theta = \sum_{m=0}^{\infty}(\Psi)^n t^n\Theta = \Theta\sum_{m=0}^{\infty}\frac{(\Psi)^n t^n}{\Gamma(0.n+1)} =\Theta E_0(\Psi T) < \infty,\ t \in [0,T]$$

which implies that

$$\sum_{n=0}^{\infty} \mathbb{E} \sup_{0\leq t\leq T} |Z_{n+1}(t) - Z_n(t)|^2 < \infty, \ a.s.. \tag{4.54}$$

Owing to Chebyshev's inequality, we infer from (4.53) and (4.54) that

$$\begin{aligned}\mathcal{P}(\sup_{t\in[0,T]} |Z_{n+1}(t) - Z_n(t))|^2 \geq 2^{-n}) \leq & 4^n \mathbb{E}[\sup_{t\in[0,T]} |Z_{n+1}(t) - Z_n(t))|^2] \\ & \leq 4^n(\Psi t)^n \Theta \leq 4^n(\Psi T)^n \Theta.\end{aligned}$$

Using the Borel-Cantelli lemma, the sequence

$$Z_n(t) = u_0 + \sum_{m=1}^{n} [Z_m(t) - Z_{m-1}(t)]$$

uniformly converges to limit u on $[0, T]$ and solves the underlying problem (4.13) a.s. We establish the continuity of u based on the continuity of $\{Z_n\}_{n=0}^{\infty}$ and the above result. From this we can therefore assert that the solution of FSDE (4.2) is the continuous function u. Let $\bar{u}(t)$ be the solution of (4.2), different from $u(t)$. By following similar procedures as applied in (4.48), we have

$$\mathbb{E}[\sup_{0\leq x\leq t} |u(x) - \bar{u}(x)|^2] \leq \Psi \int_0^t \mathbb{E}[\sup_{0\leq r\leq s} |u(r) - \bar{u}(r)|^2] ds, \forall t \in [0, T]. \tag{4.55}$$

By applying Lemma 2.3.5 on (4.55), we obtain that

$$\mathbb{E}[\sup_{0\leq x\leq t} |u(x) - \bar{u}(x)|^2] = 0.$$

This implies

$$u(t) = \bar{u}(t) \ \textbf{a.s..}$$

We conclude that the problem (4.2) admits a unique solution $u(t)$. □

In this chapter, it is crucial to note that we are mainly interested in the strong convergence of the EM scheme. Therefore, it is clear to emphasize that we need to focus on the approximation of the sample paths of the SFPDEs. Our main task is to state and prove results similar to those in [222] while showing the convergence.

The results in the above theorem can be generalized to compute the expected error $\mathbb{E}[\sup_{0\leq s\leq t} |u(s)|^p]$ for $2 \leq p < \infty$, if the assumption, $\mathbb{E}[\sup_{0\leq s\leq t} |u_0|^p] < \infty$ is satisfied. This fact is stated and proved in the result below.

THEOREM 4.2.2. *If assumption* (4.3) *to* (4.8) *hold, then FSDE* (4.2) *has a unique solution* u *such that*

$$\mathbb{E}[\sup_{0\leq x\leq t}|u(x)|^p]<\infty,\quad t\in[0,T]. \tag{4.56}$$

Proof. Recall from (4.13) that

$$\begin{aligned}u(t)=&u(0)+u(0)\int_0^t\frac{\lambda}{(1-\alpha(s))}e^{\frac{-s\alpha(s)}{(1-\alpha(s))}}ds+\int_0^t\mathcal{K}(t,s)u(s)ds\\&+\int_0^t f(u(s))ds+\int_0^t b(u(s))dW(s)\quad a.s..\end{aligned} \tag{4.57}$$

We raise (4.57) to the power p and since $p>2$, we can apply Jensen's inequality to the corresponding relation to obtain:

$$\begin{aligned}&\mathbb{E}\sup_{0\leq x\leq t}|u(t)|^p\\&\leq 5^{p-1}\mathbb{E}|u_0|^p+5^{p-1}\mathbb{E}|u_0|^p\sup_{0\leq x\leq t}\left|\int_0^x\frac{\lambda}{1-\alpha(s)}e^{\frac{-s\alpha(s)}{1-\alpha(s)}}ds\right|^p+5^{p-1}\mathbb{E}\sup_{0\leq x\leq t}\left|\int_0^x\mathcal{K}(x,s)u(s)ds\right|^p+\\&+5^{p-1}\mathbb{E}\sup_{0\leq x\leq t}\left|\int_0^x f(u(s))ds\right|^p+5^{p-1}\mathbb{E}\sup_{0\leq x\leq t}\left|\int_0^x b(u(s))dW(s)\right|^p\\&=5^{p-1}\mathbb{E}|u_0|^p+5^{p-1}\mathcal{I}_1(x)+5^{p-1}\mathcal{I}_2(x)+5^{p-1}\mathcal{I}_3(x)+5^{p-1}\mathcal{I}_4(x).\end{aligned} \tag{4.58}$$

Similarly as in the proof of Theorem 4.2.1, we can estimate the term $\mathcal{I}_1(x)$ as follows:

$$\mathcal{I}_1(x)\leq\frac{\lambda^p}{(1-\alpha^*)^p}T. \tag{4.59}$$

To estimate the term $\mathcal{I}_2(x)$, we apply Holder's inequality to get

$$\begin{aligned}\mathcal{I}_2(x)&\leq\mathbb{E}\sup_{0\leq x\leq t}\left[\int_0^x|\mathcal{K}(x,s)|^{p-1}ds\right]^{\frac{p}{p-1}}\int_0^x|u(s)|^pds\\&\leq\mathbb{E}\sup_{0\leq x\leq t}x^{\frac{p}{p-1}}\left[\frac{\lambda^{p-1}}{(1-\alpha^*)^{p-1}}\right]^{\frac{p}{p-1}}\int_0^x|u(s)|^pds\\&\leq T^{\frac{p}{p-1}}\frac{\lambda^p}{(1-\alpha^*)^p}\mathbb{E}\sup_{0\leq x\leq t}\int_0^x|u(s)|^pds.\end{aligned} \tag{4.60}$$

In order to estimate the term $\mathcal{I}_3(x)$, we deploy assumption 4.6 in item (ii) along with Holder's

inequality to obtain that

$$\begin{aligned}
\mathcal{I}_3(x) &\leq \mathbb{E}\sup_{0\leq x\leq t}\left|\int_0^x f(u(s))ds\right|^p \\
&\leq \mathbb{E}\sup_{0\leq x\leq t}\left[\left(\int_0^x 1^{(p-1)}ds\right)^{\frac{1}{p-1}}\left(\int_0^x |f(u(s))|^p ds\right)^{\frac{1}{p}}\right]^p \\
&\leq \mathbb{E}\sup_{0\leq x\leq t}\left[x^p\int_0^x |f(u(s))|^p ds\right] \\
&\leq T^p\mathbb{E}\sup_{0\leq x\leq t}\int_0^x |f(u(s))|^p ds \\
&\leq T^p L_C\mathbb{E}\sup_{0\leq x\leq t}\int_0^x (1+|u(s)|)^p ds \\
&\leq T^p C L_C^p\mathbb{E}\sup_{0\leq x\leq t}\int_0^x (1+|u(s)|^p) ds \\
&\leq T^{p+1}CL_C^p + T^pCL_C^p\mathbb{E}\sup_{0\leq x\leq t}\int_0^x |u(s)|^p ds. \qquad (4.61)
\end{aligned}$$

As for the term $\mathcal{I}_4(x)$, we use assumption (4.7) and we apply Holder and BDG inequalities to assert that there exists a constant $C>0$ such that

$$\begin{aligned}
\mathcal{I}_4(x) \leq& \mathbb{E}\sup_{0\leq x\leq t}\left|\int_0^x b(u(s))dW(s)\right|^p \\
&\leq C\mathbb{E}\left|\int_0^t |b(u(s))|^2 ds\right|^{\frac{p}{2}} \\
&\leq C\mathbb{E}\left[\left(\int_0^t 1^q ds\right)^{\frac{1}{q}}\left(\int_0^t |b(u(s))|^p ds\right)^{\frac{2}{p}}\right]^{\frac{p}{2}} \\
&\leq C\mathbb{E}\left[t^{\frac{p-2}{2}}\int_0^t |b(u(s))|^p ds\right] \\
&\leq T^{\frac{p-2}{2}}C\mathbb{E}L_C^p\int_0^t (1+|u(s)|^p)ds \\
&\leq T^{\frac{p}{2}}CL_C^p + T^{\frac{p-2}{2}}CL_C^p\mathbb{E}\sup_{0\leq x\leq t}\int_0^x |u(s)|^p ds, \qquad (4.62)
\end{aligned}$$

where q is the conjugate of $\frac{p}{2}$ and it is given by $q=\frac{p}{p-2}$.

Combining all the estimates (4.59) - (4.62), we infer from (4.58) that

$$\begin{aligned}\mathbb{E}\sup_{0\le x\le t}|u(t)|^p \le & 5^{p-1}\mathbb{E}|u_0|^p + 5^{p-1}\mathbb{E}|u_0|^p\frac{\lambda^p}{(1-\alpha^*)^p}T \\ & + 5^{p-1}T^{\frac{2p-1}{p-1}}\frac{\lambda^p}{(1-\alpha^*)^p}\mathbb{E}\sup_{0\le x\le t}\int_0^x|u(s)|^p ds + +5^{p-1}T^{p+1}CL_C^p \\ & + 5^{p-1}T^{p+1}CL_C^p\mathbb{E}\sup_{0\le x\le t}\int_0^x|u(s)|^p ds + 5^{p-1}T^{\frac{p}{2}}CL_C^p + \\ & + 5^{p-1}T^{\frac{p}{2}}CL_C^p\mathbb{E}\sup_{0\le x\le t}\int_0^x|u(s)|^p ds \end{aligned} \tag{4.63}$$

from which we infer that

$$\mathbb{E}\sup_{0\le x\le t}|u(x)|^p \le \kappa_1 + \kappa_2\mathbb{E}\sup_{0\le x\le t}\int_0^x|u(s)|^p ds, \tag{4.64}$$

where κ_1 and κ_2 are constants depending on p, T and λ.
By virtue of Gronwall's inequality applied to (4.64), we deduce that there exists a constant κ such that

$$\mathbb{E}\sup_{0\le x\le t}|u(t)|^p \le \kappa. \tag{4.65}$$

Arguing similarly as in the proof of Theorem 4.2.1, it is sufficient to assert that there exists a constant κ_3 depending only on p, T, λ such that

$$\mathbb{E}\sup_{0\le t\le T}|u(t)|^p \le \kappa_3. \tag{4.66}$$

This conclude the desired proof of the theorem.

□

4.3 Strong Convergence of the EM Scheme

In this section, we develop the EM scheme of (4.2) and conveniently investigate its strong convergence under some more weaker assumptions than those in the literature. Mainly, we will study the strong convergence of the SFPDEs with one-sided Lipschitz coefficients. Before stating and proving results similar to those above, we first construct the EM approximation scheme.

4.3.1 Derivation of the Scheme

Let us first fix $N \in \mathbb{N}$ and suppose $n \in [0, N]$ and $\tau := \frac{T}{N}$ and set $t_n := n\tau$ and $\Delta W_n = W(\tau_{n+1}) - W(\tau_n)$. Using the Euler quadrature at t_n for $n \in [1, N]$, we can discretize the

right-hand side of equation (4.13).
Firstly, let us discretize the second term by using

$$\begin{aligned} u(0)\int_0^{t_n}\frac{\lambda}{(1-\alpha(t_n))}e^{\frac{-s\alpha(t_n)}{(1-\alpha(t_n))}}ds =& u(0)\sum_{l=0}^{n-1}\int_{t_l}^{t_{l+1}}\frac{\lambda}{(1-\alpha(t_n))}e^{\frac{-s\alpha(t_n)}{(1-\alpha(t_n))}}ds \\ =& u(0)\frac{\lambda}{\alpha(t_n)}(1-e^{\frac{-t_n\alpha(t_n)}{(1-\alpha(t_n))}}). \end{aligned} \tag{4.67}$$

Secondly, we discretize the third term. Instead of classical SDEs or constant-order FSDEs, its kernel is non-local without a convolution structure. It is difficult to discretize, but to simplify, we first bound the kernel using (4.11), then discretized the bounded equation.

$$\begin{aligned} \int_0^{t_n}\mathcal{K}(t,s)u(s)ds \leq& \frac{\lambda}{1-\alpha^*}\int_0^{t_n}u(s)ds = \frac{\lambda}{1-\alpha^*}\sum_{l=0}^{n-1}\int_{t_l}^{t_{l+1}}u(s)ds \\ \approx& \frac{\lambda}{1-\alpha^*}\int_{t_l}^{t_{l+1}}u(t_l)ds = \frac{\lambda\Delta t}{1-\alpha^*}\sum_{l=0}^{n-1}u(t_l) \\ =& \frac{\lambda\tau}{1-\alpha^*}\sum_{l=0}^{n-1}u(t_l). \end{aligned} \tag{4.68}$$

Next let's discretize the fourth term

$$\begin{aligned} \int_0^t f(u(s))ds =& \sum_{l=0}^{n-1}\int_{t_l}^{t_{l+1}}f(u(s))ds \\ \approx& \int_{t_l}^{t_{l+1}}f(u(t_l))ds = \tau\sum_{l=0}^{n-1}f(u(t_l)). \end{aligned} \tag{4.69}$$

Finally let's discretize the fifth term.

$$\begin{aligned} \int_0^t b(u(s))dW =& \sum_{l=0}^{n-1}\int_{t_l}^{t_{l+1}}b(u(s))dW(s) \\ \approx& \sum_{l=0}^{n-1}\int_{t_l}^{t_{l+1}}b(u(t_l))dW(s) = \sum_{l=0}^{n-1}b(u(t_l))\Delta W_l, \end{aligned} \tag{4.70}$$

where $\Delta W_l \sim N(0,\tau)$ and $\sim N(0,\tau)$ is a Gaussian random variable with zero mean and variance τ.
The EM scheme of (4.2) is built by incorporating the discretizations (4.67) through (4.70) and (4.13) from which we define recursively v_n, for $n \in \{1,2,\ldots,N\}$ and the initial value

$v_0 := u_0$, by setting

$$\begin{aligned} v_n =& u_0 + u_0\frac{\lambda}{\alpha(t_n)}(1 - e^{\frac{-t_n\alpha(t_n)}{(1-\alpha(t_n))}}) + \int_0^{t_n} \mathcal{K}(t,s)u(s)ds \\ &+ \tau\sum_{l=0}^{n-1} f(u(t_l)) + \sum_{l=0}^{n-1} b(u(t_l))\Delta W_l \\ &\approx u_0 + u_0\frac{\lambda}{\alpha(t_n)}(1 - e^{\frac{-\alpha(t_n)(t_n)}{(1-\alpha(t_n))}}) + \frac{\lambda\tau}{1-\alpha^*}\sum_{l=0}^{n-1} u(t_l) \\ &+ \tau\sum_{l=0}^{n-1} f(u(t_l)) + \sum_{l=0}^{n-1} b(u(t_l))\Delta W_l. \end{aligned} \tag{4.71}$$

The EM approximation gives us the closest values for the solution of the underlying problem but this is done only at the grid points, hence it makes the EM approximation v_n for $n \in \{1, 2, \ldots, N\}$ much easier to implement in the numerical aspect of the problem. We now ready to introduce the following result.

THEOREM 4.3.1. *Under the assumptions* (4.3)-(4.7)*, for each* $n \in \{1, 2, 3, \ldots, N\}$*, the solution of* (4.71)*,* v_n*, satisfies the estimate*

$$\mathbb{E}|v_n^2| \leq Q_1(1 + E_{\alpha^*}(Q_2\Gamma(\alpha^*))), \tag{4.72}$$

where the constants Q_1 *and* Q_2 *are given by*

$$\begin{aligned} Q_1 &= 5\mathbb{E}[u_0^2](1 + (\frac{\lambda}{\alpha^*})^2) + 10L^2T(T+1), \\ Q_2 &= 10L^2TN(T+1) + 5N(\frac{\lambda T}{1-\alpha^*})^2. \end{aligned} \tag{4.73}$$

Proof. Using Jensen's inequality with $m = 5$ along with Cauchy inequality, we can bound the solution of (4.71), v_n, as follows:

$$\begin{aligned} \mathbb{E}|v_n^2| \leq& 5\mathbb{E}|u_0^2| + 5\mathbb{E}(u_0\frac{\lambda}{\alpha(t_n)}(1 - e^{\frac{-\alpha(t_n)(t_n)}{(1-\alpha(t_n))}}))^2 + 5\mathbb{E}(\int_0^{t_n} \mathcal{K}(t,s)u(s)ds)^2 \\ &+ 5\tau^2\mathbb{E}(\sum_{l=0}^{n-1} f(u(t_l))^2 + 5\mathbb{E}(\sum_{l=0}^{n-1} b(u(t_l))\Delta W_l)^2. \end{aligned} \tag{4.74}$$

Let bound the second term of (4.74), we have

$$\begin{aligned} 5\mathbb{E}[(u_0\frac{\lambda}{\alpha(t_n)}(1 - e^{\frac{-\alpha(t_n)(t_n)}{(1-\alpha(t_n))}})^2] &\leq 5\mathbb{E}[(u_0\frac{\lambda}{\alpha(t_n)})^2] \\ &\leq 5(\frac{\lambda}{\alpha^*})^2\mathbb{E}[(u_0)^2]. \end{aligned} \tag{4.75}$$

Next, let's bound the fourth term of (4.74) in a similar fashion as in [222]. We apply the Cauchy's inequality and use assumptions (4.3) through (4.8) to get

$$\begin{aligned}5\tau^2\mathbb{E}[(\sum_{l=0}^{n-1} f(v_l))^2] \leq & 10L^2T^2\tau\sum_{l=0}^{n-1}\mathbb{E}[1+v_l^2] \\ & \leq 10L^2T^2 + 10L^2T\tau\sum_{l=0}^{n-1}\mathbb{E}[v_l^2] \\ & \leq 10L^2T^2 + 10L^2T^2\sum_{l=0}^{n-1}\mathbb{E}[v_l^2]. \end{aligned} \tag{4.76}$$

Now we estimate the fifth term of (4.74). In a similar fashion as in [222]. We use Ito's isometry and assumption (4.3) to (4.8) to obtain the desired bound as follows:

$$\begin{aligned}5\mathbb{E}[(\sum_{l=0}^{n-1} b(v_l)\Delta w_l)^2] = & 5\tau\sum_{l=0}^{n-1}\mathbb{E}[b(v_l)^2] \leq 10L^2\tau\sum_{l=0}^{n-1}\mathbb{E}[1+v_l^2] \\ & \leq 10L^2T + 10L^2\tau\sum_{l=0}^{n-1}\mathbb{E}[v_l^2] \\ & \leq 10L^2T + 10L^2T\sum_{l=0}^{n-1}\mathbb{E}[v_l^2]. \end{aligned} \tag{4.77}$$

We will now examine the estimate of the third component of (4.74), which is unfamiliar with numerical approximations of conventional SDEs. Using assumptions (4.3) to (4.8) and the relation (4.68), we obtain the following.

$$\begin{aligned}5\mathbb{E}[(\int_0^{t_n}\mathcal{K}(t,s)u(s)ds)^2] \leq & 5\mathbb{E}((\frac{\lambda T}{1-\alpha^*})^2(\sum_{l=0}^{n-1}u(t_l))^2) \\ & = 5(\frac{\lambda T}{1-\alpha^*})^2\sum_{l=0}^{n-1}\mathbb{E}(u(t_l))^2 \\ & \leq 5(\frac{\lambda T}{1-\alpha^*})^2\sum_{l=0}^{n-1}\mathbb{E}[v_l^2]. \end{aligned} \tag{4.78}$$

Combining approximations (4.75), (4.76), (4.77) and (4.78) into (4.74) and applying the

inequality $(n-l)^{1-\alpha^*} \leq N^{1-\alpha^*}$ to infer that

$$\begin{aligned}
\mathbb{E}[v_n^2] &\leq 5\mathbb{E}[u_0^2] + 5(\frac{\lambda}{\alpha^*})^2\mathbb{E}[(u_0)^2] + 10L^2T^2 + 10L^2T^2\sum_{l=0}^{n-1}\mathbb{E}[v_l^2] + 10L^2T \\
&+ 10L^2T\sum_{l=0}^{n-1}\mathbb{E}[v_l^2] + 5(\frac{\lambda T}{1-\alpha^*})^2\sum_{l=0}^{n-1}\mathbb{E}[v_l^2] \\
&= Q_1 + (10L^2T(T+1) + 5(\frac{\lambda T}{1-\alpha^*})^2)\frac{N^{\alpha^*}}{N^{\alpha^*}}\sum_{l=0}^{n-1}\frac{\mathbb{E}[v_l^2](n-l)^{1-\alpha^*}}{(n-l)^{1-\alpha^*}} \\
&\leq Q_1 + (10L^2T(T+1) + 5(\frac{\lambda T}{1-\alpha^*})^2)\frac{N^{\alpha^*}}{N^{\alpha^*}}\sum_{l=0}^{n-1}\frac{\mathbb{E}[v_l^2](N)^{1-\alpha^*}}{(n-l)^{1-\alpha^*}} \\
&= Q_1 + (10L^2T(T+1) + 5(\frac{\lambda T}{1-\alpha^*})^2)\frac{N}{N^{\alpha^*}}\sum_{l=0}^{n-1}\frac{\mathbb{E}[v_l^2]}{(n-l)^{1-\alpha^*}} \\
&= Q_1 + \frac{Q_2}{N^{\alpha^*}}\sum_{l=0}^{n-1}\frac{\mathbb{E}[v_l^2]}{(n-l)^{1-\alpha^*}}, \qquad (4.79)
\end{aligned}$$

where Q_1 and Q_2 being given as in (4.73).
By applying the result from Lemma 2.3.6 and using (4.79) we deduce that

$$\mathbb{E}[v_n^2] \leq Q_1(1 + E_{\alpha^*}(Q_2\Gamma(\alpha^*))).$$

Hence, this concludes the proof of the desired result stated in this theorem. □

For us to study the strong convergence, we first fix $(\Omega, \mathcal{F}, \mathbb{F}, \mathbb{P})$, the filtered probability space with the complete filtration satisfying the usual conditions, $\mathbb{F}$. In the sequel, we assume the assumptions (4.3) - (4.8) hold.

4.3.2 Auxiliary Equation and Its Error Estimates

In order to study the strong convergence of the EM scheme, we construct an equivalent form of the extension of the EM approximation, which is a new continuous-time SP $v(t)$ on $[0,T]$ based on the step function $\hat{s} = \hat{s}(s)$. Suppose $\hat{s} = t_n$ for $t_n \leq s \leq t_{n+1}$ and $n \in \{0,1,2,\ldots,N-1\}$ hence the equivalent form is given by

$$\begin{aligned}
v(t) =& u(0) + u(0)\int_0^t \frac{\lambda}{(1-\alpha(s))}e^{\frac{-\alpha(s)\hat{s}}{(1-\alpha(s))}}ds + \int_0^t \mathcal{K}(t,s)v(\hat{s})ds \\
&+ \int_0^t f(v(\hat{s}))ds + \int_0^t b(v(\hat{s}))dW \quad \text{for all } t \in [t_n.t_{n+1}) \ \textbf{a.s..} \qquad (4.80)
\end{aligned}$$

LEMMA 4.3.1. *Let $\{v_n\}_{n=0}^N$ be the solution of the EM scheme and v be the continuous-time SP defined by (4.80) then $\{v(t_n)\} = v_n$ for $0 \leq n \leq N$.*

Proof. The proof of this result is a simple follow up of the result in Lemma 3.2 of Zhiwei et al. [222] where a detailed description of the proof is given. □

The aim of this section is to prove the convergence, we start by stating that the p-moment of the EM approximation can also be estimated using same techniques similar to the previous result. For this purpose, let $N \geq 1$ be a fixed natural integer and set $\Delta = \frac{T}{N}$ and $0 < t_1 < t_2 < \cdots < t_N := T$ where $\tau_n := n\Delta$ for $n \in \{1, 2, \ldots, N\}$. Now we can state the following result.

LEMMA 4.3.2. *For $n \in \{0, 1, 2, \ldots, N\}$ and N fixed, let v_n be the EM approximation at time t_n given in*

$$\begin{aligned} v_n =& u_0 + u_0 \frac{\lambda}{\alpha(t_n)}(1 - e^{\frac{-t_n\alpha(t_n)}{(1-\alpha(t_n))}}) + \int_0^{t_n} \mathcal{K}(t,s)u(s)ds \\ &+ \tau \sum_{l=0}^{n-1} f(u(t_l)) + \sum_{l=0}^{n-1} b(u(t_l))\Delta W_l \\ &\approx u_0 + u_0 \frac{\lambda}{\alpha(t_n)}(1 - e^{\frac{-\alpha(t_n)(t_n)}{(1-\alpha(t_n))}}) + \frac{\lambda\tau}{1-\alpha^*} \sum_{l=0}^{n-1} u(t_l) \\ &+ \tau \sum_{l=0}^{n-1} f(u(t_l)) + \sum_{l=0}^{n-1} b(u(t_l))\Delta W_l. \end{aligned} \tag{4.81}$$

Then, there exists a finite constant $C > 0$ such that

$$\mathbb{E}(|v_n|^p) \leq C \quad \forall\ n \geq 1 \quad \text{and} \quad p \geq 1. \tag{4.82}$$

Proof. For $n = 0$, we have $v_0 := u_0$ and since $\mathbb{E}(|u_0|^p) < \infty$ for any $p \geq 1$ by hypothesis, we can directly assert and verify that $\mathbb{E}(|v_0|^p) < \infty$. It is enough to show using mathematical induction techniques that

$$\mathbb{E}(|v_n|^p) < \infty$$

which will follow from

$$\mathbb{E}(|v_{n+1}|^p) < \infty.$$

For this purpose, we recall the EM approximation at time t_n given in

$$\begin{aligned} v_n =& u_0 + u_0\frac{\lambda}{\alpha(t_n)}(1-e^{\frac{-t_n\alpha(t_n)}{(1-\alpha(t_n))}}) + \int_0^{t_n}\mathcal{K}(t,s)u(s)ds \\ &+ \tau\sum_{l=0}^{n-1} f(u(t_l)) + \sum_{l=0}^{n-1} b(u(t_l))\Delta W_l \\ &\approx u_0 + u_0\frac{\lambda}{\alpha(t_n)}(1-e^{\frac{-\alpha(t_n)(t_n)}{(1-\alpha(t_n))}}) + \frac{\lambda\tau}{1-\alpha^*}\sum_{l=0}^{n-1} u(t_l) \\ &+ \tau\sum_{l=0}^{n-1} f(u(t_l)) + \sum_{l=0}^{n-1} b(u(t_l))\Delta W_l. \end{aligned} \tag{4.83}$$

since $v(t_n) = v_n$.
Therefore, we first fix $n \geq 1$ and we assume that

$$\mathbb{E}(|v_n|^p) < \infty.$$

In light of the above, to carry on with the required proof, it sufficient to raise the relation (4.83) to the power p and using assumption on f and b along with applying Jensen's inequality with $m = 5$, we obtain

$$\begin{aligned} &\mathbb{E}(|v_{n+1}|^p) \\ &\leq 5^{p-1}\mathbb{E}|v_0|^p + 5^{p-1}\mathbb{E}\left|u_0\frac{\lambda}{\alpha(t_n)}(1-e^{\frac{-t_n\alpha(t_n)}{(1-\alpha(t_n))}})\right|^p + 5^{p-1}\mathbb{E}\left|\int_0^{t_n}\mathcal{K}(t,s)u(s)ds\right|^p \\ &+ 5^{p-1}\mathbb{E}\left|\tau\sum_{l=0}^{n-1} f(u(t_l))\right|^p + 5^{p-1}\mathbb{E}\left|\sum_{l=0}^{n-1} b(u(t_l))\Delta W_l\right|^p \\ &\leq 5^{p-1}\mathbb{E}|v_0|^p + 5^{p-1}\frac{\lambda^p}{(\alpha(t_n))^p}\frac{1}{(1-\alpha^*)^p}\mathbb{E}|v_0|^p + 5^{p-1}\frac{\lambda^p}{(1-\alpha^*)^p}\Delta^p\mathbb{E}\left|u(t_n)\right|^p \\ &+ 5^{p-1}\Delta^p\tau^p\mathbb{E}\left|f(u(t_n))\right|^p + 5^{p-1}\Delta^p\mathbb{E}\left|b(u(t_n)\right|^p\left|\Delta W_l\right|^p \\ &\leq 5^{p-1}\mathbb{E}|v_0|^p + 5^{p-1}\frac{\lambda^p}{(\alpha(t_n))^p}\frac{1}{(1-\alpha^*)^p}\mathbb{E}|v_0|^p + 5^{p-1}\frac{\lambda^p}{(1-\alpha^*)^p}\Delta^p\mathbb{E}\left|u(t_n)\right|^p \\ &+ 5^{p-1}\Delta^p\tau^p C_2\mathbb{E}\left[1+|u(t_n)|^p\right] + 5^{p-1}\Delta^p C_3\mathbb{E}\left[1+|u(t_n)|^p\right]\mathbb{E}\left[|\Delta W_l|^{2p}\right]^{\frac{1}{2}}. \end{aligned} \tag{4.84}$$

By virtue of BDG's inequality, we assert that there exists a constant $C > 0$ such that

$$\mathbb{E}|\Delta W_l|^{2p} \leq c_p\Delta^p \leq c_p T^p, \tag{4.85}$$

from which we infer that

$$\begin{aligned} \mathbb{E}(|v_{n+1}|^p) \leq\ & 5^{p-1}\mathbb{E}|v_0|^p + 5^{p-1}\frac{\lambda^p}{(\alpha(t_n))^p}\frac{1}{(1-\alpha^*)^p}\mathbb{E}|v_0|^p + 5^{p-1}\frac{\lambda^p}{(1-\alpha^*)^p}\Delta^p\mathbb{E}\left|v_n\right|^p \\ &+ 5^{p-1}\Delta^p\tau^p C_2\mathbb{E}\left[1+|v_n|^p\right] + 5^{p-1}\Delta^p C_3\mathbb{E}\left[1+|v_n|^p\right]CT^{\frac{p}{2}}. \end{aligned} \tag{4.86}$$

Therefore, we deduce that

$$\mathbb{E}(|v_{n+1}|^p) < \infty \; for any \; n \geq 1 \; and \; p \geq 1. \tag{4.87}$$

This finally proves the desired result. □

We are now ready to state and prove the following theorem concerning the convergence of the EM approximating scheme.

THEOREM 4.3.2. *The following estimate holds for the continuous time SP v defined by (4.80) for any $t \in [t_n, t_{n+1})$ and $n \in \{0, 1, 2, \ldots, N-1\}$. Then*

$$\mathbb{E}[(v(t) - v(t_n))^2] \leq M_1 + M_2.$$

Here the constants M_1 and M_2 are given by,

$$M_1 = 6L^2\tau Q_1(1+\tau) \; and$$

$$M_2 = 6\tau Q_1[L^2(1+\tau) + 5(\frac{\lambda}{1-\alpha^*})^2][1 + E_{\alpha^*}(Q_2\Gamma(\alpha^*))]. \tag{4.88}$$

Proof. Owing to relations (4.80) and (4.13) at time t_n, for $t \in [t_n, t_{n+1})$ and $n \in [0, N-1]$ then implement Jensen's inequality at $m = 3$ to obtain

$$\left(\int_a^c f ds - \int_a^b g ds\right)^2 = \left(\int_a^b (f-g) ds + \int_b^c f ds\right)^2, \text{ for } a < b < c.$$

Hence

$$\left(\int_a^b (f-g) ds + \int_b^c f ds\right)^2 \leq 2\left(\int_a^b (f-g) ds\right)^2 + 2\left(\int_b^c f ds\right)^2$$

to obtain

$$\begin{aligned}
\mathbb{E}[(v(t) - v(t_n))^2] \leq \; & 3\mathbb{E}\left(\int_0^t \mathcal{K}(t,s)v(\hat{s})ds - \int_0^{t_n} \mathcal{K}(t_n,s)v(\hat{s})ds\right)^2 \\
& + 3\mathbb{E}\left(\int_0^t f(v(\hat{s}))ds - \int_0^{t_n} f(v(\hat{s}))ds\right)^2 \\
& + 3\mathbb{E}\left(\int_0^t b(v(\hat{s}))dW(s) - \int_0^{t_n} b(v(\hat{s}))dW(s))\right)^2 \\
& \leq 6\mathbb{E}\left(\int_0^{t_n} (\mathcal{K}(t,s) - \mathcal{K}(t_n,s))v(\hat{s})ds\right)^2 + 6\mathbb{E}\left(\int_{t_n}^t \mathcal{K}(t,s)v(\hat{s})ds\right)^2 \\
& + 3\mathbb{E}\left(\int_{t_n}^t f(v(\hat{s}))ds\right)^2 + 3\mathbb{E}\left(\int_{t_n}^t b(v(\hat{s}))dW(s)\right)^2.
\end{aligned} \tag{4.89}$$

Next, we bound the third term of (4.89) using Theorem 4.3.1 and assumption (4.3) to (4.8), we get

$$\begin{aligned} 3\mathbb{E}\left(\int_{t_n}^{t} f(v(\hat{s}))ds\right)^2 \leq\ & 3\tau\int_{t_n}^{t}\mathbb{E}[f(v(\hat{s}))^2]ds \leq 6L^2\tau\int_{t_n}^{t}(1+\mathbb{E}[|v_n|^2]ds \\ =\ & 6L^2\tau^2(1+\mathbb{E}[|v_n|^2]) \leq 6L^2\tau^2Q_1[1+(1+E_{\alpha^*}(Q_2\Gamma(\alpha^*)))]. \end{aligned} \tag{4.90}$$

We employ Itô isometry, Theorem 4.3.1 and assumption (4.3) to (4.8) to bound the last term of the right-hand side of (4.89).

$$\begin{aligned} 3\mathbb{E}\left(\int_{t_n}^{t} b(v(\hat{s}))dW(s)\right)^2 &= 3\mathbb{E}\int_{t_n}^{t} b(v(\hat{s}))^2ds \leq 6L^2\tau(1+\mathbb{E}[|v_n|^2]) \\ &\leq 6L^2\tau[1+Q_1(1+E_{\alpha^*}(Q_2\Gamma(\alpha^*)))]. \end{aligned} \tag{4.91}$$

The remaining terms of (4.89) have neither local nor convolutional structures, which are unfamiliar in conventional SDEs and constant-order FSDEs. Let us estimate them one by one. Using the Cauchy inequality and (4.11), we will link the second term (4.89).

$$\begin{aligned} 6\mathbb{E}\left(\int_{t_n}^{t}\mathcal{K}(t_n,s)v(\hat{s})ds\right)^2 &\leq 6\int_{t_n}^{t}|\mathcal{K}(t_n,s)|^2\mathbb{E}[v(\hat{s})]^2ds \\ &\leq 6(\frac{\lambda}{1-\alpha^*})^2\int_{t_n}^{t}\mathbb{E}[v(\hat{s})]^2ds \leq 6(\frac{\lambda}{1-\alpha^*})^2\tau\mathbb{E}[v_n]^2 \\ &\leq 6(\frac{\lambda}{1-\alpha^*})^2\tau Q_1[1+E_{\alpha^*}(Q_2\Gamma(\alpha^*))]. \end{aligned} \tag{4.92}$$

Next, we used Cauchy-Schwarz inequality to bound the first term of (4.89) from the inequality below:

$$\begin{aligned} &6\mathbb{E}\left(\int_0^{t_n}(\mathcal{K}(t,s)-\mathcal{K}(t_n,s))v(\hat{s})ds\right)^2 \\ &\leq 6\int_0^{t_n}|\mathcal{K}(t,s)-\mathcal{K}(t_n,s)|^2\mathbb{E}[v_n]^2ds \\ &\leq 12\int_0^{t_n}(|\mathcal{K}(t,s)|^2+|\mathcal{K}(t_n,s)|^2)\mathbb{E}[v_n]^2ds \\ &\leq 24(\frac{\lambda}{1-\alpha^*})^2\tau\mathbb{E}[v_n]^2 \leq 24(\frac{\lambda}{1-\alpha^*})^2\tau Q_1[1+E_{\alpha^*}(Q_2\Gamma(\alpha^*))]. \end{aligned} \tag{4.93}$$

Inserting the outcomes of (4.90) through (4.93) into (4.89), we get

$$\begin{aligned}\mathbb{E}[(v(t)-v(t_n))^2] &\le 6L^2\tau^2 Q_1[1+(1+E_{\alpha^*}(Q_2\Gamma(\alpha^*))]+6L^2\tau[1+Q_1(1+E_{\alpha^*}(Q_2\Gamma(\alpha^*)))]\\ &\quad+6(\frac{\lambda}{1-\alpha^*})^2\tau Q_1[1+E_{\alpha^*}(Q_2\Gamma(\alpha^*))]+24(\frac{\lambda}{1-\alpha^*})^2\tau Q_1[1+E_{\alpha^*}(Q_2\Gamma(\alpha^*))]\\ &= 6L^2\tau(Q_1\tau+1)+6\tau Q_1[L^2(1+\tau)+5(\frac{\lambda}{1-\alpha^*})^2][1+E_{\alpha^*}(Q_2\Gamma(\alpha^*))]\\ &= M_1+M_2,\end{aligned}$$

where M_1 and M_2 being given in (4.88). Hence the proof is complete. □

4.3.3 Error Estimate of the EM Scheme

In this part, we can estimate the error of the strong convergence of the EM scheme (4.71) which is the chapter's main contribution. As a matter of fact, in order to do this, we start by estimating the error of the process $u(t)-v(t)$.

THEOREM 4.3.3. *Let u and v be the solutions to the variable-order FSDE* (4.2) *and the auxiliary* (4.80)*, respectively. Then the following estimate holds*

$$\max_{t\in[0,T]}\mathbb{E}[|u(t)-v(t)|^2] \le Q_3 E_{\alpha^*}[Q_4\Gamma(\alpha^*)t^{\alpha^*}],$$

where the constants Q_3 and Q_4 are given by

$$Q_3 = 6T[M_1+M_2]((\frac{\lambda}{1-\alpha^*})^2+L^2(T+1)) \text{ and}$$

$$Q_4 = 6((\frac{\lambda}{1-\alpha^*})^2+L^2(T+1))\int_0^t \mathbb{E}[u(s)-v(s)]^2 ds. \tag{4.94}$$

Proof. For any $0\le t\le T$, let $t\in[t_n,\ t_{n+1})$ for some $n\in[0,N-1)$. Subtract equation (4.80) from equation (4.13) to obtain

$$\mathbb{E}[(u(t)-v(t))^2] = J_1+J_2+J_3, \tag{4.95}$$

$$\begin{aligned}\text{where}\quad J_1 &= 3\mathbb{E}[(\int_0^t \mathcal{K}(t,s)(u(s)-v(\hat{s}))ds)^2],\\ J_2 &= 3\mathbb{E}[(\int_0^t (f(u(s))-f(v(\hat{s}))ds)^2],\\ J_3 &= 3\mathbb{E}[(\int_0^t (b(u(s))-b(u(\hat{s}))dW))^2].\end{aligned}$$

Let bound J_1 by Lemma 4.2.1 and Theorem 4.3.2 to obtain

$$\begin{aligned}
J_1 &= 3\mathbb{E}[(\int_0^t \mathcal{K}(t,s)(u(s)-v(\hat{s}))ds)^2] \\
&\leq 6\mathbb{E}[(\int_0^t \mathcal{K}(t,s)(u(s)-v(s))ds)^2] + 6\mathbb{E}[(\int_0^t \mathcal{K}(t,s)(v(s)-v(\hat{s}))ds)^2] \\
&\leq 6(\frac{\lambda}{1-\alpha^*})^2 \int_0^t \mathbb{E}[(u(s)-v(s))]^2 ds + 6(\frac{\lambda}{1-\alpha^*})^2 \int_0^t \mathbb{E}[(v(s)-v(\hat{s}))^2]ds \\
&\leq 6(\frac{\lambda}{1-\alpha^*})^2 \int_0^t \mathbb{E}[(u(s)-v(s))]^2 ds + 6T(\frac{\lambda}{1-\alpha^*})^2[M_1+M_2]. \qquad (4.96)
\end{aligned}$$

Apply assumption (4.3) to (4.8), Cauchy inequality and Theorem 4.3.2 to estimate J_2 by the following inequality:

$$\begin{aligned}
J_2 =& 3\mathbb{E}[(\int_0^t (f(u(s)-f(v(\hat{s}))ds)^2] \\
&\leq 3TL^2[(\int_0^t \mathbb{E}((u(s)-(v(\hat{s}))ds)^2] \\
&\leq 6TL^2(\int_0^t (\mathbb{E}[|u(s)-v(s)|^2] + \mathbb{E}[|v(s)-v(\hat{s})|^2])ds \\
&= 6TL^2 \int_0^t \mathbb{E}[|u(s)-v(s)|^2]ds + 6TL^2 \int_0^t \mathbb{E}[|v(s)-v(\hat{s})|^2]ds \\
&\leq 6TL^2 \int_0^t \mathbb{E}[|u(s)-v(s)|^2]ds + 6T^2L^2[M_1+M_2]. \qquad (4.97)
\end{aligned}$$

We use Itô isometry, assumption (4.3) to (4.8), Theorem 4.3.2 and split

$$u(s)-v(\hat{s}) = (u(s)-v(s)) + (v(s)-v(\hat{s}))$$

to bound J_3 by

$$\begin{aligned}
J_3 &= 3\mathbb{E}[(\int_0^t (b(u(s))-b(u(\hat{s}))dW))^2] = 3[(\int_0^t \mathbb{E}(b(u(s))-b(u(\hat{s}))^2(dW)^2] \\
&\leq 3L^2 \int_0^t (\mathbb{E}[|u(s)-u(\hat{s})|^2]ds \leq 6L^2 \int_0^t (\mathbb{E}[|u(s)-v(s)|^2] + \mathbb{E}[|v(s)-u(\hat{s})|^2])ds \\
&= 6L^2 \int_0^t \mathbb{E}[|u(s)-v(s)|^2]ds + 6L^2 \int_0^t \mathbb{E}[|v(s)-u(\hat{s})|^2]ds \\
&\leq 6L^2 \int_0^t \mathbb{E}[|u(s)-v(s)|^2]ds + 6TL^2[M_1+M_2]. \qquad (4.98)
\end{aligned}$$

Substitute estimates (4.80), (4.97) and (4.98) in to (4.95) to obtain

$$\begin{aligned}\mathbb{E}[(u(t)-v(t))^2] &\leq 6(\frac{\lambda}{1-\alpha^*})^2\int_0^t \mathbb{E}[u(s)-v(s)]^2ds + 6T(\frac{\lambda}{1-\alpha^*})^2[M_1+M_2]\\ &+ 6TL^2\int_0^t \mathbb{E}[|u(s)-v(s)|^2]ds + 6T^2L^2[M_1+M_2]\\ &+ 6L^2\int_0^t \mathbb{E}[|u(s)-v(s)|^2]ds + 6TL^2[M_1+M_2]\\ &\leq Q_3 + Q_4\int_0^t \mathbb{E}[u(s)-v(s)]^2ds\\ &\leq Q_3 + Q_4\int_0^t \frac{\mathbb{E}[u(s)-v(s)]^2}{(t-s)^{1-\alpha^*}}ds. \end{aligned} \tag{4.99}$$

Applying results of Lemma 2.3.5 to complete the proof of the results in Theorem 3.5 from (4.94)

$$\mathbb{E}[(u(t)-v(t))^2] \leq Q_3E_{\alpha^*}[Q_4\Gamma(\alpha^*)t^{\alpha^*}].$$

Hence the proof of this theorem is complete. □

The convergence analysis of the EM scheme for the Caputo-Fabrizio FSDE (4.2) involves challenges not encountered the classical SDE framework. For classical SDEs ($\alpha = 1$), the standard Gronwall inequality suffices to establish strong convergence because error propagation is bounded exponentially. In the present model ($0 < \alpha < 1$), the Caputo-Fabrizio derivative employs a non-singular exponential kernel. However, the variable-order parameter $\alpha(t)$ destroys the convolution structure, while the non-local nature of the FD couples the error across all previous time levels. Consequently, the error equation yields an integral inequality that can be treated the generalised Gronwall inequality (2.3.5).

The error bound in Theorem 4.3.3 depends on the Mittag-Leffler function $E_{\alpha^*}(\cdot)$, where α^* is the largest value of $\alpha(t)$ on the interval $[0, T]$. In the limiting case $\alpha^* = 1$, this function reduces to the exponential and the classical SDE convergence result is recovered. For $\alpha^* < 1$, the Mittag-Leffler function grows more slowly than an exponential, which reflects the fading memory of the fractional system. The precise convergence rate is determined by the constants Q_3 and Q_4 in Theorem 4.3.3, which depend on α^*, the Lipschitz constants and other problem parameters.

4.4 Numerical Results and Simulations

In this section, we focus on the approximation and numerical methods for the problem under consideration. In this study, we conduct numerical experiments by employing the EM scheme

(4.71) to assess its efficacy and performance.

4.4.1 Strong Convergence of the EM Scheme

In this subsection, we conduct a numerical test that shows the strong convergence of the EM scheme (4.71) to (4.2), along with the calculation of the corresponding errors. For more detailed exposition in the the EM topic, we refer to the work in [162, 222]. First we deal with the numerical part of the noise by setting

$$\Delta\omega_i = Z_i\sqrt{\Delta t_i} \tag{4.100}$$

where $Z_i \in N(0,1)$ is a random discrete-time Gaussian process and normally distributed. Note that each set of $\{\omega_0, \omega_1, \ldots\ldots, \omega_n\}$ produced by the EM method is an approximate solution of SP $u(t)$. Each ω_t is an approximate solution for the FSDE produced by the EM scheme.

Let $u(t_n, \omega_j)$ be the j^{th} independent sample path of the FSDE (4.2) evaluated at t_n with the numerical approximation $v_n(\omega_j)$ defined using the EM scheme (4.71) for $n = 0, 1, 2, \cdot, N$ and $j = 1, 2, ..., M$. Computing and estimating the mean-square distance (error) between numerical solution $u(t_n, \omega_j)$ and reference solution $v_n(\omega_j)$. The sample mean of the error e_τ and the convergence rate k are defined by

$$e_\tau = \max_{0\leq n\leq N}[\frac{1}{M}\sum_{j=1}^{M}|u(t_n,\omega_j) - v_n(\omega_j)|^2]^{\frac{1}{2}} \leq QN^{-k}, \tag{4.101}$$

where

$$k = \log_2 \frac{e_\tau}{e_{\frac{\tau}{2}}}. \tag{4.102}$$

In addition the variable order $\alpha(t)$ is chosen by

$$\alpha(t) = \alpha(1) + [\alpha(0) - \alpha(1)][1 - t - \frac{\sin(2\pi(1-t))}{2\pi}] \tag{4.103}$$

for more details, we refer [105, 104, 222].

Next, by illustrations, we demonstrate the convergence and stability properties of the methods presented in this chapter.

Taking into account all of the preceding formulas, we can now define the structure algorithm:

1. Find the reference solution at $N_{ref} = 2^{10} = 1,024$ because the analytical solution is unknown a priori;

2. In the numerical experiment, the inputs for the simulation are:

- the time interval $[0, T] = [0, 1]$;
- $\lambda = 1$;
- $M = 2^{10} = 1,024$;
- with the initial condition $u(0) = u_0, \mathbb{E}[u^2(0)] = \mathbb{E}[u_0^2] < \infty$;

3. Define the corresponding grid $(\omega_j, \Delta\omega, \Delta t, t_n)$ and notice that

- $\Delta t = \frac{T}{N}$ and $t_n = n\Delta t, n = 0, 1, 2, \ldots\ldots, N$;
- $\Delta\omega_i = Z_i\sqrt{\Delta t_i}, Z_i \in N(0, 1)$;

4. Compute the variable order α using

$$\alpha(t) = \alpha(1) + [\alpha(0) - \alpha(1)][1 - t - \frac{\sin(2\pi(1-t))}{2\pi}];$$

5. Compute the sample mean of the error e_τ as follows:

$$e_\tau = \max_{0\leq n\leq N}[\frac{1}{1,024}\sum_{j=1}^{1,024}|u(t_n, \omega_j) - v_n(\omega_j)|^2]^{\frac{1}{2}} \leq QN^{-k};$$

6. Compute the convergence rate k using (4.102) and set

$$k = \log_2[\frac{e_\tau}{e_{\frac{\tau}{2}}}].$$

EXAMPLE 4.4.1. For a linear variable-order FSDE, we choose $f(u) = b(u) = -u$ and $u_0 = 0.1$ in the variable-order FSDE (4.2). We present the error e_τ for different mesh size N and different choices of $\alpha(0)$ and $\alpha(1)$ in (4.103). We observe that the EM scheme (4.71) demonstrates the convergence rates and we note that both are in agreement with the theoretical results obtained in Theorem 4.3.3.

Table 4.1: Convergence of the scheme for the linear FSDE Example.

$(\alpha(0),\ \alpha(1))$	(0.2, 0.1)		(0.6, 0.3)		(0.8, 0.5)	
N	e_τ	k	e_τ	k	e_τ	k
8	4.40 e^-3	0.00	4.73e^-3	0	8.77 e^-3	0
16	4.38 e^-3	0.0070642	5.04e^-3	0.0924739	9.49e^-3	0.1148251
32	4.33 e^-3	0.0141644	5.12e^-3	0.0222736	9.72e^-3	0.0334769
64	4.25 e^-3	0.0284441	4.96e^-3	0.0445478	9.39 e^-3	0.0494342
128	4.08e^-3	0.0570356	4.47e^-3	0.1524107	8.22 e^-3	0.1926919
256	3.78e^-3	0.1109219	3.97e^-3	0.1714552	8.22 e^-3	0.00
$min(1-\alpha^*, 0.5)$		0.5		0.4		0.2

In the next examples, we include a one sided-Lipschitz case of nonlinear function f and b in order to illustrate the numerical examples and verify the efficiency of the EM scheme and the validity of Theorems 4.2.1, 4.3.1 and 4.2.2.

EXAMPLE 4.4.2. A linear variable-order FSDE. We choose $f(u) = b(u) = \sin u$ and $u_0 = 0.1$ in the variable-order FSDE (4.2). We present the error e_τ for different mesh size N and difference choices of $\alpha(0)$ and $\alpha(1)$ in (4.103). We observe that the EM scheme (4.71) demonstrates convergence rates and we note that both are in agreement with the theoretical results obtained in Theorem 4.3.3. We present the numerical results in tables 4.2 and have the same observations as in Example 4.4.1.

Since the above results for the nonlinear are not closely related, we can compute the sample paths many times with higher sample size to conclude the outcomes for this specific exam. For the following two examples, we assert the given functions satisfy assumptions in the above theorems, therefore the result holds for this cases.

Tables 4.1 and 4.2 present the convergence behavior of the EM scheme applied to linear and nonlinear variable-order FSDEs, respectively. In Table 4.1 , the linear problem is considered with $f(u) = b(u) = -u$ and initial condition $u_0 = 0.1$, while Table 4.2 examines the nonlinear case with $f(u) = b(u) = \sin(u)$ under the same initial condition. The numerical experiments are carried out for the fractional-order parameter pairs $(\alpha(0), \alpha(1)) = (0.2, 0.1)$, $(0.6, 0.3)$ and $(0.8, 0.5)$. For both cases, the absolute errors e_τ decrease as the number of time steps N increases, demonstrating convergence of the EM scheme under mesh refinement.

Table 4.2: Convergence of scheme for the nonlinear FSDE Example.

$(\alpha(0),\ \alpha(1))$	(0.2, 0.1)		(0.6, 0.3)		(0.8, 0.5)	
N	e_τ	k	e_τ	k	e_τ	k
16	4.38 e^-2	0.009004	5.04e^-2	0.08139	9.49e^-2	0.1234129
32	4.33 e^-4	0.00900	5.12e^-3	0.02227360	9.72e^-4	0.0231000
64	6.25 e^-2	0.03411000	4.96e^-3	0.0445478	9.39 e^-1	0.0494342
128	4.08e^-2	0.32949910	4.47e^-3	0.1524107	8.22 e^-3	0.1926919
$min(1-\alpha^*, 0.5)$		0.5		0.4		0.2

In the linear case, the errors decrease monotonically and the empirical convergence rates k approach the theoretical rate $\min(1-\alpha^*, 0.5)$, where $\alpha^* = \max(\alpha(0), \alpha(1))$. In the nonlinear case, the errors are initially larger, typically of order 10^{-2} and exhibit mild oscillations due to the nonlinear nature of the $\sin(u)$ function; nevertheless, the convergence rates still tend toward the same theoretical bound, although at a slightly slower rate than in the linear case. Overall, the numerical results presented in Tables (4.1) and (4.2) are consistent with the theoretical predictions of Theorem (4.3.3) and provide strong numerical validation for the convergence analysis of the EM scheme for both linear and nonlinear variable-order FSDEs under one-sided Lipschitz conditions.

EXAMPLE 4.4.3. In this example, we investigate the strong convergence and the convergence rate for the SFPDEs on the interval $[0, 1]$. Along with the theorems mentioned above, we also verify the one-sided Lipschitz conditions on both nonlinear external terms, f and b. For a nonlinear variable-order FSDE, we choose $f(u) = e^{-u}$ and $b(u) = u + e^{-u}$ and $u_0 = 0.1$ in the variable-order FSDE (4.2).

$$du = (-\lambda\ {}_0^C D_t^\alpha u + e^{-u}dt + (u + e^{-u})dW, \quad t \in [0, T], u(0) = u_0.$$

We present the error e_τ for different mesh size N and different choices of $\alpha(0)$ *and* $\alpha(1)$ in (4.103). Again, we observe that the EM scheme (4.71) demonstrates the convergence rates that are in agreement with the theoretical analysis in Theorem (4.3.3).

Another example we can include in the following case.

EXAMPLE 4.4.4. In this example, we investigate the strong convergence and the convergence rate for the SFPDEs on the interval $[0, 1]$. Along with the theorems mentioned

above, we also verify the one-sided Lipschitz conditions on both nonlinear external terms, f and b. For a nonlinear variable-order FSDE, we choose $f(u) = \frac{\gamma_1}{u} - \gamma_2 u$ where γ_1 and γ_2 are the Lamberty constant that can be determined and $b(u) = u + \sqrt{u}$ and $u_0 = 0.1$ in the variable-order FSDE (4.2).

$$du = -\lambda\, {}_0^C D_t^{\alpha} u + (\frac{\gamma_1}{u} - \gamma_2 u)dt + (u + \sqrt{u})dW, \quad t \in [0, T], u(0) = u_0.$$

We present the error e_τ for different mesh size N and different choices of $\alpha(0)$ *and* $\alpha(1)$ in (4.103). Again, we observe that the EM scheme (4.71) demonstrates the convergence rates and we note that both are in agreement with the theoretical analysis in the result obtained in Theorem (4.3.3).

4.4.2 Performance of the Variable-Order FSDE

We compare the performance of the variable-order FSDE (4.2), for $\lambda = 0$, with the standard SDE. In this section of the numerical experiment, we used the same time interval and other variables as in the previous section. For computing various combinations of solutions of $(\alpha(0), \alpha(1))$ we use the EM scheme (4.71) with a mesh size $N = 2^{10}$.

In Figures (4.1) and (4.2) below, we show the results for $(\alpha(0), \alpha(1)) = (0.2, 0.1)$ and $(\alpha(0), \alpha(1)) = (0.8, 0, 5)$, respectively. Each figure shows the plots with values between 0.1 and 1. We note that the FSDE solution (4.2) and the standard SDE solution are nearly identical for $\lambda < 1$ (here $\lambda = 0.1$ in this case). In contrast to $\lambda = 1$, the FSDE solution (4.2) exhibits a considerable difference from the SDE solution. *

4.5 Concluding Remarks

In this chapter, we investigate a non-Lipschitz non-singular kernel variable order FSDE subjected to a nonlinear multiplicative white noise that loses the convolution structure due to the variable order fractional differential operator. In addition to the well-posedness and moment estimates of the problem, we developed and proved a generalized EM scheme and showed the strong convergence of the EM approximation scheme.

In particular, the strong convergence results obtained here in this chapter had the same result as the classical SDEs when taking $\alpha = 0$ and $\alpha = 1$ in the variable-order FSDE, we obtained the results related to the classical version of the problem under consideration.

To support the theoretical findings, we conducted numerical experiments. In particular, when the variable-order FSDE is $\alpha = 0$ and $\alpha = 1$, the behavior of the obtained convergence resembles to the well-known convergence rates of the EM scheme for the conventional SDEs.

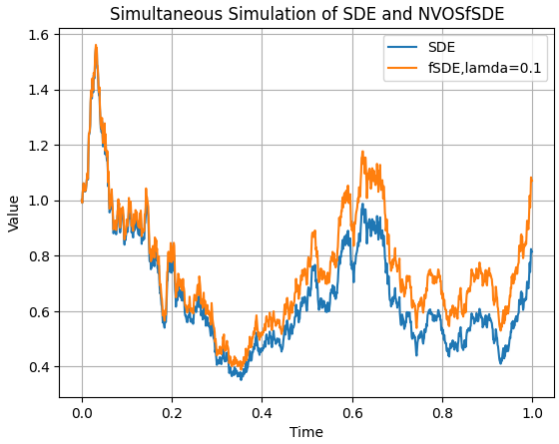

Figure 4.1: $(\alpha(0), \alpha(1))$=(0.2,0.1) and $\lambda = 0.1$

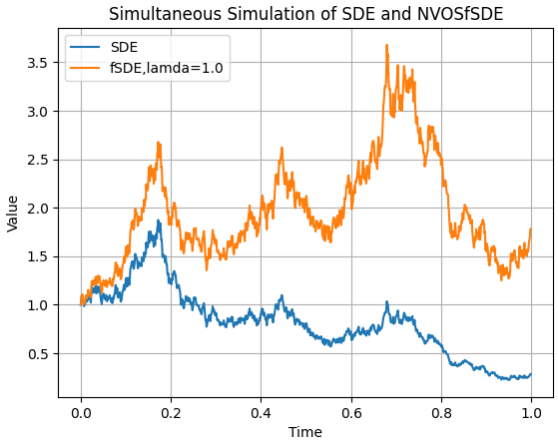

Figure 4.2: $(\alpha(0), \alpha(1))$=(0.8,0.5) and $\lambda = 1$

Plots of SDE and FSDE solutions with the same sample size: classical SDE solutions (blue color),the variable-order FSDE solutions (orange color).

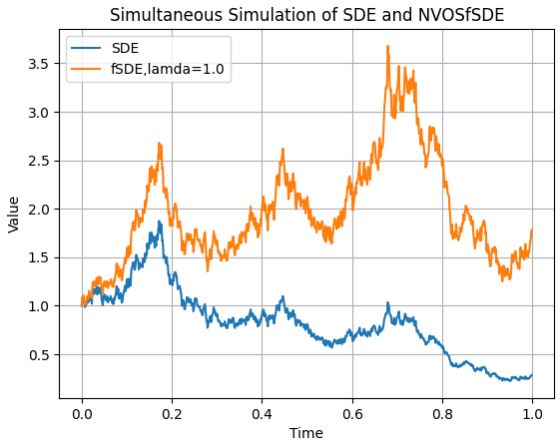

Figure 4.3: $(\alpha(0), \alpha(1))$=(0.2,0.1) and $\lambda = 1$

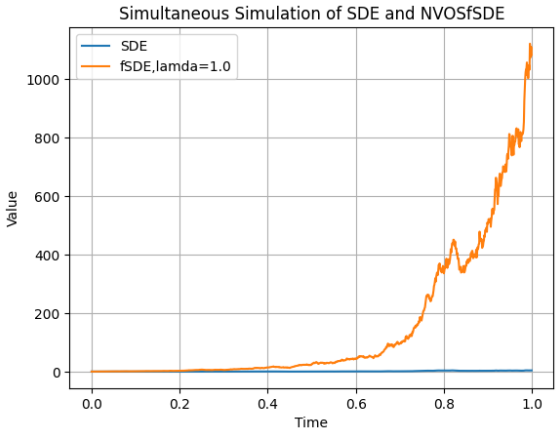

Figure 4.4: $(\alpha(0), \alpha(1))$=(0.8,0.5) and $\lambda = 1$

Plots of SDE and FSDE solutions with the same sample size: classical SDE solutions (blue color),the variable-order FSDE solutions (orange color)

There are future perspectives and research potential directions which are mainly inspired from the need of sound mathematical analysis to extend the results obtained in this chapter. We will mainly be interested in the question of global regularity and asymptotic expansion of the solutions for these SFPDEs. Additionally, many other open problems in this direction are the invariant measure and the ergodicity of the associated solutions are crucial for future perspective work. The long time behavior of a fractional stochastic system is of great relevance in long-term prediction of weather/climate or natural phenomena. Investigating the well-posedness of the the SFPDEs driven by Gaussian jumps and Levy processes and with non-regular intensity is still an open problem that can be addressed in future work.

Chapter 5

A Front Fixing Crank-Nicolson Finite-Difference for the Solvability of the APO Models

5.1 Introduction

The APO model is one of the most common derivatives instruments that are used in the valuation of financial contracts. This type of option allows investors to exercise their options at any time before the option expires and this gives the APO activity an edge over any other options in the market. Hence, a European put options are important terms to understand the value and the valuation of APOs in the derivatives market. As for further reading on this particular subject, one can turn to Riccardo et al. [75] and Company et al. [64], for instance.

The foundational work on pricing options via PDEs, with some stringent assumptions, was principally introduced by Black and Scholes and Merton in the celebrated references [30, 154], respectively, where further references can be found.We also need to credit the work of Schwartz [196] and Brennan and Schwartz [31, 32], were pioneers in solving APO problems employing the FDM, the accuracy of which has been verified by Jaillet et al. [102].Further, we acknowledge that subsequent works [64, 75, 85, 173, 207] have considered front tracking methods for monitoring the boundaries and for discretizing the problem within a changing domain.

However, we must emphasize that the complexity in pricing APOs stems from determining optimal exercise time of the underlying asset along with from solving a PDE which fulfills the requisite boundary and initial values; meaning that we must closely monitor both the fixed and the unknown free boundary conditions for clearly understand the dynamics of

the underlying problem. The FFM, which is predicated on a variable change that maps a dynamic domain onto a constant domain, can mitigate the challenges associated with free boundary problems.

A plethora of free boundary problems encountered in physics and finance have been resolved using the FFM, see for instance [44, 50, 64, 75, 93, 207, 216, 237] and the references therein; with seminal applications and solutions to free boundary option pricing using FFM by Wu and Kwok in their investigation in [216]. The FFM is advantageous for directly computing free boundary problems, in the sense of simplifying the management of computational mesh points or elements when applying FDMs and FEMs to such problems. This has motivated Landau in his work [128] to highlight that the method effectively transforms unknown, time-varying boundaries into known, fixed boundaries by altering the original problem into a nonlinear PDE within a bounded domain.

The application of FC has been instrumental in streamlining the modeling of complex systems across various disciplines, with its role intensifying over the past decade in sectors such as finance and economics, among other fields of science and engineering; where further details can be found in [126, 164, 223, 12, 19, 36, 185], among others. Nuugulu et al. [163] present a robust numerical approach in order to solve the fractional BS equation applied to value APOs. Their approach integrates FC with an implicit front-fixing algorithm, effectively addressing the complexities of the free boundary problem. The results of their study demonstrate that the proposed scheme can be characterized as consistent, convergent and stable. However, we need to clearly emphasize that the first work dealing with robust numerical approaches to solve the fractional BS differential equations with applications in pricing APOs was dully observed in the paper [9] which to the best of our knowledge was the first paper dealing with robust numerical schemes in establishing note only the uniqueness and existence of solutions for APO but also the deep investigations of their numerical treatment. The current study in this manuscript generalizes to some extent the results in the existing literature as well as some of the work in our groundbreaking paper [9].
In light of the above, we can also note that valuation of APO contracts have garnered significant attention from financial engineers and mathematicians and other scientists over the past few decades due to their status as a highly liquid and widely traded instrument within the financial options market.

In this chapter, we apply the new Caputo FDs, which do not possess a singular kernel (no blow-up at any time), as compared to the classical BS equations. Additionally, we introduce a Crank-Nicolson finite-difference scheme in conjunction with FFM to address the challenges in solving the APOs. This study focuses on developing a novel APO scheme that employs

the Crank-Nicolson finite-difference approach and the FFM, specifically in the absence of dividend payments. The proposed method transforms the variable domain problem into a bounded rectangular domain specified for the nonlinear problem using a front-fixing transformation.

This study underscores the importance of accurate and efficient numerical methods for option pricing. Among the various methods, we introduce a new variant of Crank-Nicolson FDM, dubbed the front-fixing Crank-Nicolson FDM. This method is designed to navigate the complexities exercise before the maturity feature of APOs, where the optimal exercise boundary is unknown a priori. We refer the reader to [93, 207] for further elaboration on this method. By integrating front-fixing techniques into the Crank-Nicolson scheme, we propose an enhanced numerical approach that captures the behavior of the early exercise boundary more effectively.

Furthermore, this research augments the ongoing efforts and the extant literature by developing robust and efficient numerical schemes for pricing APOs. This contribution will provide valuable insights for financial practitioners, researchers and investors engaged in option valuation and portfolio management.

5.1.1 Transition from FSDEs to APO Pricing

In chapter 4 developed a comprehensive numerical framework for solving Caputo–Fabrizio FSDEs establishing the existence and uniqueness of solutions, as well as the strong convergence of the EM scheme. In contrast, the present chapter extends these FC tools to a deterministic financial model, namely the pricing of APOs. It addressed stochastic dynamics driven by a Wiener process.

Chapter 5 focuses on deterministic dynamics incorporating a free-boundary structure arising from the early-exercise feature of APO. Despite this difference, the numerical treatment of the Caputo-Fabrizio FD remains consistent with the methodology developed in the previous chapter. In particular, the discretization scheme in is employed to approximate the fractional time derivative and the stability analysis relies on the boundedness results established in Theorem (4.3.3).

The main additional challenge in this chapter is the presence of the free boundary $X^*(\tau)$, which separates the continuation and exercise regions. This difficulty is addressed using the front-fixing (Landau) transformation, which maps the moving boundary problem onto a fixed computational domain. The resulting numerical formulation, based on a Crank-Nicolson discretisation combined with the front-fixing approach, can be interpreted as a natural extension of the EM framework developed in Chapter 4 to parabolic PDEs with free boundaries.

The chapter is structured as follows: Section 5.2 elaborates on Caputo-time fractional equation of APO. Section 5.3 introduces the fixed domain transformation of the APO problem and the Crank-Nicolson discretization of the transformed equation. Section 5.4 examines the stability and consistency of the scheme concerning time at the optimal exercise boundary. Section 5.5 presents numerical experiments and comparisons with other methodologies.

5.2 Time-Caputo-fractional equation of APO

5.2.1 The APOs Model

Let us assume that an underlying asset has a price of X at time t. Here, we consider the subsequent mathematical model for determining the value of an APO or the purpose of selling the underlying asset $V(X,\tau)$. Therefore, to address this objective, we examine the following problem

$$\begin{cases} \frac{\partial V}{\partial \tau} + \frac{1}{2}\sigma^2 X^2 \frac{\partial^2 V}{\partial^2 X} + rX\frac{\partial V}{\partial X} = rV, \text{ for } X = X^*(\tau), \text{ and } t \in [0,T], \\ V(X,T) = \max\{E - X, 0\}, \text{ for } X \geq 0, \\ \frac{\partial V}{\partial X}(X^*(\tau),\tau) = -1, \\ V(X^*(\tau),\tau) = E - X^*(\tau), \\ \lim\limits_{X\to\infty} V(X,T) = 0, \\ X^*(T) = E, \\ V(X(\tau),\tau) = E - X, \text{ for } X \in [0, X^*(\tau)), \end{cases} \tag{5.1}$$

where T is the time horizon which represents the maturity T also known to us sometimes as the expiration time, $t \geq 0$ stands for the time from 0 up to maturity T, $\tau = T - t$ represents the period until maturity T, here, $X^*(t)$ denotes the unknown early exercise-free boundary which we assume "doneravant" that $X^*(t) > 0$, E is the strike price, r risk-free interest rate and σ is the volatility parameter.
Note that to describe the problem at hand, we refer to the Black-Scholes-Merton equation (5.1) was developed by Merton [154] and Black and Scholes [30].

The historical development of FC, together with the formulation and definitions of FDs, including the Caputo, Riemann-Liouville, Jumarie, and Caputo-Fabrizio derivatives, as well as the associated fractional differential operators, has been presented in Section (1.3.2). In the next section, the derivation of the tfBS-PDE for pricing APOs without dividends is discussed. Subsequently, the classical APO pricing model described by equation (5.1) is reformulated by incorporating the Caputo-Fabrizio FD, which possesses a smoother non-singular kernel

compared with several existing FDs, such as the conformable derivative [10, 116] and the Abu-Shady-Kaabar FD [2]. Building upon these foundational concepts, the fractional Taylor series expansion is introduced, as it plays a fundamental role in the derivation of the tfBS-PDE presented in the subsequent section.

DEFINITION 5.2.1. *Fractional Taylor Series*
Let $v : \mathbb{R} \to \mathbb{R}$ be a continuous function that has a derivative of order $\alpha\zeta$, where ζ is any positive integer and $0 < \alpha \leq 1$. The fractional Taylor series is given by:

$$v(t+\kappa) = \begin{cases} \sum_{\zeta=0}^{\infty} \frac{\kappa^{\alpha\zeta}}{\Gamma(1+\alpha\zeta)} v^{(\alpha\zeta)}(t), & \eta - 1 < \alpha \leq \eta, \\ v(t) + \kappa v'(t) + \sum_{\zeta=1}^{\infty} \frac{\kappa^{\zeta\beta_e+1}}{\Gamma(\zeta\beta_e+2)} v^{(\zeta\beta_e+1)}(t), & \beta_e = \alpha - \eta, \end{cases} \tag{5.2}$$

where $\eta \in \mathbb{N}$.

5.2.2 Derivation of the tfBS-PDE

Before delving into the derivation of the time-SFPDEs, we need to introduce one important ingredient in stochastic calculus, the Itô's lemma. To frame our approach, we first define the Itô's Lemma. The later is widely used in the subsequent analysis. For a comprehensive discussion, we refer to the celebrated book [239] where the SPDEs were introduced and further discussed in great detail.

LEMMA 5.2.1. *Itô's Lemma Let X_t be an Itô process given by*

$$dX = \mu(X,t)\,dt + \sigma(X,t)\,dW_t \tag{5.3}$$

where W_t is a standard Wiener process and $\mu(X,t)$ and $\sigma(X,t)$ are sufficiently smooth functions. Let $f(t,x) \in C^2([0,\infty) \times \mathbb{R})$, i.e., f is twice continuously differentiable on $[0,\infty) \times \mathbb{R}$. Then the process $f(X,t)$ is again an Itô's process and its differential is given by

$$df = \left(\frac{\partial f}{\partial t} + \mu \frac{\partial f}{\partial X} + \frac{1}{2}\sigma^2 \frac{\partial^2 f}{\partial X^2} \right) dt + \sigma \frac{\partial f}{\partial X} dW_t \tag{5.4}$$

where the stochastic differentials satisfy the multiplication rules:

$$dt \cdot dt = dt \cdot dW_t = dW_t \cdot dt = dW_t \cdot dW_t = 0, \quad dW_t \cdot dW_t = dt. \tag{5.5}$$

For the proof of this lemma, we refer to [239]. In the derivation of the tfBS-PDE, we start by assuming that a FSDE governs the dynamics of the stock price:

$$dX = rX\ dt + \sigma\omega(t)(dt)^{\alpha/2}, \quad 0 < \alpha \leq 1, \tag{5.6}$$

where X is the stock price, σ is the volatility, r is the risk-free interest rate and $\omega(t)$ represents a standard Wiener process. Arguing similarly as in [164, 163], we can assert that using

Jumarie's fractional Taylor series, as presented in equation (5.2), the following identities are derived:

$$d^\alpha t = \frac{1}{\Gamma(2-\alpha)} t^{1-\alpha} (dt)^\alpha, \quad 0 < \alpha \leq 1, \tag{5.7}$$

$$d^\alpha X = \Gamma(1+\alpha) dX, \quad 0 < \alpha \leq 1, \tag{5.8}$$

$$\frac{d^\alpha X}{(dX)^\alpha} = \frac{1}{\Gamma(2-\alpha)} X^{1-\alpha}, \quad 0 < \alpha \leq 1. \tag{5.9}$$

Combining equations (5.7) and (5.9) results in a formula that enables the conversion between integer-order and fractional-order derivatives.

$$dX = X^{1-\alpha} \frac{\Gamma(1+\alpha)}{\Gamma(2-\alpha)} (dX)^\alpha, \quad 0 < \alpha \leq 1. \tag{5.10}$$

Now, let $V(X,t)$ be the value of an APO and assume that $V(X,t)$ satisfies the following assumption:

ASSUMPTION 5.2.1. *The function $V(X,t)$ is sufficiently smooth with respect to X and its FD with respect to time exists for some $\alpha \in (0,1)$.*

Remark 5.1. Despite remarking that in the aforementioned definitions, we used the condition $0 < \alpha \leq 1$, however, as the condition presented in the above assumption does not make use of $\alpha = 1$ due to the fact that for $\alpha = 1$ the result applies to the classical derivative.

The dynamics of the risk-free investment interest rate are given by:

$$dV = rV\, dt.$$

Multiplying both sides of this equation by $\Gamma(1+\alpha)$, we obtain:

$$\Gamma(1+\alpha) dV = \Gamma(1+\alpha) rV\, dt. \tag{5.11}$$

Using equation (5.11) and combining it with (5.7), we derive the following fractional interest rate increment:

$$d^\alpha V = \Gamma(1+\alpha) rV\, dt. \tag{5.12}$$

Now, combining equations (5.12) and (5.10), we arrive at the following fractional interest rate dynamic equation:

$$d^\alpha V = rV \frac{1}{\Gamma(2-\alpha)} t^{1-\alpha} (dt)^\alpha. \tag{5.13}$$

Since $V(X,t)$ is sufficiently smooth, applying the fractional Taylor series expansion (5.2) of order α on $V(X,t)$, we obtain:

$$dV = \frac{1}{\Gamma(1+\alpha)} \frac{\partial^\alpha V}{\partial t^\alpha} (dt)^\alpha + \frac{\partial V}{\partial X} dX + \frac{1}{2} \frac{\partial^2 V}{\partial X^2} (dX)^2. \tag{5.14}$$

Now we can apply Itô's lemma on (5.6) to find $(dX)^2$

$$\begin{aligned}(dX)^2 &= \left(rX\,dt + \sigma\omega(t)\,(dt)^{\alpha/2}\right)^2 \\ (dX)^2 &= (rX\,dt)^2 + 2\,(rX\,dt)\left(\sigma\omega(t)\,(dt)^{\alpha/2}\right) + \left(\sigma\omega(t)\,(dt)^{\alpha/2}\right)^2 \\ (dX)^2 &= 2rX\sigma\omega(t)(dt)^{1+\alpha/2} + \sigma^2\omega(t)^2\,(dt)^{\alpha} \text{ since } \quad (dt)^2 = 0 \end{aligned} \tag{5.15}$$

In Itô's calculus, $(dt)^{1+\alpha/2}$ is a higher-order term and vanishes. Since $\omega(t)$ is a SP with $\omega(t)^2 \sim 1$, the term $\left(\sigma\omega(t)\,(dt)^{\alpha/2}\right)^2$ simplifies to $\sigma^2(dt)^{\alpha}$.
Hence, (5.15) becomes:

$$(dX)^2 = \sigma^2(dt)^{\alpha} \tag{5.16}$$

Plugging equation (5.16) and by applying Itô's lemma to the expression in (5.14), we have:

$$dV = \frac{1}{\Gamma(1+\alpha)}\frac{\partial^{\alpha}V}{\partial t^{\alpha}}(dt)^{\alpha} + rX\frac{\partial V}{\partial X}\,dt + \frac{1}{2}\sigma^2X^2\frac{\partial^2V}{\partial X^2}(dt)^{\alpha}. \tag{5.17}$$

Using the conversion formula (5.13) for dt, we replace dt in equation (5.17) with:

$$dt = t^{1-\alpha}(dt)^{\alpha}\frac{1}{\Gamma(1+\alpha)\Gamma(2-\alpha)} \tag{5.18}$$

which gives:

$$dV = \frac{1}{\Gamma(1+\alpha)}\frac{\partial^{\alpha}V}{\partial t^{\alpha}}(dt)^{\alpha} + r\frac{Xt^{1-\alpha}}{\Gamma(1+\alpha)\Gamma(2-\alpha)}\frac{\partial V}{\partial X}(dt)^{\alpha} + \frac{1}{2}\sigma^2X^2\frac{\partial^2V}{\partial X^2}(dt)^{\alpha}. \tag{5.19}$$

Finally, multiplying each side of the equation (5.19) by $\Gamma(1+\alpha)$ and simplifying the terms using (5.12) to (5.14), we obtain tfBS-PDE:

$$\frac{\partial^{\alpha}V}{\partial t^{\alpha}} = \left(rV - rX\frac{\partial V}{\partial X}\right)\frac{t^{1-\alpha}}{\Gamma(2-\alpha)} - \frac{\Gamma(1+\alpha)}{2}\sigma^2X^2\frac{\partial^2V}{\partial X^2}, \text{ where }, 0 < \alpha \leq 1 \tag{5.20}$$

By introducing the change of variable $\tau = T - t$, τ is the time to maturity and incorporating the specified boundary conditions, equation (5.20) can be transformed into the following:

$$\begin{cases} \frac{\partial^{\alpha}V}{\partial\tau^{\alpha}} = [rV - rX\frac{\partial V}{\partial X}]\frac{\tau^{1-\alpha}}{\Gamma(2-\alpha)} - \frac{\Gamma(1+\alpha)\tau^{1-\alpha}}{2(T-\tau)^{1-\alpha}}\sigma^2X^2\frac{\partial^2V}{\partial X^2}, \quad X^*(\tau) \leq X \leq \infty, \text{ and } \tau \in [0,T], \\ V(X,T) = \max\{E - X, 0\}, \text{ for } X \geq 0, \\ \frac{\partial V}{\partial X}(X^*(\tau),\tau) = -1, \\ V(X^*(\tau),\tau) = E - X^*(\tau), \\ \lim\limits_{X\to\infty} V(X,T) = 0, \\ X^*(T) = E, \\ V(X(\tau),\tau) = E - X, \text{ for } X \in [0, X^*(\tau)) \end{cases} \tag{5.21}$$

Where
$\tau = T - t$ represents the period until maturity T,$X^*(t)$ unknown early exercise-free boundary with $X^*(t) > 0$,E is strike price, T expiration time, σ volatility and r the interest rate (risk-free).

5.3 The Front Fixing Method (FFM)

Free boundary problems are inherently challenging due to the requirement of solving a PDE that must satisfy boundary and initial values on both a fixed and an unidentified free boundary. To manage this complexity, these problems are typically reformulated as non-linear PDEs, treating the free boundary as an unknown variable. A prominent method to address this is the FFM, which transforms the initial PDE into a new nonlinear PDE within a bounded domain, facilitating direct computation of the free boundary.

The FFM, grounded in physics and via Landau transformation, simplifies the problem by "fixing" the unknown boundary along a vertical axis. This transformation enables a more manageable analysis. Widely applied across disciplines like physics and finance, including option pricing, the method was initially introduced by Wu and Kwok [127] in 1997 for financial applications. Since then, it has been refined by researchers such as Riccardo *et al.* [75, 73], R. Company *et al.* [44], Nielsen[161], Ševčovič [197] and Zhang and Zhu [230], among others.

A key advantage of the FFM is its capacity to directly compute the free boundary, which is crucial for analyzing the system's behavior. For instance, in the context of the BS formulae for APOs, the problem is transformed into a parabolic equation within a bounded domain, where a truncated boundary is introduced and finite-difference schemes are applied to solve the resulting approximate problem.

When $X \leq X^*(\tau)$, optimal to exercise APO, while for $X^*(\tau) < X$, the optimal strategy is to hold the option, as exercising it under these conditions is not financially viable. The value-matching condition $v(X^*(\tau), \tau) = E - X^*(\tau)$ and the smooth-pasting condition $\frac{\partial v}{\partial X}(X^*(\tau), \tau) = -1$ are essential to maintaining the financial interpretation of the continuity of v and $\frac{\partial v}{\partial X}$ across the optimal exercise boundary $X^*(\tau)$. These conditions prevent arbitrage opportunities, ensuring that transactions are self-financing *i.e.*, each portfolio adjustment is precisely funded by the proceeds from the previous position.

5.3.1 Arbitrage-Free Pricing of APOs

Ensuring arbitrage-free pricing of APOs requires adherence to two fundamental conditions: the value matching condition and the smooth pasting condition. These conditions play a critical role in eliminating arbitrage opportunities and maintaining consistency within the

financial market structure [23].

The Value Matching condition, expressed as $V(X^*(\tau), \tau) = E - X^*(\tau)$ in the APO framework, states that the option's price must equal its intrinsic value at the boundary corresponding to optimal exercise. Here, $X^*(\tau)$ denotes the optimal exercise boundary at time τ. This condition ensures that exercising the option does not produce profit beyond the guaranteed payoff $E - X^*(\tau)$, thus eliminating arbitrage opportunities. If violated, arbitrageurs could exploit pricing discrepancies by exercising the option and simultaneously trading the underlying asset to secure risk-free profits [47].

Furthermore, the principle of put-call parity reinforces the necessity of this condition in preventing arbitrage, even in nonlinear pricing models where early exercise features complicate valuation [23, 127, 163].

The smooth pasting condition, expressed as $\frac{\partial V}{\partial X}(X^*(\tau), \tau) = -1$ in the APO framework, ensures that the option value function transitions smoothly across the early exercise boundary. This condition guarantees continuity in the slope of the value function $V(X^*(\tau), \tau) = E - X^*(\tau)$ and $\frac{\partial V}{\partial X}(X^*(\tau), \tau)$, preventing abrupt changes that could create arbitrage opportunities.

A discontinuity would allow sudden changes in the hedge ratio to be exploited to construct risk-free portfolios with guaranteed profits [120]. Furthermore, arbitrage-free pricing models highlight the crucial role of smooth pasting in ensuring a seamless transition between holding and exercising AOs [47, 127, 163].

These conditions are fundamental because, in an arbitrage-free market, the transition between holding and exercising an option must occur smoothly, without introducing price discontinuities or abrupt shifts in the hedging strategy. A violation of the value matching condition would enable arbitrageurs to exploit pricing discrepancies by exercising the option and concurrently trading the underlying asset to generate risk-free profits [120, 127, 163].
At the optimal exercise boundary, an investor must decide whether to continue holding the option or exercise it immediately. The value matching condition ensures that exercising does not create unaccounted excess value, while the smooth pasting condition guarantees a seamless transition, preventing exploitable pricing discontinuities. Together, these conditions ensure that the optimal stopping problem defining $X^*(\tau)$ is well-posed within the framework of the VI governing the pricing of AOs [107, 127, 163].

A key feature of American-style derivatives is their flexibility, allowing early exercise at any time before expiration, unlike EOs. This flexibility requires that portfolio adjustments associated with early exercise remain self-financing, meaning that the reallocation of wealth

between the option and the underlying asset should not require external capital infusion. Mathematically, this is enforced by the free-boundary problem in the price of AOs, where $X^*(\tau)$ must be determined in conjunction with the PDE governing the price of the APO $V(X,\tau)$.
Since early exercise involves liquidating the option in exchange for cash while simultaneously taking a short position in the APO, any misalignment between the APO's value and intrinsic value would create arbitrage opportunities. The value matching and smooth pasting conditions eliminate such possibilities by ensuring that transactions along the free boundary satisfy the self-financing constraint. This ensures that each trade at $X = X^*(\tau)$ is precisely covered by the cash flows generated from either exercising or holding the option [107, 127, 163].

5.3.2 Derivation of the Transformed Fractional PDE

The FFM addresses the moving exercise boundary $X^*(\tau)$ by introducing a change of variables, converting the problem into a nonlinear tfBS-PDE defined over a fixed domain. This transformation allows for a given boundary position while some boundary conditions remain unidentified and computed simultaneously with the option value. For numerical implementation, the following change of variables (dimensionless variables), similar to [64, 75, 216], is introduced:

i. Logarithmic scale for stock price: $y = \ln(\frac{X}{X_f(\tau)})$, where $X_f(\tau)$ is a time-dependent scaling factor.

ii. New dependent variable: $v(y,t) = \frac{V(X,\tau)}{K}$: $K > 0$ is a constant.

iii. Scaling for $X_f(\tau) : X_f(\tau) = \frac{X^*(\tau)}{K}$.

Arguing similarly as in [128] and applying the Landau transformation given therein: $y = \ln\left(\frac{X}{X_f(\tau)}\right)$ to the asset price variable ensures that $y = 0$ whenever $X = X^*(\tau)$, thereby converting the free boundary condition into a fixed boundary condition. Consequently, the stock dynamics is modified as follows:

$$dy = \left(r - \frac{\sigma^2}{2} - \frac{X_f'(\tau)}{X_f(\tau)}\right) dt + \sigma\omega(t)(dt)^{\alpha/2}, \quad \alpha \in (0,1] \tag{5.22}$$

Using transformations of (5.22) and the above items in the change of variables, we can transform, each part of the tfBS-PDE (5.21) to new variables as follows.
The first derivative of $V(X,t)$ in terms of X is transformed as:

$$\frac{\partial V}{\partial X} = \frac{\partial}{\partial X}\left(v(y,\tau)\right) = \frac{\partial v}{\partial y}\frac{\partial y}{\partial X}$$

Using $y = \ln(\frac{X}{X_f(\tau)})$, we can have that

$$\frac{\partial y}{\partial X} = \frac{1}{X} \quad \text{and} \quad X = e^y X_f(\tau)$$

which implies that

$$\frac{\partial V}{\partial X} = \frac{\partial v}{\partial y}\frac{1}{X} = \frac{1}{e^y X_f(\tau)}\frac{\partial v}{\partial y}.$$

Therefore

$$X\frac{\partial V}{\partial X} = \frac{\partial v}{\partial y}. \tag{5.23}$$

Next, we can transform the second derivative of $V(X,t)$ in terms of X using the chain rule, hence the second derivative becomes:

$$\frac{\partial^2 V}{\partial X^2} = \frac{\partial}{\partial X}\left(\frac{\partial v}{\partial y}\frac{\partial y}{\partial X}\right) = \frac{\partial^2 V}{\partial X^2} = \frac{\partial}{\partial X}\left(\frac{1}{e^y X_f(\tau)}\frac{\partial v}{\partial y}\right).$$

Taking the derivative in terms of X and noting that

$$\frac{\partial y}{\partial X} = \frac{1}{X}$$

we obtain

$$\frac{\partial^2 V}{\partial X^2} = \frac{1}{(X_f(\tau))^2 e^{2y}}\frac{\partial^2 v}{\partial y^2} = \frac{1}{X^2}\frac{\partial^2 v}{\partial y^2}. \tag{5.24}$$

Finally, we can transform the fractional time derivative of $V(X,\tau)$ in terms of τ. Hence, applying the fractional time derivative $\frac{\partial^\alpha (V(X,\tau))}{\partial \tau^\alpha}$ involves using the chain rule to get

$$\frac{\partial^\alpha V}{\partial \tau^\alpha} = \frac{\partial^\alpha v}{\partial \tau^\alpha} + \frac{\partial y}{\partial \tau} = \frac{\partial^\alpha v}{\partial \tau^\alpha} - \frac{X_f'(\tau)}{X_f(\tau)}\frac{\partial v}{\partial y} \tag{5.25}$$

Now, using the previous change of variables we can substitute from (5.23) to (5.25) into (5.21) and factor out common terms. After simplification, the transformed equation becomes:

$$\frac{\partial^\alpha v}{\partial \tau^\alpha} = \phi(\tau)\left((rv - (r - \frac{\sigma^2}{2})\frac{\partial v}{\partial y})\frac{(T-\tau)^{1-\alpha}}{\Gamma(2-\alpha)} + \frac{X_f'(\tau)}{X_f(\tau)}\frac{\partial v}{\partial y} - \frac{\Gamma(1+\alpha)\sigma^2}{2}\frac{\partial^2 v}{\partial x^2}\right) \tag{5.26}$$

where $\phi(\tau) = \tau^{1-\alpha}(T-\tau)^{\alpha-1}$ which represents the combined influence of past and future memory contributions inherent to FC and more references can be found in the most recent papers by Nuugulu and his coauthors in [163] and by Ali, Abera and Nazir in [9, 8].
After simplifying equation (5.26), we obtain the transformed tfBS-PDE, given in (5.21). This equation is represented using the newly introduced variable y, which facilitates a more

efficient analysis of the problem. Thus far, the newly transformed fraction derivative of V can be written as:

$$\begin{cases} \frac{\partial^\alpha v}{\partial \tau^\alpha} = \theta(\tau)[rv - (r - \frac{\sigma^2}{2})\frac{\partial v}{\partial y}] - \varphi(\tau)\frac{\sigma^2}{2}\frac{\partial^2 v}{\partial y^2} + \phi(\tau)\frac{X_f'(\tau)}{X_f(\tau)}\frac{\partial v}{\partial y} = 0 \\ \theta(\tau) = \frac{\tau^{1-\alpha}}{\Gamma(2-\alpha)}, \varphi(\tau) = \frac{\Gamma(1+\alpha)\tau^{1-\alpha}}{(T-\tau)^{1-\alpha}}, \phi(\tau) = \frac{\tau^{1-\alpha}}{(T-\tau)^{1-\alpha}} \quad X^*(\tau) \leq X \leq \infty, \text{ and } t \in [0,T], \\ v(0,y) = 0, \text{ for } y \geq 0, X_f(0) = 1, \\ \lim\limits_{y\to\infty} v(\tau, y) = 0, \\ v(\tau,0) = 1 - X_f(\tau), \frac{\partial v}{\partial y}(\tau,0) = -X_f(\tau) \\ \text{ on } 0 \leq t \leq T \text{ and } 0 \leq X(\tau) \leq X^*(\tau). \end{cases} \tag{5.27}$$

5.3.3 Crank-Nicolson Finite-Difference Scheme

In the following section, we define a numerical scheme to compute the grid values of APO. For this purpose, we start by truncating $(0,\infty)$ into $0,Y)$ to solve the problem. To determine the appropriate value of $Y = y_\infty$ and ensure the accuracy of the corresponding numerical solution, we adapt the methodology proposed by Kangro and Nicolaides. That is, the problem can be studied on $(0,T]\times[0,Y]$ with $M \in \mathbb{N}$ and $\mu \in \mathbb{R}^+$; now we set the step size as follows:

$$\begin{aligned} &\Delta y = \frac{Y}{M} \\ &\Delta\tau = \mu(\Delta y)^2 \\ &\text{The integer } N = \lceil \frac{T}{\Delta\tau} \rceil \end{aligned} \tag{5.28}$$

where $\lceil . \rceil : \mathbb{R}^+ \to \mathbb{N}$ is the ceiling function from a $\mathbb{R}^+$ to $\mathbb{N}$ greater or equal to it. Hence, the grid-ratio μ is then given by

$$\mu = \frac{\Delta\tau}{(\Delta y)^2}.$$

A mesh of grid points can be introduced in the finite domain as follows:

$$\begin{aligned} &y_m = m\Delta y, \\ &\tau^n = n\Delta\tau, \text{ for } m = 0,1,\ldots,M \text{ and } n = 0,1,\ldots,N. \end{aligned}$$

To compute the grid values, we construct a numerical scheme and the free boundary values by setting

$$\begin{aligned} &v_m^n \approx v(\tau^n, y_m) \\ &X_f^n = X_f(\tau^n), \text{for } m = 0,1,\ldots,M \text{ and } n = 0,1,\ldots,N. \end{aligned}$$

Having defined the size of the mesh of grid points concerning time and space which we can use for computing a numerical scheme of the grid value of APO, we will now move to develop a new Crank-Nicolson finite-difference scheme of APO. Recalling from (5.27), we present the Crank-Nicolson finite-difference scheme, which to the best of our knowledge has never been used for this problem.
The Jumarie FD (1.3.3) and the new Caputo-Fabrizio FD (1.1) are equivalent for differentiable functions, we refer [163] for further detailed investigation in this direction.The order α in equation (5.27), the order of the FD, will be evaluated using (1.1). However, similar results can also be obtained from the other discussed definitions.

First, we discretize the terms in the FDs appearing in (5.27) using (1.1). Therefore, we have

$$\begin{aligned}
\frac{\partial^\alpha v}{\partial \tau^\alpha} &= \frac{1}{(1-\alpha)}\int_0^{t_n} v'(\tau)e^{-\frac{\alpha(t_n-\tau)}{1-\alpha}}d\tau \\
&= \frac{1}{(1-\alpha)}\sum_{j=1}^{n}\int_{(j-1)k}^{jk}\left((\frac{v_m^{j+1}-v_m^j}{\Delta\tau})+\mathcal{O}(k)\right)e^{-\frac{\alpha(t_n-\tau)}{1-\alpha}}d\tau \\
&= \frac{1}{(1-\alpha)}\sum_{j=1}^{n}\int_{(j-1)k}^{jk}\left(\frac{1}{k}(v_m^{j+1}-v_m^j)+\mathcal{O}(k)\right)e^{-\frac{\alpha(nk-\tau)}{1-\alpha}}d\tau \\
&= \frac{1}{(1-\alpha)}\sum_{j=1}^{n}\left(\frac{1}{k}(v_m^{j+1}-v_m^j)+\mathcal{O}(k)\right)\frac{(1-\alpha)}{\alpha}\int_{(j-1)k}^{jk}e^{-\frac{\alpha(nk-\tau)}{1-\alpha}}d\tau \\
&= \frac{1}{k\alpha}\sum_{j=1}^{n}\left((v_m^{j+1}-v_m^j)+\mathcal{O}(k)\right)(e^{-\frac{\alpha(n-j)k}{1-\alpha}}-e^{-\frac{\alpha(n+1-j)k}{1-\alpha}})
\end{aligned}$$

Shifting the indices in the above equation yields

$$\begin{aligned}
&= \frac{1}{k\alpha}\sum_{j=1}^{n}\left((v_m^{n-j+1}-v_m^{n-j})+\mathcal{O}(k)\right)\left(e^{-\frac{\alpha jk}{1-\alpha}}-e^{-\frac{\alpha(j+1)k}{1-\alpha}}\right) \\
&= \frac{1}{k\alpha}\left(1-e^{-\frac{\alpha k}{1-\alpha}}\right)\sum_{j=1}^{n}\left((v_m^{n-j+1}-v_m^{n-j})+\mathcal{O}(k)\right)e^{-\frac{\alpha jk}{1-\alpha}} \\
&= \beta\sum_{j=1}^{n}(v_m^{n-j+1}-v_m^{n-j})e^{-\frac{\alpha jk}{1-\alpha}}+\mathcal{O}(k)\frac{1}{k\alpha}(1-e^{-\frac{\alpha k}{1-\alpha}}) \\
&= \beta\sum_{j=1}^{n}(v_m^{n-j+1}-v_m^{n-j})e^{-\frac{\alpha jk}{1-\alpha}}+\mathcal{O}(1) \qquad (5.29)
\end{aligned}$$

where

$$\beta = \frac{1}{k\alpha}(1-e^{-\frac{\alpha k}{1-\alpha}}).$$

From the above equation (5.29) we analyze the terms as follows:

$$\mathcal{O}(k)\frac{1}{k\alpha}(1-e^{-\frac{\alpha k}{1-\alpha}})$$

First, we deal with the following:

$$\frac{O(k)}{k\alpha}$$

where

- $O(k)$: represents growth proportional to k, potentially with smaller terms.
- $k\alpha$: this grows linearly in k since α is constant.

Hence,

$$\frac{O(k)}{k\alpha} \approx \frac{D}{\alpha},$$

where D is the constant implied by $O(k)$.
Next we will see the order of

$$1-e^{-\frac{\alpha k}{1-\alpha}}.$$

Since $0<\alpha<1$, the exponent $-\frac{\alpha k}{1-\alpha}$ becomes large and negative as $k\to\infty$. Therefore,

$$e^{-\frac{\alpha k}{1-\alpha}} \to 0, \quad \text{and} \quad 1-e^{-\frac{\alpha k}{1-\alpha}} \to 1 \text{ as } k\to\infty.$$

Finally, the term becomes:

$$\frac{O(k)}{k\alpha}\cdot 1 \approx \frac{D}{\alpha}.$$

Since the right-hand side does not depend on k, we may directly assert that the error order is $O(1)$.
Subsequently, the Crank-Nicolson scheme is employed to discretize the derivative terms on the right-hand side of the FDs in equation (5.27) *i.e.,*

$$\begin{aligned}
&rv = \frac{rv_m^{n+1}+rv_m^n}{2}\\
&\frac{\partial v}{\partial y} = \frac{1}{2}\left(\frac{v_{m+1}^{n+1}-v_{m-1}^{n+1}}{2\Delta y}+\frac{v_{m+1}^{n}-v_{m-1}^{n}}{2\Delta y}\right)\\
&\frac{\partial^2 v}{\partial y^2} = \frac{1}{2}\left(\frac{v_{m-1}^{n+1}-2v_m^{n+1}+v_{m+1}^{n+1}}{\Delta y^2}+\frac{v_{m-1}^{n}-2v_m^{n}+v_{m+1}^{n}}{\Delta y^2}\right)\\
&\frac{1}{X_f^n}\frac{dX_f^n}{d\tau}\frac{\partial v}{\partial y} = \frac{1}{2X_f^n}\frac{X_f^{n+1}-X_f^n}{(\Delta\tau)}\left(\frac{v_{m+1}^{n+1}-v_{m-1}^{n+1}}{2\Delta y}+\frac{v_{m+1}^{n}-v_{m-1}^{n}}{2\Delta y}\right)\\
&\text{for } \; m=1,2,\dots M-1 \text{ and } n=1,2,\dots,N
\end{aligned} \tag{5.30}$$

By combining equations (5.29) and (5.30) we can obtain a new Crank-Nicolson finite-difference discretization time scheme for internal special nodes given by the following:

$$
\begin{aligned}
&2\beta\sum_{j=1}^{n}(v_m^{n-j+1}-v_m^{n-j})e^{-\frac{\alpha jk}{1-\alpha}}=\\
&\theta(\tau^{n+1})[(rv_m^{n+1}+rv_m^n)-(r-\frac{\sigma^2}{2})(\frac{v_{m+1}^{n+1}-v_{m-1}^{n+1}}{2\Delta y}+\frac{v_{m+1}^{n}-v_{m-1}^{n}}{2\Delta y})]\\
&-\varphi(\tau^{n+1})\frac{\sigma^2}{2}(\frac{v_{m-1}^{n+1}-2v_m^{n+1}+v_{m+1}^{n+1}}{\Delta y^2}+\frac{v_{m-1}^{n}-2v_m^{n}+v_{m+1}^{n}}{\Delta y^2})\\
&+\frac{\phi(\tau^{n+1})}{X_f^n}\frac{X_f^{n+1}-X_f^n}{(\Delta\tau)}(\frac{v_{m+1}^{n+1}-v_{m-1}^{n+1}}{2\Delta y}+\frac{v_{m+1}^{n}-v_{m-1}^{n}}{2\Delta y})
\end{aligned}
\tag{5.31}
$$

After collecting like terms, we obtain the following expression:

$$
\begin{aligned}
&-2\beta\sum_{j=1}^{n}(v_m^{n-j+1}-v_m^{n-j})e^{-\frac{\alpha jk}{1-\alpha}}+\\
&v_{m+1}^{n+1}\Big[\frac{-\theta(\tau^{n+1})(r-\frac{\sigma^2}{2})}{2\Delta y}-\varphi(\tau^{n+1})\frac{\sigma^2}{2\Delta y^2}+\frac{\phi(\tau^{n+1})}{X_f^n}\frac{X_f^{n+1}-X_f^n}{2\Delta y\Delta\tau}]+\\
&v_{m+1}^{n}\Big[\frac{-\theta(\tau^{n+1})(r-\frac{\sigma^2}{2})}{2\Delta y}-\varphi(\tau^{n+1})\frac{\sigma^2}{2\Delta y^2}+\frac{\phi(\tau^{n+1})}{X_f^n}\frac{X_f^{n+1}-X_f^n}{2\Delta y\Delta\tau}]\\
&+v_{m-1}^{n+1}\Big[\frac{\theta(\tau^{n+1})(r-\frac{\sigma^2}{2})}{2\Delta y}-\varphi(\tau^{n+1})\frac{\sigma^2}{2\Delta y^2}-\frac{\phi(\tau^{n+1})}{X_f^n}\frac{X_f^{n+1}-X_f^n}{2\Delta y\Delta\tau}]+\\
&v_{m-1}^{n}\Big[\frac{\theta(\tau^{n+1})(r-\frac{\sigma^2}{2})}{2\Delta y}-\varphi(\tau^{n+1})\frac{\sigma^2}{2\Delta y^2}-\frac{\phi(\tau^{n+1})}{X_f^n}\frac{X_f^{n+1}-X_f^n}{2\Delta y\Delta\tau}]+\\
&v_m^{n+1}\Big[\theta(\tau^{n+1})r+\varphi(\tau^{n+1})\frac{\sigma^2}{\Delta y^2}\Big]+v_m^{n}\Big[\theta(\tau^{n+1})r+\varphi(\tau^{n+1})\frac{\sigma^2}{\Delta y^2}\Big]=0
\end{aligned}
\tag{5.32}
$$

Our Crank-Nicolson numerical scheme (5.32) can be rewritten as

$$
\begin{aligned}
&\bar{A}^{n+1}v_{m+1}^{n+1}+\bar{B}^{n+1}v_{m-1}^{n+1}+\bar{C}^{n+1}v_m^{n+1}+\bar{A}^{n+1}v_{m+1}^{n}+\bar{B}^{n+1}v_{m-1}^{n}+\bar{C}^{n+1}v_m^{n}\\
&-2\beta\sum_{j=1}^{n}(v_m^{n-j+1}-v_m^{n-j})e^{-\frac{\alpha jk}{1-\alpha}}=0
\end{aligned}
$$

which becomes

$$
\begin{aligned}
&v_{m+1}^{n+1}=-(\bar{B}^{n+1}/\bar{A}^{n+1})v_{m-1}^{n+1}-(\bar{C}^{n+1}/\bar{A}^{n+1})v_m^{n+1}-(\bar{A}^{n+1}/\bar{A}^{n+1})v_{m+1}^{n}-(\bar{B}^{n+1}/\bar{A}^{n+1})v_{m-1}^{n}-\\
&(\bar{C}^{n+1}/\bar{A}^{n+1})v_m^{n}+(2\beta/\bar{A}^{n+1})\sum_{j=1}^{n}(v_m^{n-j+1}-v_m^{n-j})e^{-\frac{\alpha jk}{1-\alpha}}\ \text{for}\ m=1,2,\ldots,M-1\quad\text{and}\ n=1,\ldots,N
\end{aligned}
\tag{5.33}
$$

where

$$\begin{aligned}
\bar{A}^{n+1} &= \frac{-\theta(\tau^{n+1})(r-\frac{\sigma^2}{2})}{2\Delta y} - \varphi(\tau^{n+1})\frac{\sigma^2}{2\Delta y^2} + \frac{\phi(\tau^{n+1})}{X_f^n}\frac{X_f^{n+1}-X_f^n}{2\Delta y \Delta \tau} \\
\bar{B}^{n+1} &= \frac{\theta(\tau^{n+1})(r-\frac{\sigma^2}{2})}{2\Delta y} - \varphi(\tau^{n+1})\frac{\sigma^2}{2\Delta y^2} - \frac{\phi(\tau^{n+1})}{X_f^n}\frac{X_f^{n+1}-X_f^n}{2\Delta y \Delta \tau} \\
\bar{C}^{n+1} &= \theta(\tau^{n+1})r + \varphi(\tau^{n+1})\frac{\sigma^2}{\Delta y^2}.
\end{aligned} \tag{5.34}$$

It follows from the boundary and initial conditions in (5.27) that

$$\begin{cases}
v_0^n = 1 - X_f^n, \text{ for } n = 0, 1, \ldots, N \\
\frac{\partial v}{\partial y}(\tau, 0) = -X_f^n(\tau), \\
v_m^0 = 0, \text{ for } m = 0, 1, \ldots, M \\
X_f^0 = 1, \text{ for } m = 0, 1, \ldots, M \\
v_M^n = 0, \text{ for } n = 0, 1, \ldots, N.
\end{cases} \tag{5.35}$$

To present and validate equation (5.33) in matrix form, we intend in employing an induction technique.
To illustrate this, we start with the initial case $n = 1$, yielding:

$$\bar{A}^2 v_{m+1}^2 + \bar{B}^2 v_{m-1}^2 + \bar{C}^2 v_m^2 + \bar{A}^2 v_{m+1}^1 + \bar{B}^2 v_{m-1}^1 + \bar{C}^2 v_m^1 - 2\beta(v_m^1 - v_m^0)e^{-\frac{\alpha k}{1-\alpha}} = 0$$

from which we infer that

$$\bar{A}^2 v_{m+1}^2 + \bar{B}^2 v_{m-1}^2 + \bar{C}^2 v_m^2 = -\bar{B}^2 v_{m-1}^1 - \bar{A}^2 v_{m+1}^1 - \bar{C}^2 v_m^1 + 2\beta v_m^1 e^{-\frac{\alpha k}{1-\alpha}}. \tag{5.36}$$

For $n = 2$, we have that

$$\bar{A}^3 v_{m+1}^3 + \bar{B}^3 v_{m-1}^3 + \bar{C}^3 v_m^3 + \bar{A}^3 v_{m+1}^2 + \bar{B}^3 v_{m-1}^2 + \bar{C}^3 v_m^2 - 2\beta \sum_{j=1}^{2} (v_m^{n-j+1} - v_m^{n-j})e^{-\frac{\alpha j k}{1-\alpha}} = 0 \tag{5.37}$$

from which we infer that

$$\bar{A}^3 v_{m+1}^3 + \bar{B}^3 v_{m-1}^3 + \bar{C}^3 v_m^3 = -\bar{A}^3 v_{m+1}^2 - \bar{B}^3 v_{m-1}^2 - \bar{C}^3 v_m^2 + 2\beta \sum_{j=1}^{2} (v_m^{n-j+1} - v_m^{n-j})e^{-\frac{\alpha j k}{1-\alpha}}. \tag{5.38}$$

Similarly, we obtain for $n \geq 3$ the following result

$$\begin{aligned}
&\bar{A}^{n+1} v_{m+1}^{n+1} + \bar{B}^{n+1} v_{m-1}^{n+1} + \bar{C}^{n+1} v_m^{n+1} = \\
&- \bar{A}^{n+1} v_{m+1}^{n} - \bar{B}^{n+1} v_{m-1}^{n} - \bar{C}^{n+1} v_m^{n} + 2\beta \sum_{j=1}^{n} (v_m^{n-j+1} - v_m^{n-j}) e^{-\frac{\alpha j k}{1-\alpha}}.
\end{aligned} \tag{5.39}$$

At each time step, we have a system of linear equations involving $M-1$ variables and $M+1$ equations. These equations are valid for $m = 1, 2, 3 \ldots, M-1$, while the boundary conditions provide an extra two equations needed. The system can be expressed in matrix notation as shown below

$$\begin{bmatrix}
B^1 & C^1 & A^1 & 0 & \cdots & 0 & 0 \\
0 & B^2 & C^2 & A^2 & \cdots & 0 & 0 \\
0 & 0 & B^3 & C^3 & A^3 & \cdots & 0 \\
0 & 0 & 0 & B^4 & C^4 & A^4 & 0 \\
\vdots & \vdots & \vdots & \vdots & \ddots & \ddots & \ddots \\
0 & 0 & 0 & 0 & 0 & 0 & B^{n+1}
\end{bmatrix}
\begin{bmatrix} v_0^{n+1} \\ v_1^{n+1} \\ v_2^{n+1} \\ \vdots \\ v_M^{n+1} \end{bmatrix}
=
\begin{bmatrix}
B^1 & C^1 & A^1 & 0 & \cdots & 0 & 0 \\
0 & B^2 & C^2 & A^2 & \cdots & 0 & 0 \\
0 & 0 & B^3 & C^3 & A^3 & \cdots & 0 \\
0 & 0 & 0 & B^4 & C^4 & A^4 & 0 \\
\vdots & \vdots & \vdots & \vdots & \ddots & \ddots & \ddots \\
0 & 0 & 0 & 0 & 0 & 0 & B^{n+1}
\end{bmatrix}
\begin{bmatrix} v_0^{n} \\ v_1^{n} \\ v_2^{n} \\ \vdots \\ v_M^{n} \end{bmatrix}$$
$$+
\begin{bmatrix}
v_0^0 \\
2\beta \sum_{j=1}^{n} (v_m^{n-j+1} - v_m^{n-j}) e^{-\frac{\alpha j k}{1-\alpha}} \\
2\beta \sum_{j=1}^{n} (v_m^{n-j+1} - v_m^{n-j}) e^{-\frac{\alpha j k}{1-\alpha}} \\
2\beta \sum_{j=1}^{n} (v_m^{n-j+1} - v_m^{n-j}) e^{-\frac{\alpha j k}{1-\alpha}} \\
\vdots \\
2\beta \sum_{j=1}^{n} (v_m^{n-j+1} - v_m^{n-j}) e^{-\frac{\alpha j k}{1-\alpha}}
\end{bmatrix} \tag{5.40}$$

The matrix structure described above consists of $M-1$ rows and $M+1$ columns, aligned with the $M-1$ interior points and the $M+1$ unknowns. Note that the variables v_{N+1}^{-1} and v_{N+1}^{M+1} fall outside the computational domain. To address this challenge, we derive two additional equations from the boundary conditions, allowing us to reformulate the system as one involving square matrices where boundary constraints are fully integrated. We must emphasize that in order for us to incorporating the boundary conditions, we note the vanishing term: $v_{N+1}^{M+1} = 0$, which allows us to start the boundary application at $m = 0$. Furthermore, substituting the boundary condition of (5.27) into the main fraction differential equation that can be seen at the start of the same equations in (5.27) at $m = 0$ yields the following

modified boundary condition:

$$\frac{\partial^{\alpha}(v_0^{n+1})}{\partial t^{\alpha}} = \theta(\tau^{n+1})[r(1-X_f) + (r-\frac{\sigma^2}{2})X_f] - \varphi(\tau^{n+1})\frac{\sigma^2}{2}\frac{\partial^2 v}{\partial y^2} + \frac{\phi(\tau^{n+1})}{X_f(\tau)}\frac{dX_f(\tau)}{d\tau}\frac{\partial v}{\partial y} = 0. \tag{5.41}$$

We deduce the discretization of (5.41) as follows:

$$\begin{aligned}
&\beta\sum_{j=1}^{n}(-X^{n-j+1}+X^{n-j})e^{-\frac{\alpha jk}{1-\alpha}} = \theta(\tau^{n+1})[r-\frac{\sigma^2}{2}X_f^n]- \\
&\varphi(\tau^{n+1})\frac{\sigma^2}{4}(\frac{v_{-1}^{n+1}-2v_0^{n+1}+v_1^{n+1}}{\Delta y^2}+\frac{v_{-1}^{n}-2v_0^{n}+v_1^{n}}{\Delta y^2}) - \phi(\tau^{n+1})\frac{X_f^{n+1}-X_f^n}{\Delta\tau} = 0
\end{aligned} \tag{5.42}$$

It follows from the boundary conditions in (5.27) that

$$\begin{aligned}
&\frac{1}{4}(\frac{v_1^{n+1}-v_{-1}^{n+1}}{\Delta y}+\frac{v_1^n-v_{-1}^n}{\Delta y}) = -\frac{1}{2}(X_f^{n+1}(\tau)+X_f^n(\tau));\\
&v_{-1}^{n+1}+v_{-1}^n = v_1^{n+1}+v_1^n+2(X_f^{n+1}(\tau)+X_f^n(\tau));\\
&v_0^n = 1-X_f^n(\tau)
\end{aligned} \tag{5.43}$$

Now, inserting the boundary conditions (5.43) into (5.42) and then we obtain after easy simplification that

$$\begin{aligned}
&\beta\sum_{j=1}^{n}(X^{n-j+1}-X^{n-j})e^{-\frac{\alpha jk}{1-\alpha}} + \theta(\tau^{n+1})[r-\frac{\sigma^2}{2}X_f^n] - \phi(\tau^{n+1})\frac{X_f^{n+1}-X_f^n}{\Delta\tau}\\
&-\varphi(\tau^{n+1})\frac{\sigma^2}{4}(\frac{v_{-1}^{n+1}-2v_0^{n+1}+v_1^{n+1}+v_{-1}^n-2v_0^n+v_1^n}{\Delta y^2}) = 0
\end{aligned}$$

which implies that

$$\begin{aligned}
&\beta\sum_{j=1}^{n}(X^{n-j+1}-X^{n-j})e^{-\frac{\alpha jk}{1-\alpha}} + \theta(\tau^{n+1})[r-\frac{\sigma^2}{2}X_f^n] - \phi(\tau^{n+1})\frac{X_f^{n+1}-X_f^n}{\Delta\tau}-\\
&\varphi(\tau^{n+1})\frac{\sigma^2}{4}(\frac{2X^{n+1}\Delta y+2v_1^{n+1}-2(1-X^{n+1})+2X^n\Delta y+2v_1^n-2(1-X^n)}{\Delta y^2}) = 0
\end{aligned}$$

from which we infer that

$$\begin{aligned}
&\beta\sum_{j=1}^{n}(X^{n-j+1}-X^{n-j})e^{-\frac{\alpha jk}{1-\alpha}} + \theta(\tau^{n+1})[r-\frac{\sigma^2}{2}X_f^n] - \phi(\tau^{n+1})\frac{X_f^{n+1}-X_f^n}{\Delta\tau}-\\
&\varphi(\tau^{n+1})\frac{\sigma^2}{2}(\frac{(X^{n+1}+X^n)\Delta y+v_1^{n+1}+v_1^n-(1-X^{n+1})-(1-X^n)}{\Delta y^2}) = 0
\end{aligned}$$

which enables us to deduce that

$$\frac{2\Delta y^2}{\varphi(\tau^{n+1})\sigma^2}(\beta\sum_{j=1}^{n}(X^{n-j+1}-X^{n-j})e^{-\frac{\alpha jk}{1-\alpha}}+\theta(\tau^{n+1})[r-\frac{\sigma^2}{2}X_f^n]-\phi(\tau^{n+1})\frac{X_f^{n+1}-X_f^n}{\Delta\tau})=$$
$$(X^{n+1}+X^n)(1+\Delta y)+v_1^{n+1}+v_1^n-2$$

After reducing the above expression, we deduce that

$$v_1^{n+1}=\frac{2\Delta y^2}{\varphi(\tau^{n+1})\sigma^2}\Bigg[\beta\sum_{j=1}^{n}(X^{n-j+1}-X^{n-j})e^{-\frac{\alpha jk}{1-\alpha}}+\theta(\tau^{n+1})[r-\frac{\sigma^2}{2}X_f^n]-$$
$$\phi(\tau^{n+1})\frac{X_f^{n+1}-X_f^n}{\Delta\tau}\Bigg]-(X^{n+1}+X^n)(1+\Delta y)-v_1^n+2. \tag{5.44}$$

Combining all the above equations from (5.33) to (5.44) we deduce that

$$\mathbf{W_{n+1}v_{n+1}}+\mathbf{R_{n+1}}=\mathbf{W_nv_n}+\mathbf{L_n}+\Sigma_{n+1} \tag{5.45}$$

where

$$\mathbf{W_n}=\mathbf{W_{n+1}}\begin{bmatrix}C^1&A^1&0&\cdots&0&0&0\\0&B^2&C^2&A^2&\cdots&0&0\\0&0&B^3&C^3&A^3&\cdots&0\\0&0&0&B^4&C^4&A^4&0\\\vdots&\vdots&\vdots&\vdots&\ddots&\ddots&\ddots\\0&0&0&0&0&B^{n+1}&C^{n+1}\end{bmatrix};$$

$$\mathbf{v^n}=\begin{bmatrix}v_1^n\\v_2^n\\\vdots\\v_{M-1}^n\end{bmatrix},\quad\mathbf{v^{n+1}}=\begin{bmatrix}v_1^{n+1}\\v_2^{n+1}\\\vdots\\v_{M-1}^{n+1}\end{bmatrix};$$

$$\mathbf{L^n}=\begin{bmatrix}B^nv_0^n\\0\\\vdots\\0\\B^nv_M^n\end{bmatrix},\quad\mathbf{R^{n+1}}=\begin{bmatrix}B^{n+1}v_0^{n+1}\\0\\\vdots\\0\\B^{n+1}v_M^{n+1}\end{bmatrix};$$

$$\Sigma_{n+1} = \begin{bmatrix} 2\beta \sum_{j=1}^{n} \left(v_m^{n-j+1} - v_m^{n-j}\right) e^{-\frac{\alpha j k}{1-\alpha}} \\ 2\beta \sum_{j=1}^{n} \left(v_m^{n-j+1} - v_m^{n-j}\right) e^{-\frac{\alpha j k}{1-\alpha}} \\ 2\beta \sum_{j=1}^{n} \left(v_m^{n-j+1} - v_m^{n-j}\right) e^{-\frac{\alpha j k}{1-\alpha}} \\ \vdots \\ 2\beta \sum_{j=1}^{n} \left(v_m^{n-j+1} - v_m^{n-j}\right) e^{-\frac{\alpha j k}{1-\alpha}} \end{bmatrix}.$$

Hence, (5.45) becomes

$$\mathbf{v_{n+1}} = \mathbf{W_{n+1}^{-1}} \left(\mathbf{W_n v_n} + \mathbf{L_n} + \Sigma_{n+1} - \mathbf{R_{n+1}}\right). \tag{5.46}$$

The Crank-Nicolson discretization of APO leads to the non-linear equation (5.46) regarding price and the free boundary condition at every time step.
Now, to determine the value of X_f^n, we apply the schemes (5.32) and (5.44) at $m = 1$ and evaluate the time level n^{th} of the free boundary. Therefore,

$$\begin{aligned}
&v_2^{n+1}\Big[\frac{-\theta(\tau^{n+1})(r-\frac{\sigma^2}{2})}{2\Delta y} - \varphi(\tau^{n+1})\frac{\sigma^2}{2\Delta y^2} + \frac{\phi(\tau^{n+1})}{X_f^n}\frac{X_f^{n+1}-X_f^n}{2\Delta y \Delta\tau}\Big] + \\
&v_2^{n}\Big[\frac{-\theta(\tau^{n+1})(r-\frac{\sigma^2}{2})}{2\Delta y} - \varphi(\tau^{n+1})\frac{\sigma^2}{2\Delta y^2} + \frac{\phi(\tau^{n+1})}{X_f^n}\frac{X_f^{n+1}-X_f^n}{2\Delta y \Delta\tau}\Big] + \\
&v_0^{n+1}\Big[\frac{\theta(\tau^{n+1})(r-\frac{\sigma^2}{2})}{2\Delta y} - \varphi(\tau^{n+1})\frac{\sigma^2}{2\Delta y^2} - \frac{\phi(\tau^{n+1})}{X_f^n}\frac{X_f^{n+1}-X_f^n}{2\Delta y \Delta\tau}\Big] + \\
&v_0^{n}\Big[\frac{\theta(\tau^{n+1})(r-\frac{\sigma^2}{2})}{2\Delta y} - \varphi(\tau^{n+1})\frac{\sigma^2}{2\Delta y^2} - \frac{\phi(\tau^{n+1})}{X_f^n}\frac{X_f^{n+1}-X_f^n}{2\Delta y \Delta\tau}\Big] + \\
&v_1^{n+1}\Big[\theta(\tau^{n+1})r + \varphi(\tau^{n+1})\frac{\sigma^2}{\Delta y^2}\Big] + v_1^{n}\Big[\theta(\tau^{n+1})r + \varphi(\tau^{n+1})\frac{\sigma^2}{\Delta y^2}\Big] - \\
&2\beta\sum_{j=1}^{n}(v_1^{n+1} - v_1^n)e^{\frac{-\alpha j k}{1-\alpha}} = 0.
\end{aligned} \tag{5.47}$$

By incorporating v_0^n from equation (5.35) and v_1^n from equation (5.44) into equation (5.47),

we derive the following result:

$$
\begin{aligned}
&v_2^{n+1}\Big[\frac{-\theta(\tau^{n+1})(r-\frac{\sigma^2}{2})}{2\Delta y}-\varphi(\tau^{n+1})\frac{\sigma^2}{2\Delta y^2}+\frac{\phi(\tau^{n+1})}{X_f^n}\frac{X_f^{n+1}-X_f^n}{2\Delta y\Delta\tau}\Big]+\\
&v_2^{n}\Big[\frac{-\theta(\tau^{n+1})(r-\frac{\sigma^2}{2})}{2\Delta y}-\varphi(\tau^{n+1})\frac{\sigma^2}{2\Delta y^2}+\frac{\phi(\tau^{n+1})}{X_f^n}\frac{X_f^{n+1}-X_f^n}{2\Delta y\Delta\tau}\Big]+\\
&(1-X_f^{n+1})\Big[\frac{\theta(\tau^{n+1})(r-\frac{\sigma^2}{2})}{2\Delta y}-\varphi(\tau^{n+1})\frac{\sigma^2}{2\Delta y^2}-\frac{\phi(\tau^{n+1})}{X_f^n}\frac{X_f^{n+1}-X_f^n}{2\Delta y\Delta\tau}\Big]+\\
&(1-X_f^{n})\Big[\frac{\theta(\tau^{n+1})(r-\frac{\sigma^2}{2})}{2\Delta y}-\varphi(\tau^{n+1})\frac{\sigma^2}{2\Delta y^2}-\frac{\phi(\tau^{n+1})}{X_f^n}\frac{X_f^{n+1}-X_f^n}{2\Delta y\Delta\tau}\Big]+\\
&\Bigg(\frac{2\Delta y^2}{\varphi(\tau^{n+1})\sigma^2}\Big[\beta\sum_{j=1}^{n}(X^{n-j+1}-X^{n-j})e^{-\frac{\alpha jk}{1-\alpha}}+\theta(\tau^{n+1})[r-\frac{\sigma^2}{2}X_f^n]-\phi(\tau^{n+1})\frac{X_f^{n+1}-X_f^n}{\Delta\tau}\Big]-\\
&(X^{n+1}+X^n)(1+\Delta y)+2\Bigg)\big[\theta(\tau^{n+1})r+\varphi(\tau^{n+1})\frac{\sigma^2}{\Delta y^2}\big]-\\
&2\beta\sum_{j=1}^{n}(v_1^{n-j+1}-v_1^{n-j})e^{-\frac{\alpha jk}{1-\alpha}}=0
\end{aligned}
\tag{5.48}
$$

In a similar fashion, now we can simplify further the above equation to obtain

$$
\begin{aligned}
&v_2^{n+1}\Big[X_f^n(\frac{-\theta(\tau^{n+1})(r-\frac{\sigma^2}{2})}{2\Delta y}-\varphi(\tau^{n+1})\frac{\sigma^2}{2\Delta y^2})+\phi(\tau^{n+1})\frac{X_f^{n+1}-X_f^n}{2\Delta y\Delta\tau}\Big]+\\
&v_2^{n}\Big[X_f^n(\frac{-\theta(\tau^{n+1})(r-\frac{\sigma^2}{2})}{2\Delta y}-\varphi(\tau^{n+1})\frac{\sigma^2}{2\Delta y^2})+\phi(\tau^{n+1})\frac{X_f^{n+1}-X_f^n}{2\Delta y\Delta\tau}\Big]+\\
&(1-X_f^{n+1})\Big[X_f^n(\frac{\theta(\tau^{n+1})(r-\frac{\sigma^2}{2})}{2\Delta y}-\varphi(\tau^{n+1})\frac{\sigma^2}{2\Delta y^2})-\phi(\tau^{n+1})\frac{X_f^{n+1}-X_f^n}{2\Delta y\Delta\tau}\Big]+\\
&(1-X_f^{n})\Big[X_f^n(\frac{\theta(\tau^{n+1})(r-\frac{\sigma^2}{2})}{2\Delta y}-\varphi(\tau^{n+1})\frac{\sigma^2}{2\Delta y^2})-\phi(\tau^{n+1})\frac{X_f^{n+1}-X_f^n}{2\Delta y\Delta\tau}\Big]+\\
&X_f^n\Bigg(\frac{2\Delta y^2}{\varphi(\tau^{n+1})\sigma^2}\Big[\beta\sum_{j=1}^{n}(X^{n-j+1}-X^{n-j})e^{-\frac{\alpha jk}{1-\alpha}}+\theta(\tau^{n+1})[r-\frac{\sigma^2}{2}X_f^n]-\phi(\tau^{n+1})\frac{X_f^{n+1}-X_f^n}{\Delta\tau}\Big]-\\
&(X^{n+1}+X^n)(1+\Delta y)+2\Bigg)\big[\theta(\tau^{n+1})r+\varphi(\tau^{n+1})\frac{\sigma^2}{\Delta y^2}\big]-\\
&2X_f^n\beta\sum_{j=1}^{n}(v_1^{n-j+1}-v_1^{n-j})e^{-\frac{\alpha jk}{1-\alpha}}=0.
\end{aligned}
\tag{5.49}
$$

We observe that equation (5.49) represents a quadratic equation with complex coefficients and a constant term. At this point, the coefficients and a constant can be systematically collected for further analysis.

After factoring (X_f^{n+1}) from equation (5.49), the resulting coefficient, designated as *bb*, presented.
Let us begin by collecting the coefficients of X_f^{n+1} using

$$X_f^{n+1}\Bigg((v_2^{n+1}+v_2^n)\frac{\phi(\tau^{n+1})}{2\Delta y\Delta\tau}-(2-X_f^n)\frac{\phi(\tau^{n+1})}{2\Delta y\Delta\tau}-\big[X_f^n(\frac{\theta(\tau^{n+1})(r-\frac{\sigma^2}{2})}{2\Delta y}-\varphi(\tau^{n+1})\frac{\sigma^2}{2\Delta y^2})+$$
$$+\frac{\phi(\tau^{n+1})X_f^n}{2\Delta y\Delta\tau}\big]-X_f^n\big(\frac{2\Delta y^2}{\varphi(\tau^{n+1})\sigma^2}\frac{\phi(\tau^{n+1})}{\Delta\tau}+(1+\Delta y)\big)\big[\theta(\tau^{n+1})r+\varphi(\tau^{n+1})\frac{\sigma^2}{\Delta y^2}\big]\Bigg).$$

Hence

$$bb^{n+1}=(v_2^{n+1}+v_2^n-2)\frac{\phi(\tau^{n+1})}{2\Delta y\Delta\tau}-X_f^n\big[\frac{\theta(\tau^{n+1})(r-\frac{\sigma^2}{2})}{2\Delta y}-\varphi(\tau^{n+1})\frac{\sigma^2}{2\Delta y^2}\big]-$$
$$X_f^n\big(\frac{2\Delta y^2}{\varphi(\tau^{n+1})\sigma^2}\frac{\phi(\tau^{n+1})}{\Delta\tau}+(1+\Delta y)\big)\big[\theta(\tau^{n+1})r+\varphi(\tau^{n+1})\frac{\sigma^2}{\Delta y^2}\big] \tag{5.50}$$

After taking the term $(X_f^{n+1})^2$ as a common factoring in equation (5.49), then the resulting coefficient denoted by *aa*, can presented as:

$$aa^{n+1}=\frac{\phi(\tau^{n+1})}{2\Delta y\Delta\tau}. \tag{5.51}$$

Finally, the constant term of the quadratic equation is aggregated, resulting in the subsequent expression denoted by *cc*

$$cc^{n+1}=(v_2^{n+1}+v_2^n)X_f^n\Big[\frac{-\theta(\tau^{n+1})(r-\frac{\sigma^2}{2})}{2\Delta y}-\varphi(\tau^{n+1})\frac{\sigma^2}{2\Delta y^2}-\frac{\phi(\tau^{n+1})}{2\Delta y\Delta\tau}\Big]+$$
$$(2-X_f^n)X_f^n\Big[\frac{\theta(\tau^{n+1})(r-\frac{\sigma^2}{2})}{2\Delta y}-\varphi(\tau^{n+1})\frac{\sigma^2}{2\Delta y^2}+\frac{\phi(\tau^{n+1})}{2\Delta y\Delta\tau}\Big]+$$
$$X_f^n\Bigg(\frac{2\Delta y^2}{\varphi(\tau^{n+1})\sigma^2}\Big[\beta\sum_{j=1}^{n}(X^{n-j+1}-X^{n-j})e^{-\frac{\alpha jk}{1-\alpha}}+\theta(\tau^{n+1})(r-\frac{\sigma^2}{2}X_f^n)+\phi(\tau^{n+1})\frac{X_f^n}{\Delta\tau}\Big]-$$
$$X^n(1+\Delta y)+2\Bigg)\big[\theta(\tau^{n+1})r+\varphi(\tau^{n+1})\frac{\sigma^2}{\Delta y^2}\big]-2X_f^n\beta\sum_{j=1}^{n}(v_1^{n-j+1}-v_1^{n-j})e^{-\frac{\alpha jk}{1-\alpha}}. \tag{5.52}$$

Note that equation (5.49) has now been simplified and its simplified version can be reformulated as follows:

$$aa^{n+1}(X_f^{n+1})^2+bb^{n+1}X_f^{n+1}+cc^{n+1}=0. \tag{5.53}$$

In order for us to resolve the issue of the quadratic equation presented above, two potential roots are obtained. However, one of the roots specifically, $\frac{-bb^{n+1}+\sqrt{(bb^{n+1})^2-4aa^{n+1}cc^{n+1}}}{2aa^{n+1}}$ consistently falls outside the acceptable range defined by the free boundary X_f^{n+1}, as it is greater

than 1. Consequently, this root is deemed nonviable, as it does not satisfy the necessary constraints and is therefore excluded from consideration.
The remaining root, given by $\frac{-bb^{n+1}-\sqrt{(bb^{n+1})^2-4aa^{n+1}cc^{n+1}}}{2aa^{n+1}}$, falls within the acceptable range and satisfies all the required conditions of the problem. Thus, it is chosen as the only valid solution in this analysis. This approach ensures that only meaningful solutions are considered, consistent with the free boundary conditions of X_f^{n+1} , representing the desired outcome.

5.3.4 Algorithm

In the following section, we will demonstrate the implementation of the algorithm as outlined in section 5.3 using Python code. The algorithm incorporates all the equations discussed in section 5.3 and focuses on solving the fractional-order PDE for option pricing using a finite-difference front-fixing scheme. The primary goal is to calculate the option price, denoted $v[m, n]$, at each point on the temporal and spatial grid

i. **Initialize Parameters:**

- Set risk-free interest rate r, the fractional order α, volatility σ as well as strike price E.
- Define spatial and temporal grid sizes (M, N), step sizes (h, k) and bounds (y_∞, T).

ii. **Grid Setup:**

- Define the spatial grid y and temporal grid τ.
- Initialize matrices v, X and other auxiliary variables.

iii. **Auxilary Functions:**

- Implement auxilary functions to calculate:
  - Partial sums for FDs.
  - $\tau^{1-\alpha}$ *and* $\varphi(\tau^{n+1})$.
  - Quadratic roots for X based on coefficients $aa, bbandcc$.

iv. **Boundary Conditions:**

- Set initial conditions:

$$v[m, 0] = v_0, \quad v[0, :] = 1 - X[n].$$

v. **Crank-Nicolson Time-Stepping:**

- Iterate over time steps $n$and space steps m:

- Update auxiliary variables τ and $\varphi(\tau^{n+1})$.
- Compute coefficients $\bar{A}^{n+1}, \bar{B}^{n+1} and \bar{C}^{n+1}$ for the Crank-Nicolson scheme.

- For $m = 1$:
  - Compute partial sums and quadratic roots to update $X[n+1]$.
  - Use $X[n+1]$ to calculate $v[m, n+1]$.
- For $m > 1$:
  - Use the Crank-Nicolson formula to compute $v[m, n+1]$.

vi. **Post-Processing:**

- Plot the 3D surface of $v[m, n]$ as a function of $m and n$.
- Smooth and plot:
  - $y[m]$ vs $v[m, N-1]$.
  - $\tau[n]$ vs $X[n]$ (excluding the final time step).

vii. **Error Computation:**

- To compute the maximum error:
  - Run the algorithm twice, once with $M = 80$, $N = 320$ (fine grid) and once with $M = 20$, $N = 20$ (coarse grid).
  - Interpolate the fine grid solution onto the coarse grid and calculate the absolute difference.
  - Report the maximum error.
  - Convergence rate

5.4 Consistency and Stability

This section is devoted to the analysis of the consistency and stability of the Crank-Nicolson method of Caputo FDs for the APOs (5.33). In light of the above, we first deal with the following consistency.

5.4.1 Consistency

To deal with the issue of consistency of the scheme considered in this chapter, we need the following concept.

DEFINITION 5.4.1. *Let $\mathcal{F}(v_m^n, X_f^n)$ be the difference operator that approximates $\mathcal{L}(v, X_f)$. The local truncation error $\mathcal{T}_m^n(\bar{v}, \bar{X}_f)$ is given by the leading terms of the Taylor expansion of $\mathcal{F}(v_m^n, X_f^n) = 0$, where u satisfies $\mathcal{L}(v, X_f) = 0$.*

We remark form from the above Definition 5.4.1 that

$$\mathcal{T}_m^n(\bar{v}, \bar{X}_f) = \mathcal{F}(v_m^n, X_f^m), \text{ and}$$
$$\lim_{(\Delta\tau, \Delta y)\to(0,0)} \mathcal{T}_m^n(\bar{v}, \bar{X}_f) = 0. \tag{5.54}$$

Let's start by choosing an arbitrary location $(y, \tau) \in [0, 4E] \times [0, T]$ the mesh point (y^m, τ^n) to examine the consistency of Caputo fractional PDE as defined in (5.27) and its numerical scheme as considered in relation (5.33) by employing the Crank-Nicolson FDM. For this purpose, we consider $\bar{v}_m^n = v(\tau^n, y_m)$ to be the exact solution for the Caputo fractional PDE and $\bar{X}_f^n = X_f^n$ to be the free boundary, respectively. Namely, it means that

$$\mathcal{L}(v, X_f^n) = \frac{\partial^\alpha v}{\partial \tau^\alpha} - \theta(\tau)[rv - (r - \frac{\sigma^2}{2})\frac{\partial v}{\partial y}] + \varphi(\tau)\frac{\sigma^2}{2}\frac{\partial^2 v}{\partial y^2} - \phi(\tau)\frac{X_f'(\tau)}{X_f(\tau)}\frac{\partial v}{\partial y} = 0$$

and

$$\mathcal{F}(v_n^{m+1}, X_f^{n+1}) = 2\beta\sum_{j=1}^{n}(v_m^{n-j+1} - v_m^{n-j})e^{-\frac{\alpha j k}{1-\alpha}} =$$
$$\theta(\tau^{n+1})[(rv_m^{n+1} + rv_m^n) - (r - \frac{\sigma^2}{2})(\frac{v_{m+1}^{n+1} - v_{m-1}^{n+1}}{2\Delta y} + \frac{v_{m+1}^n - v_{m-1}^n}{2\Delta y})]$$
$$-\varphi(\tau^{n+1})\frac{\sigma^2}{2}(\frac{v_{m-1}^{n+1} - 2v_m^{n+1} + v_{m+1}^{n+1}}{\Delta y^2} + \frac{v_{m-1}^n - 2v_m^n + v_{m+1}^n}{\Delta y^2})$$
$$+\frac{\phi(\tau^{n+1})}{X_f^n}\frac{X_f^{n+1} - X_f^n}{(\Delta\tau)}(\frac{v_{m+1}^{n+1} - v_{m-1}^{n+1}}{2\Delta y} + \frac{v_{m+1}^n - v_{m-1}^n}{2\Delta y}).$$

Having derived this result which leads us to the statement of the following consistency result.

THEOREM 5.4.1. *The Crank-Nicolson finite-difference scheme of the Caputo FDs scheme method defined in equations* (5.27) *is consistent with the fixed domain model* (5.33) *of order* $\mathcal{O}(1) + \mathcal{O}((\Delta y)^2)$.

Proof. We implement Taylor's expansion similar to the techniques used in [75], taking into account the continuous partial derivatives of orders two and four in space and time, respectively to show the consistency of (5.27).
First, we examine the consistency of FDs in equation (5.27). In our earlier analysis, as outlined in equation (5.29), we developed a scheme for the Caputo FDs corresponding to certain parts of equation (5.27), establishing an order of accuracy of

$$\frac{\partial^{\alpha} v}{\partial \tau^{\alpha}} = \beta \sum_{j=1}^{n} (v_m^{n-j+1} - v_m^{n-j}) e^{-\frac{\alpha j k}{1-\alpha}} + \mathcal{O}(1) \quad \text{where} \quad \beta = \frac{1}{k\alpha}(1 - e^{-\frac{\alpha k}{1-\alpha}}) \tag{5.55}$$

with truncation denoted by

$$\mathbf{e_1} = \mathcal{O}(1) \tag{5.56}$$

Secondly, let us find the consistency of each of the last three right-hand side of our main equations considered in relation (5.27) separately, using Taylor's expansion of order two and four in time and space, respectively.
For now, let us consider the first term on the right-hand side; we proceed to estimate its truncation error (5.27) by using

$$\begin{aligned}
&\phi(\tau^{n+1})\sigma^2 \frac{\partial^2 v}{\partial y^2} = \phi(\tau^{n+1})\sigma^2 (\frac{v_{m-1}^n - 2v_m^n + v_{m+1}^n}{\Delta y^2}) \\
=&\frac{\phi(\tau^{n+1})}{\Delta y^2}\sigma^2 (v_m^n - \Delta y \frac{v_y}{1!} + (\Delta y)^2 \frac{v_{yy}}{2!} - (\Delta y)^3 \frac{v_{yyy}}{3!} + (\Delta y)^4 \frac{v_{yyyy}}{4!} + (\Delta y)^5 - \\
&2v_m^n + v_m^n + \Delta y \frac{v_y}{1!} + (\Delta y)^2 \frac{v_{yy}}{2!} + (\Delta y)^3 \frac{v_{yyy}}{3!} + (\Delta y)^4 \frac{v_{yyyy}}{4!} + (\Delta y)^5) \\
=&\phi(\tau^{n+1})\sigma^2 (\frac{\partial^2 v}{\partial^2 y} + (\Delta y)^2 \frac{1}{12} \frac{\partial^4 v}{\partial^4 y} + \mathcal{O}(\Delta y)^3).
\end{aligned} \tag{5.57}$$

Therefore the error term of (5.57) becomes

$$\mathbf{e_2} = \phi(\tau^{n+1})\sigma^2 [(\Delta y)^2 \frac{1}{12} \frac{\partial^4 v}{\partial^4 y} + \mathcal{O}(\Delta y)^3]. \tag{5.58}$$

Consider the first term on the right-hand side; we proceed to estimate its truncation error. Again, we consider the first term on the right-hand side; we proceed to estimate its truncation error (5.27)

$$\begin{aligned}
&\theta(\tau^{n+1})(\frac{\sigma^2}{2} - r)\frac{\partial v}{\partial y} = \theta(\tau^{n+1})\frac{1}{2}(\frac{\sigma^2}{2} - r)(\frac{v_{n+1}^{m+1} - v_{n+1}^{m-1}}{2\Delta y} + \frac{v_n^{m+1} - v_n^{m-1}}{2\Delta y}) \\
=&\theta(\tau^{n+1})\frac{1}{2}(\frac{\sigma^2}{2} - r)(\frac{\partial v}{\partial y} + (\Delta y)^2 \frac{1}{6} \frac{\partial^3 v}{\partial^3 y} + \mathcal{O}(\Delta y)^4).
\end{aligned} \tag{5.59}$$

Therefore the error term of (5.59) becomes

$$\mathbf{e_3} = (\Delta y)^2 \frac{1}{6} \frac{\partial^3 v}{\partial^3 y} + \mathcal{O}(\Delta y)^4. \tag{5.60}$$

Next, we consider the third term on the right-hand side; we proceed to estimate its truncation error (5.27) by relying on the expression below:

$$\varphi(\tau^{n+1})\frac{1}{X_f(\tau)}\frac{dX_f(\tau)}{d\tau}\frac{\partial v}{\partial y} = \varphi(\tau^{n+1})\frac{1}{2}(\frac{X_f^{n+1}(\tau)-X_f^n(\tau)}{\Delta\tau X_f(\tau)}(\frac{v_{n+1}^{m+1}-v_{n+1}^{m-1}}{2\Delta y}+\frac{v_n^{m+1}-v_n^{m-1}}{2\Delta y}) =$$
$$\frac{\varphi(\tau^{n+1})}{X_f(\tau)}(\frac{dX_f(\tau)}{d\tau}+(\Delta\tau)^2\frac{d^2X_f(\tau)}{d\tau^2}+\mathcal{O}((\Delta\tau)^2))(\frac{\partial v}{\partial y}+(\Delta y)^2\frac{1}{6}\frac{\partial^3 v}{\partial^3 y}+\mathcal{O}(\Delta y)^4) =$$
$$\frac{\varphi(\tau^{n+1})}{X_f(\tau)}\frac{dX_f(\tau)}{d\tau}\frac{\partial v}{\partial y}+\frac{\varphi(\tau^{n+1})}{X_f(\tau)}\frac{dX_f(\tau)}{d\tau}((\Delta y)^2\frac{1}{6}\frac{\partial^3 v}{\partial^3 y}+\mathcal{O}(\Delta y)^4)+$$
$$\frac{1}{X_f(\tau)}((\Delta\tau)^2\frac{d^2X_f(\tau)}{d\tau^2}+\mathcal{O}((\Delta\tau)^2))(\frac{\partial v}{\partial y}+(\Delta y)^2\frac{1}{6}\frac{\partial^3 v}{\partial^3 y}+\mathcal{O}(\Delta y)^4). \tag{5.61}$$

Therefore the error term of (5.61) becomes

$$\begin{aligned}\mathbf{e_4} &= \frac{\varphi(\tau^{n+1})}{X_f(\tau)}\frac{dX_f(\tau)}{d\tau}((\Delta y)^2\frac{1}{6}\frac{\partial^3 v}{\partial^3 y}+\mathcal{O}(\Delta y)^4)\\ &+\frac{\varphi(\tau^{n+1})1}{X_f(\tau)}((\Delta\tau)^2\frac{d^2X_f(\tau)}{d\tau^2}+\mathcal{O}((\Delta\tau)^2))(\frac{\partial v}{\partial y}+(\Delta y)^2\frac{1}{6}\frac{\partial^3 v}{\partial^3 y}+\mathcal{O}(\Delta y)^4)\end{aligned} \tag{5.62}$$

Lastly, we can find the truncation error of the last term of the right-hand side of (5.27)

$$rv = \frac{1}{2}(rv_{n+1}^m + rv_n^m) \tag{5.63}$$

Hence, the local truncation error of (5.27) using (5.56) to (5.63) is provided by the following expression:

$$\mathcal{T}_n^{m+1}(\bar{v},\bar{X_f}) = \mathbf{e_1}+\mathbf{e_2}+\mathbf{e_3}+\mathbf{e_4} = \mathcal{O}(1)+\mathcal{O}(\Delta\tau)+\mathcal{O}((\Delta y)^2). \tag{5.64}$$

We now proceed to determine the local truncation error of the boundary conditions of equations (5.27), (5.42) and (5.41). For us to get the boundary conditions, we use the following normal derivatives:

$$\begin{cases}\mathcal{L}_1(v,X_f) = v(\tau,0)-1+X_f(\tau)=0\\ \mathcal{L}_2(v,X_f) = \frac{\partial v}{\partial y}(\tau,0)+X_f(\tau)=0,\\ \mathcal{L}_3(v,X_f) = -{}_0^cD_t^\alpha(1-X_f(\tau))+\theta(\tau^{n+1})[r(1-X_f)+(r-\frac{\sigma^2}{2})X_f]-\varphi(\tau^{n+1})\frac{\sigma^2}{2}\frac{\partial^2 v}{\partial y^2}\\ +\frac{\varphi(\tau^{n+1})}{X_f(\tau)}\frac{dX_f(\tau)}{d\tau}\frac{\partial v}{\partial y}=0\end{cases} \tag{5.65}$$

from which we deduce the numerical boundary scheme:

$$\begin{cases}\mathcal{F}_1(v_{n+1}^0,X_f^{n+1}) = v_{n+1}^0-1+X_f^{n+1}\\ \mathcal{F}_2(v_{n+1}^0,X_f^{n+1}) = \frac{v_{n+1}^1-v_{n+1}^{-1}+v_n^1-v_n^{-1}}{2\Delta y}+X_f^{n+1}\\ \mathcal{F}_3(v_{n+1}^0,X_f^{n+1}) = -\beta\sum_{j=1}^n(-X^{n-j+1}+X^{n-j})e^{-\frac{\alpha jk}{1-\alpha}}+\theta(\tau^{n+1})[r-\frac{\sigma^2}{2}X_f^{n+1}]-\\ \varphi(\tau^{n+1})\frac{\sigma^2}{4}(\frac{v_{-1}^{n+1}-2v_0^{n+1}+v_1^{n+1}}{\Delta y^2}+\frac{v_{-1}^n-2v_0^n+v_1^n}{\Delta y^2})-\frac{X_f^{n+1}-X_f^n}{\Delta\tau}=0.\end{cases} \tag{5.66}$$

By following the same steps we just used as done for relations (5.56) to (5.63) for (5.65) and (5.66), we obtain the following local truncation error

$$\mathcal{O}(1) + \mathcal{O}(\Delta\tau) + \mathcal{O}((\Delta y)^2). \tag{5.67}$$

It follows now that

$$\begin{aligned}
\mathcal{T}_1^0(\bar{v}, \bar{X}_f) &= \mathcal{F}_1(V_{n+1}^0, X_f^{n+1}) = 0, \\
\mathcal{T}_2^0(\bar{v}, \bar{X}_f) &= (\Delta y)^2 \frac{1}{3} \frac{\partial^3 v}{\partial^3 y} + \mathcal{O}(\Delta y)^4, \\
\mathcal{T}_3^0(\bar{v}, \bar{X}_f) &= \mathcal{O}(\Delta\tau) + \mathcal{O}((\Delta y)^2).
\end{aligned}$$

As a result of (5.64) and (5.67), we can now assert that the Crank-Nicolson finite scheme provided by (5.33) is a compatible model defined on a fixed domain (5.21) of order

$$\mathcal{O}(1) + \mathcal{O}((\Delta y)^2).$$

This proves the desired result for the consistency. □

5.4.2 Stability

In this section, we introduce the stability properties of the numerical scheme (5.33). We begin by defining the stability used in the section for the sake of several concepts of stability used in the literature. In order to define the concept of stability that we deal with in this chapter we borrow some basic notions from the papers [64, 46].

DEFINITION 5.4.2. *The numerical scheme* (5.33) *is said to be* $\|v^n\|_\infty$ *stable in the domain, if for every partition of the domain* $[0, \infty] \times [0, T]$ *we set* $\Delta\tau = \frac{T}{N}$ *and* $\Delta y = \frac{Y}{M}$, $\exists \zeta > 0$ *which is constant:*

$$\|v^n\|_\infty \leq \zeta, \ \ for\ 0 \leq n \leq N \tag{5.68}$$

where ζ *does not depend on* $\Delta\tau, \Delta y$ *and* $n = 1, 2, \ldots, N$.

Having defined the notion of stability that we are using here, we can state another main result of this chapter in the following lemma.

LEMMA 5.4.1. *Let* (v_n^m, X_f^n) *be the computed numerical solution and for sufficiently small values of* Δy, *we have:*

(i) X_f^n *is positive and decreasing for* $n = 0, 1, \ldots, N$;

(ii) the vectors v_n^m *have positive components for* $n = 0, 1, \ldots, N$;

(iii) the vectors v_n^m are decreasing w.r.t m for each fixed $n = 0, 1, \ldots, N$.

Proof. The lemma can be proven following a methodology analogous to that used in R. Company et al. [43], Riccardo et al. [75] and R.Company et al. [64] and S.Nuugulu. et al. [163]. For a comprehensive presentation of the proof, see the corresponding discussions in these references. □

We can now define and prove another fundamental result of general stability in the theorem presented below.

THEOREM 5.4.2. *The Crank-Nicolson finite-difference Caputo FD scheme method defined by equations* (5.33) *is unconditionally stable.*

Proof. For a given fixed value of n, v_m^n is a nonincreasing sequence w.r.t m, following the prescribed boundary condition (5.33) and positivity of X_f^n as defined in Lemma 5.4.1, we obtain

$$\|v^n\|_\infty = v_0^n = 1 - X_f^n \leq 1, \text{ for } 0 \leq n \leq N. \tag{5.69}$$

Therefore, we conclude that the Crank-Nicolson scheme for the APO with Caputo fractional order derivative is $(\|.\|_\infty)$ unconditionally stable. Thus far, this proves the desired stability result. □

5.5 Numerical Result

In the following section, we illustrate the previous theoretical outcomes of numerical experiments showing the potential advantages of the proposed method, such as retaining the fundamental qualitative features of the theoretical solution of APO, such as stability and consistency. In addition, in this section, a comparison with other approaches is also presented.

In the absence of an analytical solution for the fractional APO model under the Caputo-Fabrizio derivative, a numerical reference solution is constructed using the proposed Crank-Nicolson scheme on a highly refined computational grid. Owing to the nonlocal nature of the fractional operator and the free-boundary structure of the APO problem, closed-form analytical solutions are generally unavailable. Consequently, the refined grid numerical solution is adopted as the benchmark against which numerical approximations obtained on coarser grids are evaluated. Where necessary, values from the refined-grid solution are matched or interpolated to ensure consistency during the comparison process. The pointwise error at each grid node is computed as the absolute difference between the coarse-grid approximation and the corresponding benchmark solution value.

In numerical error analysis, it is important to distinguish among several related but fundamentally different concepts. In general, the term error refers to the discrepancy between a numerical approximation and the reference solution without reference to a specific norm or measurement criterion. It therefore provides a qualitative indication of the inaccuracy associated with the numerical approximation.

The maximum error, commonly associated with the discrete L^∞-norm, is defined as

$$E_{\max} = \max_{i,j} \left| V_{i,j}^{\text{ref}} - V_{i,j} \right|,$$

where $V_{i,j}^{\text{ref}}$ denotes the reference solution and $V_{i,j}$ represents the numerical approximation at the grid point (i, j). This metric measures the largest deviation over the entire computational domain and is particularly effective for detecting localized instability, oscillatory behavior, or spurious numerical artifacts near the free boundary. Consequently, the maximum error serves as an important indicator of the boundedness, robustness and stability of the numerical scheme.

The root mean square error (RMSE), corresponding to the discrete L_2-norm, is defined by

$$\text{RMSE} = \sqrt{\frac{1}{MN} \sum_{i=1}^{M} \sum_{j=1}^{N} \left(V_{i,j}^{\text{ref}} - V_{i,j} \right)^2},$$

where M and N denote the numbers of spatial and temporal grid points, respectively. Unlike the maximum error, RMSE provides a global measure of numerical accuracy over the entire computational domain and is less sensitive to isolated outliers. Since larger deviations are amplified through the squaring operation, RMSE effectively captures the overall distribution of numerical error and therefore provides a reliable measure of approximation quality and convergence performance.

The mean-based convergence rate refers to the rate at which the average numerical error, typically measured using RMSE, decreases as the spatial and temporal discretizations are progressively refined. This quantity characterizes the asymptotic convergence behavior of the numerical method and provides important insight into the consistency, accuracy and reliability of the proposed numerical scheme.

The selection of RMSE as the principal convergence metric is motivated by its favorable numerical and statistical properties. In particular, RMSE provides a smooth and differentiable measure of global error while remaining less sensitive to isolated pointwise anomalies than the maximum error. As a result, it is well-suited for quantifying the average reduction in error under mesh refinement. Nevertheless, the maximum error is retained as a complementary metric for monitoring local stability and detecting potential nonphysical oscillations, especially near the early exercise boundary, where the solution may exhibit non-smooth behavior. Collectively, RMSE and the maximum error provide a comprehensive validation

framework for the proposed numerical method. RMSE characterizes global convergence behavior, whereas the maximum error assesses local robustness and numerical stability.

The APO problems (5.21) were solved using the parameters listed below:

$$r = 0.1, \sigma = 0.2, T = 1, \alpha = 0.5.$$

To evaluate the convergence, error metrics, including maximum error and RMSE have been calculated in relation to a reference solution derived from a highly refined grid. The convergence rate is subsequently determined using the following formula:

i.

$$\gamma(h_1, h_2) = \frac{\ln(\text{RMSE}_{h_1}) - \ln(\text{RMSE}_{h_2})}{\ln(h_1) - \ln(h_2)}, \tag{5.70}$$

- RMSE_{h_1} and RMSE_{h_2} are the root mean square errors
- h_1 and h_2 are the respective grid spacings.

ii.

$$\text{Convergence Rate} = \frac{\log\left(\frac{E_{\text{coarse}}}{E_{\text{fine}}}\right)}{\log\left(\frac{h_{\text{coarse}}}{h_{\text{fine}}}\right)} \tag{5.71}$$

where

- $\boldsymbol{E}_{\text{fine}}$: The error associated with the finer grid, calculated using a chosen error norm, such as the maximum error or root mean square error.
- $\boldsymbol{E}_{\text{coarse}}$: The error associated with the coarser grid, computed in the same manner as $\boldsymbol{E}_{\text{fine}}$.
- $\boldsymbol{h}_{\text{fine}}$: The grid spacing for the finer grid, typically represented as Δy (spatial step).
- $\boldsymbol{h}_{\text{coarse}}$: The grid spacing for the coarser grid, similarly represented as Δy.

In light of this defined the convergence rate and the errors needed, we intend to now compute the errors related to the associated problem in order to validate the scheme used. For this purpose, we fix y_∞ in the table below and compute the errors for the given values for each N.

Table 5.1: Free boundary location at t = T=1.

$Y = y_\infty$	$N = 20$	$N = 40$	$N = 80$
1	0.72636032	0.62031929	0.50841141
2	0.72637032	0.62032529	0.50836313
4	0.72637632	0.62032829	0.50836513

We focus on determining a suitable value for the truncated boundary, $Y = y_\infty$ and subsequently analyze how the choice of $Y = y_\infty$ influences the numerical solution. A straightforward approach involves monitoring the computing values of the free boundary, X_f^n, at $t = T$. Table 5.1 provides a comparative analysis of the numerical results of the sample for X_f^n obtained with varying grid step values, while keeping $\mu = 20$ and setting $y_\infty = 1, y_\infty = 2, y_\infty = 4$. The findings presented in Table 5.1 reveal that, for a constant value of $\mu = 20$, the calculated values of X_f^n remain consistent up to the first four decimal places in different values of the grid step. Based on these observations, we selected $y_\infty = 1$ for subsequent calculations. This result aligns with the preliminary numerical results derived from the implementation of explicit and implicit finite difference methods, as reported by Riccardo [73] and Riccardo et al. [75] respectively.

In the above table the boundary solutions calculated, we now turn our attention to compute the maximum absolute error in the table below.

α	$N = 20$	$N = 40$	$N = 80$	$N = 160$
0.1	6.69e-03	2.36e-03	2.50e-03	0.00e+00
0.2	5.34e-03	6.77e-04	6.73e-04	0.00e+00
0.3	2.38e-03	0.00e+00	0.00e+00	0.00e+00
0.4	3.07e-03	0.00e+00	0.00e+00	0.00e+00
0.5	2.21e-03	0.00e+00	0.00e+00	0.00e+00
0.6	1.58e-03	0.00e+00	0.00e+00	0.00e+00
0.7	1.32e-03	0.00e+00	0.00e+00	0.00e+00
0.8	1.68e-03	0.00e+00	0.00e+00	0.00e+00
0.9	2.57e-03	0.00e+00	0.00e+00	0.00e+00

Table 5.2: The table presents the maximum absolute errors calculated for various fractional orders of α, spanning from 0.1 to 0.9 in increments of 0.1

Table 5.2 illustrates the maximum absolute errors associated with various values fractional parameters of α and different grid sizes N within a numerical method. The data reveal a consistent reduction in error as α and N increase. Specifically, the maximum absolute errors

approximately halve with each doubling of N. In coarser grids $N = 10$, $N = 20$ and $N = 40$, the errors demonstrate greater variability relative to α; however, this sensitivity diminishes significantly in finer grids $N = 160$ and $N = 320$, where the errors converge to negligible levels across all values of α. This trend underscores the reliability of the method and the effectiveness of grid refinement in attaining enhanced accuracy, while also indicating a reduced sensitivity at higher resolutions.

α	$N = 20$	$N = 40$	$N = 80$
0.1	6.90e-01	1.26e+00	2.44e+00
0.2	6.92e-01	1.26e+00	2.44e+00
0.3	6.96e-01	1.26e+00	2.45e+00
0.4	7.01e-01	1.27e+00	2.45e+00
0.5	7.08e-01	1.27e+00	2.46e+00
0.6	7.15e-01	1.28e+00	2.47e+00
0.7	7.22e-01	1.28e+00	2.47e+00
0.8	7.30e-01	1.29e+00	2.48e+00
0.9	7.53e-01	1.32e+00	2.53e+00

Table 5.3: The table presents the convergence rates computed based on the mean values for various fractional orders of α, ranging from 0.1 to 0.9 in increments of 0.1.

α	$N = 20$	$N = 40$	$N = 80$
0.1	5.03e-01	9.71e-01	1.96e+00
0.2	5.02e-01	9.70e-01	1.95e+00
0.3	5.03e-01	9.70e-01	1.96e+00
0.4	5.05e-01	9.70e-01	1.96e+00
0.5	5.08e-01	9.74e-01	1.96e+00
0.6	5.13e-01	9.78e-01	1.97e+00
0.7	5.20e-01	9.83e-01	1.97e+00
0.8	5.31e-01	9.93e-01	1.98e+00
0.9	5.53e-01	1.02e+00	2.02e+00

Table 5.4: The table presents the convergence rates calculated using the RMSE for the example problem, with fractional orders of α varying from 0.1 to 0.9 in increments of 0.1.

Table 5.3 illustrates the convergence rates associated with various values of α and grid sizes N in the numerical method, as determined by equation (5.70). For coarser grids $N = 20$,

$N = 40$ and $N = 80$, the convergence rates are approximately 0.69, 1.26 and 2.44, respectively. As α increases from 0.1 to 0.9, these rates improve to 0.753, 1.32 and 2.53. This trend suggests that the method nearly achieves optimal second-order convergence as grid resolution of the grid improves. Similarly, Table 5.4 exhibits the convergence rates for the same grid sizes $N = 20$, $N = 40$ and $N = 80$, which begin at 0.503, 0.971 and 1.96, respectively and further increase to 0.553, 1.02 and 2.02 with the escalation of α from 0.1 to 0.9. These results also indicate second-order convergence, consistent with the calculations derived from equation (5.71). The uniformity of convergence rates across varying α values in both tables underscores the robustness of the numerical method. This characteristic ensures consistent performance regardless of the parameter α and highlights the reliability and precision of the approach, particularly as the resolution of the grid improves.

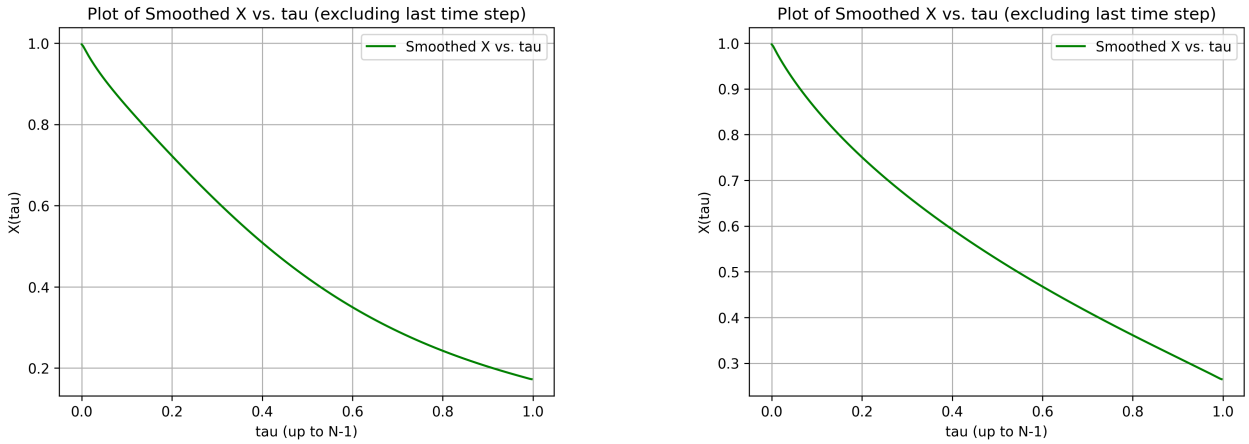

$\alpha = 0.9$ $\alpha = 0.5$

Figure 5.1: The figure presents the numerical results obtained using the Crank-Nicolson method, plotting X_f^n versus τ_n, with $\alpha = 0.9$ on the left and $\alpha = 0.5$ on the right.

The figures 5.1 present two graphs of X_f^n versus τ_n: the graph on the right corresponds to $\alpha = 0.5$, while the graph on the left also represents $\alpha = 0.9$. These results were generated using the Crank-Nicolson finite-difference scheme with $N = 320$, $M = 80$ and $\mu = 20$. The findings indicate that the effectiveness of the approach increases as the parameter values become larger $\alpha = 0.5$. This observation aligns with expectations, as $\alpha > 0.5$ characterizes scenarios in which increases in the underlying stock exhibit a persistent positive correlation.

Figures 5.2 and 5.3 illustrate the results obtained from the Crank-Nicolson finite difference scheme, presenting both the graphs $2D$ and $3D$ of v_m^n versus y, respectively. The graph on the right corresponds to $\alpha = 0.5$, while the graph on the left represents $\alpha = 0.9$. These

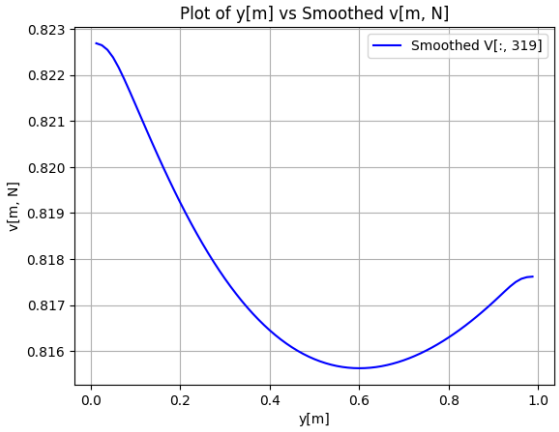

$\alpha = 0.9$

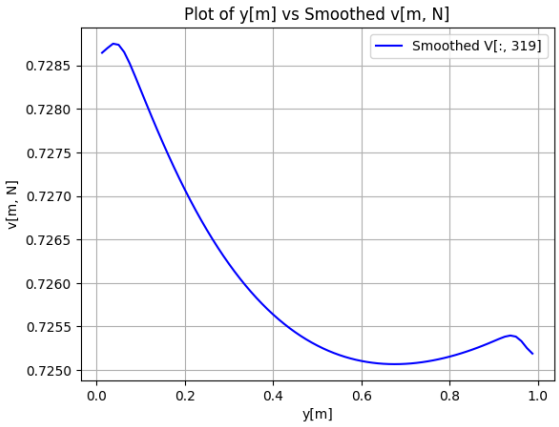

$\alpha = 0.5$

Figure 5.2: Maturity payoffs of an APO plotted as V versus τ for different values of α.

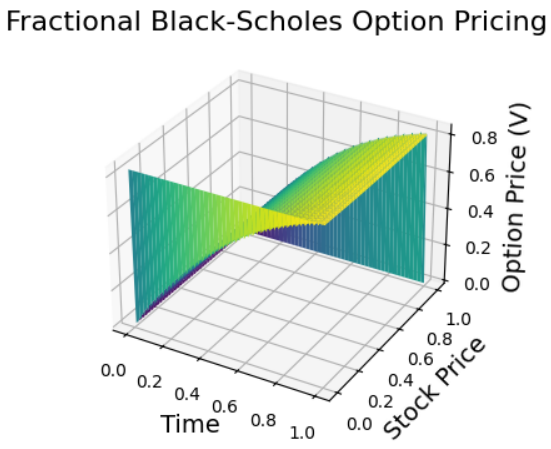

$\alpha = 0.9$

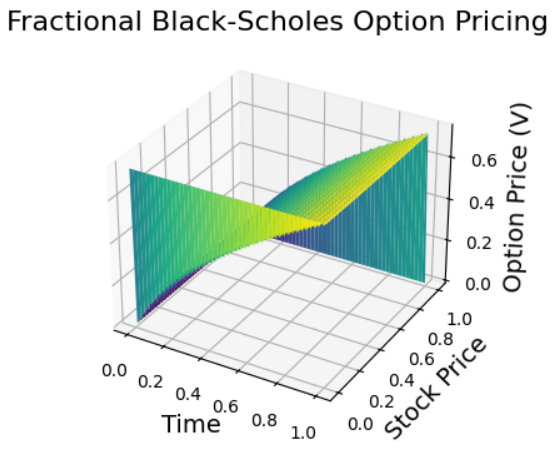

$\alpha = 0.5$

Figure 5.3: The figure shows the 3D plot of the numerical solution v_m^n, with $\alpha = 0.9$ on the left and $\alpha = 0.5$ on the right.

results were computed with the parameters $N = 320$, $M = 80$ and $\mu = 20$. The analysis indicates that the method demonstrates improved performance for larger $\alpha > 0.5$ values.This observation is consistent with expectations, as $\alpha > 0.5$ reflects scenarios where increases in the underlying stock exhibit a persistent positive correlation.

The Figure 5.3 represents the $3D$ profiles of the numerical solution v_m^n for different fractional orders are illustrated in the above Figure, where the plot corresponds to $\alpha = 0.5$. The $3D$ profiles of the numerical solution v_m^n for different fractional orders are presented in Figure 5.3, where the first surface corresponds to $\alpha = 0.9$ and the second to $\alpha = 0.5$. The figure clearly illustrates the influence of the fractional parameter α on the behavior of the solution. This is to clearly demonstrate the variation in solution profiles with respect to the fractional order. As shown above, this is also to reveal how the fractional order parameter affects the amplitude and smoothness of the solution surface.

Author	Research Focus and Methodology	Key Findings and Strengths	Limitations	Identified Research Gap
Company et al. [43]	Front-fixing method for classical AOs; Numerical analysis of front-fixing FD schemes	Validated convergence and stability for classical free-boundary PDEs; Rigorous error analysis; computationally efficient	Limited to non-fractional, non-jump models	No extension to fractional/jump-diffusion frameworks
Fazio et al. [73]	Richardson's extrapolation and error estimator for APOs; Front-fixing finite difference scheme with Richardson extrapolation	Improved accuracy via a posteriori error estimation; validated convergence rates; Explicit error control; efficient for classical BS models	Limited to integer-order PDEs; no fractional extensions	Lack of error estimators for fractional free-boundary problems
Fazio et al. [75]	Implicit finite difference method for APOs; Front-fixing implicit FD scheme; nonlinear solver (Newton-Raphson)	Stable convergence for free boundaries under classical BS model; Robust for non-smooth payoffs; handles early exercise constraints	Computationally intensive for fine grids; no stochastic volatility	No extension to fractional operators or multi-asset models
Company et al. [44]	AOs under jump-diffusion models; Front-fixing ETD (Exponential Time Difference) method	Stabilized scheme for jump-induced discontinuities; Handles jumps; robust for non-smooth payoffs	High runtime for fine grids; no fractional operators	Integration of jumps with fractional calculus unexplored
Kumar et al. [126]	Numerical computation of fractional BS equation; Finite difference method for fractional PDEs	Solved fractional BS for EOs; Early work on fractional BS; validated accuracy	Focused on EOs; no free boundaries	No treatment of AOs or early exercise
Nuugulu et al. [163]	Robust numerical scheme for AOs under time-fractional BS model; Front-fixing method with finite differences; simultaneous boundary/price solve; Consistent, stable, convergent scheme for free boundaries in fractional PDEs	Handles non-locality of FDs; guarantees positivity	First-order in time; limited to time-fractional models	Higher-order schemes, space-time fractional models
Ali et al.[8]	A Front Fixing Crank-Nicolson Finite-difference for the APOs Model; front-fixing method with finite differences; simultaneous boundary/price solve;Consistent, stable, convergent scheme for free boundaries in Caputo fractional PDEs	Handles non-locality of Caputo Fabrizio FDs; guarantees positivity	First order in time; limited to time-fractional models	**Addressed gaps**: Simultaneous Free Boundary Computation under Fractional Calculus. **Remaining gaps**: Higher-order schemes, space-time fractional models; Future research should integrate machine learning with stochastic volatility models for precise, data-driven parameter estimation, enhancing accuracy and realism.

Table 5.5: State-of-the-Art Research Gap Analysis for Fractional BS Models in AO Pricing

A comparative summary of recent contributions in the field of fractional BS models for AO pricing is presented in Table 5.5. The table highlights the current state-of-the-art approaches, their methodologies and the specific research gaps that persist in this domain. Notably, while several studies have introduced fractional-order formulations to capture memory effects and market irregularities, most of them focus primarily on EOs and overlook the numerical stability and convergence characteristics crucial for AOs. The proposed method in this work addresses these gaps by providing a more robust numerical framework that ensures both convergence and stability across varying fractional orders. This improvement reinforces the reliability of the fractional BS model for practical financial applications.

5.6 Managerial and Policy Implications

This research introduces a transformation framework designed for financial professionals and policymakers that addresses critical challenges in the pricing of AOs and risk management. For portfolio managers, the integration of FC allows for precise valuation by concurrently calculating optimal exercise boundaries and option premiums. This methodology effectively captures long-range dependencies and non-local effects in asset price dynamics, thereby enhancing hedging strategies for volatile assets and complex derivatives[167, 184, 215, 103]. Furthermore, the front-fixing algorithm improves efficiency by minimizing computational overhead while ensuring numerical stability [231, 65, 204, 45]. Financial institutions can leverage this framework for real-time dynamic hedging of large portfolios, even among turbulent markets [166, 11, 125, 118, 179, 56, 106, 183, 220] and for cost-effective evaluations of path-dependent options, such as convertible bonds, without the need for computationally intensive simulations.

From a regulatory point of view, the framework aligns with empirical market behavior by incorporating memory effects and anomalous diffusion. This provides policymakers with valuable tools to mitigate systemic risks in derivatives markets [194, 213, 195, 76, 150]. Its consistency and stability support standardized fair value measurements under regulatory frameworks, particularly for illiquid or long-dated options, where traditional models often underestimate tail risks. In addition, its robustness improves stress testing protocols for evaluating institutional resilience [151, 77, 170]. Regulatory pilots can also support the development of innovative financial instruments, such as climate-linked derivatives, within fractal-structured markets such as cryptocurrencies, fostering financial innovation while maintaining regulatory oversight through rigorous validation.

Despite these advancements, persisting challenges require resolution, notably the computational complexity inherent to nonlocal fractional operators and the sensitivity in parameter

calibration, particularly for fractional order α. Future research could investigate the integration of machine learning techniques for data-driven parameter estimation or combine this framework with stochastic volatility models to improve realism. By bridging fractional calculus with practical finance, this study lays the groundwork for more transparent, efficient and resilient financial markets that will benefit industry practitioners and regulatory bodies alike.

5.7 Limitations of the Study

The proposed numerical scheme offers significant advances in the pricing of AOs within the tfBS framework; however, several limitations merit careful consideration.

A primary challenge arises from the computational complexity associated with the non-local characteristics of FDs. Although the FFM reduces the necessity of iterative boundary adjustments, the scheme's reliance on dense matrix operations for time-fractional discretization may adversely affect stability, particularly in high-dimensional or multi-asset contexts [203]. Moreover, the accuracy is highly sensitive to the precise calibration of the fractional order, which dictates the memory effects of the underlying process. Estimating this order from market data presents challenges due to inherent noise and dynamism, potentially undermining the reliability of the results [131].

Furthermore, the model presumes constant parameters such as interest rates, volatility and dividend yields even if actual markets frequently exhibit stochastic or regime-switching behaviors that remain unaccounted for within this framework [39]. The theoretical analysis also assumes certain smoothness and differentiability conditions, including the differentiability of the function up to order. However, these assumptions may not hold in markets characterized by abrupt shocks or discontinuous price trajectories by limiting the method's applicability during periods of market turbulence. Although the numerical experiments were carried out in line with theoretical expectations, they were performed under controlled parameters, necessitating further validation against real-market data, especially for long-dated options or assets exhibiting heavy-tailed returns, to assess practical effectiveness.

This study predominantly employs Caputo's FD; however, conducting a comparative analysis using alternative fractional definitions, such as Jumarie' or Riemann-Louville, [188] could yield a more comprehensive theoretical foundation, as different frameworks of FC may influence pricing accuracy. Lastly, although the method is specifically designed for APOs, extending it to encompass other option types, such as American calls or hybrid derivatives with early exercise and path-dependent features, would require additional algorithmic refinements.

5.8 Conclusion

Over the last decade, the field of financial modeling has made substantial advances, particularly the introduction of various mathematical frameworks that aim to capture the complex dynamics of financial markets. Among these, FC based models serve as a fundamental tool, balancing the need to explain the intricate behaviors of stock market evolutions while maintaining mathematical tractability. Despite the significant mathematical challenges associated with designing analytic solutions for fractional models, our work addresses this gap by proposing a robust numerical scheme to solve tfBS equations to price APO contracts.

This study introduces a numerical approach rooted in the front-fixing algorithm, which simplifies the inherent complexity of early exercise boundaries by transforming them into fixed boundaries. This transformation enables simultaneous computation of optimal exercise boundaries and the fair premiums charged for the options. The theoretical properties of the proposed scheme consistency, stability and convergence up to order $\mathbf{O}(1, \Delta y^2)$ have been rigorously demonstrated. Moreover, the scheme guarantees the positivity and monotonicity of the option premium solutions v_n^m and the free boundary X_f^n under all potential market conditions.

To validate the theoretical assertions,a numerical experiment was conducted, simulating a practical scenario of the APO with market parameters such as an interest rate of $r = 0.10$, $T = 1$ and $\sigma = 0.20$. Importantly, our results align with findings reported in the existing literature, underscoring the reliability and effectiveness of FC frameworks for modeling financial markets. From a broader perspective, this work supports the consensus that FC provides a comprehensive framework for capturing and explaining stylized facts of market dynamics, which often elude classical modeling approaches.

A particularly notable finding is that the proposed model delivers more accurate results when the fractional order $\alpha > 0.5$, consistent with the view that markets exhibit long memory. Under such conditions, the underlying fractal processes display persistence and positive correlation. Although the proposed method demonstrates robustness, efficiency and accuracy in pricing AOs, it also opens avenues for future research. Upcoming efforts will focus on calibrating similar fractional models to real-time market data and developing higher-order numerical schemes to price both APOs and other financial instruments. By addressing these challenges, we aim to further enhance the practical applicability and precision of FC based financial models, contributing to the broader field of quantitative finance.

Chapter 6

Conclusion and Future Perspectives

6.1 Conclusion

This thesis primarily comprises two published papers in peer-reviewed international journals. In Chapter 4, in this thesis, we first prove the existence and uniqueness of the solution to a variable-order Caputo-Fabrizio FSDE driven by a multiplicative white noise, which describes random phenomena with non-local effects and non-singular kernels. The EM scheme is extended to develop the EM method and the strong convergence of the proposed method is demonstrated. The main difference between our work and the existing literature is the fact that our assumptions on the nonlinear external forces are those of one-sided Lipschitz conditions on both the drift and the nonlinear intensity of the noise, as well as the proofs of the higher integrability of the solution and the approximating sequence. Finally, to validate the numerical approach, current results from the numerical implementation are presented to test the efficiency of the scheme used in order to substantiate the theoretical analysis.

In Chapter 5, in this thesis, we present a novel approach to solving the APOs pricing model by hugely relying on a front-fixing Crank-Nicolson FFM. Since the APO pricing model is a widely used financial model for valuing an option with the right to sell an underlying asset at a fixed price, which generally decided in advance. The method we proposed here, solves the problem of early exercise by introducing a FFM that permits for efficient and accurate valuation of an APO. As in the comparison to other approaches in the existing literature, we can assert that this method is stable, accurate, consistent and efficient. The results that we obtained here from the numerical experiments demonstrate not only the efficacy of the proposed method but also in consistently and accurately pricing APOs with a stable scheme. Under some appropriate conditions on the step size discretization, we also show the positivity and monotonicity of the coefficient involved in the numerical scheme used.

6.2 Future work

The importance of research into FSDEs, time FDE and their significance to future applications in financial derivatives warrants the continued study. Future work is presented in distinct sections for each of the two interconnected papers.

6.2.1 Future work Strong Convergence of Euler-Type Methods for Nonlinear FSDEs without Singular Kernel

i. **High-Dimensional and Spatially Extended Systems** The research can be extended to FSPDEs with spatial dependencies or multi-dimensional noise sources, such as Lévy processes. Major challenges include addressing cross-correlated noise structures and anisotropic fractional operators in higher dimensions, which are particularly relevant to turbulent fluid dynamics and spatially distributed biological systems.

ii. **Advanced Numerical Algorithms** Further work should focus on the development of higher-order discretization schemes (e.g., Milstein methods, stochastic Runge–Kutta techniques) and adaptive time-stepping strategies to enhance computational efficiency in variable-order dynamics. A key research objective is to evaluate the trade-offs among accuracy, stability and computational cost, with particular attention to behavior near critical regimes where $\alpha(t) \approx 1$.

iii. **Generalized Assumptions on Nonlinearities** Relaxing traditional one-sided Lipschitz constraints would enable the framework to accommodate monotone, polynomially bounded, or discontinuous coefficients. This line of research also encompasses the study of FSDEs driven by jump-diffusion processes, such as Poisson noise, with a focus on establishing well-posedness under weaker regularity conditions.

iv. **Domain-Specific Modeling Applications** The validated framework can be applied across a range of domain-specific contexts to model anomalous transport phenomena. In biophysics, it provides a means of capturing neuron firing dynamics where ion channel gating exhibits memory-dependent behavior. In quantitative finance, the approach offers a robust foundation for option pricing under non-Markovian asset volatility, reflecting long-range dependence and market irregularities. Similarly, in materials science, it enables the analysis of stress relaxation in viscoelastic polymers, where fractional-order dynamics capture complex hereditary effects. Collectively, these applications underscore the versatility of the framework and its potential to address fundamental challenges in diverse scientific disciplines.

v. **Long-Term System Behavior** Finally, research should investigate ergodicity, invariant measures and asymptotic stability in non-singular kernel FSDEs. An important aspect of this study is to characterize how variable-order fractional operators affect steady-state distributions and convergence rates in dissipative systems.

6.2.2 Future work A Front Fixing Crank-Nicolson Finite-difference for the APOs Model

i. **Arbitrage-Free Fractional Option Pricing with Transaction Costs**

This study extends the tfBS framework to incorporate transaction costs while enforcing arbitrage-free conditions in fractional markets. The methodology integrates Leland's transaction cost adjustment into the fractional PDE and examines its implications for option pricing and hedging strategies. By addressing the arbitrage limitations inherent in fractional models, this work preserves the memory effects that distinguish FC from classical approaches, offering a more robust pricing tool for illiquid or inefficient markets.

ii. **Empirical Performance of the tfBS Model in High-Volatility Regimes**

This research evaluates the tfBS model's accuracy in pricing options during extreme market conditions (e.g., financial crises). Using historical high-volatility datasets, we conduct comparative analyses between the tfBS model, classical BS and stochastic volatility models (e.g., Heston). The results are expected to demonstrate the tfBS model's superior ability to capture tail risks and market anomalies, providing empirical validation for its use in turbulent markets.

iii. **Numerical Solutions for Multi-Asset Fractional BS Models**

We develop efficient numerical methods for pricing multi-asset options (e.g., basket options) under the Fractal Market Hypothesis. The methodology adapts FDM to solve high-dimensional fractional PDEs, addressing computational challenges in multi-asset derivatives. This extension enhances the tfBS framework's applicability to correlated asset dynamics, with implications for portfolio optimization and risk management.

iv. **Deep Learning for Fast Pricing of Fractional PDEs in Finance**

This work investigates PINNs to solve high-dimensional fractional PDEs efficiently. By training PINNs to approximate tfBS-PDE solutions, we reduce computational costs compared to traditional numerical methods. The proposed data-driven approach enables real-time pricing of complex derivatives, offering scalability for high-frequency and algorithmic trading applications.

v. **Time-Varying Fractional Derivatives in Asset Pricing**

We introduce a dynamic tfBS model where the fractional order α evolves as a stochastic or time-dependent process, $\alpha(t)$. The methodology integrates state-dependent FC and calibrates $\alpha(t)$ using market data. This framework captures shifting market inefficiencies and regime changes more flexibly than constant-α models, improving adaptability to economic fluctuations.

vi. **Fractional Models for Cryptocurrency Option Pricing**

This research adapts the tfBS model to price cryptocurrency options (e.g., Bitcoin), which exhibit strong fractal properties. After calibrating the tfBS model to crypto volatility surfaces, we compare its performance against jump-diffusion and stochastic volatility models. The study addresses the limitations of traditional models in crypto markets, particularly their inability to account for extreme volatility and long-memory effects.

vii. **Fractional Stochastic Volatility Models**

This work unifies the tfBS framework with rough volatility models (e.g., fractional Heston) to improve volatility dynamics modeling. The methodology combines fBM for asset prices with fractional volatility processes, deriving closed-form approximations or robust numerical solutions. By bridging fractal asset paths and rough volatility, this integration enhances pricing and hedging accuracy for exotic and path-dependent derivatives.

6.3 Recommendations

The importance of research into FSDEs, time FDEs and their significance to recommendation applications warrants the continued study. Recommendations are presented in distinct sections for each of the two interconnected chapters.

6.3.1 Recommendations Strong Convergence of Euler-Type Methods for Nonlinear FSDEs without Singular Kernel

The recommendations arising from this study highlight several critical directions for advancing research in FSDEs. First, significant attention should be given to *computational infrastructure optimization*. Implementing Graphics Processing Unit accelerated parallelization techniques, such as Compute Unified Device Architecture, will be essential for efficiently performing large-scale Monte Carlo simulations of high-dimensional FSDEs. In parallel, the development of open-source, modular software libraries in Python or Julia, equipped with

the EM scheme and its extensions, would enhance accessibility and foster broader adoption within the scientific community.

On the theoretical front, further progress requires the establishment of weak convergence rates for the EM scheme, thereby enabling reliable applications in financial and statistical contexts such as derivative pricing. Additionally, rigorous analysis of pathwise solution regularity, particularly the Hölder continuity of solutions under variable-order Caputo-Fabrizio operators, will contribute to a deeper mathematical understanding of the models.

Equally important are *interdisciplinary validation studies*, which should involve close collaboration with domain specialists. Such efforts would enable benchmarking of model predictions against experimental data, for example in polymer rheology and electrophysiological recordings. Furthermore, comparative studies evaluating the performance of the EM scheme against emerging machine learning-based solvers, such as neural SDEs, are vital for assessing accuracy and scalability in high-dimensional applications.

Finally, advancing FSDE modeling will benefit from *algorithm–hardware co-design*. In particular, hardware-aware optimizations, including Field-Programmable Gate Array based acceleration and the potential use of quantum computing architectures, should be explored to address the memory-intensive requirements of non-singular kernel operations. Collectively, these recommendations emphasize the importance of integrating computational innovation, theoretical rigor, interdisciplinary validation and hardware-aware design in order to establish a robust foundation for future research and applications.

6.3.2 Recommendations A Front Fixing Crank-Nicolson Finite-difference for the APOs Model

Accurately modeling financial markets under conditions characterized by extreme volatility and fractal dynamics remains a significant challenge in modern quantitative finance. This complex problem requires a multidimensional research approach that combines advanced mathematical theories, computational innovations and rigorous empirical validation. The application of FC in market analysis offers profound insights into phenomena such as long-memory effects, non-Gaussian return distributions and extreme tail risks features that conventional financial models tend to underestimate or overlook.

This study highlights the substantial potential of tfBS models to improve option pricing accuracy and enhance risk management frameworks. Nonetheless, several practical obstacles must be addressed to realize their full utility. These include issues related to arbitrage opportunities, high computational demands and challenges in model calibration. To facilitate the broader adoption and continued refinement of fractional models, the following strategic recommendations are proposed.

For financial institutions and regulatory bodies, it is imperative to undertake compre-

hensive empirical validations of tfBS models, leveraging high-frequency market data, especially during periods of financial stress and crises. Such validation efforts will help establish the predictive reliability and practical robustness of these models. Furthermore, regulatory frameworks should be updated to include standardized protocols for trading FDs, encompassing mechanisms for arbitrage mitigation, transaction cost modeling and adjustments for market frictions.

Within the quantitative research community, fostering interdisciplinary collaboration among financial mathematicians, computational finance experts, data scientists and machine learning specialists is crucial. Such collaboration will accelerate the development of efficient numerical methods capable of solving high-dimensional fractional PDEs. Moreover, research should focus on hybrid modeling strategies that integrate the tfBS framework with stochastic volatility models, jump diffusion processes and rough volatility dynamics, thereby capturing a richer spectrum of market behaviors.

Regarding financial data infrastructure, enhanced accessibility to high-quality market data is essential. This includes detailed intraday volatility surfaces, limit order book dynamics and high-frequency price series. Additionally, the establishment of centralized repositories for fractal market metrics such as standardized calculations of the Hurst exponent, memory effect quantifications and scaling property analyses will provide valuable resources for both researchers and practitioners.

Policy makers and funding agencies are encouraged to promote strategic partnerships between academia, the financial industry and technology providers. Such collaborations are vital to accelerate the translation of FC research from theoretical frameworks into practical applications. Priority should be given to funding initiatives focused on fractional modeling applications in emerging markets, cryptocurrency valuation and systemic risk assessment, areas where traditional models frequently fall short.

While acknowledging current limitations related to computational complexity and calibration precision, fractional models represent a paradigm shift in financial mathematics. This research underscores the urgent need to incorporate FC principles into mainstream quantitative finance methodologies. Enhanced cooperation between theoretical researchers and industry practitioners will ensure that modeling frameworks evolve in parallel with the increasingly complex and dynamic nature of global financial markets. The development of robust and scalable fractional pricing models will be pivotal to maintaining the relevance, accuracy and effectiveness of financial risk management in the decades ahead.

Bibliography

[1] M. Abu-Shady and M. K. Kaabar. A generalized definition of the fractional derivative with applications. *Mathematical Problems in Engineering*, 2021(1):9444803, 2021. 19, 47

[2] M. Abu-Shady and M. K. Kaabar. A novel computational tool for the fractional-order special functions arising from modeling scientific phenomena via abu-shady-kaabar fractional derivative. *Computational and Mathematical Methods in Medicine*, 2022(1):2138775, 2022. 13, 94

[3] R. A. Adams and J. J. Fournier. *Sobolev Spaces*. Academic Press, 2nd edition, 2003. 23, 27

[4] R. Agarwal, S. Hristova, and D. O'Regan. Stability concepts of riemann-liouville fractional-order delay nonlinear systems. *Mathematics*, 9(4):435, 2021. 16

[5] N. Agrawal and Y. Hu. Jump models with delay-option pricing and logarithmic euler-maruyama scheme. *Mathematics*, 8(11):1932, 2020. 48

[6] A. Ahmadova and N. I. Mahmudov. Strong convergence of a euler–maruyama method for fractional stochastic langevin equations. *Mathematics and Computers in Simulation*, 190:429–448, 2021. 48

[7] E. Aksoy, M. Kaplan, and A. Bekir. Exponential rational function method for space–time fractional differential equations. *Waves in random and complex media*, 26(2):142–151, 2016. 47

[8] Z. Ali, M. A. Abebe, and T. Nazir. Strong convergence of euler-type methods for nonlinear fractional stochastic differential equations without singular kernel. *Mathematics (2227-7390)*, 12(18), 2024. 14, 100, 126

[9] ALI.ZI, Abera.MA, and Nazir.T. A front fixing implicit finite difference for the american put options model. *Preprint*, 2022. 14, 91, 100

[10] D. R. Anderson and D. J. Ulness. Newly defined conformable derivatives. *Adv. Dyn. Syst. Appl*, 10(2):109–137, 2015. 94

[11] S. S. M. Asif. Create an ai-based model for dynamic risk management in equity portfolios that accounts for extreme market events (eg, pandemics, financial crises). 2024. 127

[12] A. Atangana and D. Baleanu. New fractional derivatives with nonlocal and non-singular kernel: theory and application to heat transfer model. *arXiv preprint arXiv:1602.03408*, 2016. 18, 91

[13] A. Atangana and E. F. D. Goufo. Cauchy problems with fractal–fractional operators and applications to groundwater dynamics. *Fractals*, 28(08):2040043, 2020. 18

[14] A. Atangana and A. Secer. A note on fractional order derivatives and table of fractional derivatives of some special functions. In *Abstract and applied analysis*, volume 2013, page 279681. Wiley Online Library, 2013. 14

[15] U. Ayub, S. Mubeen, A. Abbas, A. Khan, and T. Abdeljawad. Some transforms, riemann–liouville fractional operators, and applications of newly extended m–l (p, s, k) function. *Open Physics*, 22(1):20240005, 2024. 17

[16] L. Bachelier. "theory of speculation", doctoral thesis (1900), coot-ner (ed),'random character of stock market prices', massachusetts institute of technology (1964), pp. 17-78. In *The History of Actuarial Science Vol VII*, pages 15–78. Routledge, 2024. 41

[17] R. L. Bagley and P. J. Torvik. Fractional calculus a different approach to the analysis of viscoelastically damped structures. *AIAA Journal*, 21(5):741–748, 1983. 12

[18] D. Baleanu, K. Diethelm, E. Scalas, and J. J. Trujillo. *Fractional Calculus: Models and Numerical Methods*. World Scientific, 2017. 13

[19] D. Baleanu, Z. B. Güvenç, J. T. Machado, et al. *New trends in nanotechnology and fractional calculus applications*, volume 10. Springer, 2010. 91

[20] D. Baleanu, A. Mousalou, and S. Rezapour. A new method for investigating approximate solutions of some fractional integro-differential equations involving the caputo-fabrizio derivative. *Advances in Difference Equations*, 2017(1):1–12, 2017.

[21] A. Barth and A. Lang. Deep learning for high-dimensional spdes. *Journal of Machine Learning Research*, 22:1–45, 2021. 37

[22] M. H. Bashar, S. Ghosh, and M. Rahman. Dynamical exploration of optical soliton solutions for m-fractional paraxial wave equation. *Plos one*, 19(2):e0299573, 2024. 47

[23] L. Bastianello, A. Chateauneuf, and B. Cornet. Put–call parities, absence of arbitrage opportunities, and nonlinear pricing rules. *Mathematical Finance*, 34(4):1242–1262, 2024. 98

[24] I. M. Batiha, A. A. Abubaker, I. H. Jebril, S. B. Al-Shaikh, and K. Matarneh. A numerical approach of handling fractional stochastic differential equations. *Axioms*, 12(4):388, 2023. 48

[25] C. Bayer, P. Friz, and J. Gatheral. Pricing under rough volatility. *Quantitative Finance*, 16(6):887–904, 2016. 11

[26] C. Bayer, R. Tempone, and S. Wolfers. Pricing american options by exercise rate optimization. *Quantitative Finance*, 20(11):1749–1760, 2020. 45

[27] S. Becker, P. Cheridito, and A. Jentzen. Deep optimal stopping. *Journal of Machine Learning Research*, 20(74):1–25, 2019. 45

[28] A. Bensoussan and J.-L. Lions. *Impulse Control and Quasi-Variational Inequalities*. Gauthier-Villars, 1982/1984. Original French edition: 1982. English translation: 1984. 42

[29] G. Beylkin, R. Coifman, and V. Rokhlin. Fast wavelet transforms and numerical algorithms i. *Communications on pure and applied mathematics*, 44(2):141–183, 1991. 45

[30] F. Black and M. Scholes. The pricing of options and corporate liabilities. *Journal of Political Economy*, 81(3):637–654, 1973. 1, 3, 40, 90, 93

[31] M. J. Brennan and E. S. Schwartz. The valuation of american put options. *The Journal of Finance*, 32(2):449–462, 1977. 90

[32] M. J. Brennan and E. S. Schwartz. Finite difference methods and jump processes arising in the pricing of contingent claims: A synthesis. *Journal of Financial and Quantitative Analysis*, 13(3):461–474, 1978. 90

[33] H. Brézis. *Functional Analysis, Sobolev Spaces and Partial Differential Equations*. Springer, 2011. 22, 23, 28

[34] G. Campolieti and R. N. Makarov. *Financial Mathematics: A Comprehensive Treatment*. CRC Press, Boca Raton, FL, 1 edition, 2018. Series: Textbooks in Mathematics. 1, 4

[35] M. Caputo. Linear models of dissipation whose q is almost frequency independent-ii. *Geophysical Journal International*, 13(5):529–539, 1967. 12, 14

[36] M. Caputo and M. Fabrizio. A new definition of fractional derivative without singular kernel. *Progr. Fract. Differ. Appl*, 1(2):73–85, 2015. 14, 48, 49, 50, 91

[37] Ã. Cartea and D. del Castillo-Negrete. Fractional diffusion models of option prices in markets with jumps. *Physica A: Statistical Mechanics and its Applications*, 374:749–763, 2007. 10

[38] D. M. Chance and R. Brooks. *An introduction to derivatives and risk management*. Cengage Learning, 2013. 2

[39] X. Chen and Y. Wang. Regime-switching models in option pricing: A non-parametric approach. *Quantitative Finance*, 23(5):789–812, 2023. 128

[40] Chicago Board Options Exchange (CBOE). Understanding options: Contract specifications. Technical report, CBOE, 2023. 2

[41] C. Christara and D.-M. Dang. Adaptive and high-order methods for valuing american options. *Journal of Computational Finance, Forthcoming*, 2010. 5

[42] A. Cohen. *Wavelet Methods in Numerical Analysis*, volume 7 of *Studies in mathematics and its applications 32*. Elsevier, Amsterdam, 1st ed edition, 2003. 45

[43] R. Company, V. N. Egorova, and L. Jódar. Solving american option pricing models by the front fixing method: Numerical analysis and computing. In *Abstract and Applied Analysis*, volume 2014, page 146745. Wiley Online Library, 2014. 118, 126

[44] R. Company, V. N. Egorova, and L. Jódar. A front-fixing etd numerical method for solving jump–diffusion american option pricing problems. *Mathematics and Computers in Simulation*, 189:69–84, 2021. 7, 91, 97, 126

[45] R. Company, V. N. Egorova, and L. Jódar. An etd method for vulnerable american options. *Mathematics*, 12(4):602, 2024. 127

[46] R. Company, L. Jódar, and J.-R. Pintos. A consistent stable numerical scheme for a nonlinear option pricing model in illiquid markets. *Mathematics and Computers in Simulation*, 82(10):1972–1985, 2012. 3, 117

[47] A. M. Cox and C. Hoeggerl. Model-independent no-arbitrage conditions on american put options. *Mathematical Finance*, 26(2):431–458, 2016. 98

[48] J. C. Cox, S. A. Ross, and M. Rubinstein. Option pricing: A simplified approach. *Journal of Financial Economics*, 7(3):229–263, 1979. 3, 4

[49] M. G. Crandall and P.-L. Lions. Viscosity solutions of hamilton-jacobi equations. *Transactions of the American mathematical society*, 277(1):1–42, 1983. 43

[50] J. Crank and J. Crank. *Free and moving boundary problems*. Oxford University Press, USA, 1984. 91

[51] J. Cresson and A. Szafrańska. Comments on various extensions of the riemann–liouville fractional derivatives: About the leibniz and chain rule properties. *Communications in Nonlinear Science and Numerical Simulation*, 82:104903, 2020. 47

[52] G. Da Prato and J. Zabczyk. *Stochastic Equations in Infinite Dimensions*. Cambridge University Press, 2nd edition, 2014. 21, 27

[53] W. Dahmen. Wavelet and multiscale methods for operator equations. *Acta Numerica 1997-jan vol. 6*, 6, jan 1997. 45

[54] I. Daubechies. Ten lectures on wavelets. 1992. 45

[55] J. J. De Espíndola, C. A. Bavastri, and E. M. de Oliveira Lopes. Design of optimum systems of viscoelastic vibration absorbers for a given material based on the fractional calculus model. *Journal of Vibration and Control*, 14(9-10):1607–1630, 2008. 48

[56] M. Devan, K. Thirunavukkarasu, and L. Shanmugam. Algorithmic trading strategies: real-time data analytics with machine learning. *Journal of Knowledge Learning and Science Technology ISSN: 2959-6386 (online)*, 2(3):522–546, 2023. 127

[57] A. Dhiman and Y. Hu. Physics informed neural network for option pricing. *arXiv preprint arXiv:2312.06711*, 2023. 5

[58] K. Diethelm and N. Ford. The analysis of fractional differential equations. *Lecture notes in mathematics*, 2004, 2010. 46

[59] K. Diethelm, N. J. Ford, and A. D. Freed. A predictor-corrector approach for the numerical solution of fractional differential equations. *Nonlinear Dynamics*, 29(1–4):3–22, 2002. 13

[60] X.-L. Ding and J. J. Nieto. Analytical solutions for multi-time scale fractional stochastic differential equations driven by fractional brownian motion and their applications. *Entropy*, 20(1):63, 2018. 48

[61] T. S. Doan, P. T. Huong, P. E. Kloeden, and A. M. Vu. Euler–maruyama scheme for caputo stochastic fractional differential equations. *Journal of Computational and Applied Mathematics*, 380:112989, 2020. 48

[62] J. Dong, N. Du, and Z. Yang. A distributed-order fractional stochastic differential equation driven by lévy noise: Existence, uniqueness, and a fast em scheme. *Chaos: An Interdisciplinary Journal of Nonlinear Science*, 33(2), 2023. 48

[63] Y. Duan, Y. Jiang, Y. Wei, and J. Zhou. The solution of stochastic evolution equation with the fractional derivative. *Physica Scripta*, 99(2):025219, 2024. 47

[64] V. Egorova, L. Jódar, et al. Solving american option pricing models by the front fixing method: Numerical analysis and computing. In *Abstract and Applied Analysis*, volume 2014. Hindawi, 2014. 90, 91, 99, 117, 118

[65] V. N. Egorova, S.-H. Tan, C.-H. Lai, R. Company, and L. Jódar. Moving boundary transformation for american call options with transaction cost: finite difference methods and computing. *International Journal of Computer Mathematics*, 94(2):345–362, 2017. 127

[66] N. El Karoui, C. Kapoudjian, E. Pardoux, S. Peng, and M.-C. Quenez. Reflected solutions of backward sde's, and related obstacle problems for pde's. *the Annals of Probability*, 25(2):702–737, 1997. 42

[67] A. El-Nabulsi. Fractional derivatives generalization of einstein's field equations. *Indian Journal of Physics*, 87(2):195–200, 2013. 48

[68] R. A. El-Nabulsi. Modifications at large distances from fractional and fractal arguments. *Fractals*, 18(02):185–190, 2010. 48

[69] R. A. El-Nabulsi. Gravitons in fractional action cosmology. *International Journal of Theoretical Physics*, 51(12):3978–3992, 2012. 48

[70] N. Engheta. On fractional calculus and fractional multipoles in electromagnetism. *IEEE Transactions on Antennas and Propagation*, 44(4):554–566, 1997. 12

[71] L. Euler. *Introductio in Analysin Infinitorum*. Marcum-Michaelis, Lausanne, 1748. 9

[72] L. C. Evans. *Partial Differential Equations*. American Mathematical Society, 2nd edition, 2010. 21, 22, 27

[73] R. Fazio. American put option: Richardson's extrapolation and a posteriori error estimator for a front-fixing finite difference scheme. *by: Appl. Math. E-Notes*, 10, 2020. 97, 121, 126

[74] R. Fazio, A. Insana, and A. Jannelli. A front-fixing implicit finite difference method for the american put options model. *Mathematical and Computational Applications*, 25(2):27, 2020. 7

[75] R. Fazio, A. Insana, and A. Jannelli. A front-fixing implicit finite difference method for the american put options model. *Mathematical and Computational Applications*, 26(2):30, 2021. 90, 91, 97, 99, 114, 118, 121, 126

[76] E.-C. N. FULGA. Exploring the dynamics of derivative markets. a comprehensive study on futures, options, and swaps in modern finance. *Revista tinerilor economişti*, (43):97–108, 2024. 127

[77] L. Galbusera, D. Ward, G. Giannopoulos, et al. Developing stress tests to improve the resilience of critical infrastructures: a feasibility analysis. 2014. 127

[78] F. Gatta, V. S. Di Cola, F. Giampaolo, F. Piccialli, and S. Cuomo. Meshless methods for american option pricing through physics-informed neural networks. *Engineering Analysis with Boundary Elements*, 151:68–82, 2023. 6

[79] O. Gelderblom and J. Jonker. Amsterdam as the cradle of modern futures trading and options trading, 1550-1650. In *The origins of value: the financial innovations that created modern capital markets/Goetzmann, William N.[edit.]; et al.*, pages 189–206. 2005. 2

[80] H. A. Ghany, A.-A. Hyder, and M. Zakarya. Exact solutions of stochastic fractional korteweg de–vries equation with conformable derivatives. *Chinese Physics B*, 29(3):030203, 2020. 47

[81] A. K. Grünwald. Über "begrenzte" derivationen und deren anwendung. *Zeitschrift für Mathematik und Physik*, 12:441–480, 1867. 9, 13, 17

[82] X.-M. Gu, J. Liu, and C. W. Oosterlee. Parallel-in-time iterative methods for pricing american options. *arXiv preprint arXiv:2405.08280*, 2024. 7

[83] O. Guner, E. Aksoy, A. Bekir, and A. C. Cevikel. Different methods for (3+ 1)-dimensional space–time fractional modified kdv–zakharov–kuznetsov equation. *Computers & Mathematics with Applications*, 71(6):1259–1269, 2016. 47

[84] B. Guo, X. Pu, and F. Huang. *Fractional partial differential equations and their numerical solutions*. World Scientific, 2015. 47

[85] H. Han and X. Wu. A fast numerical method for the black–scholes equation of american options. *SIAM Journal on Numerical Analysis*, 41(6):2081–2095, 2003. 90

[86] J. Han, A. Jentzen, and W. E. Solving high-dimensional partial differential equations using deep learning. *Proceedings of the National Academy of Sciences*, 115(34):8505–8510, 2018. 11

[87] T. Han, Z. Li, J. Wen, and J. Yuan. Classification of all single traveling wave solutions of (3+ 1)-dimensional jimbo-miwa equation with space-time fractional derivative. *Advances in Mathematical Physics*, 2022(1):2466900, 2022. 47

[88] T. Han, Z. Li, and K. Zhang. Exact solutions of the stochastic fractional long–short wave interaction system with multiplicative noise in generalized elastic medium. *Results in Physics*, 44:106174, 2023. 47

[89] T. Han, Z. Zhao, K. Zhang, and C. Tang. Chaotic behavior and solitary wave solutions of stochastic-fractional drinfel'd-sokolov-wilson equations with brownian motion. *Results in Physics*, 51:106657, 2023. 47

[90] S. Heidari and H. Azari. A front-fixing finite element method for pricing american options under regime-switching jump-diffusion models. *Computational and Applied Mathematics*, 37:3691–3707, 2018. 6

[91] S. L. Heston. A closed-form solution for options with stochastic volatility with applications to bond and currency options. *The review of financial studies*, 6(2):327–343, 1993. 43

[92] R. Hilfer. Mathematical and physical interpretations of fractional derivatives and integrals. *Handbook of Fractional Calculus with Applications*, 1:47–85, 2019. 46

[93] A. D. Holmes, H. Yang, and S. Zhang. A front-fixing finite element method for the valuation of american options with regime switching. *International Journal of Computer Mathematics*, 89(9):1094–1111, 2012. 91, 92

[94] M. Houas, A. Devi, and A. Kumar. Existence and stability results for fractional-order pantograph differential equations involving riemann-liouville and caputo fractional operators. *International Journal of Dynamics and Control*, 11(3):1386–1395, 2023. 17

[95] S. Hristova, S. Tersian, and R. Terzieva. Lipschitz stability in time for riemann-liouville fractional differential equations. *Fractal and Fractional*, 5(2):37, 2021. 16

[96] Z. Hu, K. Kawaguchi, Z. Zhang, and G. E. Karniadakis. Tackling the curse of dimensionality in fractional and tempered fractional pdes with physics-informed neural networks. *Computer Methods in Applied Mechanics and Engineering*, 432:117448, 2024. 13

[97] J. Huang, L. Shao, and J. Liu. Euler–maruyama methods for caputo tempered fractional stochastic differential equations. *International Journal of Computer Mathematics*, 101(9-10):1113–1131, 2024. 48

[98] J. Hull and A. White. Pricing interest-rate-derivative securities. *The Review of Financial Studies*, 3(4):573–592, 1990.

[99] J. C. Hull. *Options, futures, and other derivatives*. Pearson, 11th edition, 2021. 1, 4

[100] K. Itô and H. P. J. McKean. *Diffusion Processes and Their Sample Paths*. Classics in Mathematics. Springer, 1996. Reprint of the 1974 edition. 42

[101] K. ItÃ´. On stochastic differential equations. *Memoirs of the American Mathematical Society*, 4:1–51, 1951. 36

[102] P. Jaillet, D. Lamberton, and B. Lapeyre. Variational inequalities and the pricing of american options. *Acta Applicandae Mathematica*, 21(3):263–289, 1990. 5, 90

[103] D. Jakhongir and N. Raju. The effectiveness of hedging strategies in volatile markets: Literature review. *Recent Trends in Commerce and Business Management*, page 82. 127

[104] J. Jia, Z. Yang, H. Wang, et al. Analysis and numerical approximation for a nonlinear hidden-memory variable-order fractional stochastic differential equation. *East Asian Journal on Applied Mathematics*, 12(3), 2022. 83

[105] J. Jia, X. Zheng, H. Fu, P. Dai, and H. Wang. A fast method for variable-order space-fractional diffusion equations. *Numerical Algorithms*, 85:1519–1540, 2020. 83

[106] G. Jiang, L. J. Hong, and H. Shen. Real-time derivative pricing and hedging with consistent metamodels. *INFORMS Journal on Computing*, 36(5):1168–1189, 2024. 127

[107] M. Johnson and L. Wang. Principled pasting in risk-neutral densities. *Quantitative Finance*, 23, 2023. 98, 99

[108] G. Jumarie. Merton's model of optimal portfolio in a black-scholes market driven by a fractional brownian motion with short-range dependence. *Insurance: Mathematics and Economics*, 37(3):585–598, 2005. 14

[109] G. Jumarie. Modified riemann-liouville derivative and fractional taylor series of non-differentiable functions further results. *Computers & Mathematics with Applications*, 51(9-10):1367–1376, 2006. 14, 15

[110] G. Jumarie. Stock exchange fractional dynamics defined as fractional exponential growth driven by (usual) gaussian white noise. application to fractional black–scholes equations. *Insurance: Mathematics and Economics*, 42(1):271–287, 2008. 14

[111] G. Jumarie. Derivation and solutions of some fractional black-scholes equations in coarse-grained space and time. application to merton's optimal portfolio. *Computers & mathematics with applications*, 59(3):1142–1164, 2010. 13, 14

[112] O. Kallenberg. *Foundations of Modern Probability*. Springer, 2nd edition, 2002. 27

[113] B. Kaltenbacher and W. Rundell. Some inverse problems for wave equations with fractional derivative attenuation. *Inverse Problems*, 37(4):045002, 2021. 47

[114] A. Kaneko. Multi-stage euler–maruyama methods for backward stochastic differential equations driven by continuous-time markov chains. *Japan Journal of Industrial and Applied Mathematics*, 41(2):1223–1276, 2024. 29, 31, 32

[115] I. Karatzas, S. E. Shreve, I. Karatzas, and S. E. Shreve. *Methods of mathematical finance*, volume 39. Springer, 1998. 42

[116] R. Khalil, M. Al Horani, A. Yousef, and M. Sababheh. A new definition of fractional derivative. *Journal of computational and applied mathematics*, 264:65–70, 2014. 94

[117] M. A. Khan. The dynamics of a new chaotic system through the caputo–fabrizio and atanagan–baleanu fractional operators. *Advances in Mechanical Engineering*, 11(7):1687814019866540, 2019. 18

[118] R. Khatwani, P. Shah, R. Sekhar, H. R. Penubadi, P. K. Mitra, L. Shrotriya, and S. Das. Deep learning models for hedging strategies in derivative markets. In *2024 International Conference on Intelligent Systems and Advanced Applications (ICISAA)*, pages 1–7. IEEE, 2024. 127

[119] A. A. Kilbas, H. M. Srivastava, and J. J. Trujillo. *Theory and applications of fractional differential equations*, volume 204. elsevier, 2006. 46

[120] E. Kim, T. Nie, and M. Rutkowski. Arbitrage-free pricing of american options in nonlinear markets. *arXiv preprint arXiv:1804.10753*, 2018. 98

[121] H. Kim, R. Sakthivel, A. Debbouche, and D. F. Torres. Traveling wave solutions of some important wick-type fractional stochastic nonlinear partial differential equations. *Chaos, Solitons & Fractals*, 131:109542, 2020. 47

[122] P. E. Kloeden, E. Platen, P. E. Kloeden, and E. Platen. *Stochastic differential equations*. Springer, 1992. 29, 31

[123] R. Koeller. Applications of fractional calculus to the theory of viscoelasticity. 1984. 48

[124] C. Kuehn and M. D. Chekroun. Spdes in climate modeling. *Nonlinear Processes in Geophysics*, 29:1–22, 2022. 36

[125] K. Kumar. Cross-asset correlation shifts in crisis periods: A framework for portfolio hedging. *Journal of Data Analysis and Critical Management*, 1(01):40–51, 2025. 127

[126] S. Kumar, D. Kumar, and J. Singh. Numerical computation of fractional black–scholes equation arising in financial market. *Egyptian Journal of Basic and Applied Sciences*, 1(3-4):177–183, 2014. 91, 126

[127] Y. Kwok. Mathematical models of financial derivatives, 2008. 97, 98, 99

[128] H. G. Landau. Heat conduction in a melting solid. *Quarterly of Applied Mathematics*, 8(1):81–94, 1950. 91, 99

[129] Z. K. Lawal, H. Yassin, D. T. C. Lai, and A. Che Idris. Physics-informed neural network (pinn) evolution and beyond: A systematic literature review and bibliometric analysis. *Big Data and Cognitive Computing*, 6(4):140, 2022. 6

[130] J.-F. Le Gall and J.-F. Le Gall. Brownian motion and partial differential equations. *Brownian Motion, Martingales, and Stochastic Calculus*, pages 185–208, 2016. 35

[131] H. Lee, S. Kim, and R. Patel. Robust calibration of fractional order parameters under noisy financial data. *SIAM Journal on Financial Mathematics*, 13(2):112–135, 2022. 128

[132] G. W. Leibniz. *Leibnizens mathematische Schriften*, volume 1. H. W. Schmidt, 1849. 8

[133] A. V. Letnikov. Theory of differentiation with an arbtraly indicator. *Matem Sbornik*, 3:1–68, 1868. 17

[134] C. Li, D. Qian, and Y. Chen. On riemann-liouville and caputo derivatives. *Discrete Dynamics in Nature and Society*, 2011(1):562494, 2011. 13, 14

[135] M. Li, X. Dai, and C. Huang. Fast euler–maruyama method for weakly singular stochastic volterra integral equations with variable exponent. *Numerical Algorithms*, 92(4):2433–2455, 2023. 48

[136] X. Li and X. Yang. Error estimates of finite element methods for stochastic fractional differential equations. *Journal of Computational Mathematics*, pages 346–362, 2017. 48

[137] F. A. Longstaff and E. S. Schwartz. Valuing american options by simulation: A simple least-squares approach. *Review of Financial Studies*, 14(1):113–147, 2001. 3, 6, 45

[138] G. J. Lord, C. E. Powell, and T. Shardlow. *An Introduction to Computational Stochastic PDEs*. Cambridge Texts in Applied Mathematics. Cambridge University Press, 2014. 20, 21, 24, 25, 26, 27, 29, 30, 31, 33, 34, 37, 38, 39

[139] G. J. Lord and A. Tambue. Stochastic exponential integrators for the finite element discretization of spdes for multiplicative and additive noise. *IMA Journal of Numerical Analysis*, 33(2):515–543, 2013. 37

[140] J. Losada and J. J. Nieto. Properties of a new fractional derivative without singular kernel. *Progr. Fract. Differ. Appl*, 1(2):87–92, 2015. 50

[141] Y. Luchko. Fractional derivatives and the fundamental theorem of fractional calculus. *Fractional Calculus and Applied Analysis*, 23(4):939–966, 2020. 16

[142] J. Ma and C. Xu. Sparse grids for regime-switching lcps. *Journal of Computational Finance*, 25(4):1–35, 2021. 3

[143] D. MacKenzie and Y. Millo. Constructing a market, performing theory: The historical sociology of a financial derivatives exchange. *American journal of sociology*, 109(1):107–145, 2003. 2

[144] R. L. Magin. *Fractional Calculus in Bioengineering*. Begell House, 2006. 10

[145] F. Mainardi. *Fractional Calculus and Waves in Linear Viscoelasticity: An Introduction to Mathematical Models*. World Scientific, 2010. 10

[146] Z. S. Makumbe. Approximate option pricing for jump-diffusion stochastic volatility models. Tesis doctoral, Facultat de Matemàtiques i Informàtica, 9 2024. 3, 7

[147] B. B. Mandelbrot and J. W. Van Ness. Fractional brownian motions, fractional noises and applications. *SIAM Review*, 10(4):422–437, 1968. 13

[148] S. Mandt, M. D. Hoffman, and D. M. Blei. Stochastic gradient descent as approximate bayesian inference. *Journal of Machine Learning Research*, 18(134):1–35, 2017. 29

[149] X. Mao. *Stochastic differential equations and applications*. Elsevier, 2007. 30, 31

[150] M. S. M. Markose. *Systemic risk from global financial derivatives: a network analysis of contagion and its mitigation with super-spreader tax*. International Monetary Fund, 2012. 127

[151] R. Marmo, B. T. Adey, and G. Celentano. Stress testing hospitals using service measures and resilience indicators. *International Journal of Disaster Risk Reduction*, page 105492, 2025. 127

[152] F. Martínez and M. K. Kaabar. A novel theoretical investigation of the abu-shady–kaabar fractional derivative as a modeling tool for science and engineering. *Computational and Mathematical Methods in Medicine*, 2022(1):4119082, 2022. 47

[153] H. P. McKean Jr. A free boundary problem for the heat equation arising from a problem in mathematical economics. *Indust. Manag. Rev.*, 6:32–39, 1965. 42

[154] R. C. Merton. Theory of rational option pricing. *The Bell Journal of economics and management science*, pages 141–183, 1973. 4, 90, 93

[155] R. C. Merton. Option pricing when underlying stock returns are discontinuous. *Journal of financial economics*, 3(1-2):125–144, 1976. 43

[156] R. Metzler and J. Klafter. The random walk's guide to anomalous diffusion: A fractional dynamics approach. *Physics Reports*, 339(1):1–77, 2000. 10

[157] F. S. Mishkin and S. G. Eakins. *Financial markets and institutions*. Pearson, 9th edition, 2015. 3

[158] W. W. Mohammed, N. Iqbal, A. M. Albalahi, A. Abouelregal, D. Atta, H. Ahmad, and M. El-Morshedy. Brownian motion effects on analytical solutions of a fractional-space long–short-wave interaction with conformable derivative. *Results in Physics*, 35:105371, 2022. 47

[159] K.-S. Moon, H. Kim, and Y. Jeong. A series solution of black-scholes equation under jump diffusion model. *Economic Computation and Economic Cybernetics Studies and Research*, 48(1):127–39, 2014. 45

[160] V. F. Morales-Delgado, J. F. Gómez-Aguilar, K. Saad, and R. F. Escobar Jiménez. Application of the caputo-fabrizio and atangana-baleanu fractional derivatives to mathematical model of cancer chemotherapy effect. *Mathematical Methods in the Applied Sciences*, 42(4):1167–1193, 2019. 18

[161] B. F. Nielsen, O. Skavhaug, and A. Tveito. Penalty and front-fixing methods for the numerical solution of american option problems. *Journal of Computational Finance*, 5(4):69–98, 2002. 97

[162] K. Nouri, H. Ranjbar, and L. Torkzadeh. Solving the stochastic differential systems with modified split-step euler-maruyama method. *Communications in Nonlinear Science and Numerical Simulation*, 84:105153, 2020. 83

[163] S. Nuugulu, F. Gideon, and K. Patidar. A robust numerical simulation of a fractional black–scholes equation for pricing american options. *Journal of Nonlinear Mathematical Physics*, 31(1):40, 2024. xii, 15, 91, 94, 98, 99, 100, 102, 118, 126

[164] S. M. Nuugulu, F. Gideon, and K. C. Patidar. A robust numerical scheme for a time-fractional black-scholes partial differential equation describing stock exchange dynamics. *Chaos, Solitons & Fractals*, 145:110753, 2021. 15, 91, 94

[165] S. M. Nuugulu, K. C. Patidar, and D. T. Tarla. A physics informed neural network approach for solving time fractional black-scholes partial differential equations. *Optimization and Engineering*, pages 1–30, 2024. 6, 13

[166] A. Odunaike. Integrating real-time financial data streams to enhance dynamic risk modeling and portfolio decision accuracy. *Int J Comput Appl Technol Res*, 14(08):1–16, 2025. 127

[167] P. G. Ogundu. The strategic implications of financial derivatives in hedging corporate exposure to global economic volatility. 2025. 127

[168] B. Øksendal. *Stochastic Differential Equations: An Introduction with Applications*. Universitext. Springer, 6th edition, 2003. 28, 29

[169] K. B. Oldham and J. Spanier. *The Fractional Calculus: Theory and Applications of Differentiation and Integration to Arbitrary Order*. Academic Press, 1974. 12, 15

[170] J. Osterrieder, V. Arakelian, I. F. Coita, B. Hadji-Misheva, A. Kabasinskas, M. Machado, and C. Mare. An overview-stress test designs for the evaluation of ai and ml models under shifting financial conditions to improve the robustness of models. *Available at SSRN 4634266*, 2023. 127

[171] H. M. Ozaktas, Z. Zalevsky, and M. A. Kutay. *The Fractional Fourier Transform: With Applications in Optics and Signal Processing*. Wiley, 2001. 12

[172] G. Pang, L. Lu, and G. E. Karniadakis. fpinns: Fractional physics-informed neural networks. *SIAM Journal on Scientific Computing*, 41(4):A2603–A2626, 2019. 13

[173] K. Pantazopoulos, E. Houstis, and S. Kortesis. Front-tracking finite difference methods for the valuation of american options. *Computational Economics*, 12(3):255–273, 1998. 90

[174] É. Pardoux. Equation aux derivees partielles stochastiques non lineaires monotones. *These, Universite Paris*, 1975. 36, 55

[175] E. Pardoux and S. Peng. Adapted solution of a backward stochastic differential equation. *Systems & control letters*, 14(1):55–61, 1990. 42

[176] J.-C. Pedjeu and G. S. Ladde. Stochastic fractional differential equations: Modeling, method and analysis. *Chaos, Solitons & Fractals*, 45(3):279–293, 2012. 48

[177] C. Peng and Z. Li. Dynamic effects on traveling wave solutions of the space-fractional long-short-wave interaction system with multiplicative white noise. *Results in Physics*, 53:106931, 2023. 47

[178] J. Persson and L. von Sydow. Pricing american options using a space-time adaptive finite difference method. *Mathematics and Computers in Simulation*, 80(9):1922–1935, 2010. 5

[179] A. Peters. Risk-sensitive fractional hjb framework for tokenized asset markets in the digital economy. *Available at SSRN 5532244*, 2025. 127

[180] E. Platen and N. Bruti-Liberati. *Numerical Solution of Stochastic Differential Equations with Jumps in Finance*, volume 64 of *Stochastic Modelling and Applied Probability*. Springer, Berlin, Heidelberg, 2010. 20

[181] I. Podlubny. *Fractional differential equations: an introduction to fractional derivatives, fractional differential equations, to methods of their solution and some of their applications*, volume 198. elsevier, 1998. 12

[182] I. Podlubny and K. V. T. (Eds.). *Fractional Differential Equations: An Introduction to Fractional Derivatives, Fractional Differential Equations, to Methods of Their Solution and Some of Their Applications*. Mathematics in Science and Engineering 198. Academic Press, 1st edition, 1998. 34

[183] E. Popovska and G. Georgieva-Tsaneva. Fractal-based robotic trading strategies using detrended fluctuation analysis and fractional derivatives: A case study in the energy market. *Fractal and Fractional*, 9(1):5, 2024. 127

[184] H. Purnomo, B. Sugeng, and P. Handayati. Strategy of derivatives hedging: Maintaining and increasing firm value amidst market volatility in indonesia. *Shafin: Sharia Finance and Accounting Journal*, 4(2):66–84, 2024. 127

[185] S. Qureshi, N. A. Rangaig, and D. Baleanu. New numerical aspects of caputo-fabrizio fractional derivative operator. *Mathematics*, 7(4):374, 2019. 91

[186] B. Riemann. *Gesammelte Mathematische Werke*. Teubner, 1876. 9

[187] J. A. Roberts and P. A. Robinson. Spdes in neural field theory. *Physical Review E*, 69:051901, 2004. 36

[188] G. Rossi and T. Brown. Comparative analysis of fractional derivative definitions in financial modeling. *Applied Mathematical Finance*, 27(4):287–310, 2020. 128

[189] B. L. Rozovskii. *Stochastic evolution systems: linear theory and applications to nonlinear filtering*, volume 35. Springer Science & Business Media, 2012. 42

[190] W. Rudin. *Real and Complex Analysis*. McGraw-Hill, 3rd edition, 1987. 21

[191] J. Ruf and W. Wang. Neural networks for option pricing and hedging: A literature review. *Journal of Computational Finance*, 24(1):1–29, 2020. 3

[192] K. Sakamoto and M. Yamamoto. Initial value/boundary value problems for fractional diffusion-wave equations and applications to some inverse problems. *Journal of Mathematical Analysis and Applications*, 382(1):426–447, 2011. 48

[193] S. G. Samko, A. A. Kilbas, and O. I. Marichev. *Fractional Integrals and Derivatives: Theory and Applications*. Gordon and Breach, 1993. 9, 10, 15

[194] M. S. Scholes. Global financial markets, derivative securities, and systemic risks. *Insurance Mathematics and Economics*, 3(19):267, 1997. 127

[195] S. L. Schwarcz. Derivatives and collateral: balancing remedies and systemic risk. *U. Ill. L. Rev.*, page 699, 2015. 127

[196] E. S. Schwartz. The valuation of warrants: Implementing a new approach. *Journal of Financial Economics*, 4(1):79–93, 1977. 90

[197] D. Ševcovic. An iterative algorithm for evaluating approximations to the optimal exercise boundary for a nonlinear black–scholes equation. *Canad. Appl. Math. Quarterly*, 15(1):77–97, 2007. 97

[198] S. E. Shreve et al. *Stochastic calculus for finance II: Continuous-time models*, volume 11. Springer, 2004. 29

[199] J. Shu, P. Li, J. Zhang, and O. Liao. Random attractors for the stochastic coupled fractional ginzburg-landau equation with additive noise. *Journal of Mathematical Physics*, 56(10), 2015. 47

[200] W. L. Silber. Innovation, competition, and new contract design in futures markets. *Journal of Futures Markets*, 3(2):123–156, 1983. 2

[201] B. K. Singh and A. Kumar. New approximate series solutions of conformable time–space fractional fokker–planck equation via two efficacious techniques. *Partial Differential Equations in Applied Mathematics*, 6:100451, 2022. 47

[202] A. V. Skorokhod. *Studies in the Theory of Random Processes*. Addison-Wesley, 1965. 36

[203] A. B. Smith and C. D. Johnson. Computational bottlenecks in high-dimensional fractional pde discretization. *Journal of Computational Finance*, 25(3):45–67, 2021. 128

[204] F. Soleymani. Numerical analysis of novel finite difference methods. *Novel Methods in Computational Finance*, 25:171, 2017. 127

[205] M. Stynes, E. O'Riordan, and J. L. Gracia. Error analysis of a finite difference method on graded meshes for a time-fractional diffusion equation. *SIAM Journal on Numerical Analysis*, 55(2):1057–1079, 2017. 47, 48

[206] P. L. Swan and J. Westerholm. The impact of market architectural features on world equity market performance: A structural equation approach. Technical report, Working Paper, University of New South Wales, 2004. 2

[207] D. Tangman, A. Gopaul, and M. Bhuruth. A fast high-order finite difference algorithm for pricing american options. *Journal of Computational and Applied Mathematics*, 222(1):17–29, 2008. 90, 91, 92

[208] V. E. Tarasov. No nonlocality. no fractional derivative. *Communications in Nonlinear Science and Numerical Simulation*, 44:52–60, 2018. 13

[209] V. V. Uchaikin. *Fractional derivatives for physicists and engineers*, volume 2. Springer, 2013. 46

[210] H. Wang and X. Li. Gpu-accelerated psor for high-dimensional american options. *Journal of Parallel and Distributed Computing*, 152:1–15, 2021. 7

[211] H. Wang and X. Zheng. Wellposedness and regularity of the variable-order time-fractional diffusion equations. *Journal of Mathematical Analysis and Applications*, 475(2):1778–1802, 2019. 48

[212] Q. Wang, K. Serkh, and C. C. Christara. High-order deferred correction and penalty iteration for american option pricing. *Journal of Computational Finance*, 25(3):45–77, 2022. 5

[213] N. Wellink. Mitigating systemic risk in otc derivative markets. *FSR FINANCIAL*, page 2010131, 2010. 127

[214] P. Wilmott. *Paul Wilmott on quantitative finance*. Wiley, 2nd edition, 2013. 3

[215] H. Windcliff, P. A. Forsyth, and K. R. Vetzal. Pricing methods and hedging strategies for volatility derivatives. *Journal of Banking & Finance*, 30(2):409–431, 2006. 127

[216] L. Wu and Y.-K. Kwok. A front-fixing finite difference method for the valuation of american options. *Journal of Financial Engineering*, 6(4):83–97, 1997. 91, 99

[217] Z. Wu, X. Zhang, J. Wang, and X. Zeng. Applications of fractional differentiation matrices in solving caputo fractional differential equations. *Fractal and Fractional*, 7(5):374, 2023. 15

[218] A. Xiao, X. Dai, and W. Bu. Well-posedness and em approximation for nonlinear stochastic fractional integro-differential equations with weakly singular kernels. *arXiv*, 2019, 2019. 48

[219] D. K. Yadav, A. Bhardwaj, and A. Kumar. Operator splitting method to solve the linear complementarity problem for pricing american option: An approximation of error. *Computational Economics*, pages 1–27, 2024. 5

[220] J. Yang, Y. Tang, Y. Li, L. Zhang, and H. Zhang. Dynamic hedging strategies in derivatives markets with llm-driven sentiment and news analytics. *arXiv preprint arXiv:2504.04295*, 2025. 127

[221] X.-J. Yang. *General fractional derivatives: theory, methods and applications*. Chapman and Hall/CRC, 2019. 13, 14

[222] Z. Yang, X. Zheng, Z. Zhang, and H. Wang. Strong convergence of a euler-maruyama scheme to a variable-order fractional stochastic differential equation driven by a multiplicative white noise. *Chaos, Solitons & Fractals*, 142:110392, 2021. 35, 48, 49, 53, 59, 68, 74, 76, 83

[223] M. Yavuz and N. Özdemir. A different approach to the european option pricing model with new fractional operator. *Mathematical Modelling of Natural Phenomena*, 13(1):12, 2018. 91

[224] Y. Yu. Convergence of relative entropy for euler–maruyama scheme to stochastic differential equations with additive noise. *Entropy*, 26(3):232, 2024. 48

[225] F. L. Yuen and H. Yang. Option pricing with regime switching by trinomial tree method. *Journal of computational and applied mathematics*, 233(8):1821–1833, 2010. 11

[226] O. P. Yves Achdou. *Computational Methods for Option Pricing*. Frontiers in Applied Mathematics. Society for Industrial and Applied Mathematics (SIAM), 2005. 44

[227] N. A. Zabidi, Z. A. Majid, A. Kilicman, and Z. B. Ibrahim. Numerical solution of fractional differential equations with caputo derivative by using numerical fractional predict-correct technique. *Advances in Continuous and Discrete Models*, 2022(1):26, 2022. 15

[228] C. Zhang and L. Huang. A quantum model for the stock market. *Physica A: Statistical Mechanics and Its Applications*, 389(24):5769–5775, 2010. 3

[229] J. Zhang, Y. Tang, and J. Huang. A fast euler-maruyama method for fractional stochastic differential equations. *Journal of Applied Mathematics and Computing*, 69(1):273–291, 2023. 48

[230] J. Zhang and S. Zhu. A hybrid finite difference method for valuing american puts. In *Proceedings World Congress on Engineering*, pages 1131–1136, 2009. 97

[231] K. Zhang, H. Song, and J. Li. Front-fixing fems for the pricing of american options based on a pml technique. *Applicable Analysis*, 94(5):903–931, 2015. 127

[232] Q. Zhang, Q. Wang, P. Zuo, H. Du, and F. Wu. Projection and contraction method for pricing american bond options. *Mathematics*, 11(22):4689, 2023. 5

[233] X. Zheng, H. Wang, and H. Fu. Well-posedness of fractional differential equations with variable-order caputo-fabrizio derivative. *Chaos, Solitons & Fractals*, 138:109966, 2020. 54

[234] X. Zheng, Z. Zhang, and H. Wang. Analysis of a nonlinear variable-order fractional stochastic differential equation. *Applied Mathematics Letters*, 107:106461, 2020. 48, 54

[235] S. Zhou and H. Jin. The truncated euler-maruyama method for highly nonlinear stochastic differential equations with multiple time delays. *Numerical Algorithms*, 94(2):581–617, 2023. 31, 32

[236] Y. Zhou. Fractional evolution equations and inclusions. *Analysis and control*, 2015. 47

[237] Y.-l. Zhu, B.-m. Chen, H. Ren, and H. Xu. Application of the singularity-separating method to american exotic option pricing. *Advances in Computational Mathematics*, 19(1):147–158, 2003. 91

[238] G.-a. Zou and B. Wang. Stochastic burgers' equation with fractional derivative driven by multiplicative noise. *Computers & Mathematics with Applications*, 74(12):3195–3208, 2017. 47

[239] B. Ã˜ksendal. *Stochastic Differential Equations: An Introduction with Applications*. Universitext. Springer, 6th edition, 2003. 94